Cooperative Porphyrin Assemblies

Een wetenschappelijke proeve op het gebied van de
Natuurwetenschappen, Wiskunde en Informatica

Proefschrift

Ter verkrijging van de graad van doctor
aan de Radboud Universiteit Nijmegen
op gezag van de rector magnificus prof. Mr. S.C.J.J. Kortmann,
volgens besluit van het College van Decanen
in het openbaar te verdedigen op dinsdag 7 oktober
om 13:30 precies

door

Paul Johannes Thomassen

geboren op 14 september 1979
te ’s-Hertogenbosch

Promotores
Prof. dr. A.E. Rowan
Prof. dr. R.J.M. Nolte

Copromotor
Dr. J.A.A.W. Elemans

Manuscripcommissie
Prof. dr. J.C.M. van Hest
Prof. dr. R.P. Sijbesma (Technische Universiteit Eindhoven)
Prof. dr. J.N.H. Reek (Universiteit van Amsterdam)
Dr. M.C. Feiters

Paranimfen
Ribera Jordana i Lluch
Nico Veling

The work described in this thesis was financially supported by the "Nederlandse Organisatie voor Wetenschappelijk Onderzoek" (NWO).

Printing: PrintParners Ipskamp
Praktische uitvoering kaft: Ton Dirks

ISBN: 970-90-9023366-6

Come on, world, cheer up! It may bloody never happen!

- Edina Monsoon -

Contents

Chapter 1. Literature review: cooperative porphyrin assemblies

1.1 Introduction

Cooperative interactions play a ubiquitous role in Nature; they are employed to influence the composition and the function of hierarchical, complex self-assembled systems such as the tobacco mosaic virus, but also to transfer information, as in the binding of oxygen to haemoglobin.[1,2] Cooperative interactions also play a critical role in gene transcription; for instance, cyclic AMP has a strong cooperative effect upon the binding of the gene-transcription-regulating cAMP receptor protein (CRP) to DNA.[3]

Chemists have only recently recognised that cooperative interactions might also help in the construction of functional nanoscale objects. In the past few decades this type of interactions have received increasing attention and a myriad of self-assembled structures that employ cooperative effects have been developed. This being the case, it is a matter of ongoing debate what exactly the definition is of cooperativity and how one can prove which self-assembled structures actually show evidence of employing cooperativity.

In the literature, various definitions of cooperativity can be found, which only differ slightly.[4] A general one seems to be: "cooperativity is the interaction process by which binding of a ligand to one site of a (macro)molecule (enzyme, receptor, etc.) influences binding of another ligand at a second remote site". When the association constant of the second binding event is increased, the cooperative effect is positive; when this association constant is decreased, the effect is negative. If the effector molecule, which is the molecule involved in the first binding event, is the same as the molecule involved in the second binding event, the cooperative effect is defined as homotropic; if this is not the case, then the cooperative effect is termed heterotropic.

Cooperative effects have also been made evident with the help of mathematics. Consider the common case depicted in Figure 1a:

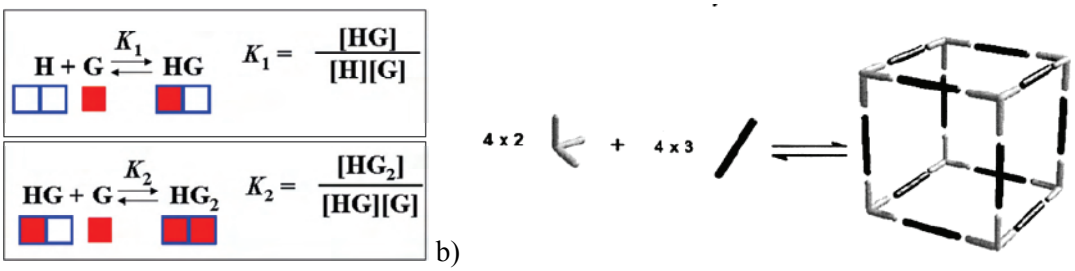

a) b)

Figure 1. *a) Two binding events involving a ditopic host. b) Self-assembly of a cube by two predisposed building blocks.*

One can easily deduce that when there are no additional (cooperative) interactions $4 \cdot K_2 = K_1$. The ratio $4 \cdot K_2/K_1$ is termed α: binding behaviour with $\alpha<1$ indicates negative cooperativity, $\alpha>1$ positive cooperativity.
Another method of quantifying the extent of any cooperative effects is by calculating the Hill coefficient *n* of the system, $\theta = [L]^n/\{(K_A)^n + [L]^n\}$, with θ = the fraction of ligand binding sites that are filled, [L] = ligand concentration, K_A = the ligand concentration at which half the binding sites are occupied. As in the case for α, binding behaviour with $n<1$ indicates negative cooperativity, $n>1$ positive cooperativity.
A special case of cooperativity, in which the host molecule changes its conformation upon binding of the effector molecule, is called "allosterism", also sometimes called "allostery" or "allostericity".
There are systems in which the self-assembled structures are more complex and of a higher order than the one shown in Figure 1a, e.g. in the case of intramolecular cyclisation processes (e.g. Figure 1b). These assemblies display enhanced thermodynamic stability compared with the non-cyclic analogues, because no entropy penalty has to be overcome in the step(s) that close(s) the "circle". This increase in stability is quantified by the parameter EM, the effective molarity of the intramolecular process, which is defined as the ratio of the association constant of the intramolecular interaction to the association constant of the corresponding intermolecular interaction.[5] The former can be determined by measuring the stability of the self-assembled structure; the latter value is generally determined by using simple monofunctional reference compounds. Ercolani *et al.* have developed a model which treats the competition, under thermodynamic control, between self-assembly and nonlinear random polymerisation, based on the EM of the assembly and the equilibrium constant for the intermolecular model reaction between monofunctional reactants.[6] This model provides a method to assess whether cooperative effects play a role in higher-order assemblies. In cases where the degree of cyclicity can be systematically increased, a plot of $-\Delta G°$ against the number of cyclic substructures of the assembly is expected to be linear with a positive slope in the absence of cooperativity. A positive or negative deviation from this linearity is evidence of positive or negative cooperativity, respectively.[7]

1.2 Scope of this literature review

A large number of artificial cooperative systems has been reported in the literature and the majority of these include one or more crown ether moieties.[8,9] Numerous so-called crown porphyrin molecules, which combine a crown ether moiety and a porphyrin unit, have been described in the past decade, some of which show cooperative behaviour; the binding of an appropriate cation into the crown-ether can

cause a conformational change in the molecule, changing the binding behaviour of the porphyrin moiety.[10] An overview of allosteric supramolecular receptors and catalysts, of which most contain a crown-ether and some a porphyrin moiety, was recently given by Kovbasyuk and Krämer.[11] Several reviews have been written on the of self-assembly of porphyrin arrays, but only Baldini and Hunter mention both cooperative and non-cooperative systems.[12] A review on the use of double helical DNA as a template for the controlled assembly of chromophore aggregates, e.g. porphyrins, is given by Armitage.[13] The more recent developments in cooperative assembly of porphyrins will be discussed here.

1.3 The early years

In the 1970's and 1980's, research into cooperative effects mostly involved iron porphyrins and the binding of small molecules such as oxygen, carbon dioxide and carbon monoxide to these dye compounds. Most of this research was directed towards the elucidation of the mechanism by which the protein haemoglobin operates. Collman *et al.* found that in the solid state picket-fence porphyrins show positive cooperativity towards the binding of oxygen, probably because of a change in their molecular dimension upon oxygenation, which is subsequently communicated from site to site by changes in the crystal packing forces.[14]

Oxygen binding has been a subject of continuing research. A more recent example is given by Fournier *et al.* who investigated the oxygen binding properties of the self-assembled complex $Co^{II-\delta}P^{4+}/(Al^{III}Pc^{4-})^{+\delta}$, which consists of a tetracationic cobalt porphyrin, $Co^{II}P^{4+}$, and a tetraanionic sulfoaluminium phthalocyanine, $Al^{III}Pc^{4-}$.[15] The unconventional properties of the resultant self-assembled structure include a severely lowered oxidation potential of the phthalocyanine moiety by at least 500 mV to a point where oxidation of the phthalocyanine occurred before oxidation of the Co^{II}-ion. In addition, the zwitterionic complex was found to bind oxygen to form the charge-transfer species $^{-}O_2Co^{II}P^{4+}/(Al^{III}Pc)^{0+}$. Upon photo-excitation, singlet oxygen was photo-ejected exclusively from this complex. Since singlet oxygen is a known cytotoxic intermediate in the photodynamic therapy of cancer, the potential of the complex as a sensitizer for the photodynamic inactivation of cancer cells was investigated; however, disappointingly the complex showed too little activity for this purpose.

1.4 Multiporphyrin systems linked by spacers

Ditopic ligands, such as diazibicyclo[2.2.2]octane (**dabco**), diamines ($H_2N(CH_2)_nNH_2$) and 4,4'-bipyridine, have been used extensively as bridges between two porphyrins. Although the binding behaviour of **dabco** sandwiched between two loose zinc(II)

porphyrins does not display any cooperativity, Hunter *et al*. have shown that when the porphyrins are attached *via* a spacer (**1**, Figure 2a) negative cooperativity with $\alpha = 0.8$ is observed.[16] This observation has led to the development of a wealth of different bisporphyrins linked by different spacers.

Ema *et al.* have studied the bisporphyrin system **2** depicted in Figure 2b.[17] The optically active cyclophane spacer causes the two porphyrin chromophores to adopt a slipped cofacial disposition. The asymmetric geometry was found to be tuneable by the cooperative coordination of diamines with various chain lengths, clearly indicated by changes in the CD spectrum of the different bisporphyrin/diamine complexes.

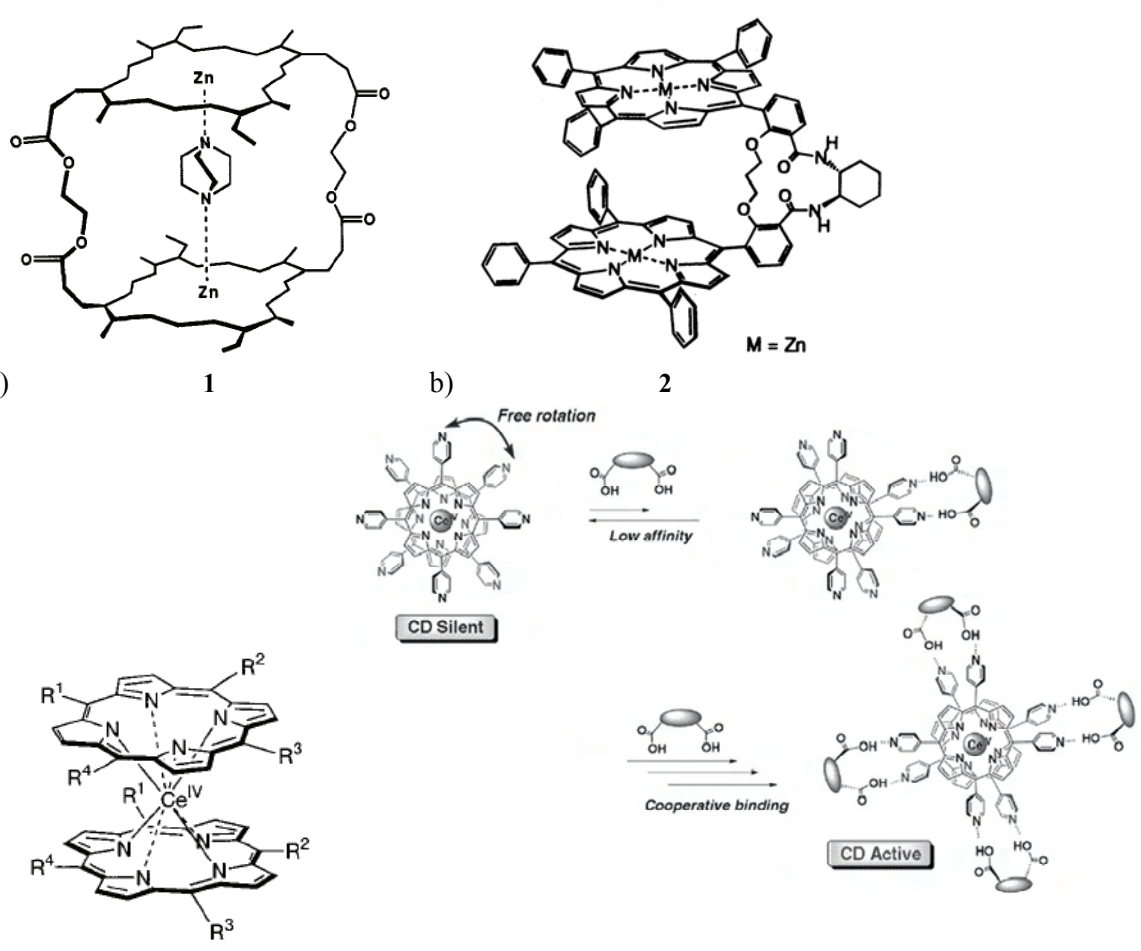

a) **1** b) **2**

c) **3** d)

Figure 2. *a) Bisporphyrin/**dabco** complex **1** studied by Hunter. b) Chiral bisporphyrin system **2** studied by Ema. c) Cerium (IV) bis(porphyrinate) double decker **3** of Shinkai. d) Highly cooperative binding of a ditopic ligand to a cerium bisporphyrin sandwich complex.*

The group of Shinkai has prepared numerous multiporphyrin systems that display allosteric behaviour upon the binding of ditopic ligands. In these systems, the porphyrins

are connected *via* several different kinds of linkers, such as a metal ion, a C-C-spacer, a butadiynyl or *p*-terphenyl spacer and *via* calix[3]arene linker groups.

Two tetra-pyridyl porphyrins sandwiched *via* a Ce^{IV} ion (complex **3**) can freely rotate, however, binding of a ditopic ligand like (1*R*,2*R*)-1,2 cyclohexanedicarboxylic acid suppresses this rotation, making a second, third and fourth binding event possible to occur (Figure 2c and d).[18] In a recent paper Ercolani has shown that the source of cooperativity in this homotropic allosteric system is mainly the torsional strain induced by binding of the ligands and the subsequent alignment of the pyridyl groups.[19]

A porphyrin-homooxacalix[3]arene conjugate **4** creating a C_3-symmetrical capsular space that is capable of binding tris(2-aminoethyl)amine (TREN) has been reported (Figure 3a).[20] Upon the addition of $NaClO_4$ to a $CHCl_3$ solution of this capsule, the geometry of the system changed, because of the coordination of sodium ions to the lower rims of the calixarenes. This coordination resulted in an increase in the binding affinity for TREN by three orders of magnitude, i.e. from $K_a = 1.7 \times 10^5\ M^{-1}$ to $K_a = 1.5 \times 10^8\ M^{-1}$.

A porphyrin tetramer with a butadiynyl rotational axis (compound **5**) was shown to bind two molecules of 1,3-di(4-piperidyl)propane (DPP) with positive homotropic allosterism and a Hill coefficient of 1.9 (Figure 3b).[21,22] The binding of a first ligand molecule in the cleft between one of the porphyrin pairs enhances the affinity of the other pair of porphyrins toward a second ligand molecule, due to preorganisation and alignment of the second binding site.

In a later report Shinkai *et al.* showed a porphyrin tetramer with 5-hexene tails, which can be preorganised with two 2,5-diiodo-1,4-bis(*N*-methylaminomethyl)benzene guest molecules for ring closing metathesis using the Hoveyda-Grubbs catalyst (Figure 3c).[23] After removal of the guests, the resulting compound still showed positive homotropic allosteric binding behaviour towards this guest, with $\alpha = 1.16$.

A porphyrin tetramer related to the compound depicted in Figure 3b, with a *p*-terphenyl axis that could bind two C_{60} fullerenes was designed (Figure 3d, compound **6**).[24] A positive homotropic allosteric effect was observed with an α-value of 1.38 and significantly higher association constants were measured than in the case of mono-porphyrin analogues.

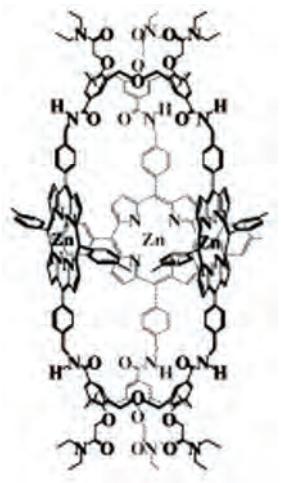

a) **4**

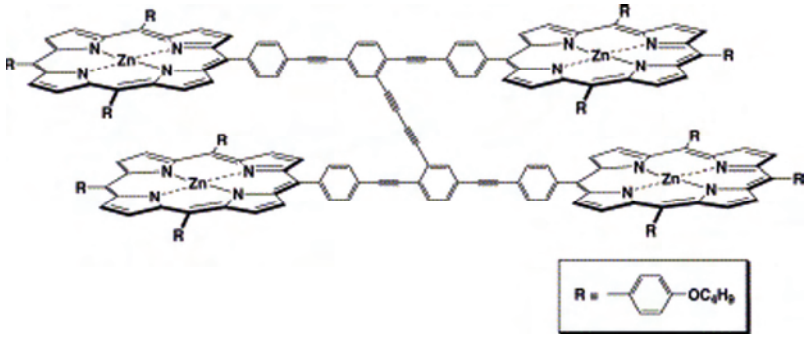

b) **5**

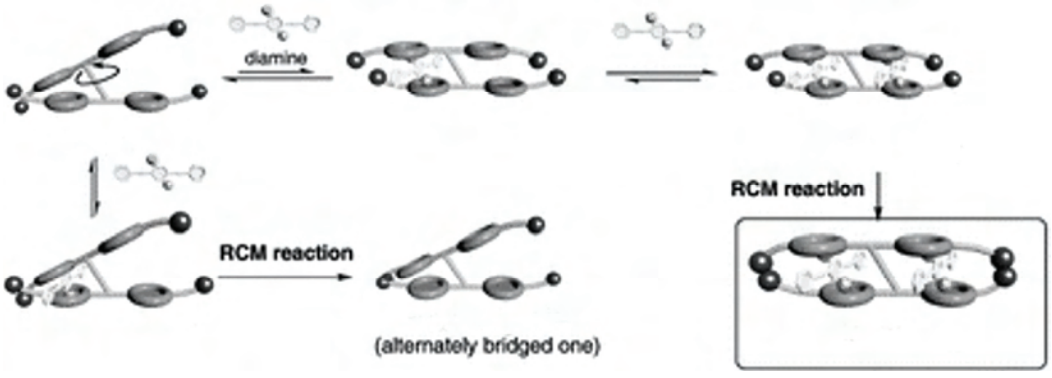

c)

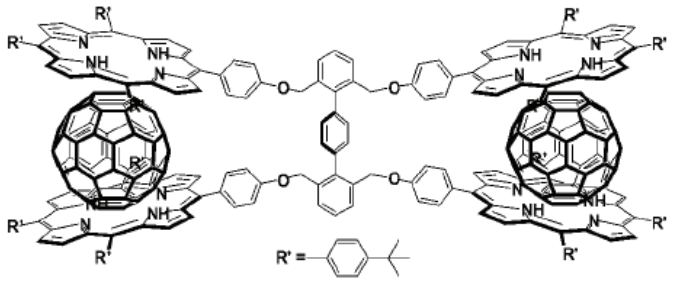

d) **6**

Figure 3. *a) Molecular capsule consisting of three zinc porphyrins and two ionophoric calixarenes* ***4*** *reported by Shinkai. b) Porphyrin tetramer with a butadiynyl rotational axis (****5****) by Shinkai. c) Preorganisation of the olefinic tails of* ***5*** *for ring closing metathesis. d) Porphyrin tetramer with a p-terphenyl axis (****6****) binding two [60]fullerenes published by Shinkai.*

The related porphyrin tetramer with the butadiynyl rotational axis **5** has recently been used in combination with the porphyrin hexamer molecule **7** (Figure 4a).[25] It was shown that both molecules bind the reference compound MCP (*N*-methyl-{2,5-diiodo-4-[(methylamino)methyl]phenyl}methanamine) with large positive homotropic allosteric behaviour, with $\alpha = 7.5$ for **5** and $\alpha_1 = 4.2$ and $\alpha_2 = 20.9$ for **7**. Both molecules were

found to allosterically align the conjugated polymer CP into supramolecular bundles, as was proven by AFM and TEM techniques (Figure 4).

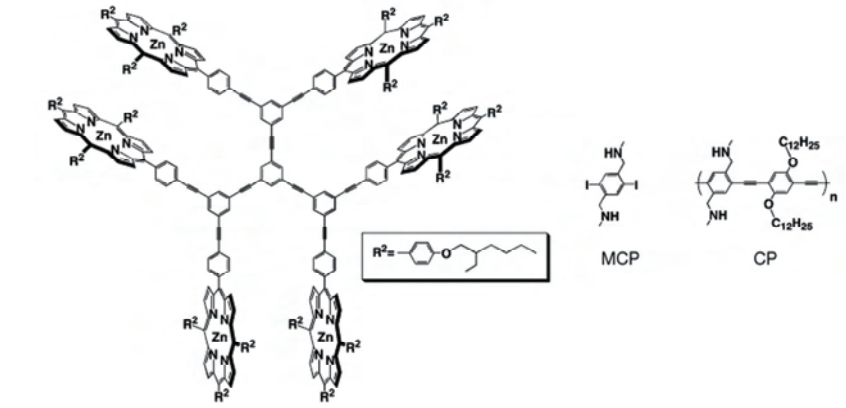

a) **7**

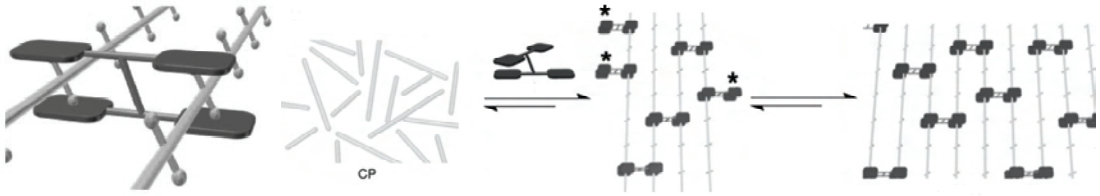

b)

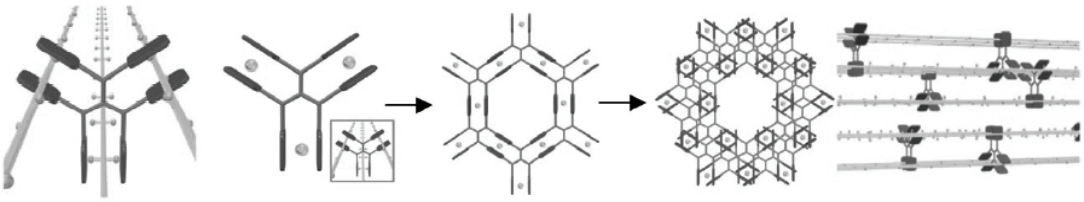

c)

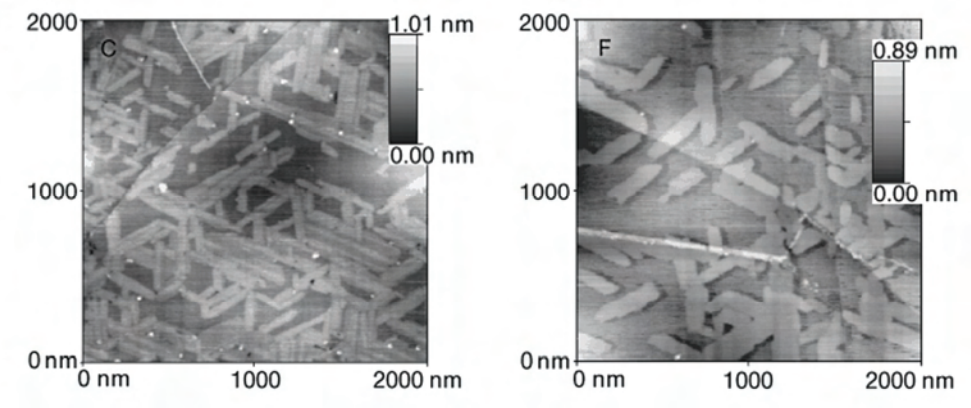

d)

Figure 4. *a) Porphyrin hexamer **7** prepared by Shinkai, reference compound MCP and conjugated polymer CP. b) Alignment of CP polymers by **5**. c) Alignment of CP polymers by **7**. d) Representative AFM images of [**5**·CP] and [**7**·CP] assemblies deposited from a $CHCl_3$ solution onto HOPG. CP:**5** = 9.1 in the picture on the left; CP:**7** = 5.9 in the picture on the right.*

Each pair of cofacially aligned porphyrinato zinc tweezers in **5** and **7** binds to a diamine moiety of the polymer to form polymer bundles; in this process, the binding of the first

polymer to an aligner molecule facilitates the binding of the second, which results in the ready formation of aligned assemblies. The asterisks in Figure 4b denote clefts that have enhanced affinity for polymer binding, as a result of preorganisation by the first polymer binding event. The assemblies of the hexamer and CP probably possess multi-walled tubular structures.

In an analogous approach, the group of Hunter has also reported several multiporphyrin systems in which the porphyrins are linked by spacers.[14] A molecule consisting of two porphyrins bridged by a naphthalene diimide moiety (compound **8**) was self-assembled into a dimer by the addition of **dabco**, the process displayed negative cooperativity and an effective molarity for the cyclisation of 2mM (Figure 5a).[26] The potential of the sandwich complex to function as a molecular receptor was investigated, but it failed to bind aromatic substrates.

If calixarenes are used as spacers between porphyrins, the addition of **dabco** to a calix[4]arene with two zinc porphyrins attached (**9**) and one with four porphyrins attached (**10**) induces self-assembly (Figure 5b and c).[27] In above cases, binding behaviour displaying minimal negative cooperativity was observed. At approximately a 1:1 ratio in solution the calix-bisporphyrin forms a 2:2 complex with **dabco**, generating a large cavity of which the potential to act as a supramolecular host is currently under investigation (Figure 5b). Upon further addition of **dabco** a 2:1 **dabco**:**9** complex is obtained. The calix-tetraporphyrin **10** can form four different complexes with **dabco**, depending on the stoichiometry and concentration of the components. The major species present at a 2:1 **dabco**:**10** ratio is a dimeric cage. Upon further addition of **dabco** this species dissociates *via* a 3:1 complex that contains one **dabco** molecule bound in a sandwich complex geometry to the 4:1 species (Figure 5c).

A series of three isomeric bisporphyrins with an isophthalic acid linker moiety (**11-13**) differing in the substitution pattern on the *meso* phenyl groups was reported by Hunter *et al.* (Figure 5d).[28] Whereas no cooperativity was observed for the binding of **dabco** in the *meta* and *para* isomers, the *ortho* isomer displayed negative cooperativity with $\alpha = 0.4$. Apparently in the case of the latter isomer a weak intramolecular interaction between the two porphyrins is disrupted upon the coordination of **dabco**. Upon the addition of one equivalent of **dabco**, the *ortho* and *meta* substituted bisporphyrins form 1:1 intramolecular sandwich complexes; the *para*-substituted bisporphyrin, however, can not adopt this conformation and forms a 2:2 intermolecular assembly, which is stable over a wide concentration range of **dabco**.

Another example of dimerisation by the addition of **dabco** is discussed in a report about a zinc trisporphyrin molecule (**14**) that forms a stable 2:3 porphyrin:**dabco** double-decker molecular coordination cage upon the addition of **dabco** (Figure 5e).[29] It was remarkable that at micromolar concentration the self-assembly of the coordination cage was an all-or-nothing process, while at millimolar concentration the relative stabilities of the

intermediate species increased, leading to a stepwise self-assembly process. Subsequently a 2:2 intermediate species could be clearly observed with ^{1}H NMR spectroscopy. The resulting double-decker cage was able to bind a benzene-1,3,5-tricarboxamide guest molecule inside its cavity by the formation of six N-H···O=C hydrogen bonds.

a)

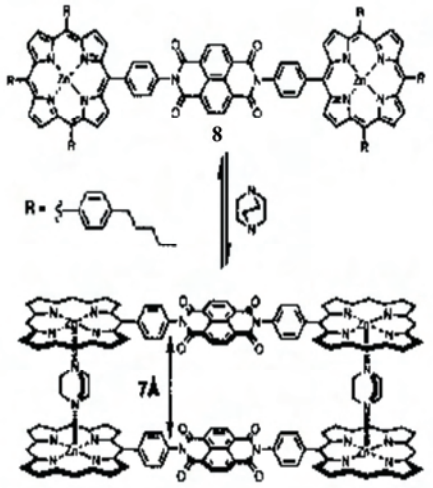

b)

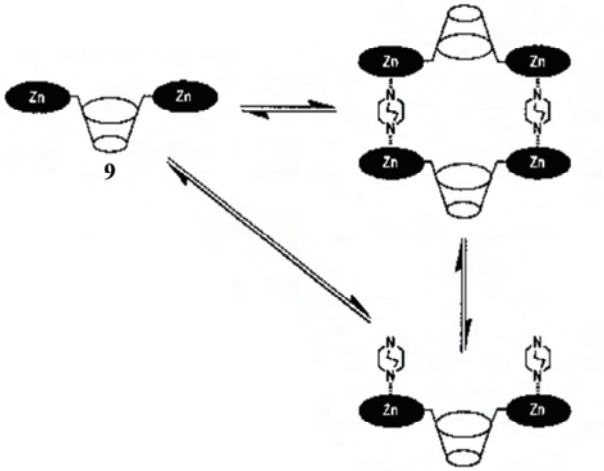

c)

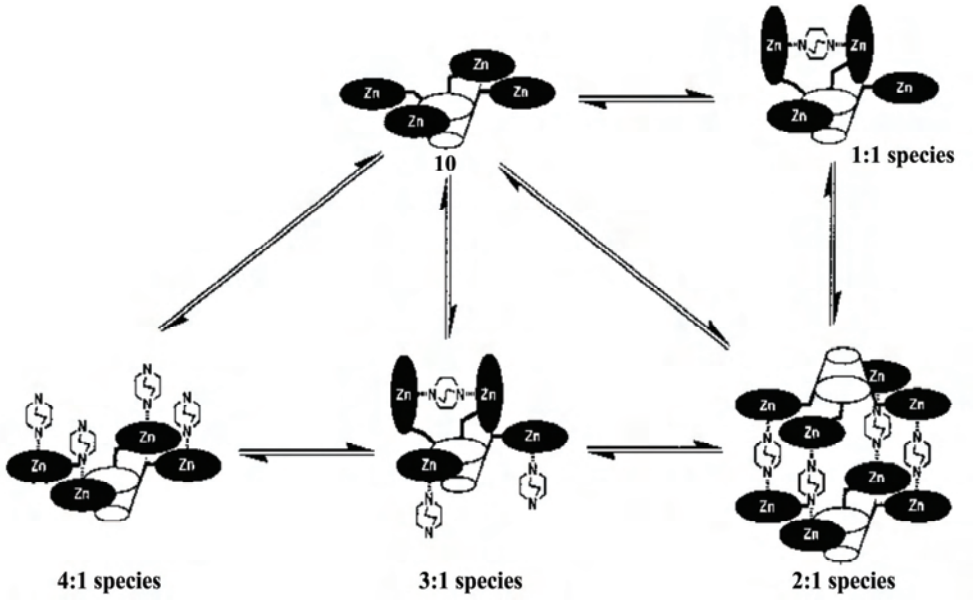

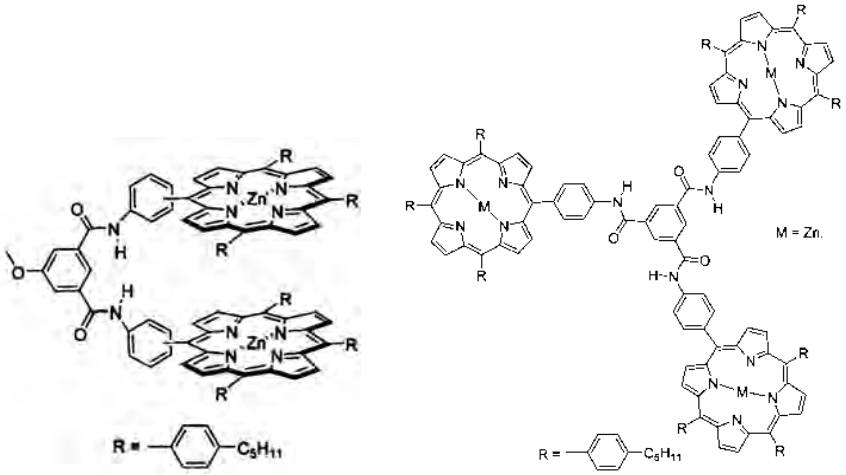

d) **11-13** e) **14**

Figure 5. *a) Dimerisation of a bisporphyrin-naphtalene diimide system by a* ***dabco*** *ligand. b) Various complexes that are formed by a calix[4]arene with two porphyrins attached upon the step-wise addition of* ***dabco****. c) Idem, in case of a calix[4]arene with four porphyrins attached. d) Bisporphyrins with an isophtalic acid linker by Hunter. e) Trisporphyrin system studied by Hunter.*

Closely related to Hunter's calixarene-based zinc porphyrins (Figure 5b), Dudič *et al.* have described the binding behaviour of calix[4]arenes to which two zinc porphyrins are attached (**15-16**; Figure 6a).[30] In contrast to Hunter's systems, which could form dimers upon the addition of **dabco**, in this molecule the amide spacers are not flexible enough to allow such a geometry. Titrations in which **dabco** was added, showed that the thiacalix[4]arene **16** prefers intramolecular **dabco** complexation in a 1:1 ratio up until a high excess of ligand. For the classical calix[4]arene **15** this 1:1 species is only an intermediate, and eventually the separate ligation of both zinc porphyrins in a 2:1 **dabco**:calix[4]arene ratio is preferred. For both calixarene molecules clear cooperative binding behaviour is observed. The difference in binding behaviour is ascribed to the larger cavity of the thiacalix[4]arene, which might be better capable of accommodating the **dabco** ligand.

The synthesis of two electron-deficient porphyrin building blocks and their resulting coordinatively linked assemblies have been reported by Splan *et al*.[31] The porphyrins with two perfluorophenyl and two pyridyl substituents were reacted with $Re(CO)_5Cl$ to give a discrete dimer (**17**) and a discrete tetramer (**18**), as was dictated by the geometry of the porphyrin monomer (Figure 6b). An enhanced affinity for nitrogen donor ligands was observed because the electron-withdrawing substituents on the porphyrin increase the zinc centre's Lewis acidity. Dimerisation of the dimer with 4,4'-bipyridine appeared to occur in a cooperative manner.

Related to Hunter's bisporphyrin-naphtalene diimide structure, You *et al*. have reported two bis-zinc-porphyrin perylene triads with bulky phenoxy substituents attached (**19**-**20**) to the perylene moiety (Figure 6c).[32] Addition of one equivalent of 4,4-bipyridine to the triad in solution leads to the formation of a zigzag oligomer with, on average, six bidentate ligands and triads (Figure 6d).

a)

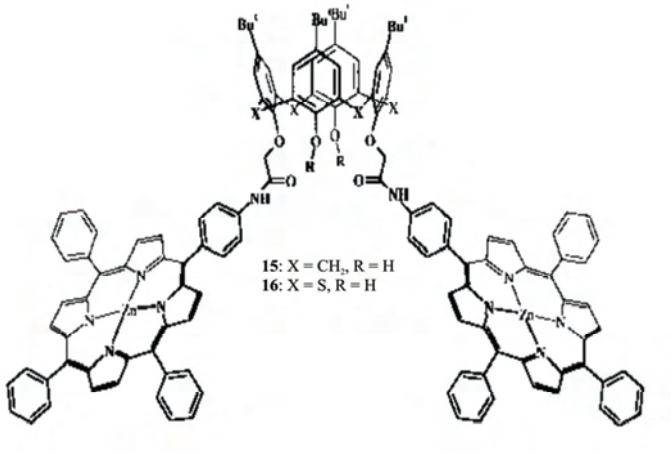

b)

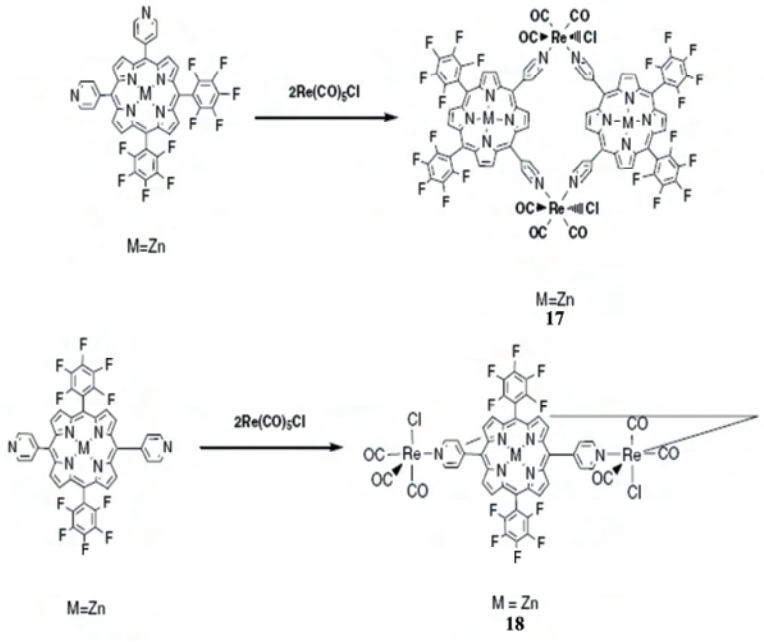

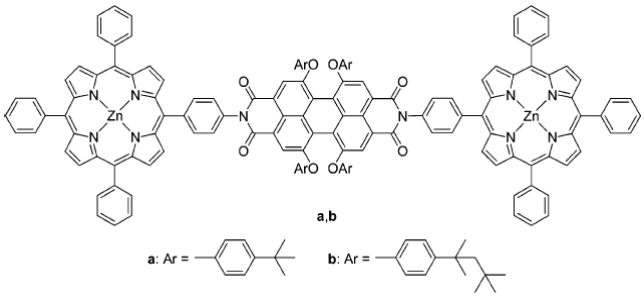

c) **19** **20** d)

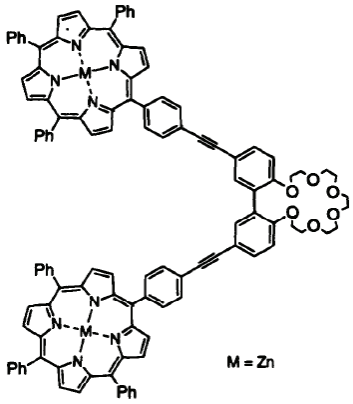

e) **21**

Figure 6. *a) Calixarene-based zinc porphyrin dimer studied by Dudič. b) Dimer and square formation upon reaction of bis-pyridyl porphyrins with $Re(CO)_5Cl$ as studied by Splan. c) Bisporphyrin perylene triad studied by You. d) Example of zigzag oligomer formed upon addition of 4,4'-bipyridine to the bisporphyrin perylene triad. e) Biphenyl-20-crown-6-derived zinc porphyrin dimer studied by Kubo.*

Kubo *et al*. combined crown ethers and zinc porphyrin systems to give a tweezer (**21**) that shows allosteric binding behaviour (Figure 6e).[33] The biphenyl-20-crown-6 porphyrin dimer can bind the α,ω-diamine 1,4-bis(3-aminopropyl)piperazine with an association constant K_a= 7.9 x 10^5 M^{-1}. The addition of an excess of $Ba(ClO_4)_2$, surprisingly decreased the amount of bound guest by approximately 50%. This behaviour is attributed to Ba^{2+} ions which bind in the crown ether moiety, thereby causing a conformational change in the molecule and a change in the porphyrin-porphyrin distance, as a result of which the association constant decreases significantly. This behaviour was also used for control of chirality-transfer. The addition of either the *R,R*- or the *S,S*-isomer of a Tröger's base to the zinc porphyrin dimer gave rise to exciton-coupled CD spectra with opposite sign. The addition of a large excess $Ba(ClO_4)_2$ resulted in a significant decrease in the CD signal intensity, however the subsequent addition of achiral 1,10-diaminodecane showed a clear increase in the CD signal again. This behaviour clearly indicated that the achiral ditopic ligand fixed the chirality which was induced by the previously bound chiral ligand. Addition of the barium salt before the addition of the

chiral ditopic ligand hardly resulted in the emergence of any signals in the CD spectrum, indicating suppression of chirality-transfer.

Albrecht-Gary *et al.* have reported that the binding of the pyridine sub-unit containing fullerene derivatives **22** and **23** to the ditopic and polytopic zinc porphyrin receptors **24** and **25** exhibits a positive cooperative binding effect.[34] This binding behaviour was attributed to intramolecular π-π stacking and hydrophobic interactions between the different fullerene sub-units.

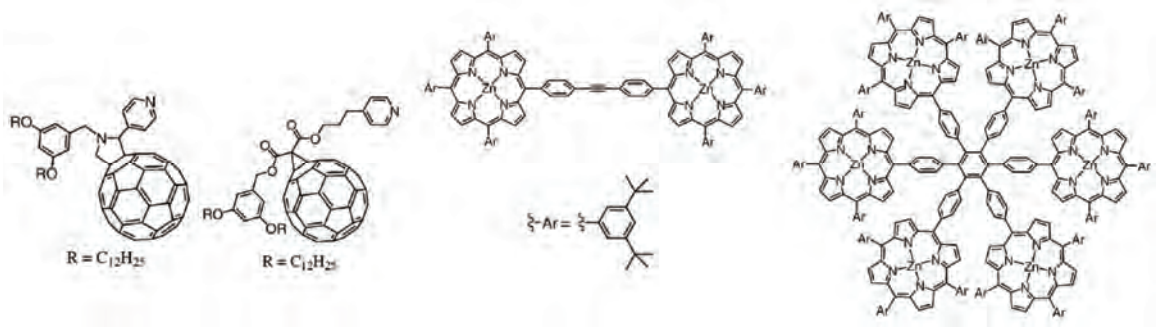

22 **23** **24** **25**

Figure 7. *Fullerene derivatives **22** and **23** with zinc(II) porphyrin receptors **24** and **25** studied by Albrecht-Gary.*

Fused porphyrins

Sato *et al*. have reported cooperative effects in the binding behaviour of a fused porphyrin system with π-electronically coupled binding sites (**26**; Figure 8a).[35] Negative homotropic cooperativity was found for the binding of two molecules of 4,4'-bipyridine, N,N,N',N'-tetramethylhexane-1,6-diamine and C_{60} fullerene. A combination of either of the two nitrogen donor ligands with the fullerene, however, displayed positive heterotropic cooperative behaviour. The strong negative cooperativity in the complexation events of two 4,4'-bipyridine guests enabled stepwise guest inclusion to form 1:1 and 1:2 host-guest complexes selectively.

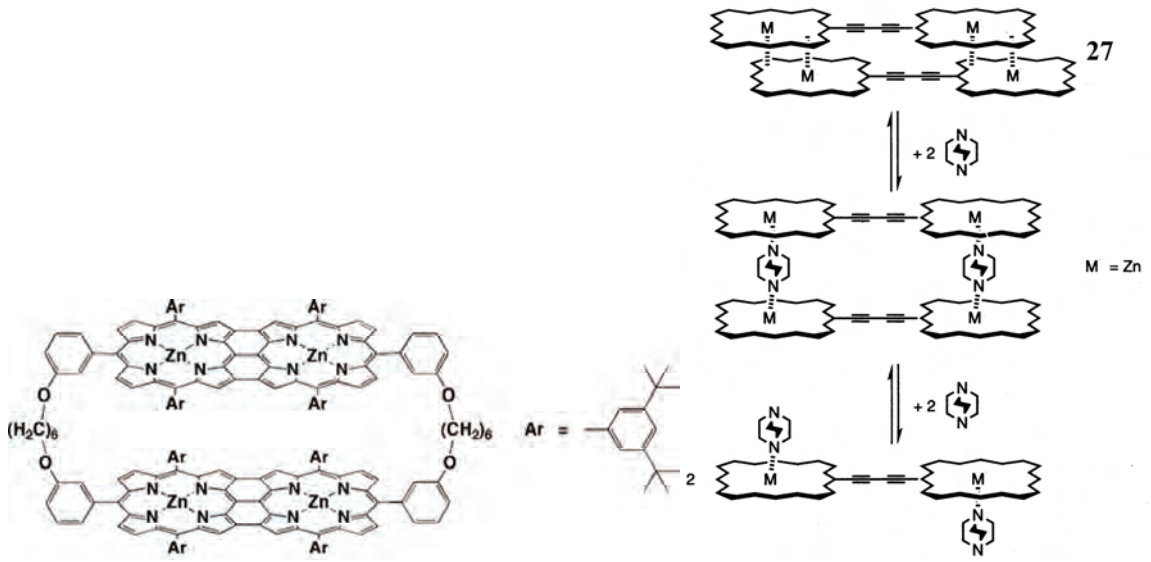

a) **26** b)

Figure 8. *a) Fused zinc porphyrin system studied by Sato. b) Anderson's first* ***dabco*** *ladder assembly.*

Ladders and zippers

The first coordination complexes with a ladder structure were reported by Anderson in 1994. Ladders are prepared from the assembly of covalently linked metalloporphyrin oligomers by coordination to bidentate ligands, for example from a butadieyne-linked zinc porphyrin dimer (**27**) by coordination to **dabco**, 4,4'-bipiperidine and 4,4'-bipyridine (Figure 8b). [36] The addition of an excess of the bidentate ligand leads to the disassembly of the ladder in favour of the formation of complexes in which each ligand is bound to only one porphyrin. Anderson and others have extended the research on this topic, which in 2002 has been reviewed by Baldini and Hunter.[12a]

Since ladder formation is a two-state, all-or-nothing process and ladders containing longer porphyrin oligomers display higher stability than those containing smaller oligomers, Anderson and others concluded that ladder formation was a positive homotropic cooperative process. Ercolani disagreed with this conclusion and stated that chelate effects in cyclisation reactions should not be confused with cooperativity.[7] The application of his model which is based on i) the reference constant for the intermolecular processes; ii) the reference constant for the intramolecular processes; iii) the number of intermolecular and intramolecular interactions required to build the assembly and iv) the symmetry factor of the self-assembly reaction, gave no evidence of cooperative effects.

Some of the later reports of ladder-assemblies in the literature still call this process cooperative and since this debate is still on-going, ladder structures will be discussed further in this review.

Camara-Campos *et al*. have investigated the self-assembly of ladder structures with calorimetric techniques.[37] Positive cooperativity stabilises a system as progressively more interactions are added and the origin of the beneficial free energy can be entropic or enthalpic in origin. The "enthalpic chelate effect", which has been proposed to operate through structural tightening upon ladder formation and increased functional group interactions in a tightly-bound complex, is not evident in the self-assembly process of porphyrin ladder systems. Camara-Campos *et al*. found that the enthalpies of individual interactions in ladder systems are merely additive and not cooperative.

The group of Anderson has reported that optical nonlinearity is amplified by an order of magnitude per macrocycle in porphyrin ladders **28**, self-assembled from zinc porphyrin oligomers and 4,4'-bipyridine (Figure 9a).[38] In addition, they have described a similar system in which the two-photon absorption by oligomer **29** increased 500-fold compared to the parent monomer and by a factor of 11 compared to the corresponding butadiyne-linked dimer.[39] Upon the addition of 4,4'-bipyridine, the oligomers assemble into double-strand ladders, in which the porphyrins are almost perfectly coplanar, resulting in a further two-photon absorption increase by a factor of 1.4 (Figure 9b).

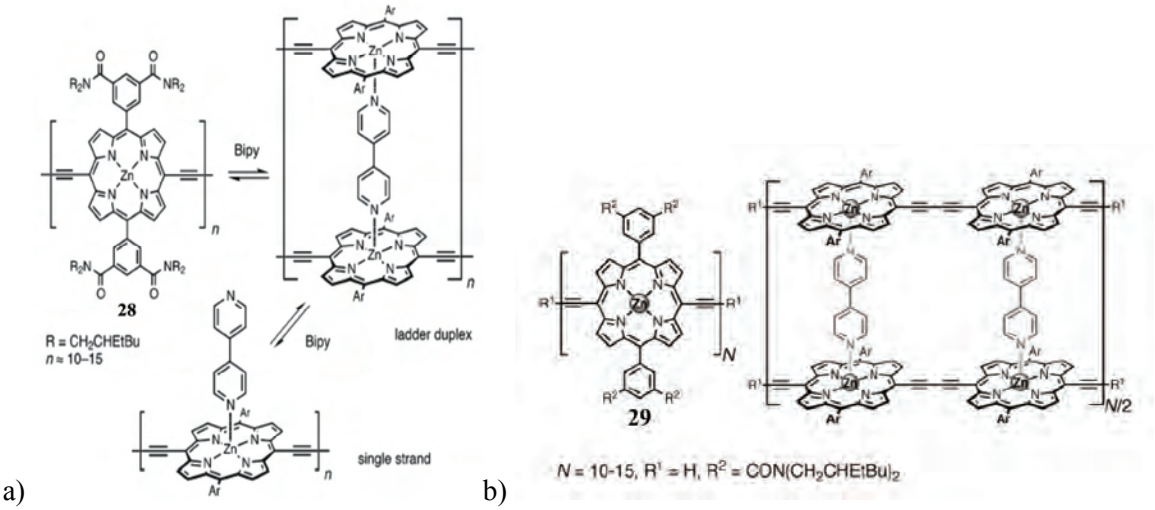

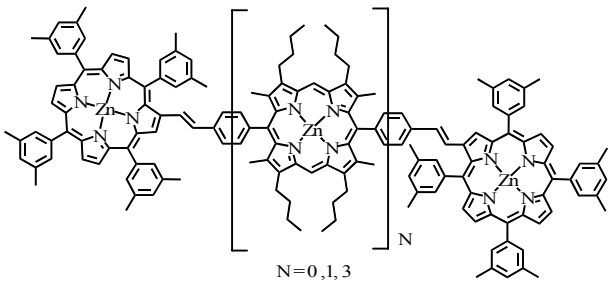

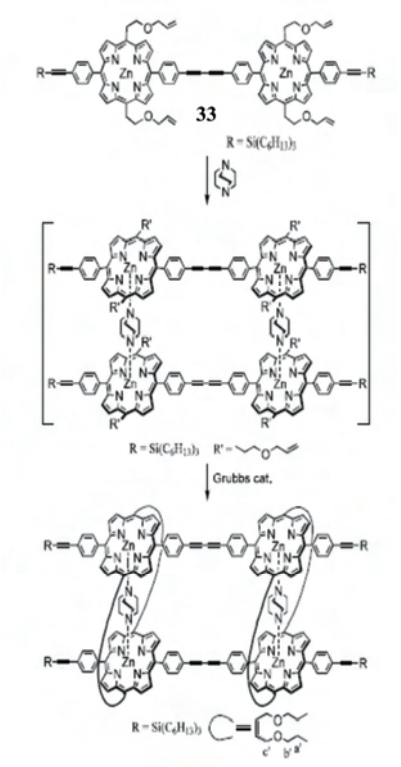

d)

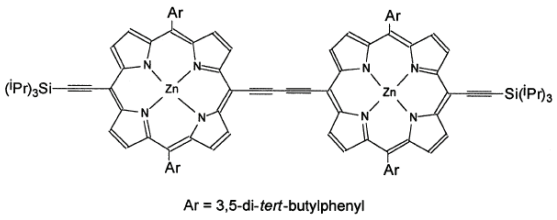

e) **34**

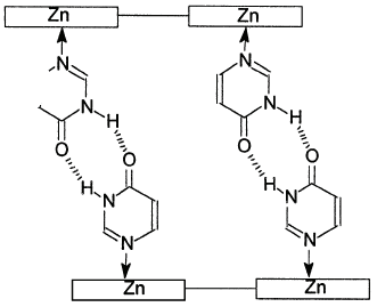

f)

Figure 9. *a) Porphyrin ladders studied by Screen. b) Porphyrin oligomers studied by Drobizhev. c) Porphyrin oligomers studied by Plieger. d) Synthesis of a molecular tube by Ishida. e) Zinc porphyrin dimer* ***34*** *studied by Plater. f) Porphyrin zipper obtained by Plater.*

Plieger *et al.* have investigated the self-assembly of a series of a dimeric, trimeric and pentameric zinc porphyrin systems (**30-32**) with **dabco** and 4,4'-bipyridine (Figure 9c).[40] The porphyrins in these molecules are connected by either β-pyrrolic or *meso*-aryl linkages, whereas Anderson's systems are *meso*-linked. Addition of 4,4'-bipyridine to the oligomers led to the desired sandwich structures, which are, however, in equilibrium with the various components. The higher binding affinity of **dabco** for zinc porphyrins resulted in the all-or-nothing formation of ladder structures. The binding constants for both 4,4'-bipyridine and **dabco** increased upon increasing the number of porphyrins in

the oligomers, however no cooperative effects were evident from the calculated concentrations of half-formed sandwich complexes.
Ishida *et al*. have used a ladder system of two diacetylene-linked zinc porphyrins with terminal alkenes (**33**) dimerised by **dabco** as a scaffold to prepare a molecular tube.[41] Olefin metathesis performed by the first generation Grubbs catalyst transformed the ladder complex into a covalently linked tubular nanostructure (Figure 9d).
In a different approach Plater *et al*. have reported a technique to self-assemble a porphyrin zipper structure, based on porphyrin ladder systems.[42] Instead of a simple ditopic ligand, e.g. **dabco**, 4(3*H*)pyrimidone was used as an axial ligand for the zinc porphyrin dimer **34** (Figure 9e). The resulting structures display both *N*-pyridyl zinc coordination and hydrogen bonding between the ligands, resulting in the formation of a double-stranded hydrogen bonded porphyrin zipper (Figure 9f).

Dendritic porphyrin systems

Dendrimers have been synthesised since the mid-1980's and have found an increasing use in different fields of chemistry and technology.[43] A small number of metalloporphyrin dendrimers that display cooperative behaviour has been reported.
The group of Sanders has synthesised two dendrimers with six zinc porphyrin arms and a zinc porphyrin core (**35**-**36**; Figure 10a).[44] Three **dabco** molecules could be bound between two zinc porphyrins in these dendrimers. Positive homotropic cooperative behaviour was observed, although no precise association constants were obtained. The second association constant of the first **dabco** binding event seemed to be at least 100-fold higher than the first association constant. In addition, the first binding of **dabco** pre-organises the other binding sites, leading to even further allosterically increased association constants.
Shinkai *et al.* have also ventured into the field of dendrimers. They have reported a dendrimer with six zinc porphyrin arms and an aryl core (**37**; Figure 10b).[45] C_{60} fullerenes could be complexed between two zinc porphyrins, a process which was accompanied by a profound positive homotropic cooperative effect, again because of pre-organisation of the second and third binding site by the first binding event. From UV-Vis absorption data they could conclude that cavity B is the acting binding site and not cavity A (see Figure 10b). In later research, this same molecule was used to align a conjugated polymer into a supramolecular bundle (*vide supra*).[25]

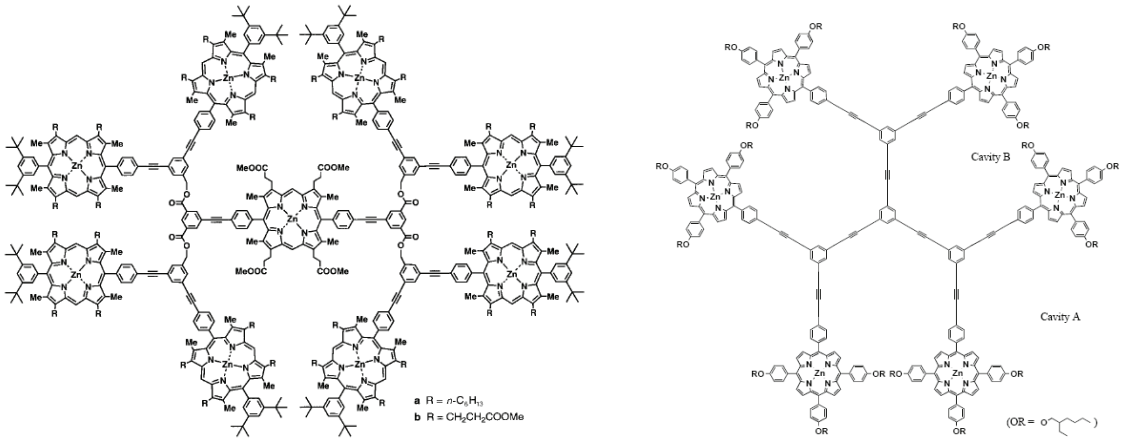

a) **35-36** b) **37**

Figure 10. *a) Porphryin dendrimers studied by Mak. b) Porphyrin dendrimer studied by Shinkai.*

1.5 Architectures without spacers based on ditopic ligands

Sanders *et al*. have reported in two papers that the dimerisation of both Ru(II) and Rh(III) porphyrins by **dabco** and the dimerisation of Rh(III) porphyrins by 4,4'-bipyridine display weak negative cooperative behaviour.[46] In both papers also higher-order porphyrin assemblies were reported, although no cooperative behaviour involving these systems was described.

Iengo *et al*. have reported the synthesis of 2 + 2 molecular squares which were obtained by a reaction of the octahedral Ru(II) complexes *trans*-$RuCl_2(DMSO\text{-}S)_4$), *trans*-$RuCl_2(DMSO\text{-}O)_2(CO)_2$ and *trans*-$RuCl_2(DMSO)_3(CO)$ with a stoichiometric amount of 5,10-bis(4'-pyridyl)-15,20-diphenylporhyrin (Figure 11).[47] One of these molecular squares (**38**) was metallated with zinc and dimerisation with the ditopic ligands 4,4'-bipyridine and two different *trans*-substituted bis-pyridyl porphyrins was investigated. Analogous to ladder structures, dimerisation proved to be an all-or-nothing process, showing no intermediate structures. The authors deem the dimerisation process to be considerably cooperative. While all sandwich-complexes formed discrete supramolecular boxes in solution, it was shown that the system with 4,4'-bipyridine as the ligand adopted a stair like polymeric wire conformation in the solid state, in which the axial ligand binds to the opposite sides of each square.

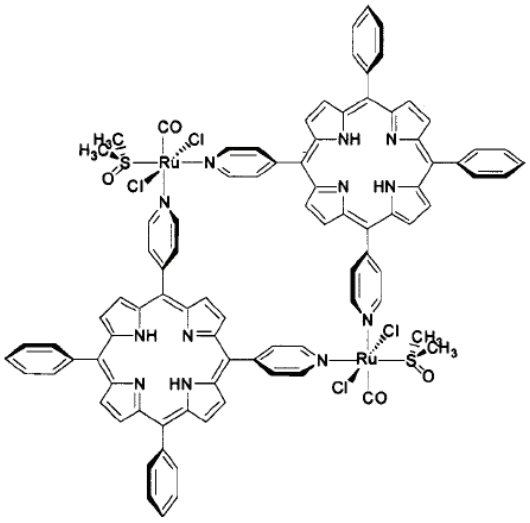

38

Figure 11. *Example of a molecular square studied by Iengo.*

1.6 Crown-porphyrins

As mentioned earlier the majority of allosteric systems were based upon crown ethers. A large number of porphyrin systems with covalently attached crown ether moieties has also been reported in the literature.[9] A few examples of cooperative systems within this category will be discussed here.

Thanabal *et al.* reported the synthesis of a zinc porphyrin with four appended 15-crown-5 units (**39**; Figure 12a).[48] Potassium ions are too big to fit inside one crown ether moiety and they therefore promote dimerisation of the porphyrins in order to achieve sandwich-like complexation. The stability of the 4:2 complex between K^+ and the porphyrins was found to be 10^{23} M^{-5}, which is many orders of magnitude larger than that observed for a single non-sandwich K^+-crown ether interaction (~10^2 M^{-1}). This increased stability was ascribed to cooperative interactions, although no α-values were reported.
Gubelmann *et al.* have reported the synthesis of a strapped porphyrin system, with two [18]-diazocrown receptor moieties incorporated into the strap (Figure 12b).[49] Addition of silver salts leads to fluorescence quenching, both of the free base (**40**) and the zinc porphyrin derivative (**41**). The observed sigmoidal curve obtained upon plotting the fluorescence quenching versus the silver ion concentration indicated that the two subsequent binding events of silver ions into the crown ether receptors occur with positive cooperativity. The average association constant of the two silver ions in **37** was calculated to be K_a= 6.1 x 10^{11} M^{-1}, whereas the association constant of Ag^+ for a simple reference [18]-diazocrown ether molecule was K_a= 8.7 x 10^7 M^{-1}.

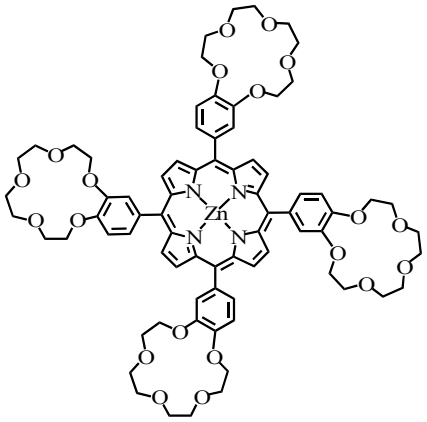

a) **39**

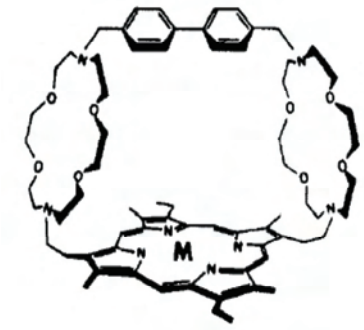

b)

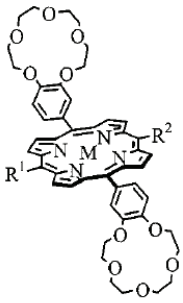

c) **42**

Figure 12. *a) Porphyrin system with four crown ether moieties studied by Thanabal. b) Porphyrin bis-crown ether system studied by Gubelmann. c) Porphyrin system with two crown ether moieties studied by Shinmori.*

The dimerisation behaviour of crown ether appended porphyrins has been further investigated by Shinmori *et al*. They reported that a zinc porphyrin with only two benzocrown ether moieties but lacking the other two *meso*-phenyl substituents (**42**), dimerises upon the addition of potassium salts, with higher stability constants than reported for the tetra-crown ether system described by Thanabal *et al*., calculated per binding site ($\approx 10^9$ M^{-1} compared to $\approx 10^6$ M^{-1}; Figure 12c).[50] This stronger binding was attributed to enhanced π–π interactions between the porphyrins, which was supported by NMR data. The addition of potassium salts to the analogous di-crown ether system with *meso*-phenyl substituents did not result in any significant changes in the UV-vis and fluorescence spectra, indicating low levels of dimerisation, probably due to steric hindrance.

The groups of Nolte and Rowan have reported the synthesis of a U-shaped receptor molecule (**43**) that includes a porphyrin, a crown ether and a glycoluril moiety, which can strongly bind viologen derivatives (**V**) inside the cavity (Figure 13a). [51] The zinc derivative of this "porphyrin clip" can coordinate nitrogen donor ligands, either on the outside of the cavity when the ligand is sterically too demanding to fit inside, or on the

inside of the cavity in which case the association constant is considerably increased because of additional stabilising interactions. Using a combination of these two types of ligands results in positive heterotropic allosteric binding behaviour: coordination of 4-*tert*-butyl-pyridine (**tbpy**) on the outside of the clip increases the association constant of viologens on the inside, and *vice versa* (Figure 13b). This behaviour has allowed the construction of several multicomponent complexes by allosteric self-assembly. In the case of the self-assembly of four zinc porphyrin clips around a central tetrakis(*meso*-4-pyridyl)porphyrin, the ratio of the 4:1 complex is greatly increased upon the binding of viologen molecules inside the cavities of the host (Figure 13c).[52] The ratio of clips in the 4:1 complex at 1 mM concentration was increased from 1% to 32% due to allosteric magnification. The manganese(III) derivative of **43** has been applied as an oxygenation catalyst. Upon the coordination of 4-*tert*-butylpyridine this catalyst shows remarkable stability during the epoxidation reaction of olefins.[53] In addition, a rotaxane was synthesised consisting of manganese clips threaded onto a polybutadiene polymer endcapped with bulky stoppers (Figure 13d). Using iodosylbenzene as oxygen donor the polymer was fully epoxidised.[54] The kinetics and thermodynamics of the treading and dethreading process of polymers through the cavity of **43** was investigated by studying its complexation with a series of end-functionalized polymers of different lengths with a viologen end-group (Figure 13e).[55] The system was designed in such a way that complexation was only observed if the host had travelled all the way across the polymer. Detailed kinetic investigations using fluorescence spectroscopy have revealed that the barrier for this process is length dependent.

Highly negative allosteric binding was reported for a double cavity porphyrin system (**44** Figure 13f).[56] This host molecule has the ability to bind two dimethyl viologen molecules, but the association constant for the second binding (5×10^4 M^{-1}) is considerably lower than for the first binding event (7×10^7 M^{-1}; $\alpha = 0.0029$). A combination of the NMR data with computational modelling indicated that this was not due to electronic repulsion between the two guests, but because of conformational changes in the host molecule. It was shown that one of the cavities is 0.6 Å wider than the other and this is the cavity that is occupied by the first viologen guest. This binding is accompanied by a simultaneous pinching of the second cavity, which thereby decreases its affinity for the second viologen guest.

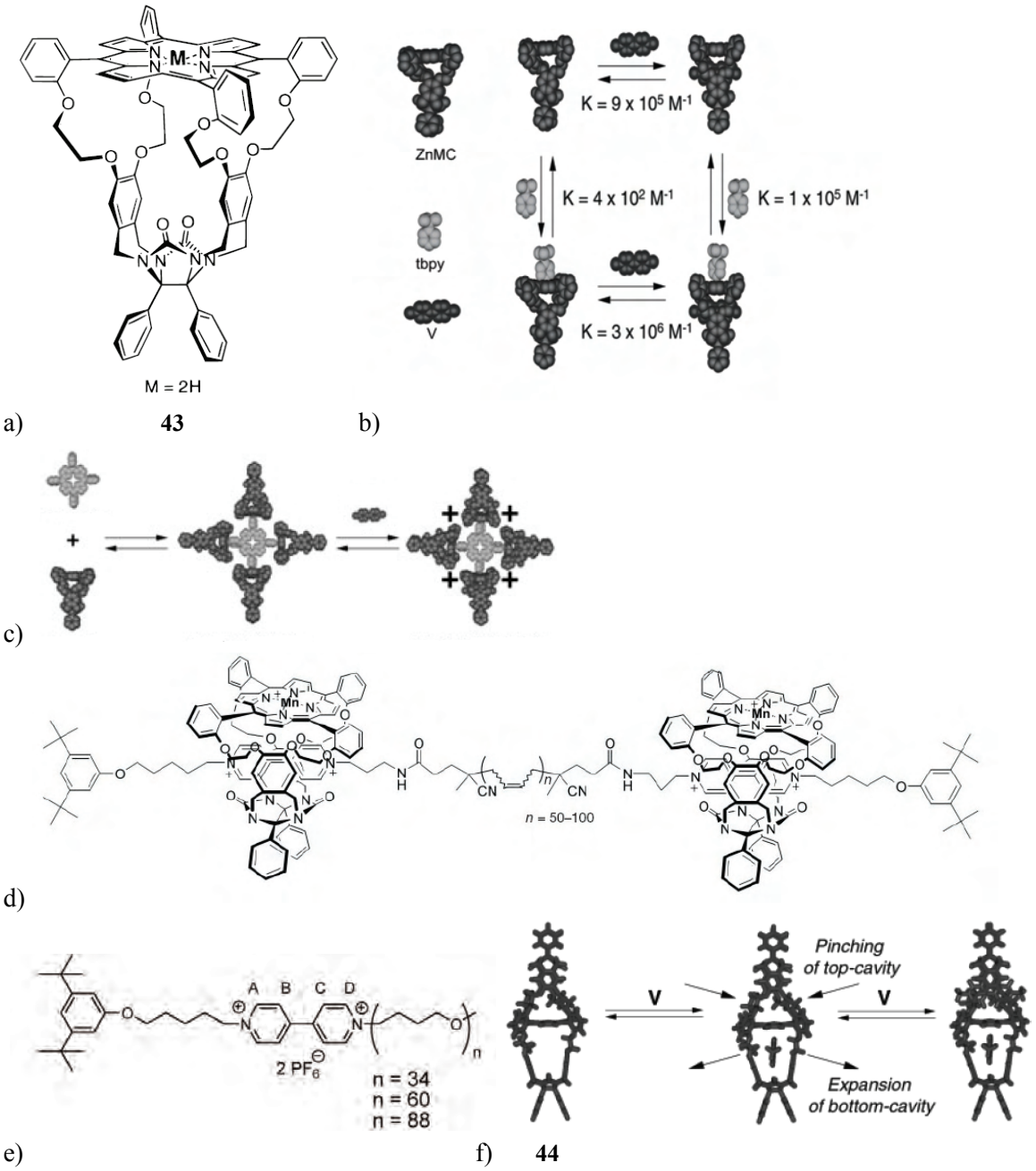

a) **43** b)

c)

d)

e) f) **44**

Figure 13. *a) Porphyrin clip studied by Rowan and Nolte. b) Allosteric binding behaviour of the zinc clip. c) Self-assembly of four zinc clips around a tetra-pyridyl porphyrin. The + signs indicate the positive cooperativity. d) [3]-Rotaxane constructed by Rowan and Nolte. e) Polymers used to study the threading and dethreading of polymers though the cavity of* ***43****. f) Molecular modelling figures of the complexes formed upon viologen binding in the double cavity porphyrin system* ***40****.*

1.7 Scope of this thesis

In this thesis porphyrin host molecules are used both as catalysts and as building blocks in the construction of multi-component self-assembled systems. In chapter 2 the synthesis of several porphyrin host molecules containing two cavities is described. Chapter 3 describes the catalytic properties of the manganese derivative of one of these hosts. This manganese "double clip" appears to be exceptionally stable in the epoxidation of simple alkenes, such as styrene, *cis*-stilbene and *trans*-stilbene. Self-assembly studies of allosteric complexes based on the zinc derivates of mono- and double-cavity-containing porphyrin hosts with three different bifunctional guest molecules are reported in chapter 4. These bifunctional guests, containing pyridine and/or viologen moieties, were synthesised in order to obtain supramolecular polymers upon their binding with the hosts. Instead of polymeric assemblies, however, discrete low-order assemblies were obtained. Chapter 5 describes the self-assembly of complexes in which mono-substituted bipyridinium guests are complexed inside the cavity of a zinc porphyrin host with the aim to construct photosynthetic antenna mimics. Photophysical studies have been performed to investigate the electron transfer process between the donor porphyrin host and a guest in which the mono-substituted bipyridinium moiety is attached to a gold(III) porphyrin acceptor. The synthesis of a zinc porphyrin host that is functionalised with four hydroxy groups positioned on top of the meso phenyl rings of the porphyrin is described in chapter 6. This host was designed with the objective to form strong dimeric complexes with a neighbouring host upon the addition of the bidentate ligand **dabco**. With the aim to construct even more complex self-assembled architectures by allosteric interactions, the self-assembly of a complex consisting of a central tetra-viologen porphyrin guest and four hydroxy-functionalised clips is discussed, together with the dimerisation of this complex upon the addition of **dabco** to give a 14-component self-assembled system. Finally, chapter 7 describes the first attempts to synthesise a double-cavity, double-porphyrin containing host molecule.

References

1. A. Klug, *Angew. Chem. Int. Ed. Engl.*, 1983, **22**, 565-582.
2. a) G.K. Ackers, M.L. Doyle, D. Myers, M.A. Daugherty, *Science*, 1992, **255**, 54-63.
   b) Y.W. Huang, M.L. Doyle, G.K. Ackers, *Biophys. J.*, 1996, **71**, 2094-2105.
   c) M.L. Johnson, *Methods Enzym.*, 2000, **323**, 124-155.
3. J.G. Harman, *Biochim. Biophys. Acta*, 2001, **1547**, 1-17.
4. a) K.J. Laidler, P.S. Bunting, in *The Chemical Kinetics of Enzyme Action*, Clarendon Press, Oxford, 2nd edition, 1973.
   b) J. Monod, J.-P. Changeux, F. Jacob, *J. Mol. Biol.*, 1963, **6**, 306-329.

c) J. Monod, J. Wyman, J.-P. Changeux, *J. Mol. Biol.*, 1965, **12**, 88-118.
d) B. Perlmutter-Hayman, *Acc. Chem. Res.*, 1986, **19**, 90-96.
e) K.A. Connors, in *Binding Constants*, John Wiley & Sons, New York, 1987.
f) M. Campbell, *Biochemistry*, Saunders College Publishing, Philadelphia, 2nd ed., 1995.
g) S. Shinkai, M. Ikeda, A. Sugasaki, M. Takeuchi, *Acc. Chem. Res.*, 2001, **34**, 494-503.
h) M. Takeuchi, M. Ikeda, A. Sugasaki, S. Shinkai, *Acc. Chem. Res.*, 2001, **34**, 865-873.
5. a) A.J. Kirby, *Adv. Phys. Org. Chem.*, 1980, **17**, 183-278.
b) L. Mandolini, *Adv. Phys. Org. Chem.*, 1986, **22**, 1-111.
6. G. Ercolani, *J. Phys. Chem. B*, 2003, **107**, 5052-5057.
7. G. Ercolani, *J. Am. Chem. Soc.*, 2003, **125**, 16097-16103.
8. I. Tabushi, S. Kugiyama, *Biomat., Art. Cells, Art. Org.*, 1988, **16**, 321-329.
9. a) T. Nabeshima, *Coord. Chem. Rev.*, 1996, **148**, 151-169.
b) Y. Kubo, Y. Ishii, *J. Nanosci. Nanotechno.*, 2006, **6**, 1489-1509.
10. P. Even, B. Boitrel, *Coord. Chem. Rev.*, 2006, **250**, 519-541.
11. L. Kovbasyuk, R. Krämer, *Chem. Rev.*, 2004, **104**, 3161-3187.
12. a) L. Baldini, C.A. Hunter, *Adv. Inorg. Chem.*, 2002, **53**, 213-259.
b) L. Flamigni, A.M. Talarico, B. Ventura, *J. Porphyrins Phthalocyanines*, 2003, **7**, 318-327.
c) H. Imahori, *J. Phys. Chem. B*, 2004, **108**, 6130-6143.
d) C.M. Drain, I. Goldberg, I. Sylvain, A. Falber, *Top. Curr. Chem.*, 2005, **245**, 55-88.
e) J.A.A.W. Elemans, R. van Hameren, R.J.M. Nolte, A.E. Rowan, *Adv. Mater.*, 2006, **18**, 1251-1266.
f) K. Ogawa, Y. Kobuke, *J. Photochem. Photobiol, C: Photochem. Rev.*, 2006, **7**, 1-16.
g) C.M. Drain, G. Smeureanu, S. Patel, X. Gong, J. Garno, J. Arijeloye, *New J. Chem.*, 2006, **30**, 1834-1843.
h) D. Bonifazi, A. Kiebele, M. Stohr, F. Cheng, T. Jung, F. Diederich, H. Spillmann, *Adv. Funct. Mater.*, 2007, **17**, 1051-1062.
i) M.O. Senge, M. Fazekas, E.G.A. Notaras, W.J. Blau, M. Zawadzka, O.B. Locos, E.M.N. Mhuircheartaigh, *Adv. Mater.*, 2007, **19**, 2737-2774.
13. B.A. Armitage, *Mol. Supramol. Photochem.*, 2006, **14**, 255-287.
14. J.P. Collman, J.I. Brauman, E. Rose, K. Suslick, *Proc. Natl. Acad. Sci. USA*, 1978, **75**, 1052-1055.
15. T. Fournier, Z. Liu, T.-H. Tran-Thi, D. Houde, N. Brasseur, C. La Madeleine, R. Langlois, J.E. van Lier, D. Lexa, *J. Phys. Chem. A*, 1999, **103**, 1179-1186.
16. a) C.A. Hunter, M.N. Meah, J.K.M. Sanders, *J. Am. Chem. Soc.*, 1990, **112**, 5773-5780.
b) H.L. Anderson, C.A. Hunter, M.N. Meah, J.K.M. Sanders, *J. Am. Chem. Soc.*, 1990, **112**, 5780-5789.
17. T. Ema, S. Misawa, S. Nemugaki, T. Sakai, M. Utaka, *Chem. Lett.*, 1997, 487-488.
18. a) S. Shinkai, M. Ikeda, A. Sugasaki, M. Takeuchi, *Acc. Chem. Res.*, 2001, **34**, 494-503.
b) M. Takeuchi, M. Ikeda, A. Sugasaki, S. Shinkai, *Acc. Chem. Res.*, 2001, **34**, 865-873.
c) T. Ikeda, O. Hirata, M. Takeuchi, S. Shinkai, *J. Am. Chem. Soc.*, 2006, **128**, 16008-16009.
19. G. Ercolani, *Org. Lett.*, 2005, **7,** 803-805.
20. M. Kawagucki, A. Ikead, S. Shinkai, *Tetrahedron Lett.*, 2001, **42**, 3725-3728.

21. Y. Kubo, M. Ikeda, A. Sugasaki, M. Takeuchi, S. Shinkai, *Tetrahedron Lett.*, 2001, **42**, 7435-7438.
22. a) B. Perlmutter-Hayman, *Acc. Chem. Res.*, 1986, **19**, 90-96.
    b) K.A. Connors, in *Binding Constants*, John Wiley & Sons, New York, 1987.
23. R. Wakabayashi, Y. Kubo, O. Hirata, M. Takeuchi, S. Shinkai, *Chem. Commun.*, 2005, 5742-5744.
24. Y. Kubo, A. Sugasaki, M. Ikeda, K. Sugiyasu, K. Sonoda, A. Ikeda, M. Takeuchi, S. Shinkai, *Org. Lett.*, 2002, **4**, 925-928.
25. Y. Kubo, Y. Kitada, R. Wakabayashi, T. Kishida, M. Ayabe, K. Kaneko, M. Takeuchi, S. Shinkai, *Angew. Chem. Int. Ed.*, 2006, **45**, 1548-1553.
26. C.A. Hunter, R. Tregonning, *Tetrahedron*, 2002, **58**, 691-697.
27. L. Baldini, P. Ballester, A. Casnati, R.M. Gomila, C.A. Hunter, F. Sansone, R. Ungaro, *J. Am. Chem. Soc.*, 2003, **125**, 14181-14189.
28. P. Ballester, A. Costa, A. Castilla, P.M. Deyà, A. Frontera, R.M. Gomila, C.A. Hunter, *Chem. Eur. J.*, 2005, **11**, 2196-2206.
29. P. Ballester, A.I. Oliva, A. Costa, P.M. Deyà, A. Frontera, R.M. Gomila, C.A. Hunter, *J. Am. Chem. Soc.*, 2006, **128**, 5560-5569.
30. M. Dudič, P. Lhoták, H. Petříčková, I. Stibor, K. Lang, J. Sýkora, *Tetrahedron*, 2003, **59**, 2409-2415.
31. K.E. Splan, C.L. Stern, J.T. Hupp, *Inorg. Chim. Acta*, 2004, **357**, 4005-4014.
32. C.-C. You, F. Würthner, *Org. Lett.*, 2004, **6**, 2401-2404.
33. a) Y. Kubo, Y. Murai, J. Yamanaka, S. Tokita, Y. Ishimaru, *Tetrahedron Lett.*, 1999, **40**, 6019-6023.
    b) Y. Kubo, T. Ohno, J. Yamanaka, S. Tokita, T. Iida, Y. Ishimaru, *J. Am. Chem. Soc.*, 2001, **123**, 12700-12701.
34. A. Trabolsi, M. Maxence, J.L. Delgado, F. Ajamaa, M. Elhabiri, N. Solladie, J.-F. Nierengarten, A.-M. Albrecht-Gary, *New J. Chem.*, 2008, **32**, 159-165.
35. a) H. Sato, K. Tashiro, H. Shinmori, A. Osuka, Y. Murata, K. Komatsu, T. Aida, *J. Am. Chem. Soc.*, 2005, **127**, 13086-13087.
    b) H. Sato, K. Tashiro, H. Shinmori, A. Osuka, T. Aida, *Chem. Commun.*, 2005, 2324-2326.
36. H.L. Anderson, *Inorg. Chem.*, 1994, **33**, 972-981.
37. A. Camara-Campos, C.A. Hunter, S. Tomas, *Proc. Natl. Acad. Sci. USA*, 2006, **103**, 3034-3038.
38. a) T.E.O. Screen, J.R.G. Thorne, R.G. Denning, D.G. Bucknall, H.L. Anderson, *J. Am. Chem. Soc.*, 2002, **124**, 9712-9713.
    b) T.E.O. Screen, J.R.G. Thorne, R.G. Denning, D.G. Bucknall, H.L. Anderson, *J. Mater. Chem.*, 2003, **13**, 2796-2808.
39. M. Drobizhev, Y. Stepanenko, A. Rebane, C.J. Wilson, T.E.O. Screen, H.L. Anderson, *J. Am. Chem. Soc.*, 2006, **128**, 12432-12433.
40. P.G. Plieger, A.K. Burrell, S.B. Hall, D.L. Officer, *J. Inclusion Phenom. Macrocyclic Chem.*, 2005, **53**, 143-148.
41. T. Ishida, Y. Morisaki, Y. Chujo, *Tetrahedron Lett.*, 2006, **47**, 5265-5268.

42. J.H. Plater, S. Aiken, G. Bourhill, *Tetrahedron Lett.*, 2001, **42**, 2225-2229.
43. B. Helms, E.W. Meijer, *Science*, 2006, **313**, 929-930.
44. C.C. Mak, N. Bampos, J.K.M. Sanders, *Angew. Chem. Int. Ed.*, 1998, **37**, 3020-3023.
45. M. Ayabe, A. Ikeda, Y. Kubo, M. Takeuchi, S. Shinkai, *Angew. Chem. Int. Ed.*, 2002, **41**, 2790-2792.
46. a) C.C. Mak, N. Bampos, J.K.M. Sanders, *Chem. Commun.*, 1999, 1085-1086.
    b) J.E. Redman, N. Feeder, S. J. Teat, J.K.M. Sanders, *Inorg. Chem.*, 2001, **40**, 2486-2499.
47. E. Iengo, E. Zangrando, R. Minatel, E. Alessio, *J. Am. Chem. Soc.*, 2002, **124**, 1003-1013.
48. V. Thanabal, V. Krishnan, *J. Am. Chem. Soc.*, 1982, **104**, 3643-3650.
49. M. Gubelmann, A. Harriman, J.-M. Lehn, J.L. Sessler, *J. Phys. Chem.*, 1990, **94**, 308-315.
50. H. Shinmori, Y. Yasuda, A. Osuka, *Eur. J. Org. Chem.*, 2002, 1197-1205.
51. a) A.E. Rowan, P.P.M. Aarts, K.W.M. Koutstaal, *Chem. Commun.*, 1998, 611-612.
    b) J.A.A.W. Elemans, M.B. Claase, P.P.M. Aarts, A.E. Rowan, A.P.H.J. Schenning, R.J.M. Nolte, *J. Org. Chem.*, 1999, **64**, 7009-7016.
52. P. Thordarson, R.G.E. Coumans, J.A.A.W. Elemans, P.J. Thomassen, J. Visser, A.E. Rowan, R.J.M. Nolte, *Angew. Chem. Int. Ed.*, 2004, **43**, 4755-4759.
53. a) J.A.A.W. Elemans, E.J.A. Bijsterveld, A.E. Rowan, R.J.M. Nolte, *Chem. Commun.*, 2000, 2443-2444.
    b) J.A.A.W Elemans, E.J.A. Bijsterveld, A.E.Rowan, R.J.M. Nolte, *Eur. J. Org. Chem.*, 2007, 751-757.
54. P. Thordarson, E.J.A. Bijsterveld, A.E. Rowan, R.J.M. Nolte, *Nature*, 2003, **424**, 915-918.
55. R.G.E. Coumans, J.A.A.W. Elemans, R.J.M. Nolte, A.E. Rowan, *Proc. Natl. Acad. Sci. USA*, 2006, **103**, 19647-19651.
56. P. Thordarson, E.J.A. Bijsterveld, J.A.A.W. Elemans, P. Kasák, R.J.M. Nolte, A.E. Rowan, *J. Am. Chem. Soc.*, 2003, **125**, 1186-1187.

Chapter 2. Synthesis and binding properties of double-cavity porphyrin molecules

2.1 Introduction

In earlier research in our group a number of cavity-appended porphyrin host systems has been developed that were shown to display allosteric binding behaviour.[1,2] The most extensively studied host molecule was the mono-cavity-appended zinc porphyrin **ZnMC**, which is depicted in Figure 1a.[1] This "porphyrin clip" was found to bind viologen derivatives (**V**) extremely strongly inside its cavity and was also able to coordinate nitrogen donor ligands, either on the inside or on the outside of the cavity. The latter binding mode occurs when the ligand is sterically too demanding to fit inside the cavity.

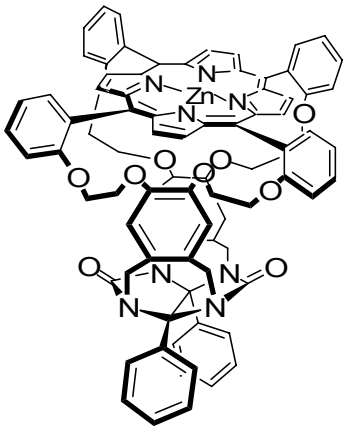

a)

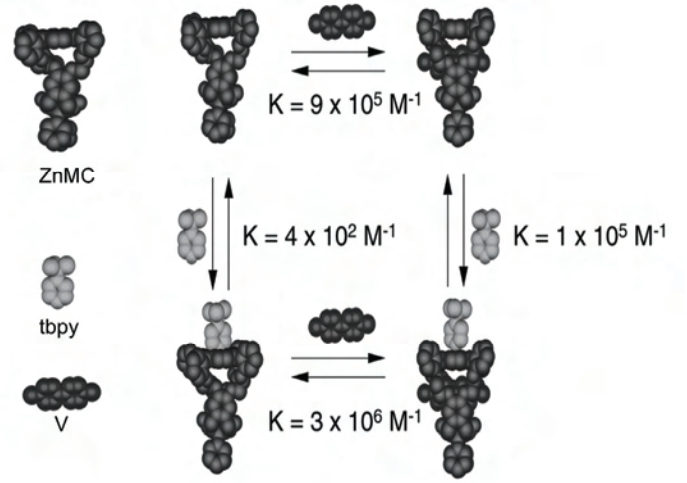

b)

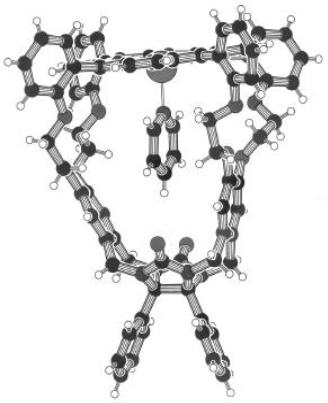

c)

Figure 1. *a) Structure of porphyrin host* ***ZnMC****. b) Allosteric binding behaviour of* ***ZnMC*** *(V = PF_6 salt of 4,4'-dimethyl-viologen). c) X-ray crystal structure of* ***ZnMC*** *with a pyridine molecule bound in its cavity.*

Using a combination of this ligand and the viologen guest a positive heterotropic allosteric binding behaviour was observed; coordination of 4-*tert*-butyl-pyridine (**tbpy**) on the outside of the clip was found to increase the association constant of viologens on the inside, and *vice versa* (Figure 1b). One origin of this allosteric behaviour was thought to be the relocation of the zinc ion out of the porphyrin plane towards the external axial ligand, e.g. **tbpy**. This relocation increases the binding because it a) diminishes the repulsive electrostatic forces between the positively charged zinc ion and **V** and b) prevents competitive solvent molecules from binding in the cavity, creating more room in the host cavity. The reverse relocation effect in which the zinc ion is pulled into the cavity upon the binding of a pyridine (**py**) guest inside the host's cavity, can be clearly observed from the crystal structure of the guest complex in Figure 1c.

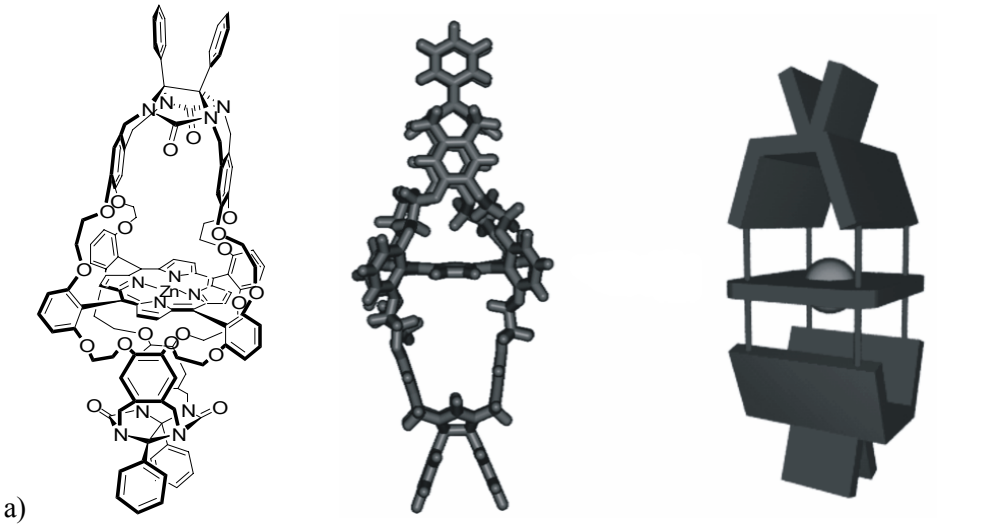

Figure 2. *a) ZnDC, its structure calculated by molecular modelling, and its schematic representation. b) Negative homotropic allosteric binding behaviour of DC (Viologen = PF_6 salt of 4,4'-dimethyl-viologen).*

In addition to the **ZnMC**, the double-cavity porphyrin molecule doubleclip (**DC)** has been previously reported (Figure 2a).[2] This host was observed to exhibit a negative homotropic allosteric binding behaviour upon the simultaneous binding of two viologen

guests (Figure 2b). From NMR studies and computational modelling it was concluded that the considerable decrease in the association constant of the second viologen guest, when compared to that of the first viologen guest, was due to allosteric conformational changes in the host molecule (Chapter 1). It was postulated from modelling studies that one of the cavities is 0.6 Å wider than the other and it is within this cavity that the first viologen guest binds. This binding is accompanied by an induced fit which causes a pinching of the connected second cavity. This constricted second cavity has a much reduced affinity for the second viologen guest.

One of the major problems in studying this intriguing double-cavity molecule is its difficult synthesis. The overall yield in the synthesis of the double-cavity host molecule **DC** has been reported to be extremely low (<1%).[2] In order to increase this yield, its synthesis route is further explored in this chapter. A number of the various reaction products in the synthesis of **DC** has been identified for the first time. In addition, the binding behaviour of the zinc derivative of **DC**, **ZnDC**, towards the simultaneous binding of a viologen (**V**) and a pyridine (**py**) guests has been studied.

2.2 Synthesis of double-cavity porphyrin molecules

In the previously reported synthesis of **DC** two separate routes to obtain this host molecule were described (Figure 3a).[2] The first was a one-step reaction in DMF between the octa-hydroxy porphyrin **1** and two equivalents of tetra-tosylate molecule **2** (route B in Figure 3a). A second alternative route involved the addition of one equivalent of **2** to **1** in acetonitrile to yield an intermediate tetra-hydroxy mono-cavity-appended porphyrin clip (isomer I in Figure 3b). This isomer could then be further reacted with an excess of **2** in DMF to yield **DC** (route A in Figure 3a). In both approaches the formation of two double-cavity porphyrin isomers were obtained in a 10:1 ratio: isomer III (**DC**) and isomer IV (Figure 3c). The low yields obtained in the synthesis of **DC** as compared to **MC** suggest that the final cyclisation is extremely difficult due to significantly more strain in the former molecule. The unequal product ratio of isomer III and isomer IV typically has its origin in the *C*2-symmetry of the cavity in isomer I, which results in the reaction with a second molecule of **2** being energetically more favorable for one orientation than for the other.

a)

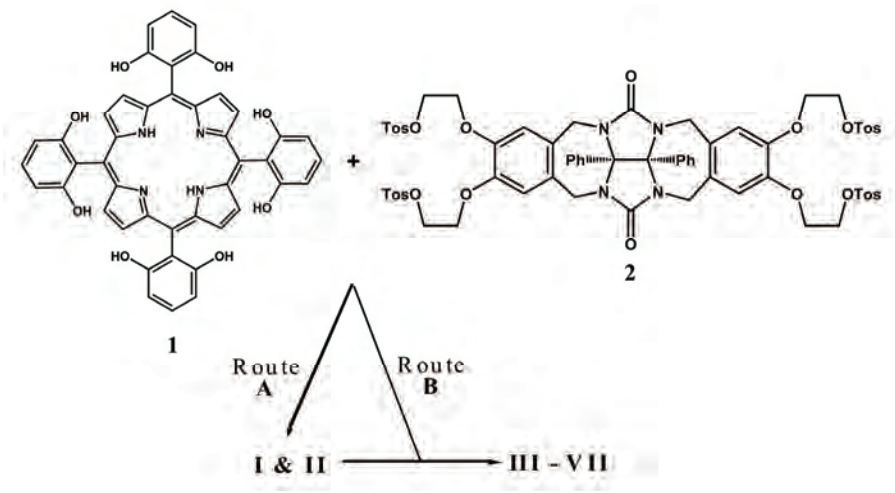

b)

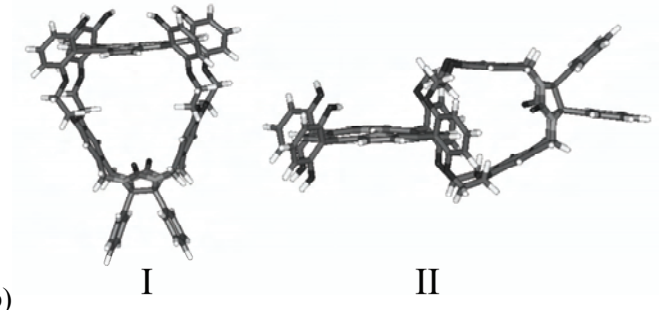

c)

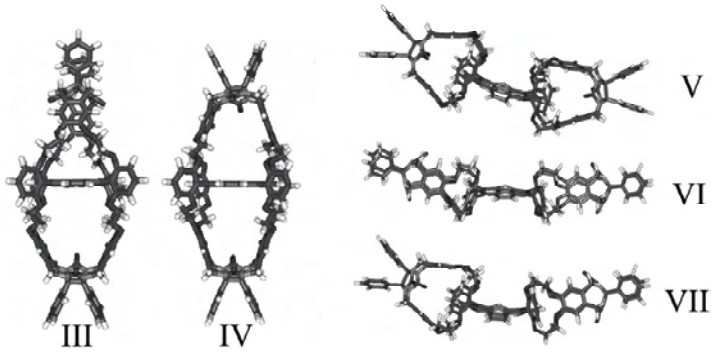

Figure 3. *a) Synthesis of mono- and double-cavity porphyrins. Route A, step 1: K_2CO_3/CH_3CN/ reflux, 16h, ratio **1**:**2** = 1:1; step 2: K_2CO_3/DMF/90°C, 16h, excess **2**; route B: K_2CO_3/DMF/90°C, 16h, ratio **1**:**2** = 1:2. b) The two tetra-hydroxy mono-cavity porphyrin clip isomers formed from the reaction between one molecule **2** and one porphyrin **1**. c) The five different double-cavity porphyrin isomers formed from the reaction between two molecules **2** and one porphyrin **1** or one molecule **2** with one tetra-hydroxy mono-cavity porphyrin.*

During the synthesis of **DC** an additional double-cavity porphyrin isomer could also be isolated, which had an identical mass to that of **DC**, as was demonstrated by MALDI-TOF spectroscopy (isomer V; Figure 3c). In addition, an intermediate of this isomer, isomer II of the tetra-hydroxy mono-cavity porphyrin, was also isolated (Figure 3b). In these isomers (II and V) the porphyrin plane is not orthogonal to the cavity of the clip,

but attached in a "sideways" geometry. This geometry is confirmed by the observation that the signals of the β-pyrrolic protons of these isomers positioned inside the cavity exhibit a significant upfield shift (Δδ≈ -0.8 ppm) when compared to those situated on the outside (Figure 4b and 5c).

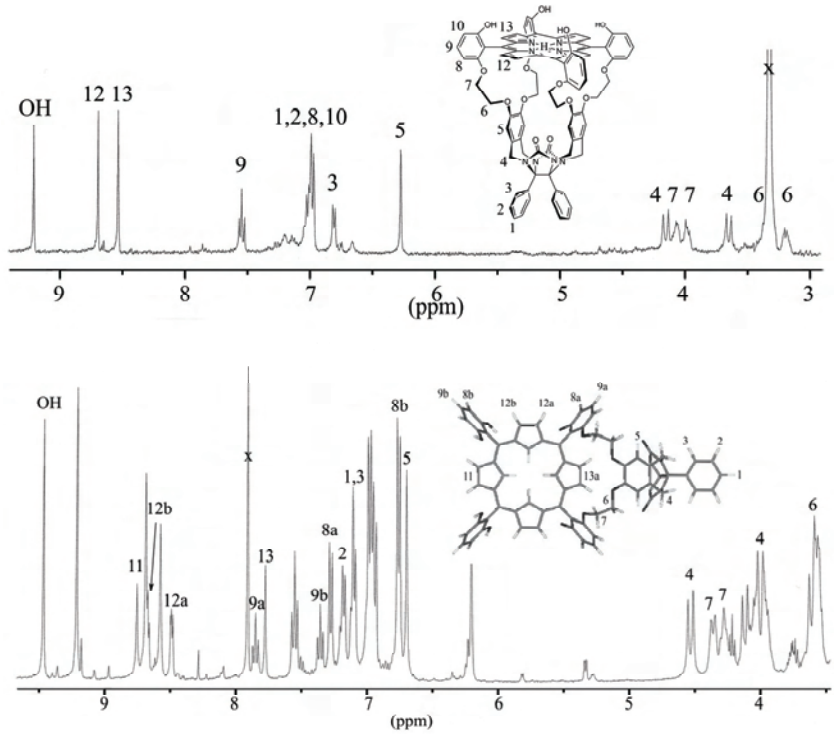

Figure 4. *a) Downfield region of the ^{1}H-NMR spectrum (400.18 MHz, 298K, DMSO-d_6) of tetra-hydroxy mono-cavity porphyrin isomer I. b) Idem, of a mixture of tetra-hydroxy mono-cavity porphyrin isomers I and II with proton assignments for isomer II.*

A ^{1}H NMR spectrum containing a mixture of all the reaction products (all with a mass equal that of **DC)**, obtained *via* column chromatography, showed trace amounts of two other species, which we tentatively identify as isomers VI and VII (Figure 3c). These additional isomers could not be isolated from the mixture due to their low yield. The formation of the different isomers appeared to be kinetically determined, since the ratios in which they were formed varied in every batch of double-cavity porphyrin molecules that was synthesised.

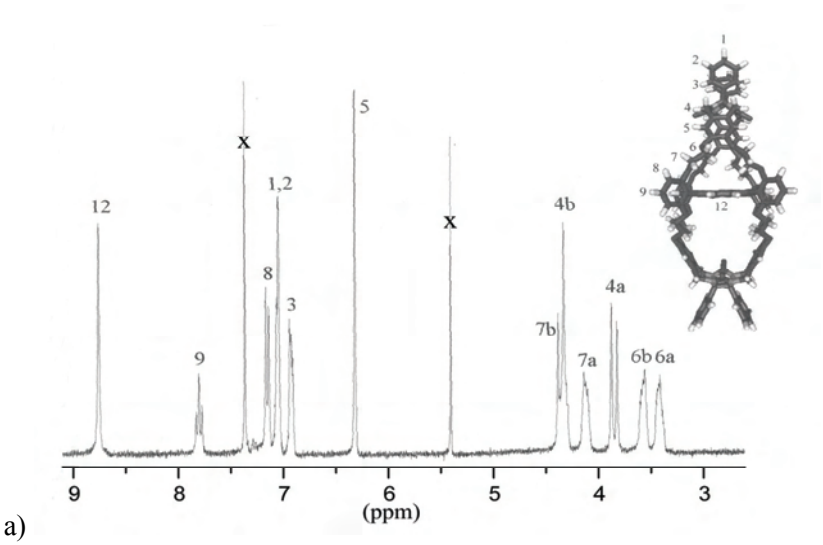

Figure 5. *a) Downfield region of the ^{1}H-NMR spectrum (400.18 MHz, 298K, $CDCl_3$) of* ***DC****. b) Idem, of double-cavity porphyrin isomer IV. The β-pyrrole protons are designated 12 and 13. For numbering of the other protons see Figure 5a. c) Idem, of double-cavity porphyrin isomer V. The β-pyrrole protons are designated 12 and 13. For numbering of the other protons see Figure 5a.*

Since the effective yield of **DC** (isomer III) was very low (<1%), several attempts were undertaken to optimise its synthesis. No significant improvement, however, could be made upon changes in a) the reaction time (0.5-3 days), b) the solvent (acetonitrile or DMF) or c) the base (K_2CO_3 or Cs_2CO_3). When a 1:1 mixture of clip molecule **2** and porphyrin **1** was employed, both mono-cavity and double-cavity porphyrins were formed in both the solvents CH_3CN and DMF. When the ratio of clip molecule **2** to porphyrin **1** was maintained at 1:1 the number of oligomeric side products was reduced when compared to a 2:1 mixture of **2** and **1**. The decrease in side products resulted in an increase in the overall yield of **DC** and also the yield of the mono-cavity isomer I. The isomer I could be reacted further with clip molecule **2** to form **DC** and isomer IV. The different isomers for both mono-cavity and double-cavity porphyrins were always formed in spite of whatever synthetic route was followed. Refluxing a 1:1 acetonitrile solution of clip molecule **2** and porphyrin **1** with an excess of K_2CO_3 overnight, was finally found to be the most straightforward procedure for the synthesis of **DC**. This was concluded since any variations in the yield of the different products in the reaction itself due to different reaction parameters were indistinguishable after the subsequent purification steps.

The isolation of **DC** appeared to be an additional and very important yield-determining factor in the sense that while the double-cavity porphyrin isomers were easily separable from the their mono-cavity analogues *via* column chromatography, the R_f-values within each set of isomers (I-II and III-V) were very similar. Careful column chromatography using a gradient ranging from 1.2% to 1.6% methanol in chloroform, with incremental increases of 0.05%, was necessary to separate and isolate the different double-cavity porphyrins. This last purification step could only be performed successfully after the purification of the double-cavity porphyrin isomers from the other species. This latter separation was accomplished by column chromatography over silica and alumina (to remove any traces of tetra-hydroxy functionalised mono-cavity porphyrins), followed by the insertion of a zinc ion into the porphyrin isomers and column chromatography over silica with 1% (v/v) pyridine present in the eluent (employing the different binding behaviour towards **py** for cavity-appended and non-cavity-appended porphyrins). The penultimate step was treatment of the cavity molecules with hydrochloric acid to remove the zinc ions from the porphyrins. The unavoidable small loss of the desired product in each of the purification steps is also responsible for the low overall yield of **DC**.

Attempts to perform the reaction with the zinc(II) derivative of **1** in the presence of pyridine, in order to template cavity formation, actually hindered the reaction, resulting in the formation of no **DC** and none of the above mentioned isomers.

2.3 Binding properties of double-cavity porphyrin molecules

In previous work, binding studies of **DC** (isomer III) and the PF_6 salt of 4,4'-dimethyl-viologen (**V**) as a guest molecule, have already been described.[2] The potential of the other two isolated double-cavity porphyrin isomers to act as a host were therefore also studied. Whereas double-cavity porphyrin isomer IV could not be obtained in sufficient amounts to perform binding studies, the binding behaviour of double-cavity porphyrin isomer V could be investigated. According to ^{1}H NMR spectroscopy the addition of 2 equivalents of **V** to a solution of this isomer in $CDCl_3/CD_3CN$ 1:1 (v/v) did not result in the formation of any noticeable host-guest complex, since no shifts in the signals from the double-cavity molecule could be observed. In addition, when a 10-fold excess of **V** was added to a solution of isomer V in $CHCl_3/CH_3CN$ 1:1 (v/v), the fluorescence of the porphyrin molecule was not significantly quenched. This strongly indicates that the guest is unable to approach near enough to the porphyrin. In accordance with these experiments, a CPK-model of isomer V confirmed that its cavities are too sterically hindered to allow the entrance of a viologen guest molecule.

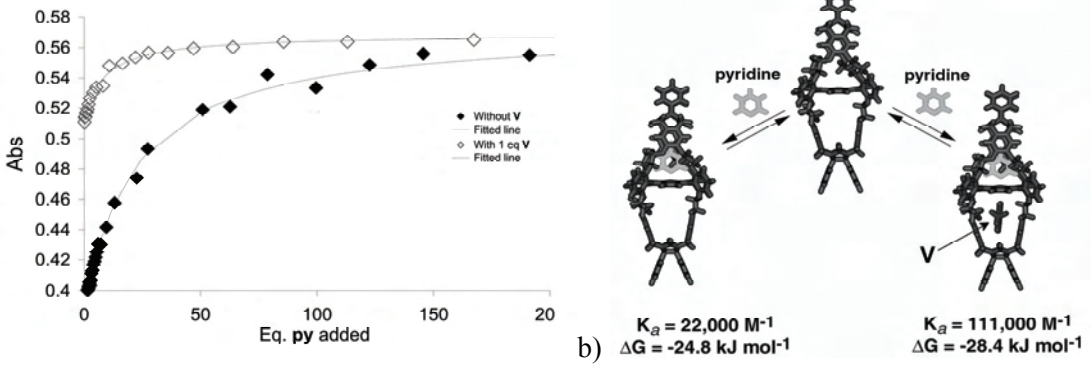

Figure 6. *a) Binding curves of **ZnDC** with **py** in the absence and in the presence of one equivalent of **V**, obtained by UV-Vis spectroscopy in $CHCl_3/CH_3CN$ 4:1 (v/v). b) The positive heterotropic allosteric binding behaviour of **ZnDC**.*

In contrast to the above mentioned isomers, **ZnDC** (the zinc(II) derivative of isomer III) could be synthesised in large enough quantities to allow a thorough study of its allosteric binding behaviour. The association constant between **ZnDC** and **py** was determined using UV-Vis spectroscopic studies in both the absence and in the presence of one equivalent of **V**. In the absence of **V** the association constant in $CHCl_3/CH_3CN$ 4:1 (v/v) was measured to be $K_a = 2.2 \times 10^4$ M^{-1}, which is only slightly lower than the association constant between **py** and **ZnMC** ($K_a = 7.5 \times 10^4$ M^{-1}).[1] The association constant between **py** and **ZnDC** in the presence of one equivalent of **V** increased 5-fold to $K_a = 11 \times 10^4$ M^{-1} (Figure 6a and b), which indicates a significant positive heterotropic allosteric binding behaviour. This allosteric effect is slightly bigger than for the binding of **tbpy** to **ZnMC**

in the presence and absence of **V**, which increases 2.5-fold from 4 x 10^2 M^{-1} to 1 x 10^5 M^{-1} upon the addition of 1 eq of **V**. This indicates that the induced pinching of the second cavity upon the binding of **V** is actually favourable for the binding of **py** inside this cavity.

2.4 Conclusions

The double-cavity porphyrin molecule **DC** has been synthesised and the isolation of two of its isomers has been achieved. The additional formation of two other double-cavity porphyrin species is also proposed. The intermediate of the synthesis of **DC**, the tetra-hydroxy functionalised mono-cavity porphyrin has been found to exist in at least two isomeric forms (I and II), which explains the formation of five different double-cavity porphyrin isomers. In three of these isomers, the porphyrin is bridging the two clip moieties in a "sideways" geometry and the cavities of these isomers are too sterically crowded to allow the binding of guest molecules. In the case of **ZnDC** strong positive heterotropic allosteric binding was observed upon the binding of one **py** and one **V**.

2.5 Experimental

^{1}H-NMR and ^{13}C-NMR spectra were recorded on Bruker DMX-300, Varian Unity Inova 400 and Bruker FDRX-500 instruments at 298 K. FAB mass spectra were recorded on a Finnigan MAT 900 S with m-nitrobenzylalcohol as a matrix. UV-Vis spectra were measured on a Varian Cary 50 UV-Vis spectrophotometer, GC-spectra were measured on a Varian GC3800 instrument and IR spectra were measured on a ATI Mattson Genesis FT-IR spectrometer, equipped with a Harrick Split Pea ATR apparatus. Melting points were recorded on a Jeneval polarization microscope THMS 600 hot stage and MALDI-TOF MS spectra were recorded on a Bruker Biflex III spectrometer.
All solvents were distilled under nitrogen prior to use. Acetonitrile was distilled from CaH_2, chloroform from $CaCl_2$ and dichloromethane from CaH_2. DMF was predried over BaO for one week and then distilled under reduced pressure, and the first and last 25% of the distillate was discarded. K_2CO_3 was dried in an oven (150°C). All other solvents and chemicals were commercial materials and used without purification. Acros Aluminium oxide 90 (activity III) and Merck Silica Gel 60 and 60H were used for column chromatography. 5,10,15,20-Tetrakis(2,6-dihydroxyphenyl)porphyrin **1**[2] and tetrakis-(tolylsulfonyl-ethoxy)clip **2**[1] were synthesised according to literature procedures.
Association constants were determined using a literature procedure.[4]

Synthesis of double-cavity porphyrin isomers III-V.
To a mixture of porphyrin **1** (180 mg, 0.24 mmol), clip **2** (327 mg, 0.24 mmol), K_2CO_3 (332 mg, 2.40 mmol) and finely grounded zinc powder (5 mg, 0.08 mmol), under an argon atmosphere, was added freshly distilled CH_3CN (150 mL) that had previously been purged with argon. The mixture was refluxed for 16 h under an argon atmosphere. After cooling, aqueous HCl (1 M) was added until the solution turned green and then a few drops of saturated aqueous $NaHCO_3$ were added until a brown coloured solution was obtained (pH 8-9). The mixture was filtered and the residue washed with $CHCl_3$ and CH_3CN until the filtrate remained colourless. The combined filtrates were evaporated to dryness and the residue was subjected to column chromatography (Merck 60, $CHCl_3/CH_3OH$, 97:3 (v/v)) to yield both a mixture of mono-cavity porphyrin isomers I and II as well as a mixture of double-cavity porphyrin isomers III-VII.
To a mixture of clip **2** (27 mg, 0.020 mmol), dried K_2CO_3 (40 mg, 0.30 mmol), finely grounded zinc powder (5 mg, 0.08 mmol) and the mixture of mono-cavity porphyrin isomers I and II (23 mg, 0.016 mmol), under an argon atmosphere, was added freshly distilled DMF (15 mL) that had previously been purged with argon. The mixture was stirred at 90-100 °C for 16 h under an argon atmosphere. After cooling, aqueous HCl (1 M) was added until the solution turned green and then a few drops of saturated aqueous $NaHCO_3$ were added to until a brown coloured solution was obtained (pH 8-9). The mixture was filtered and the residue washed with $CHCl_3$ and CH_3CN until the filtrate remained colourless, and the combined filtrates were evaporated to dryness. At this point the previously obtained mixture of double-cavity porphyrin isomers III-VII was added. Column chromatography over silica (Merck 60H, $CHCl_3/CH_3OH$, 98:2 (v/v)) was followed by column chromatography over alumina ($CHCl_3/CH_3OH$, 99.5:0.5 (v/v)). Zinc(II) was inserted in the porphyrin mixture by refluxing the compounds in the presence of 10 eq of $Zn(OAc)_2{\cdot}2H_2O$ in $CHCl_3/CH_3OH$ 3:1 (v/v) for 3 h. Column chromatography over silica (Merck 60, $CHCl_3/CH_3OH$/Pyridine, 98:2:1 (v/v)) afforded a mixture of the different double-cavity porphyrin isomers III-V (10 mg) with high purity (>99%). Demetallation using aqueous HCl (6 M) in CH_2Cl_2 and, after neutralisation, further chromatography over silica (Merck 60, $CHCl_3/CH_3OH$, 98.8:1.2 → 98.4:1.6 (v/v)) yielded the separate isomers III-V. Yield isomer III: 0.5%, traces of isomer IV and V.

Isomer I: m.p. > 300°C; IR (KBr-pellet) ν: 3945, 3692, 3055, 2987, 2686, 2522, 2411, 2306, 2155, 2126, 2055, 1706, 1674, 1604, 1550, 1422, 1264, 1177, 896, 738 and 716 cm^{-1}; UV-Vis (CH_2Cl_2) λ/nm: 420, 515, 543, 588, 650; ^{1}H-NMR ($CDCl_3$, 300 MHz): δ = 8.90 (s, 4H, *H12*), 8.79 (s, 4H, *H13*), 7.65 (t, 4H, ^3J= 8.2 Hz, *H9*), 7.07 (d, 8H, ^3J= 8.3 Hz, *H8,10*), 7.08-6.91 (m, 6H, *H1,2*), 6.80-6.76 (m, 4H, *H3*), 6.16 (s, 4H, *H5*), 4.88 (bs, 4H, O*H*), 4.30-4.20 (m, 4H, *H7*), 4.21 (d, 4H, ^2J= 15.9 Hz, *H4*), 4.13-4.08 (m, 4H, *H7*),

3.72 (d, 4H, ^2J= 16.2 Hz, *H4*), 3.54-3.48 (m, 4H, *H6*), 3.40-3.32 (m, 4H, *H6*), -2.74 (bs, 2H, N*H*) ppm; FAB-MS *m/z*: 1409 $(M+H)^+$.

Isomer II: ^{1}H NMR (DMSO-d_6, 400.15 MHz): δ = 9.50 (s, 4H, O*H*), 8.78 (s, 2H, *H11*), 8.70 (d, 4H, ^3J = 4.7 Hz, *H12b*), 8.52 (d, 4H, ^3J = 4.7 Hz, *H12a*), 7.88 (t, 2H, ^3J = 8.4 Hz, *H9a*), 7.81 (s, 2H, *H13*), 7.39 (t, 2H, ^3J = 8.2 Hz, *H9b*), 7.31 (d, 4H, ^3J = 8.4 Hz, *H8a*), 7.25-7.18 (m, 4H, *H2*), 7.18-7.10 (m, 6H, *H1,3*), 6.79 (d, 4H, ^3J = 8.2 Hz, *H8b*), 6.73 (s, 4H, *H5*), 4.57 (d, 4H, ^2J = 15.7 Hz, *H4*), 4.46-4.37 (m, 4H, *H7*), 4.37-4.28 (m, 4H, *H7*), 4.04 (d, 4H, ^2J = 15.7 Hz, *H4*), 3.68-3.56 (m, 8H, *H6*), -2.85 (br, 2H, N*H*) ppm; MS (MALDI-TOF) *m/z*: 1409 $(M+H)^+$.

DC (isomer III): m.p. > 300°C; IR ($CHCl_3$) ν: 2956, 2923, 2856, 1702, 1589, 1511, 1461, 1425, 1307, 1272, 1247, 1216, 1141, 1112, 1016, 964, 943, 794, 765, 721 and 696 cm^{-1}; UV-Vis ($CHCl_3$/CH_3CN 4:1 (v/v)) λ/nm ($\log(\varepsilon/M^{-1}cm^{-1})$): 276 (4.36), 405sh (4.68), 423 (5.43), 517 (4.06), 549 (3.49), 591 (3.56), 571 (3.68), 651 (3.00) nm; ^{1}H-NMR ($CDCl_3$, 300 MHz): δ = 8.65 (s, 8H, *H12*), 7.70 (t, 4H, ^3J= 8.4 Hz, *H9*), 7.04 (d, 8H, ^3J= 8.4 Hz, *H8*), 6.97-6.92 (m, 12H, *H1,2*), 6.82-6.78 (m, 8H, *H3*), 6.21 (s, 8H, *H5*), 4.25 (d, 8H, ^2J= 15.7 Hz, *H4*), 4.28-4.17 (m, 8H, *H7*), 4.04-3.97 (m, 8H, *H7*), 3.74 (d, 8H, ^2J= 15.7 Hz, *H4*), 3.49-3.43 (m, 8H, *H6*), 3.35-3.27 (m, 8H, *H6*), -2.58 (s, 2H, N*H*) ppm; ^{13}C-NMR ($CDCl_3$, 100 MHz): δ = 159.88, 156.93, 146.80, 133.69, 129.94, 129.67, 128.41, 128.10, 122.06, 115.71, 09.87, 105.94, 84.71, 67.72, 67.18, 44.36 ppm; MS (HR-MALDI-TOF) *m/z*: 2074.697 [$(M)^+$, calcd for $C_{124}H_{98}N_{12}O_{20}$: 2074.702].

Isomer IV: m.p. > 300°C; ^{1}H-NMR ($CDCl_3$, 500.14 MHz): δ = 8.76 (s, 4H, *H12*), 8.60 (s, 4H, *H13*), 7.67 (t, 4H, ^3J= 8.1 Hz, *H9*), 7.05 (d, 8H, ^3J= 8.2 Hz, *H8*), 6.95-6.93 (m, 12H, *H1,2*), 6.83-6.81 (m, 8H, *H3*), 6.15 (s, 8H, *H5*), 4.22 (d, 8H, ^2J= 15.9 Hz, *H4*), 4.06-4.05 (m, 8H, *H7*), 4.02-4.00 (m, 8H, *H7*), 3.72 (d, 8H, ^2J= 15.9 Hz, *H4*), 3.57-3.54 (m, 8H, *H6*), 3.26-3.25 (m, 8H, *H6*), -2.51 (s, 2H, N*H*) ppm; MS (HR-MALDI-TOF) *m/z*: 2074.697 [$(M)^+$, calcd for $C_{124}H_{98}N_{12}O_{20}$: 2074.702].

Isomer V: m.p. > 300°C; IR ν: 3745, 3459, 2923, 2850, 1696, 1592, 1519, 1458, 1419, 1286, 1221, 1095, 940, 879, 793, 767, 724, 693, 581 cm^{-1}; UV-Vis ($CHCl_3$) λ/nm: 418, 556, 588; ^{1}H-NMR ($CDCl_3$, 400.15 MHz): δ = 8.78 (s, 4H, *H12*), 7.94 (s, 4H, *H13*), 7.85 (t, 4H, ^3J= 8.3 Hz, *H9*), 7.19-7.13 (m, 28H, *H1,2,3,8*), 6.77 (s, 8H, *H5*), 4.68 (d, 8H, ^2J= 15.9 Hz, *H4*), 4.23-4.16 (m, 16H, *H7*), 4.12 (d, 8H, ^2J= 15.6 Hz, *H4*), 3.67-3.62 (m, 8H, *H6*), 3.58-3.53 (m, 8H, *H6*), -2.55 (s, 2H, N*H*) ppm; MS (MALDI-TOF) *m/z*: 2075 $(M)^+$.

Synthesis of ZnDC.

To a solution of isomer III (4.7 mg, 0.0026 mmol) in $CHCl_3$ (15 mL) was added $Zn(OAc)_2{\cdot}2H_2O$ (4 mg, 0.018 mmol) in dry CH_3OH (8 mL). The reaction mixture was refluxed for 4 h under a nitrogen atmosphere in the absence of light. After cooling to room temperature, the solvent was removed under reduced pressure and the crude product

was purified by column chromatography (Merck 60, $CHCl_3$/MeOH 98.2:1.8 (v/v)). Yield: 92%.

M.p. > 300°C; IR (KBr-pellet) ν: 2956, 2892, 2846, 1702, 1625, 1581, 1509, 1457, 1421, 1307, 1261, 1118, 1099, 1016, 995, 941, 806, 765, 746, 719, 694, 669 cm^{-1}; UV-Vis ($CHCl_3$/CH_3CN 4:1 (v/v)) λ/nm (log(ε/$M^{-1}cm^{-1}$): 282 (4.16), 431 (5.35), 561 (3.97), 601 (3.24); ^{1}H-NMR (500.14 MHz, $CDCl_3$): δ = 8.75 (s, 8H, *H12*), 7.69 (t, 4H, ^3J= 8.0 Hz, *H9*), 7.07 (d, 8H, ^3J= 7.4 Hz, *H8*), 6.97-6.91 (m, 6H, *H1,2*), 6.83-6.78 (m, 4H, *H3*), 6.18 (s, 4H, *H5*), 4.24 (d, 8H, ^2J= 15.8 Hz, *H4*), 4.25-4.20 (m, 8H, *H7*), 4.00-3.80 (m, 8H, *H7*), 3.74 (d, 8H, ^2J= 15.8 Hz, *H4*), 3.43-3.28 (m, 8H, *H6*), 3.25-3.10 (m, 8H, *H6*) ppm; ^{13}C-NMR (100 MHz, $CDCl_3$): δ = 159.20, 148.04, 134.10, 129.68, 129.19, 128.58, 128.26, 117.21, 85.96, 69.02, 45.50 ppm; MS (HR-MALDI-TOF) *m/z*: 2136.631 [$(M)^+$, calcd for $C_{124}H_{96}N_{12}O_{20}Zn$: 2136.615].

References

1. a) A.E. Rowan, P.P.M. Aarts, K.W.M. Koutstaal, *Chem. Commun.*, 1998, 611-612.
   b) J.A.A.W. Elemans, M.B. Claase, P.P.M. Aarts, A.E. Rowan, A.P.H.J. Schenning, R.J.M. Nolte, *J. Org. Chem.*, 1999, **64**, 7009-7016.
   c) P. Thordarson, R.G.E. Coumans, J.A.A.W. Elemans, P.J. Thomassen, J. Visser, A.E. Rowan, R.J.M. Nolte, *Angew. Chem. Int. Ed.*, 2004, **43**, 4755-4759.
2. P. Thordarson, E.J.A. Bijsterveld, J.A.A.W. Elemans, P. Kasák, R.J.M. Nolte, A.E. Rowan, *J. Am. Chem. Soc.*, 2003, **125**, 1186-1187.
3. E. Tsuchida, T. Komatsu, H. Etsuo, H. Nishide, *J. Chem. Soc., Dalton Trans.*, 1990, 2713-2738.
4. P. Thordarson, E.J.A. Bijsterveld, J.A.A.W. Elemans, P. Kasák, R.J.M. Nolte, A.E. Rowan, *J. Am. Chem. Soc.*, 2003, **125**, 1186-1187, suppl. inf.

Chapter 3. Catalytic properties of double-cavity porphyrin molecules

3.1 Introduction

The enzyme cytochrome P450 plays an essential role in everyday life, since it is a key component in the detoxification system within our liver.[1] It contains an iron porphyrin (haem) in its active site and is extremely versatile, since it performs sulfoxidation, epoxidation and hydroxylation reactions. Its exact mechanism and the intermediate structures of the mono-oxygenation reactions it catalyses have been extensively studied.[2] The wealth of information that has been obtained has enabled (bio)organic chemists to develop simple organic analogues, both as models to further understand the mechanism of enzyme action, and as functional catalytic systems.[3]

Manganese(III) porphyrins and corroles have been extensively used as models for cytochrome P450 and the mechanisms of their catalytic cycles have been studied in depth, in particular the effect of substituents on the porphyrin, axially binding ligands and the oxygenation methodology.[4-6]

Efforts to mimic the binding site of cytochrome P450 have lead to the synthesis of a class of molecules called "picket-fence" and "double picket" porphyrins.[7,8] The straps (or caps) attached to the porphyrin catalysts have provided chemists with the opportunity to perform the oxygenation reactions under steric control while they also inhibit catalyst decomposition.[9] The introduction of chiral functional groups into the pickets has also led to the ability to perform the oxygen transfer stereoselectively.[10] One of the effects of the pickets was the increase in the stability of the manganese(III) porphyrins during the oxygenation reactions by hindering the proposed catalyst-deactivation, i.e. the formation of μ-oxo manganese(IV) porphyrin dimers (Figure 1).[11]

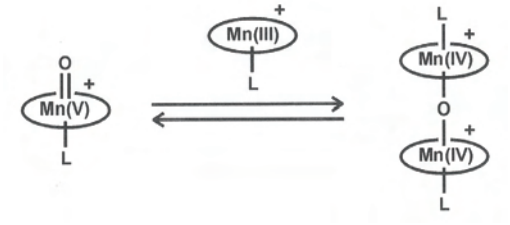

Figure 1. *Proposed deactivation of Mn-porphyrin catalysts due to the formation of inactive μ-oxo dimers.*[11]

Increasing the stability and reusability of manganese porphyrin catalysts has long been a goal and a myriad of approaches have been investigated, e.g. immobilisation of the catalyst *via* covalent attachment to support molecules, immobilisation *via* encapsulation within or adsorption onto a support matrix, and increasing the water-solubility by the

attachment of sugar-groups to the porphyrin.[12,13,14,15] Supramolecular chemistry has been utilised to encapsulate porphyrin catalysts inside a molecular square or to bring the catalyst and the substrate closely together.[16,17]

Our group has previously reported the use of a porphyrin functionalised cavity-containing catalyst **MnMC** (manganese monoclip; Figure 2a), as an epoxidation catalyst. It was demonstrated that **MnMC** had enhanced activity and stability in the epoxidation of alkenes when compared to electronically analogous porphyrins without an attached cavity.[18] In **MnMC** the manganese(III) porphyrin roof is positioned symmetrically above the receptor, thus creating a rigid and relatively closed cavity with a diameter of 8 Å.[19,20] (Figure 2a). Using both the biphasic dichloromethane-aqueous NaOCl and the single phase iodosylbenzene systems as oxygen donors, the simple alkenes *cis*-stilbene, *trans*-stilbene and α-pinene were readily epoxidised. More remarkably, it was also shown that the polyalkene polybutadiene could be epoxidised. In this latter case **MnMC** mimicked the action of processive enzymes in Nature, since it slides over the polymer chain thereby epoxidising its double bonds without falling off.[18b]
It was shown that the coordination of an electron-donating axial ligand increased the activity of the catalyst, as expected for manganese porphyrin catalysts.[21] In the case of pyridine (**py**), which is small enough to fit inside the cavity, the oxygenation reaction occurred on the outside of the porphyrin clip (approach A in Figure 2b). When 4-*tert*-butyl-pyridine (**tbpy**) which is too sterically demanding to fit inside the cavity was used, oxygenation occurred inside the cavity in a pseudo-rotaxane geometry (approach B in Figure 2b). The difference in the two approaches was evident from a difference in the reaction rate of epoxidation and in the stability of the catalyst, with approach B showing a dramatic increase in stability of the catalyst compared to approach A and to an electronically related manganese porphyrin without a protecting cavity. Due to the weak binding, 500 equivalents of **tbpy** were, however, necessary to completely block the outside of the cavity. In contrast, as a result of a much stronger binding, in approach A already one equivalent of axial ligand was effective in significantly increasing the activity of the catalyst.

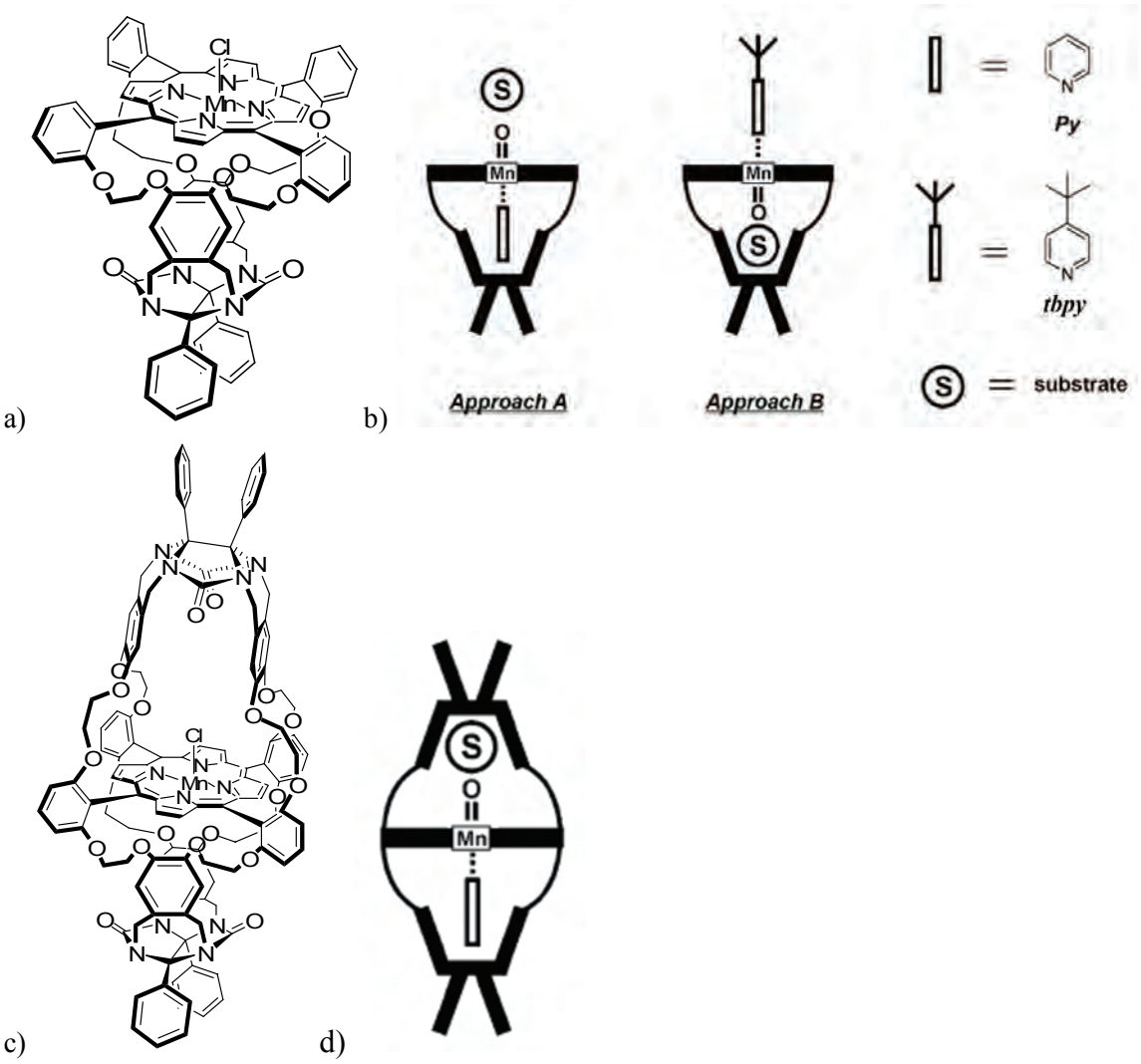

Figure 2. *a) Mono-cavity manganese(III) porphyrin* ***MnMC****. b) Two approaches in which* ***MnMC*** *is used as an epoxidation catalyst in combination with* ***py*** *or* ***tbpy*** *as the axial ligand. c) Double-cavity manganese(III) porphyrin* ***MnDC****. d) Simultaneous combination of approaches A and B in a manganese double-clip catalyst.*

The synthesis of the double-cavity analogue of **MC** (monoclip), **DC** (doubleclip), has been described in the previous chapter. The manganese(III) derivative of this molecule, **MnDC** (Figure 2c), has been designed in order to combine approaches A and B, i.e. catalyst activation by only one equivalent of axial ligand and an increased catalyst stability compared to non-picketed porphyrins. Moreover, communication between the two connected cavities of **MnDC** might provide stereo- and/or electronic control of catalysis in one cavity *via* binding of a guest or axial ligand inside the opposite cavity of the catalyst (Figure 2d).

3.2 Synthesis of MnDC

A manganese ion was inserted into **DC** by refluxing this compound under an argon atmosphere in DMF in the presence of an excess of MnI_2. Stirring the product for three days under air in a two-phase system of chloroform and brine exchanged the iodide for a chloride anion and oxidised the manganese(II) ion to manganese(III). Remarkably, manganese insertion with the salt which is normally used, $Mn(OAc)_2 \cdot 4H_2O$, failed. This is probably due to the stronger bonding of the acetate ion to the manganese cation in DMF compared to an iodide ion (hard-soft metal-ligand principle),[22] making it less favourable for the metal to enter the sterically demanding encapsulating environment of the porphyrin.

3.3 Catalytic properties

The oxygenation of the manganese porphyrin catalyst with an oxygen donor in the absence of substrate was first investigated. When a dichloromethane solution of **MnDC** was thoroughly mixed with an aqueous NaOCl solution, the UV-Vis spectrum clearly showed a shift of the porphyrin Soret band from 479 to 425 nm. Based on similar experiments reported in the literature, the structure (P)Mn(IV)OCl is proposed for the formed species.[23] Apparently despite the steric restraints, the manganese ion could be readily oxidised by hypochlorite. The mixture was allowed to stand at room temperature and UV-Vis spectra showed that the intensity of the band at 425 nm gradually decreased, accompanied by an increase in intensity of the band at 479 nm, which corresponds to the $[(P)Mn(III)]^+$ species (Figure 3a). Remarkably, the decay process of the Mn(IV) species back to Mn(III) took approximately 20 minutes for **MnDC**, whereas the complete decay for **MnMC** was observed to take approximately 15 minutes (see Figure 3b). For a standard manganese(III) tetra-phenyl porphyrin **MnTPP** decay occurs within only 2 minutes. These experiments suggest that the oxidised species of **MnDC** is somewhat more stable than that of **MnMC**, whereas they are both considerably more stable than that of **MnTPP**. In addition to the long lifetime of the active catalyst, no decomposition was observed for **MnDC** despite the absence of a substrate, which is clearly a strong indication that the previously proposed primary decomposition route of an active catalyst does indeed proceed *via* a μ-oxo dimer.[11] Moreover, the rigidity of the cavities apparently prevents the oxidation of the molecule itself.

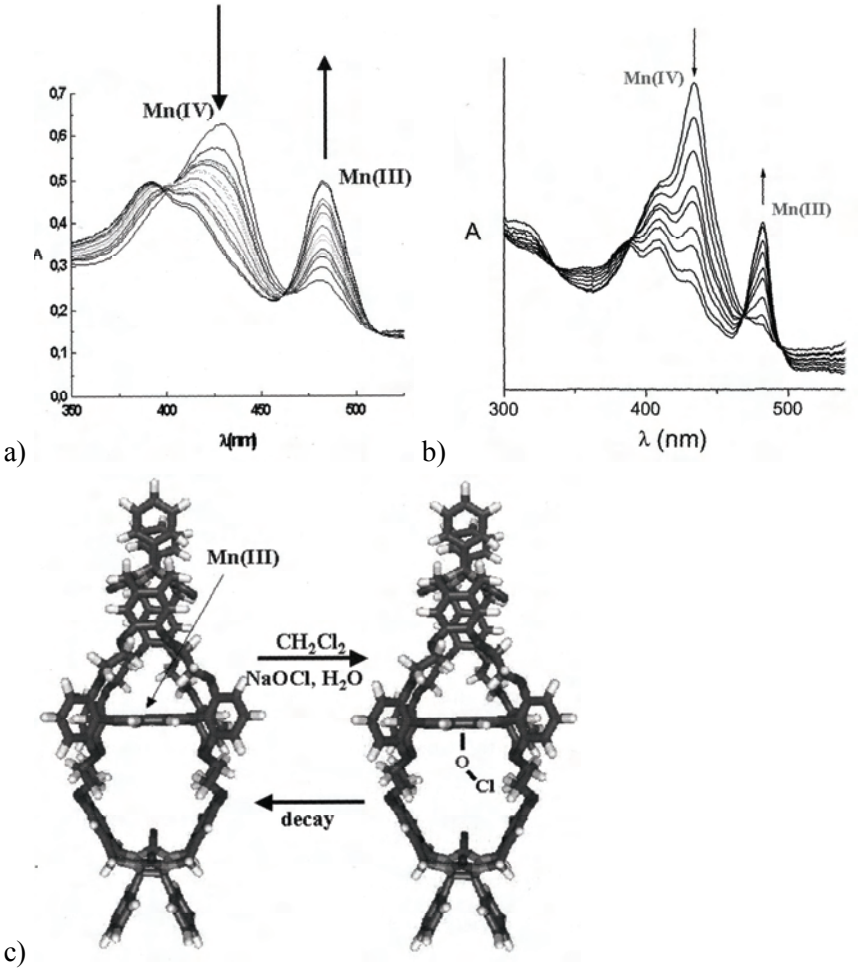

Figure 3. *a) UV-Vis spectra of* ***MnDC*** *in CH_2Cl_2 after treatment with an aqueous NaOCl-solution. b) Idem, of* ***MnMC****. c) Formation and decay of (P)Mn(IV)OCl.*

In a second series of experiments the epoxidation of alkenes was investigated employing the standard two-phase hypochlorite-dichloromethane reaction conditions already reported for **MnMC** (Table 1).[18]

Initially, the epoxidation of simple *cis*-stilbene using **MnDC** as the catalyst was investigated. Upon the binding of one equivalent of **py** in its cavity, the reaction rate increased, in a similar fashion to that observed for **MnMC**. The addition of more equivalents of **py** to **MnDC** resulted in a subsequent decrease in reaction rate, indicating that both cavities of the catalyst become occupied by axial ligands that block the approach of substrates to reach the catalytic metal centre. The binding of two pyridine ligands to a manganese(III) porphyrin has been reported, and is known to exhibit strong negative cooperative binding behavior.[24] The measured reaction rates were significantly lower than the rates observed when the electronically analogous reference catalyst *o*-octa-methoxy-porphyrin **Mn-o.m.p.** was used (Figure 4). In contrast to **MnDC**, this porphyrin catalyst exhibited an increased activation upon an increase in the amount of added axial

ligand (Table 1). This reduced rate is a result of the reaction occurring within a sterically demanding cavity.

Table 1. *Epoxidation of olefins by* ***MnDC*** *and the reference catalysts* ***MnMC*** *and* ***Mn-o.m.p*** *(see Figure 4).*

Substrate	**Axial ligand**	**Eq axial ligand**	**Rate MnDC[a]**	**Rate MnMC[a]**	**Rate Mn-o.m.p.[a]**	**MnDC f.c.[b]**	**MnDC c:t[c]**	**Mn-o.m.p. c:t[c]**
Cis-stilbene[d]		0	0.5	n.d.[e]	0.08	>99%	46:54	99:1
Cis-stilbene[d]	**py**	1	0.7	20	2.6	>99%	39:61	97:3
Cis-stilbene[d]	**py**	10	0.5	n.d.	45	>99%	55:45	96:4
Cis-stilbene[d]	**py**	500	0.4	n.d.	91	n.d.	67:33	99:1
Cis-stilbene[d]	**tbpy**	500	n.d.	15.5[f]	n.d.	n.d.	n.d.	n.d.
Trans-stilbene[d]		0	1.6	n.d.	0.03	n.d.	-[g]	-[g]
Trans-stilbene[d]	**py**	1	2	19	0.2	n.d.	-[g]	-[g]
Trans-stilbene[d]	**py**	10	0.5	n.d.	0.3	>99%	-[g]	-[g]
Trans-stilbene[d]	**py**	500	0.3	n.d.	1.3	n.d.	-[g]	-[g]
Trans-stilbene[d]	**tbpy**	500	n.d.	24	n.d.	n.d.	n.d.	n.d.
Styrene[h]	**py**	500	1.4	n.d.	>500[i]	>99%		
Styrene[j]	**tbpy**	500	n.d.	11.1	n.d.	n.d.		
α-Pinene[k]	**py**	1	n.d.	12	n.d.	n.d.		
α-Pinene[l]	**py**	500	-[m]	n.d.	72	n.d.		
α-Pinene[n]	**tbpy**	500	n.d.	11	n.d.	n.d.		

[a] Initial rate of olefin conversion x 10^{-5} mol dm^{-3} s^{-1}. Estimated error: 50%. [b] f.c.= Final conversion. [c] Ratio cis-trans epoxide product after 4 h. [d] The blank epoxidation rate with all the components present except ***MnDC*** *in the same ratios and amounts as in a typical epoxidation experiment was 0.0 mol dm^{-3} s^{-1} within experimental error. [e] Not determined. [f] Ratio cis-trans epoxide product after 3 h. = 90:10. [g] No cis-epoxide was detected. [h] The blank-value measured without catalyst was 0.3 x 10^{-5} mol dm^{-3} s^{-1}. [i] Too fast to measure. [j] The blank-value measured without catalyst was 1.5 x 10^{-5} mol dm^{-3} s^{-1}. [k] The blank-value measured without catalyst was 0.8 x 10^{-5} dm^{-3} s^{-1}. [l] The blank-value measured without catalyst was 1.35 x 10^{-5} mol dm^{-3} s^{-1}. [m] The measured rate was equal to the blank-value measured without catalyst. [n] The blank-value measured without catalyst was 0.7 x 10^{-5} mol dm^{-3} s^{-1}.*

When **Mn-o.m.p.** was used as the catalyst in the epoxidation of *cis*-stilbene, almost exclusively the *cis*-epoxide was formed. This is in stark contrast to the situation in which **MnDC** was used as the catalyst, where, depending on the amount of axial ligand present, also a significant amount of *trans*-epoxide was formed. Similar behaviour has also been observed when **MnMC** was used as the catalyst in combination with **tbpy** as the axial ligand.[18] The above results indicate that the pseudo-rotaxane geometry of the catalyst-substrate complex imposes steric constraints on the bulky reaction intermediate in the transition state, causing its partial isomerisation.

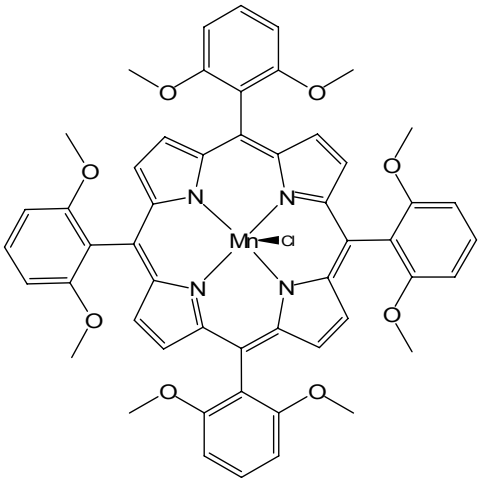

Figure 4. *Reference porphyrin catalyst* ***Mn-o.m.p.***

Molecular modelling studies reveal that the *trans*-stilbene and *trans*-stilbene oxide fit better in the cavities of **MnDC**. This finding is supported by the initial reaction rates which for the epoxidation of *trans*-stilbene in the presence of one equivalent of **py** are higher than that for *cis*-stilbene under similar conditions. The fact that the ratio between *cis* and *trans* oxide products obtained from the epoxidation of *cis*-stilbene depends on the **MnDC**:**py** ratio can be explained by the mechanism of the epoxidation reaction. This reaction has been speculated to proceed either *via* a) a radical mechanism or b) a concerted mechanism.[3] It has been speculated that the epoxidation of cyclohexane by (tetraphenylporphyrin)Mn-Cl (**TPPMnCl)** in the presence of iodosylbenzene as the oxygen-donor proceeds *via* a radical mechanism.[25] This was concluded from the observation by EPR of **TPPMn^{II}** in the reaction mixture, which was formed by the reaction between a cyclohexane radical and **TPPMnCl.** The cyclohexane radical resulted from hydrogen abstraction by **TPP$^{\cdot+}$Mn^{IV}O** (forming **TPPMn^{IV}OH**), itself the product of the reaction between **TPPMnCl** and iodosylbenzene. However, when imidazole was added to the reaction mixture, the epoxidation proceeded much faster and no **TPPMn^{II}** could be detected anymore.[5b] These observations indicated that the reaction did in this case not proceed *via* the radical mechanism, but *via* a concerted mechanism involving **TPPMn^{V}O**. In the case of **MnDC** the ratio of **py** to catalyst might therefore also influence the competition between the radical and concerted pathways, favouring the latter and the formation of **Mn^{V}DC(O)**.

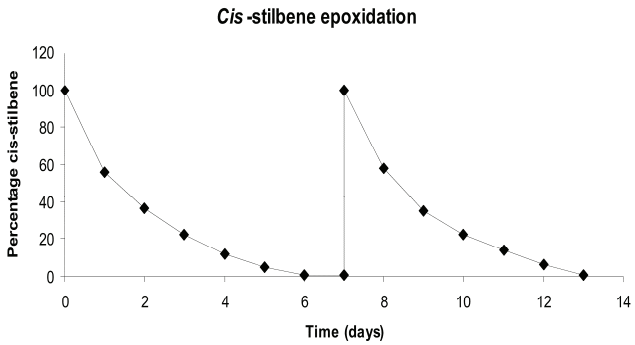

Figure 5. *Epoxidation of twice 250 equivalents of cis-stilbene by* ***MnDC*** *in the presence of one equivalent of* ***py****. Epoxidation of a second batch reveals an identical rate of epoxidation.*

The stability of the **MnDC** catalyst was found to be remarkably high. Although the rates of epoxidation for both *cis*- and *trans*-stilbene were very low, the reaction went to completion in all cases (Table 1). In the presence of one equivalent of **py** it took six days to complete the epoxidation of *cis*-stilbene without catalyst decomposition. The addition of a second batch of substrate again resulted in a complete conversion into the epoxide, with no apparent loss of activity of the catalyst (Figure 5). After thirteen days, the main products were *cis*- and *trans*-stilbene oxide, with only a trace of benzaldehyde. During the reaction time, the brown colour of the dichloromethane phase had not changed observably, which is an indication that the catalyst was not destructed. In contrast, under the same reaction conditions **Mn-o.m.p.** decomposed within 24 hours. This remarkable difference in catalyst stability can be attributed to the shielding of the manganese porphyrin by the two clips in **MnDC**, which prevents μ-oxo dimer formation, an effect that is absent in **Mn-o.m.p**, and the inability of the active catalyst to oxidise itself. This latter effect clearly demonstrates that the epoxidation in the presence of **py** does probably not occur *via* a radical mechanism.

In the presence of 500 equivalents of **py** styrene could also epoxidised by **MnDC**, with a slightly higher initial reaction rate than observed for *cis*-stilbene, which might be caused by the fact that styrene is a somewhat less bulky substrate (Table 1). Also the epoxidation went to completion, while the initial rate was significantly lower than the rate observed when **Mn-o.m.p.** was used as the catalyst. The latter rate could not be accurately determined, since the conversion of the substrate was too fast to be measured reliably by GC analysis.
Surprisingly, in the presence of 500 equivalents of **py** the normally highly reactive substrate α-pinene was not epoxidised by **MnDC**. The formation of a little α-pinene epoxide was observed, however, the rates of product formation and substrate disappearance were equal to the values observed in a blank measurement in which no porphyrin catalyst was present. The fact that this blank epoxidation rate appeared to be

dependent on the amount and type of axial ligand (**py** or **tbpy**), suggests that these bases are responsible for the observed oxidation reaction. Such a non-innocence of nitrogen-donor ligands in epoxidation reactions has been demonstrated before.[5f]

In order to compare the influence of the cavity of **MnDC** with that of **MnMC**, a situation had to be established in which both the manganese porphyrins experienced a similar activation by an axial ligand, which can only be achieved when **MnDC** is used in combination with one equivalent of **py** and **MnMC** with 500 equivalents of **tbpy**. Taking the association constants into account, it can be calculated that in both cases >99% of the hosts coordinates an axial ligand, whereas at the same time the cavities remain available for catalysis. Compared to **MnDC**, it was found that **MnMC** epoxidised *cis*-stilbene 22 times faster and *trans*-stilbene 12 times, which suggests that the cavity of **MnDC** is more sterically hindered. It had been previously shown (Chapter 2) that binding in one cavity squeezes the second cavity resulting in a negative allosteric effect. The lack of activity of **MnDC** compared to **MnMC** is in agreement with this observation. Another observation that supports this hypothesis is that the use of the more sterically demanding oxygen donor iodosylbenzene in combination with **MnDC** did not result in the epoxidation of any substrate, neither did the addition of this oxygen donor to a dichloromethane solution of **MnDC** result in changes in the UV-vis spectrum. In contrast, the formation of the catalytically active manganese species and the epoxidation of styrene, *cis*- and *trans*-stilbene and polybutadiene have been reported for **MnMC** in combination with iodosylbenzene.[18]

The epoxidation of polybutadiene derivatives by catalyst **MnMC**, is an important research goal, since the catalyst mimics the working mechanism of a processive enzyme.[18b] The oxidation of *cis*-polybutadiene[26] with NaOCl using **MnDC** as the catalyst in the presence of one equivalent of **py** was visible even with the naked-eye, since after a few hours the two-phase system turned cloudy and separate evaporation of the two phases after two days afforded only polymeric products in the water layer. ^{1}H-NMR and IR-spectroscopy showed in these products that some double bonds were still present, but that the majority had been converted into epoxides and their ring-opened products (alcohols). Simultaneous to this epoxidation reaction, a blank experiment was performed containing the same reagents in equal amounts and with identical reaction conditions, except that **MnDC** was absent. Unfortunately, this blank reaction proceeded with a similar, though a little lower rate, than the catalysed oxygenation, judged by the naked eye. Analysis of the mixture after two days again only afforded polymeric material in the water layer and this product proved to have a slightly higher ratio of double bonds to epoxides and alcohols than the product of the reaction containing **MnDC**. This indicates that **py** is non-innocent in the epoxidation of this polymer, but that **MnDC** does show activity as an oxidation of

cis-polybutadiene. However, both the catalysis and the blank reaction were only performed once, and therefore no strong conclusions can be drawn from these experiments.

The very low initial epoxidation rates observed when **MnDC** is used as a catalyst are remarkable. From the allosteric binding behaviour exhibited by the related molecule **ZnDC** it is known that the two cavities influence each other upon the binding of guests.[27] For example, when two viologen molecules are bound, the first binding event expands one cavity, resulting in a concomitant pinching of the second cavity, as a result of which the binding constant for the second viologen molecule drops significantly. In addition, the association constant for a viologen molecule is increased upon the binding of **py** in one of the cavities of **ZnDC**, as a result of pinching of the opposite cavity, which, among others, increases the favourable π-π interactions between the viologen and the aromatic sidewalls of the host molecule. One could envisage that a similar process can occur upon the binding of **py** in one cavity of **MnDC**, i.e. a pinching of the opposing cavity resulting in a decrease in the ease of substrate entrance.

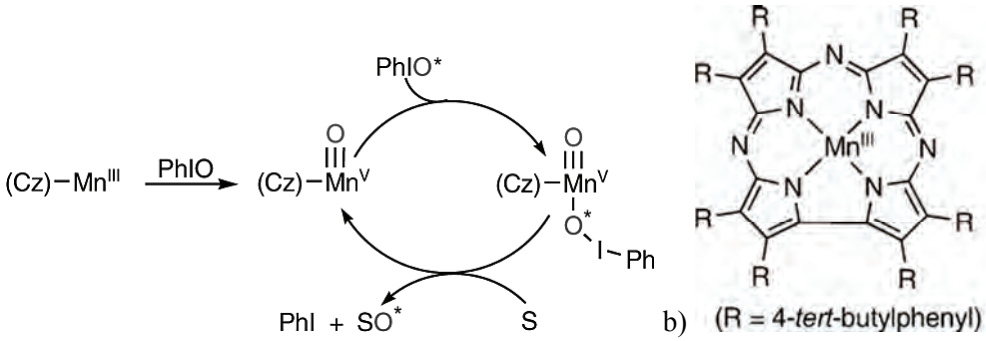

Figure 6. *a) Proposed mechanism of oxygen atom transfer for manganese corroles with iodosylbenzene as the oxygen donor, according to Goldberg et al. b) Manganese corrolazine (Cz)-Mn^{III} studied by Goldberg et al.*

Another factor that should be taken into account is the mechanism of the epoxidation reaction itself. Goldberg *et al.* have shown that when manganese corroles are used as epoxidation catalysts, it is not the oxygen atom of the oxygen donor that is incorporated into the epoxide, but an oxygen atom from a molecule of water or from a second oxygen donor molecule (see Figure 6).[5g,h] It was proposed that this mechanism could also explain many observations in epoxidation catalysis using manganese porphyrins. Although in the corrole mechanism no axial ligands are involved and a different oxygen donor is present, it still might explain some of our observations for **MnDC**. It can be envisaged that the entrance of not only one but of two oxygen donor molecules into the narrow cavities of **MnDC** that are filled with solvent, axial ligand or substrate is cumbersome.

3.5 Molecular modelling

To obtain a better idea of the structure of **MnDC** with various bound substrates, molecular modelling calculations were carried out (see experimental section for details). The catalytic host was modelled as the Mn(V)-oxo complex, activated by an axially coordinating **py** ligand on the of the cavities. Molecular modelling calculations were carried out on this complex and a variety of substrate molecules in the adjoining, available cavity. The results are shown in Table 2 and Figure 7.

Table 2. *Molecular modelling calculations[a] of the cavities of various **MnDC** molecules as their Mn(V)-oxo complexes in the presence of a pyridine axial ligand in one of the cavities and a variety of substrates in the other.*

Substrate	Size of the cavity containing substrate[b]	Size of the cavity containing axial ligand[b]
None[c]	5.0 Å	6.2 Å
styrene	6.3 Å	6.5 Å
cis-stilbene	6.1 Å	6.6 Å
trans-stilbene-**1**[d]	6.3 Å	6.5 Å
trans-stilbene-**2**[d]	7.2 Å	6.4 Å
α-pinene	7.7 Å	6.8 Å

*[a] See experimental section for details. [b] Measured as the average distance between the centres of the two aromatic side-walls. [c] From the X-ray structure of the complex between **ZnMC** and **py** the distance between the cavity side-walls was determined to be 6.2 Å, a value which is in excellent agreement with the calculated structure here. [d] The structure of these complexes differ only by the initial orientation of the substrate in the cavity, with trans-stilbene-**1** being more perpendicular to the porphyrin plane than trans-stilbene-**2**. As explained in the experimental section, the orientation trans-stilbene-**1** is converted to the orientation of trans-stilbene-**2** by simulated annealing.*

The calculations indicate that upon binding a substrate, both the cavity that accommodates the substrate and the cavity that binds the axial ligand have to expand. For the bulkiest substrate, α-pinene, it is calculated that the cavity should expand more than 50%, which probably explains why α-pinene is not epoxidised by this catalyst. In the case of the other substrates, their entrance into a pinched cavity which subsequently is being forced to expand explains the observed low epoxidation rates.

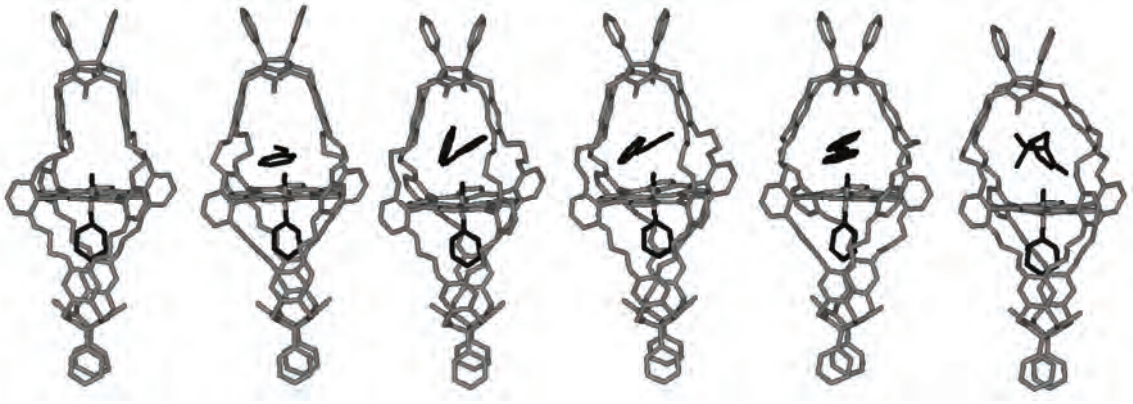

Figure 7. *Structures calculated by molecular modelling of* ***MnDC*** *as the Mn(V)-oxo complex activated by a* ***py*** *ligand in the bottom cavity, with different substrates: from left to right: none, styrene, cis-stilbene, trans-stilbene-1, trans-stilbene-2 and α-pinene. See Table 2 for details.*

3.6 Conclusions

Porphyrin epoxidation catalyst **MnDC** combines both the supramolecular activation induced by the binding of only one equivalent of axial ligand with a huge increase in catalyst stability. Although the observed epoxidation reaction rates are very low, the catalyst remains stable for at least two weeks without showing any signs of decomposition, which is attributed to the impossibility to form μ-oxo dimeric species. According to molecular modelling simulations, the low epoxidation rates seem to originate from the unfavourable binding of the substrate into a pinched cavity and the energetically unfavourable strained conformation of the resulting Mn(V)-oxo complexes containing an axially binding **py** ligand in one cavity and a substrate in the other.

3.7 Experimental

UV-Vis spectra were measured on a Varian Cary 50 UV-Vis spectrophotometer, GC-spectra were measured on a Varian GC3800 instrument and IR spectra were measured on a ATI Mattson Genesis FT-IR spectrometer, equipped with a Harrick Split Pea ATR apparatus. Melting points were recorded on a Jeneval polarization microscope THMS 600 hot stage and MALDI-TOF MS spectra were recorded on a Bruker Biflex III spectrometer.

All solvents were distilled under nitrogen prior to use. Dichloromethane was distilled from CaH_2. DMF was predried over BaO for one week and then distilled under reduced pressure, discarding the first and last 25% of the distillate. **DC** was synthesised as described in Chapter 2. All other solvents and chemicals were commercial materials and used without purification. Merck Silica Gel 60 was used for column chromatography.

Synthesis of MnDC.

DC (isomer III; see Chapter 2 Figure 3b) (3.5 mg, 1.7 μmol) was dissolved in dry DMF (2 mL) and to this solution was added MnI_2 (75 mg, 0.25 mmol) and NaOAc (1.1 mg, 0.013 mmol). The reaction mixture was stirred overnight under an argon atmosphere in the absence of light at 160°C. After cooling, the solvent was removed under reduced pressure. $CHCl_3$ (20 mL) and brine (20 mL) were added and the two-phase system was stirred vigorously for three days. The organic layer was washed with water three times and evaporated to dryness. The crude product was purified by column chromatography (Merck 60, $CHCl_3$/MeOH 98.5:1.5 → 95:5 (v/v)). Yield: 83% (green solid).

M.p. > 300°C; IR[§] (KBr-pellet) ν: 2962, 2915, 2879, 2855, 1712, 1695, 1590, 1515, 1468, 1454, 1425, 1303, 1251, 1106, 1076, 1012, 944, 796, 767, 721, 696 cm^{-1}; UV-Vis (CH_2Cl_2, λ/nm (log(ε/$M^{-1}cm^{-1}$): 279 (4.25), 342 (4.23), 392 (4.46), 415 (4.33), 479 (4.58), 493 (4.29), 571 (3.68), 651 (3.00); ^{1}H-NMR was not possible because of paramagnetic broadening; MS (HR-MALDI-TOF) *m/z*: 2127.621 [$(M\text{-}Cl)^+$, calcd for $C_{124}H_{96}N_{12}O_{20}Mn$: 2127.624].

[§] *The manganese – iodide bond is expected to have an absorption in the IR spectrum at 190 cm^{-1}.[28] No measurements in this IR region have been performed. A manganese – chloride bond should be easily distinguishable from the manganese – iodide bond with an absorption at 262 cm^{-1}.*

Epoxidation reaction conditions: to a CH_2Cl_2 solution (0.65 mL) of the substrate (0.626 M), the manganese catalyst (2.5 mM), the phase transfer catalyst tetrabutylammonium chloride (5 mM), the axial ligand, and an internal standard (1,3,5-tri-*tert*-butylbenzene; 0.17 M) in a Schlenck tube was added an aqueous NaOCl solution (2 mL, 0.6 M). The mixture was stirred vigorously at a constant rate under nitrogen and during the course of the reaction samples were taken from the organic layer for ^{1}H-NMR and/or GC-analysis. All experiments were performed in triplicate.

Molecular modelling: The molecular modelling studies were performed with the Hyperchem 6.03 package[29] for Windows using a MM+ force field modified for porphyrins.[30-32] Geometric optimisation of all the structures was carried out by energy minimisation using the Polak-Ribiere conjugate gradient algorithm until either a root mean square gradient termination cut-off of 0.0001 kcal/Å had been reached or the total strain energy had not changed for at least 100 cycles. A conformational search was then carried out by molecular dynamics using the method of simulated annealing (run time 25 ps).[33] The resulting structures were then subjected to another round of geometric optimisation as described above to arrive at the structure which was finally reported. An exception to this is conformer **1** in which trans-stilbene is bound to the Mn(V)**DC**-oxo-**py** complex, which is the structure obtained before simulated annealing, as annealing caused

it to convert to conformer **2**. The starting point for the optimisation of **MnDC** as a Mn(V)-oxo complex with bound **py** was an approximate model which was created using the inbuilt model builder of HyperChem, and the resulting structure was used as the starting point for all the other complexes studied. For all the alkene substrates, distance restraints (force constant 20 kcal mol^{-1} $Å^{-2}$) were applied between the unsaturated C-atoms and the O-atom bound to Mn (Mn(V)-oxo). The same distance restraints were also used for the Mn-O bond in the Mn(V)-oxo complexes. The distances used were 1.64 Å for the unsaturated C-O bond and 1.54 Å for the Mn-O bond, based on a previously obtained transition state-like structure (Structure 3) reported in a DFT study on the epoxidation of cyclohexane by manganese porphyrins.[34]

References

1. J.T. Groves, Y.Z. Han, in '*Cytochrome P450. Structure, Mechanism and Biochemistry',* ed. P.R. Ortiz de Montellano, Plenum Press, New York, 1995, pp 3-48.
2. a) I.G. Denisov, T.M. Makris, S.G. Sligar, I. Schlichting, *Chem. Rev.*, 2005, **105**, 2253-2277.
   b) S. Shaik, D. Kumar, S.P. de Visser, A. Altun, W. Thiel, *Chem. Rev.*, 2005, **105**, 2279-2328.
3. *Reviews:* a) A.M.d'A. Rocha Gonsalves, M.M. Pereira, *J. Mol. Catal. A: Chem.*, 1996, **113**, 209-211.
   b) W.A. Reiter, A. Gerges, S. Lee, T. Deffo, T. Clifford, A. Danby, K. Bowman-James, *Coord. Chem. Rev.*, 1998, **174**, 343-359.
   c) M.C. Feiters, A.E. Rowan, R.J.M. Nolte, *Chem. Soc. Rev.*, 2000, **29**, 375-384.
   d) G. Simonneaux, P. Tagliatesta, *J. Porphyrins Phthalocyanines*, 2004, **8**, 1166-1171.
   e) T. Punniyamurthy, S. Velusamy, J. Iqbal, *Chem. Rev.*, 2005, **105**, 2329-2363.
   A recent example: f) G. Yin, M. Buchalova, A.M. Danby, C.M. Perkins, D. Kitko, J.D. Carter, W.M. Scheper, D.H. Busch, *Inorg. Chem.*, 2006, **45**, 3467-3474.
4. *Some examples:* a) D. Ostovic, T.C. Bruice, *Acc. Chem. Res.*, 1992, **25**, 314-320.
   b) R. Zhang, M. Newcomb, *J. Am. Chem. Soc.*, 2003, **125**, 12418-12419.
   c) R. Zhang, J.H. Horner, M. Newcomb, *J. Am. Chem. Soc.*, 2005, **127**, 6573-6582.
5. *Some examples:* a) S. Banfi, F. Montanari, S. Quici, *J. Org. Chem.*, 1989, **54**, 1850-1859.
   b) Y. Iamamoto, M.D. Assis, K.J. Ciuffi, C.M.C. Prado, B.Z. Prellwitz, M. Moraes, O.R. Nascimento, H.C. Sacco, *J. Mol. Catal. A: Chem.*, 1997, **116**, 365-374.
   c) J.P. Collman, A.S Chien, T.A. Eberspacher, M. Zhong, J.I. Brauman, *Inorg. Chem.*, 2000, **39**, 4625-4629.
   d) G.B. Shul'pin, *J. Mol. Catal. A: Chem.*, 2002, **189**, 39-66.
   e) M.D. Godbole, A.C.G. Hotze, R. Hage, A.M. Hills, H. Kooijman, A.L. Spek, E. Bouwman, *Inorg. Chem.*, 2005, **44**, 9253-9266.
   f) J.P. Collman, A.S Chien, T.A. Eberspacher, M. Zhong, J.I. Brauman, *Inorg. Chem.*, 2000, **39**, 4625-4629.
   g) S.H. Wang, B.S. Mandimutsira, R. Todd, B. Ramdhanie, J.P. Fox, D.P. Goldberg, *J. Am.*

Chem. Soc., 2004, **126**, 18-19.
h) W.J. Song, M.S. Seo, S. DeBeer George, T. Ohta, R. Song, M.-J. Kang, T. Tosha, T. Kitagawa, E.I. Solomon, W. Nam, *J. Am. Chem. Soc.*, 2007, **129**, 1268-1277.

6. a) B.S. Mandimutsira, B. Ramdhanie, R.C. Todd, H. Wang, A.A. Zareba, R.S. Czernuszewicz, D.P. Goldberg, *J. Am. Chem. Soc.*, 2002, **124**, 15170-15171.
   b) Z. Gross, H.B. Gray., *Adv. Synth. Catal.*, 2004, **346**, 165-170.
   c) D.E. Lansky, D.P. Goldberg, *Inorg. Chem.*, 2006, **45**, 5119-5125.
7. *The first examples:* a) J.P. Collman, J.I. Brauman, K.M. Doxsee, T.R. Halbert, S.E. Hayes, K.S. Suslick, *J. Am. Chem. Soc.*, 1978, **100**, 2761-2766.
   b) J.P. Collman, R.R. Gagne, T.R. Halbert, J.C. Manchon, C.A. Reed, *J. Am. Chem. Soc.*, 1973, **95**, 7868-7870.
   Recent examples: c) D.H. Burns, K. Calderon-Kawasaki, S. Kularatne, *J. Org. Chem.*, 2005, **70**, 2803-2807.
   d) J. Goodwin, T. Kurtikyan, J. Standard, R. Walsh, B. Zheng, D. Parmley, J. Howard, S. Green, A. Mardyukov, D.E. Przybyla, *Inorg. Chem.*, 2005, **44**, 2215-2223.
8. *Some examples:* a) E. Rose, A. Kossanyi, M. Quelquejeu, M. Soleilhavoup, F. Duwavran, N. Bernard, A. Lecas, *J. Am. Chem. Soc.*, 1996, **118**, 1567-1568.
   b) S.Smeets, C.V. Asokan, F. Motmans, W. Dehaen, *J. Org. Chem.*, 2000, **65**, 5882-5885.
   c) B. Boitrel, V. Baveux-Chambenoit, P. Richard, *Eur. J. Org. Chem.*, 2001, **22**, 4213-4221.
   d) D. Ricard, M. L'Her, P. Richard, B. Boitrel, *Chem. Eur. J.*, 2001, **7**, 3291-3297.
   e) E. Rose, M. Quelquejeu-Ethève, B. Andrioletti, *J. Porphyrins Phthalocyanines*, 2003, **7**, 375-381.
   f) Z. Halime, S. Balieu, M. Lachkar, T. Roisnel, P. Richard, B. Boitrel, *Eur. J. Org. Chem.*, 2006, 1207-1215.
9. *Reviews:* a) B. Meunier, *Chem. Rev.*, 1992, **92**, 1411-1456.
   b) J.P. Collman, L. Fu, *Acc. Chem. Res.*, 1999, **32**, 455-463.
   c) J.P. Collman, X. Zhang, V.J. Lee, E.S. Uffelman, J.I. Brauman, *Science*, 1993, **261**, 1404-1411.
10. E. Rose, B. Andrioletti, S. Zrig, M. Quelquejeu-Ethève, *Chem. Soc. Rev.*, 2005, **34**, 573-583.
11. A.W. van der Made, R.J.M. Nolte, W. Drenth, *Recl. Trav. Chim. Pays-Bas*, 1990, **109**, 537-551.
12. a) F.G. Doro, J.R.L. Smith, A.G. Ferreira, M.D. Assis, *J. Mol. Catal. A: Chem.*, 2000, **164**, 97-109.
    b) E. Brulé, K.K. Hii, Y.R. de Miguel, *Org. Biomol. Chem.*, 2005, **3**, 1971-1976.
13. a) I.O. Benítez, B. Bujoli, L.J. Camus, C.M. Lee, F. Odobel, D.R. Talham, *J. Am. Chem. Soc.*, 2002, **124**, 4363-4370.
    b) I.D. Cunningham, T.N. Danks, J.N. Hay, I. Hamerton, S. Gunathilagan, C. Janczak, *J. Mol. Catal. A: Chem.*, 2002, **185**, 25-31.
    c) M.V. Avdeev, E.I. Bagrii, G.B. Maravin, Y.M. Korolev, *Kinet. Catal.*, 2002, **43**, 38-44.
    d) R. Naik, P. Joshi, S. Umbarkar, R.K. Deshpande, *Catal. Commun.*, 2005, **6**, 125-129.
14. F. Chen, S.-H. Cheng, C.-H. Yu, M.-H. Liu, Y.O. Su, *J. Electroanal. Chem.*, 1999, **474**, 52-59.

15. X.-B. Zhang, C.-C. Guo, J.-B. Xu, R.-Q. Yu, *J. Mol. Catal. A: Chem.*, 2000, **154**, 31-38.
16. M.L. Merlau, M.P. Mejia, S. T. Nguyen, J.T. Hupp, *Angew. Chem. Int. Ed.*, 2001, **40**, 4239-4242.
17. a) P. Thordarson, R.J.M. Nolte, A.E. Rowan, *Aust. J. Chem.*, 2004, **57**, 323-327.
    b) L. Kovbasyuk, R. Krämer,. *Chem. Rev*, 2004, **104**, 3161-3187.
18. a) J.A.A.W. Elemans, E.J.A. Bijsterveld, A.E. Rowan, R.J.M. Nolte, *Chem. Commun.*, 2000, 2443-2444.
    b) P. Thordarson, E.J.A. Bijsterveld, A.E. Rowan, R.J.M. Nolte, *Nature*, 2003, **424**, 915-918.
    c) J.A.A.W. Elemans, E.J.A. Bijsterveld, A.E. Rowan, R.J.M. Nolte, *Eur. J. Org. Chem.*, **2007**, 751-757.
19. *A review on the clip:* A.E. Rowan, J.A.A.W. Elemans, R.J.M. Nolte, *Acc. Chem. Res.*, 1999, **32**, 995-1006.
20. a) A.E. Rowan, P.P.M. Aarts, K.W.M. Koutstaal, *Chem. Commun.*, 1998, 611-612.
    b) J.A.A.W Elemans, M.B. Claase, P.P.M. Aarts, A.E. Rowan, A.P.H.J. Schenning, R.J.M. Nolte, *J. Org. Chem.*, 1999, **64**, 7009-7016.
21. A.W. Van der Made, R.J.M. Nolte, *J. Mol. Catal.*, 1984, **26**, 333-335; E. Guilmet, B. Meunier, *Nouv. J. Chim.*, 1982, **6**, 511-513.
22. R.H. Crabtree, in *The Organometallic Chemistry of the Transition Metals*, John Wiley & Sons Inc., Hoboken, 4th edition, 2005, p.8.
23. a) J.T. Groves, M.K. Stern, *J. Am. Chem. Soc.*, 1988, **110**, 6828-6838.
    b) J.T. Groves, J. Lee, S.S. Marla, *J. Am. Chem. Soc.*, 1997, **119**, 6269-6273.
    c) R.D. Arasasingham, G.-X. He, T.C. Bruice, *J. Am. Chem. Soc.*, 1993, **115**, 7985-7991.
24. a) E.M. Davoras, R. Diaper, A. Devissi, M.J. Tornaritis, A.G. Coutsolelos, *J. Porphyrins Phthalocyanines*, 1998, **2**, 53-60.
    b) A. Nascimento de Sousa, M.E. Moreira Dai de Carvalho, Y.M. Idemori, *J. Mol. Catal. A*, 2001, **169**, 1-10.
25. J.A. Smegal, C.L. Hill, *J. Am. Chem. Soc.*, 1983, **105**, 3515-3521.
26. Acros, M_w ~ 300,000, 98% cis. Analysed by IR-spectroscopy and ^{1}H-NMR.
27. P. Thordarson, E.J.A. Bijsterveld, J.A.A.W. Elemans, P. Kasák, R.J.M. Nolte, A.E. Rowan, *J. Am. Chem. Soc.*, 2003, **125**, 1186-1187.
28. L.J. Boucher, *J. Am. Chem. Soc.*, 1968, **90**, 6640-6645.
29. *Hyperchem 6.03*, Hypercube Inc., Gainesville, FL, 2000.
30. O. Q. Munro, J. C. Bradley, R. D. Hancock, H. M. Marques, F. Marsicano, P. W. Wade, *J. Am. Chem. Soc.* 1992, **114**, 7218-7230.
31. O. Q. Munro, H. M. Marques, P. G. Debrunner, K. Mohanrao, W. R. Scheidt, *J. Am. Chem. Soc.* 1995, **117**, 935-954.
32. H.M. Marques, O. Q. Munro, N. E. Grimmer, D. C. Levendis, F. Marsicano, G. Pattrick, T. Markoulides, *J. Chem. Soc., Faraday Trans.* 1995, **91**, 1741-1749.
33. S. Kirkpatrick, C. D. Gelett, Jr, M. P. Vecchi, *Science* 1983, **220**, 671-680.
34. D. Rutkowska-Zbik, M. Witko, E. M. Serwicka, *Catalysis Today*, 2004, **91-92**, 137-141.

Chapter 4. Construction of supramolecular multi-component assemblies by allosteric interactions

4.1 Introduction

The formation of well-defined assemblies and polymers by the association of monomers through reversible, non-covalent interactions is a major area of interest in the field of supramolecular chemistry. The first supramolecular polymers, reported by Lehn and co-workers, were based upon complementary hydrogen bonding units, mimicking systems found in Nature.[1] Meijer *et al.* further developed the concept and successfully used triple and quadruple hydrogen bonding moieties to synthesize supramolecular polymers, with high binding constants between the monomers ($K_{dim} > 6 \times 10^7$ M^{-1}) and high degrees of polymerisation (>100).[2] The directionality and the selectivity of multiple hydrogen bonds allow a high degree of control over the resulting macromolecular architectures. A variety of other hydrogen bonding motives and non-hydrogen bonding supramolecular interactions have also been used to form supramolecular polymers.[3,4]

In principle, if numerous cooperating non-covalent interactions are simultaneously applied, an even greater control over the macromolecule architecture can be obtained. One such approach would be to build allosteric supramolecular assemblies. This application of allosteric assembly has been largely unexplored in the field of supramolecular polymers, even though such an approach is seen throughout Nature as a subtle means to construct hierarchical, complex systems.[5,6] Allosterism is a special case of cooperativity, in the sense that a binding event at one site in a multivalent host causes a discrete, reversible alteration in the structure of the host at a remote binding site.[7] Allosteric interactions can be both positive and negative in nature, and act between a host and identical guests (homotropic), or between a host and different types of guests (heterotropic).

In previous research a number of cavity-appended porphyrin hosts has been developed that display such an allosteric binding behaviour.[8] The most extensively studied host molecule is the mono-cavity appended zinc porphyrin **ZnMC**, which is depicted in Figure 1a. Its allosteric binding behaviour has been discussed in Chapter 1 and is summarised in Figure 1b.

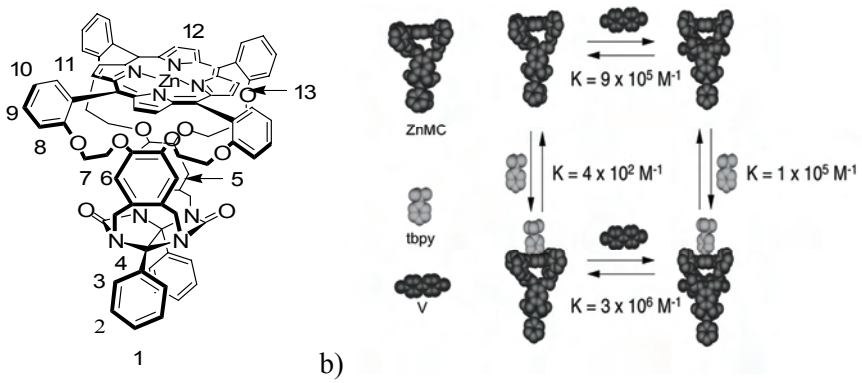

a) b)

Figure 1. *a) Structure of porphyrin host **ZnMC**, together with the relevant proton numbering. b) Schematic representation of the allosteric binding properties of this molecule.*

It was found that **ZnMC** can bind viologen molecules with high binding constants. The addition of a nitrogen-donor ligand that is too bulky to fit inside the cavity, such as 4-*tert*-butyl-pyridine (**tbpy**), results in a positive heterotropic allosteric effect, which is demonstrated by an increase in the binding constant between dimethylviologen (**V**) and **ZnMC** (Figure 1b). An increase in the binding constant of **tbpy** to **ZnMC** was observed upon the addition of viologen molecules to a mixture of the host and the axial ligand. Since the research described in this thesis was performed, a detailed investigation into the allosteric binding properties of **ZnMC** was performed, which also took into account the competitive association constants of solvent molecules. The updated association constants still reveal the same allosteric binding behaviour. With these numbers, however, the total ΔG-value of the two binding events is irrespective of the order in which **tbpy** and **V** are bound, in contrast to the situation depicted in Figure 1b.

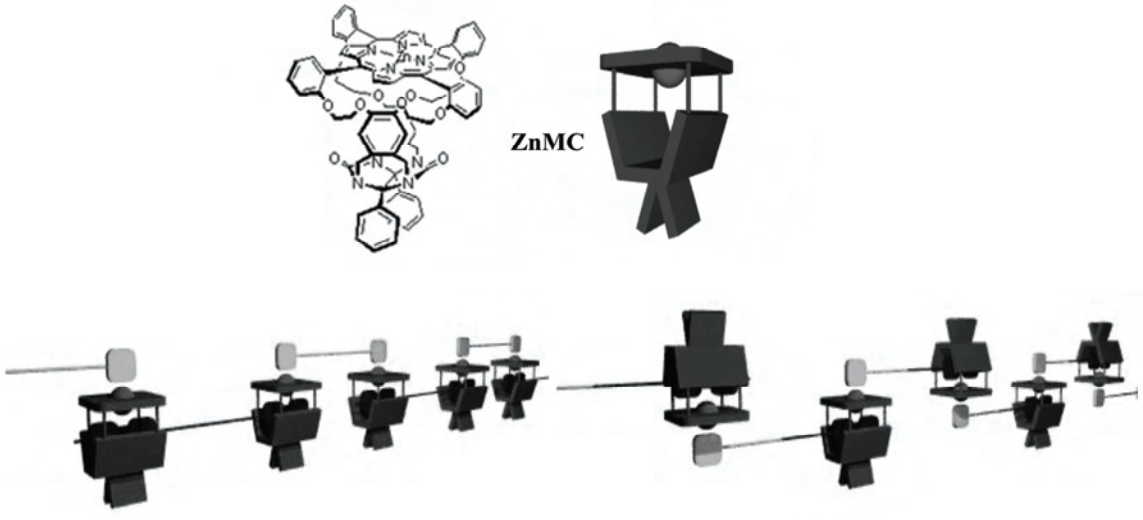

Figure 2. *Schematic and modelled structure of **ZnMC** and examples of the proposed supramolecular polymers based on **ZnMC** and three different bifunctional guests.*

As a continuation of the research described above, this chapter describes the attempts to construct more complex self-assembled allosteric complexes that contain derivatives based upon modified **V** and **py** ligands, in combination with both **ZnMC** and **ZnDC** (Chapter 2). The ultimate goal of this research is to bind bifunctional guests into the hosts **ZnMC** or **ZnDC** forming supramolecular polymers and lock them in place using allosteric interactions (Figure 2).

4.2 Synthesis of bifunctional guests

To achieve the above goal three different bifunctional guests with equal spacer length were synthesised, one containing two pyridine moieties (**PyPy**), one containing two viologen-moieties (**VV**) and one containing one pyridine and one viologen moiety (**VPy**) (Figure 3a).

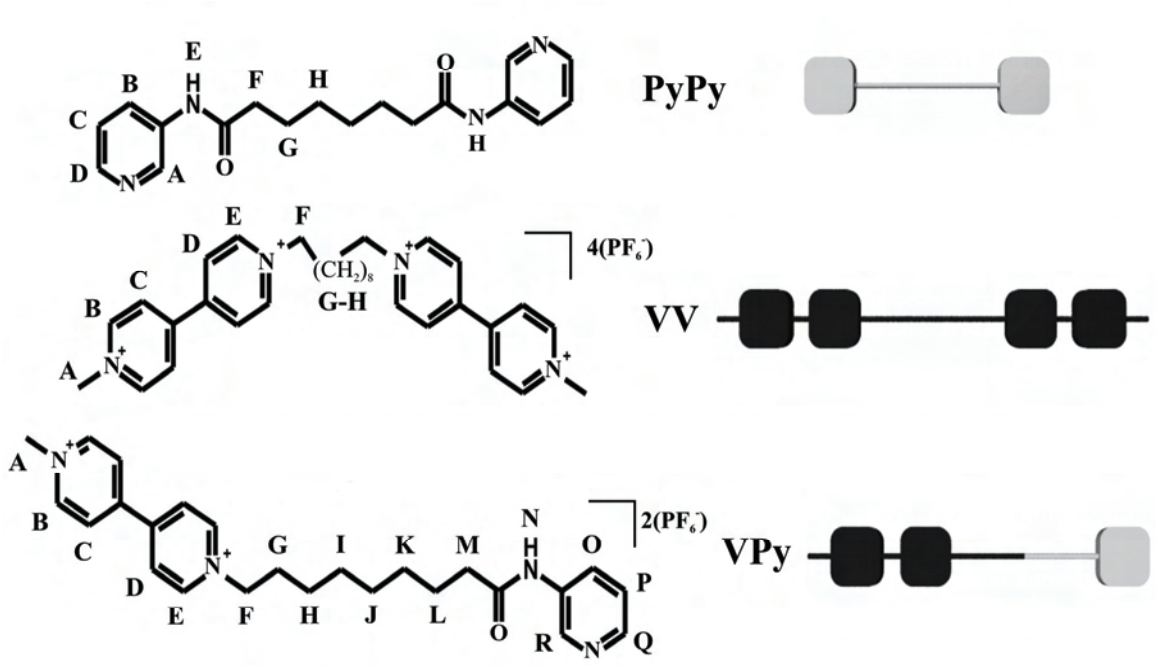

Figure 3. *Chemical and schematic structure of the three different bifunctional guests used in this study with their proton assignment.*

Bis-pyridine bifunctionalised guest **PyPy** was synthesised by a straightforward reaction of suberoyl chloride with 3-aminopyridine (Scheme 1). An amide linker was chosen because it has been reported that it increases the binding of the pyridine guest in **ZnMC** due to an additional hydrogen bond with one of the carbonyl groups of the cavity of the host.[8d] A disadvantage of this linker was that the presence of the amide bonds in **PyPy** resulted in a hydrogen-bonding network, causing the guest to be poorly soluble in most solvents, and making its purification difficult.

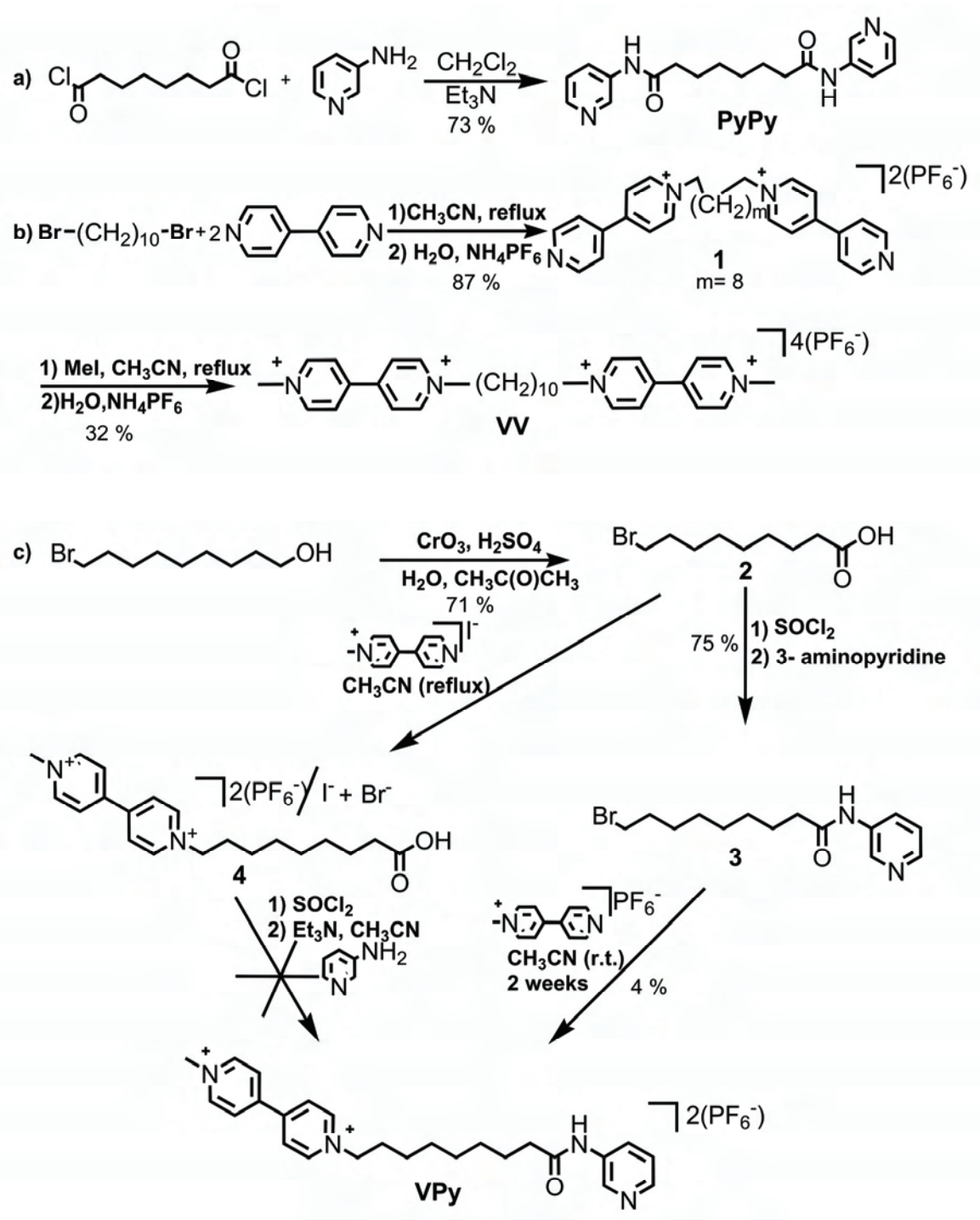

Scheme 1. *Synthesis of a)* ***PyPy****, b)* ***VV*** *and c)* ***VPy****.*

To synthesize the di-viologen bifunctionalised guest **VV**, 1,12-dibromodecane was reacted with an excess amount of 4,4'-bipyridine to give **1** (Scheme 1), which was then reacted with iodomethane. Once formed, anion exchange was carried out by dissolving

the compound in a hot aqueous solution of ammonium hexafluorophosphate. Upon cooling, the desired product **VV** precipitated out as the tetrakis-hexafluorophosphate salt.
The synthesis of **VPy** was less straightforward than that of **VV**. First the acid **2** was synthesised from 9-bromo-1-nonanol, which only yielded the desired product upon a 20-fold decrease in the concentration of the reactants when compared to the literature procedure (Scheme 1).[9] This original procedure yielded predominantly the ester of **2** and the starting alcohol. In the next step, compound **2** was reacted with mono-methylated bipyridine. This reaction proceeded as expected, however the resulting product **4**, was found to be insoluble in most organic solvents. The counter ions were therefore exchanged for hexafluorophosphate ions, as described previously, dramatically increasing the solubility. Compound **4** was converted into an acid-chloride, however surprisingly in acetonitrile no reaction could be observed between this compound and 3-aminopyridine to give the desired product **VPy**.
In an alternative route to synthesise **VPy**, acid **3** was first converted into an acid chloride using thionyl chloride, and then reacted with 3-aminopyridine to yield compound **3**. When the reaction of **3** with mono-methylated bipyridine was carried out at elevated temperatures (35 ºC) an inseparable mixture of products was obtained. According to ^{1}H NMR these were mainly cyclised products in which the pyridine moiety of **3** had carried out a nucleophilic intramolecular attack on the carbon atom to which the bromide is attached. This cyclisation could be avoided by performing the reaction at room temperature, however, in that case the formation of **VPy** was very slow, and occurred in a very low yield.

4.3 Self-assembled complexes containing ZnMC

The first step in forming self-assembled architectures was to measure the association constants using UV-vis spectroscopic titrations between the three new guest molecules and host **ZnMC** in acetonitrile/chloroform 1:1 (v/v; Table 1). All the association constants were obtained assuming independent (non-cooperative) binding of the separate binding moieties of the guest molecules. (In most cases this gave a reasonable fit, although the deviations of the fit from the binding curve that were present indicate additional interactions between host and guests.)
The association constant obtained for the binding of **VV** to **ZnMC** was calculated to be about five times higher than that obtained for **V** (K_a= 9 x 10^5 M^{-1}), which is in line with the general observation that viologens equipped with long alkyl chains bind more strongly in **ZnMC**.[8b] The accuracy of the fit decreased at higher concentrations of the guest, which is tentatively ascribed to other binding geometries, e.g. the formation of [4]-pseudo-rotaxanes in which three molecules of **ZnMC** bind on one strand of **VV** (Figure 4a). A 40-fold increase in association constant was observed upon the addition of an

excess **tbpy** to this mixture. It was noticed that after the addition of only half an equivalent of **VV** to **ZnMC** the titration curve reached saturation, while a full equivalent was needed to reach complete binding in the absence of **tbpy** (Figure 4).

Table 1. *Association constants K_a[a] and binding free energies ΔG for the complexation of* ***ZnMC*** *with different guests.*

Guest	K_a (M^{-1})	ΔG (kJ mol^{-1})
VV	4.6 x 10^6	-38
VV[b]	2.2 x 10^8	-48
PyPy	5 x 10^5	-33
VPy	1.0 x 10^7	-38

*[a] $CHCl_3/CH_3CN$ = 1/1 (v/v) at 298 K, [**ZnMC**] = 1.5 x 10^{-6} M, determined by UV-Vis spectroscopy. Association constants obtained from fluorescence (excitation wavelength = 426 nm; emission wavelength (max) = 605 nm) data have been compared with the reported K_{ass}-values determined from UV-vis data. They were found to be similar and are therefore not mentioned. In their calculation it was assumed that the quantum yield of the host and of the host-guest complexes are the same .[b] Association constant in the presence of 500 equivalents* ***tbpy****.*

a) 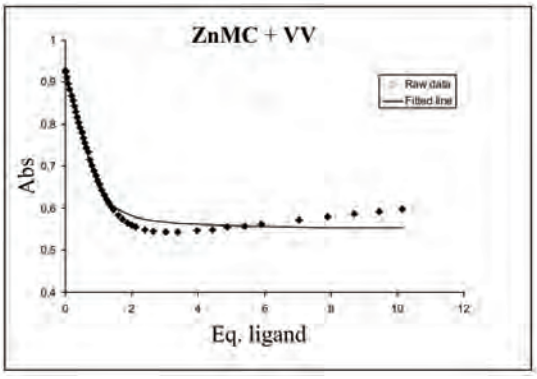

b) 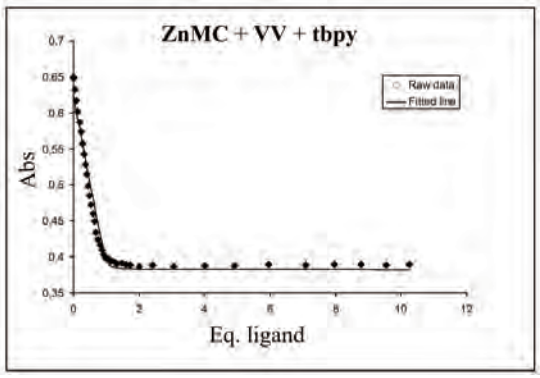

Figure 4. *Titration curves for the binding of* ***VV*** *in* ***ZnMC*** *obtained by UV-Vis spectroscopy in $CHCl_3/CH_3CN$ 1:1 (v/v): a) in the absence of* ***tbpy*** *and b) in the presence of 500 equivalents of* ***tbpy****.*

^{1}H-NMR studies confirmed the observed allosteric assembly, revealing a 1:1 stoichiometry for the **VV**:**ZnMC** complex and a 1:2:2 stoichiometry for the **VV**:**ZnMC**:**tbpy** complex. ^{1}H-NMR, COSY- and NOESY 2D NMR spectra indicated the geometry of the 1:2:2 **VV**:**ZnMC**:**tbpy** complex (Figure 5a and b). The addition of 10 eq of **tbpy** to a solution of **VV**/**ZnMC** (1:2) in $CDCl_3/CD_3CN$ 1:1 (v/v) resulted in a sharpening up of the crown ether proton signals of **ZnMC** and the viologen moiety of **VV**, indicating the formation of a more defined complex. A splitting up of proton signals 5-7 and 11-13 into two sets of signals for each proton was observed (Table 2). This asymmetry is attributed to the non-symmetrical complexation of a guest inside the cavity.

In contrast, only very broad signals were found for the free **tbpy** ligand (indicated by asterisks in Figure 5b), indicating that it is in exchange with axially coordinated **tbpy**. Other clear indications of the complexation of the viologen moieties of **VV** were the significant upfield shifts for protons B to F and the NOE signals observed between protons C and E with protons 6 of **ZnMC**. COSY NMR was indispensable for assigning the signals in the ^{1}H NMR spectrum to their corresponding guest protons, since both sets of protons B-E and F-I can be easily distinguished with this technique. The NOESY spectrum showed two clear NOE couplings between protons A and B and between E and F, resulting in a complete assignment of the guest signals in the ^{1}H NMR of the complex. The ^{1}H NMR signals arising from **ZnMC** in the complex, did not experience a significant shift compared to free **ZnMC**, affording easy assignment with the expected COSY and NOE signals that have been described earlier.[10]

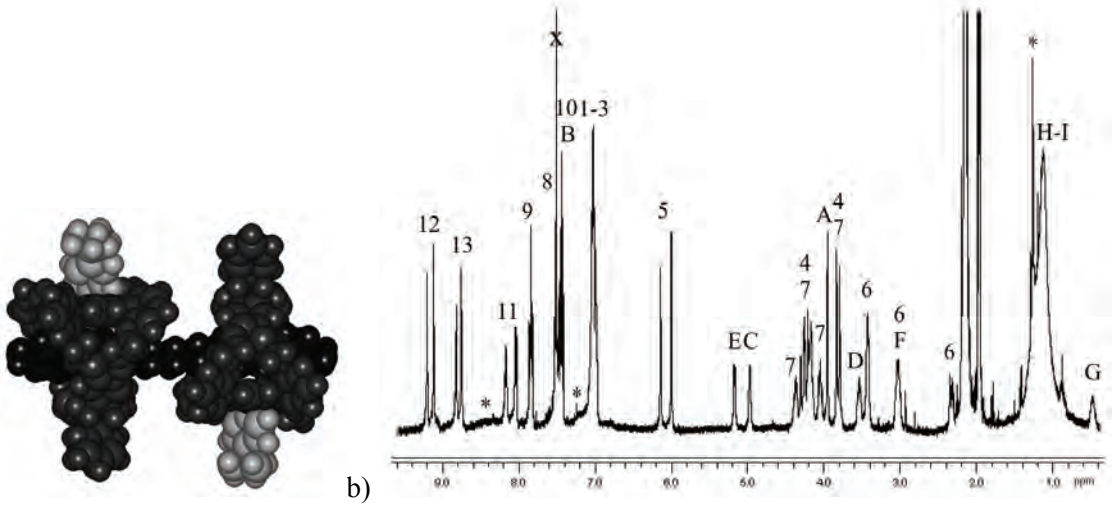

Figure 5. *a) Computer modelled structure of a) the 1:2:2 assembly of **VV**, **ZnMC** and **tbpy**; b) ^{1}H NMR spectrum (400.15 MHz, $CDCl_3/CD_3CN$ = 1/1 (v/v), 298K, [**ZnMC**] = 2.90 x 10^{-3} M) of a 1:2:10 **VV**/**ZnMC**/**tbpy** mixture, the proton assignments of **tbpy** are indicated by an asterisk. For proton numbering see Figures 1 and 3.*

Assuming independent binding of the pyridine moieties, the association constant calculated for the binding of **PyPy** (K_a= 5 x 10^5 M^{-1}), is more than five times higher than the association constant of pyridine bound inside the cavity of **ZnMC** (K_a= 1 x 10^5 M^{-1} in chloroform; Figure 6a). To investigate the reason for this increase, which may be a result of the presence of the amide substituents and their ability to form hydrogen bonds with the carbonyl groups of the host, the reference guest *N*1-(3-pyridyl)butanamide (Figure 6b) was synthesised. The association constant of this guest with **ZnMC** was measured to be K_a= 2.7 x 10^5 M^{-1} in $CHCl_3/CH_3CN$ 1:1 (v/v), indicating that a hydrogen bonding interaction is only partially responsible for the observed increase in association constant.

The increase is thought to be a combination of effects, one being the effects of the long alkyl spacer in the guest molecule.

a) 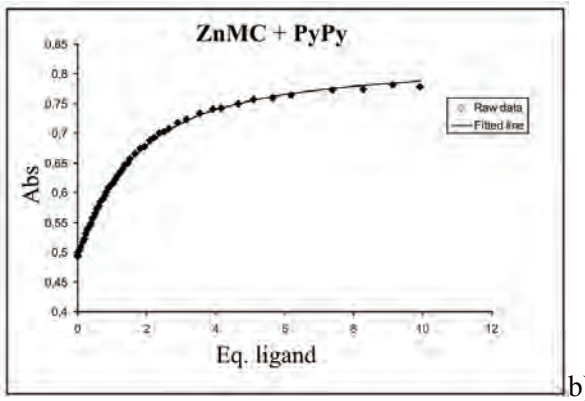

b) 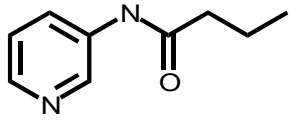

Figure 6. *a) Titration curve for the binding of **PyPy** in **ZnMc** obtained by UV-Vis spectroscopy in $CHCl_3/CH_3CN$ 1:1 (v/v). b) Reference guest N1-(3-pyridyl)butanamide.*

Since it had been demonstrated that both **VV** and **PyPy** are excellent guests for **ZnMc**, the architecture formed upon the combination of these three components was studied. ^{1}H-NMR, COSY- and NOESY 2D NMR studies of a 2:1:1 mixture of **ZnMC**, **VV** and **PyPy** in $CDCl_3/CD_3CN$ 1:1 (v/v) revealed that discrete self-assembled complexes had been exclusively formed (Figure 7a).

a) 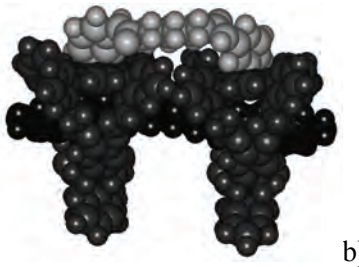
b) 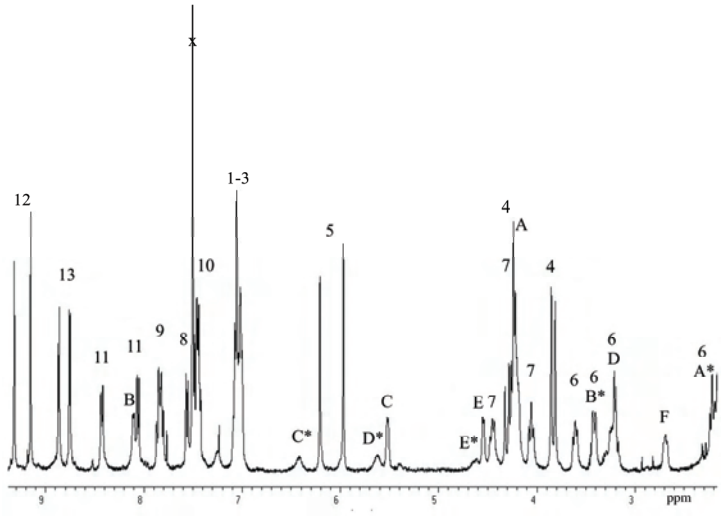

Figure 7. *a) Computer modelled structure of the 2:1:1 assembly of **ZnMC**, **VV**, and **PyPy**. b) ^{1}H NMR spectrum (400.15 MHz, $CDCl_3/CD_3CN$ = 1/1 (v/v), 298K, [**ZnMC**] = 2.16 x 10^{-3} M) of a 1:2:1 **VV**/**ZnMC**/**PyPy** mixture, the proton assignments of **PyPy** are indicated by an asterisk. For proton numbering see Figures 1 and 3.*

Table 2. *Chemical shifts[a] and Δδ values (in ppm) of* ***ZnMC*** *and its complexes with the bifunctional guests.*

ZnMc	without guest	**VPy**	**VV/tbpy**	**VV/PyPy**	
1	6.97 (m)	6.99-7.0 (m)	6.99-7.05 (m)	7.00-7.05 (m)	
2	6.97 (m)	6.99-7.0 (m)	6.99-7.05 (m)	7.00-7.05 (m)	
3	6.85 (m)	6.99-7.0 (m)	6.99-7.05 (m)	7.00-7.05 (m)	
4a	4.13 (d)	4.2 (d)	4.2 (d)	4.20+4.30 (m)	
4b	3.7 (d)	4.0 (d)	3.8 (d)	3.82 (d)	
5	6.21 (s)	6.03 (s)	6.14 (s)	6.2 (s)	
		5.97 (s)	6.00 (s)	5.96 (s)	
6a	3.23 (m)	3.4 (br)	2.3+3.42 (br)	2.21+3.43 (br)	
6b	3.53 (m)	2.8 (br)	3.02+3.55 (br)	3.23+3.61 (br)	
		2.35 (br)			
7a	4.15 (m)	4.2 (m)	4.04+4.18 (m)	4.06+4.19 (m)	
7b	4.1 (m)	4.04 (m)	4.16+4.38 (m)	4.21+4.46 (m)	
8	7.38 (d)	7.41 (br)	7.52 (m)	7.55 (m)	
9	7.77 (t)	7.82 (m)	7.84 (m)	7.8 (m)	
		7.5-7.4 (br)			
10	7.44 (t)	7.3 (br)	7.41 (m)	7.45 (m)	
		7.4 (br)			
11	7.99 (d)	8.14 (d)	8.04 (d)	8.05 (d)	
		8.22 (d)	8.17 (d)	8.42 (d)	
12	8.64 (s)	9.12 (br)	9.12 (s)	9.15 (s)	
			9.20 (s)	9.32 (s)	
13	8.85 (s)	8.73 (d)	8.75 (d)	8.75 (d)	
		8.78 (d)	8.82 (d)	8.86 (d)	
Guest		**VPy**	**VV**	**VV**	**PyPy**
A		3.81 (s, -0.58)	3.95 (s, -0.45)	4.25 (br, -0.15)	2.2 (br, -6.4)[b]
B		7.17 (br, -1.68)	7.5 (m, -1.3)	8.10 (d, -0.75)	3.3 (br, -5.0)[b]
C		4.61 (br, -3.74)	4.97 (d, -3.40)	5.51 (d, -2.86)	6.4 (br, -0.8)[b]
D		3.4 (br, -4.9)	3.4 (br, -5.0)	3.19 (d, -5.18)	5.62 (br, -2.5)[b]
E		5.43 (br, -3.42)	5.17 (d, -3.68)	4.54 (d, -4.31)	4.7 (br, -3.5)[b]
F		3.4 (br, -1.2)	3.03 (br, -1.57)	2.69 (t, -1.91)	1.86 (br, -0.51)
G		0.62 (m, -1.40)	0.48 (br, -1.52)	0.1 (br, -1.9)	1.41 (br, -0.32)
H		1.05 (m, -0.35)	1.1 (br, -0.3)	1.02 (br, -0.35)	1.17 (br, -0.26)
I		1.3-1.1 (br, -0.2)	1.1-1.3 (br, -0.2)	1.1 (br, -0.3)	-
J		1.3-1.1 (br, -0.2)	1.1-1.3 (br, -0.2)	1.2 (br, -0.3)	-
K		1.3-1.1 (br, -0.2)	-	-	-
L		1.3-1.1(br, -0.4)	-	-	-
M		1.47 (m, -0.87)	-	-	-
N		4.45 (br, -3.90)	-	-	-
O		5.67 (br, -2.33)	-	-	-
P		6.56 (br, -0.74)	-	-	-
Q		3.1 (br, -5.14)	-	-	-
R		2.18 (br, -6.52)	-	-	-

[a] s = singlet, d = doublet, t = triplet, m = multiplet, br = broad. A negative Δδ value corresponds to an upfield shift. $CDCl_3/CD_3CN$ 1:1 (v/v), 298 K, 400.15 MHz. For proton numbering see Figure 1a and 3. [b] Signals too small to detect COSY and NOESY couplings, peaks assigned according to ***ZnMc/VPy*** *data.*

Doubling of the signals of protons 5-7 and of 11-13 in the ^{1}H NMR indicated the complexation of an asymmetric guest inside the host cavities, whereas the signals for the protons of both the viologen and pyridine moieties of both bifunctional guests experienced upfield shifts due to complexation to **ZnMC** (Table 2). Again, NOE signals were observed between protons C and E from **VV** with protons 6 from **ZnMC**. Additional NOE signals between protons D from **PyPy** and protons 11 and 13 from **ZnMC** indicated the axial ligation of the host by the pyridine moieties of **PyPy**.
It is remarkable that three complex molecules are driven to assemble and form a defined species with a mass of 3739 D (excluding the 4 PF_6^- counter-ions). This allosteric complex demonstrates the power of hierarchical assembly.

UV-vis titration studies of the hetero-bifunctional guest **VPy** with the host **ZnMC** revealed an association constant of roughly $K_a = 1.0 \times 10^7\ M^{-1}$ (Figure 8a). The poor fit to a simple 1:1 complex is a result of several possible binding geometries. The increase in the association constant when compared to that of **VV** ($K_a = 4.6 \times 10^6\ M^{-1}$), might indicate that the ligand acts as its own allosteric effector. (The formation of the 2:1 complex between **ZnMC** and **VPy** in which both ends of the guest molecule are bound to a different host cavity was not taken into account in the fitting model.) Molecular modelling studies suggest that a 1:1 complex between **ZnMC** and **VPy** can not adopt a conformation in which both binding moieties of the guest bind to the same host molecule, i.e. the viologen moiety of **VPy** inside the cavity of **ZnMC** and the pyridine moiety bound to the porphyrin zinc ion on the outside of the host.
The assumption that the ligand acts as its own allosteric effector in combination with the observed step in the titration, suggest that the viologen moiety is bound first, followed by allosteric assembly of two complexes into a 2:2 architecture (Figure 8b). According to ^{1}H NMR spectroscopy, the addition of 1 q equivalent of **VPy** to **ZnMC** in $CDCl_3/CD_3CN$ 1:1 (v/v) resulted in the full complexation of the viologen moiety inside the cavity and a full axial binding of pyridine to the zinc ion. The complexation of a non-symmetrical viologen inside the cavity, in combination with the axial complexation of a non-symmetrical pyridine on top of the host, evident by a upfield shift of the signal for the pyridine protons, results in a high asymmetry of the host **ZnMC**. This asymmetry is highlighted by the splitting of the NMR signals for protons 5-7, 9-11 and 13 (Table 2). The non-symmetrical conformation of the complex was also confirmed by an unequal upfield shift of the signals for the B and C protons compared to the D and E protons. The formation of a discrete 2:2 assembly could be deduced by integration from ^{1}H NMR studies. The geometry of this 2:2 assembly was deduced from COSY and NOESY 2D NMR spectra, since again NOE contacts were visible between the 6 protons and the protons C and E of the guest and between the Q protons with both 11 and 13 (Figure 8b).

a)

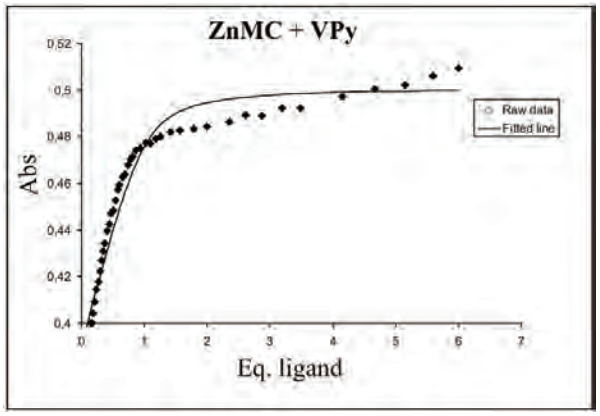

b)

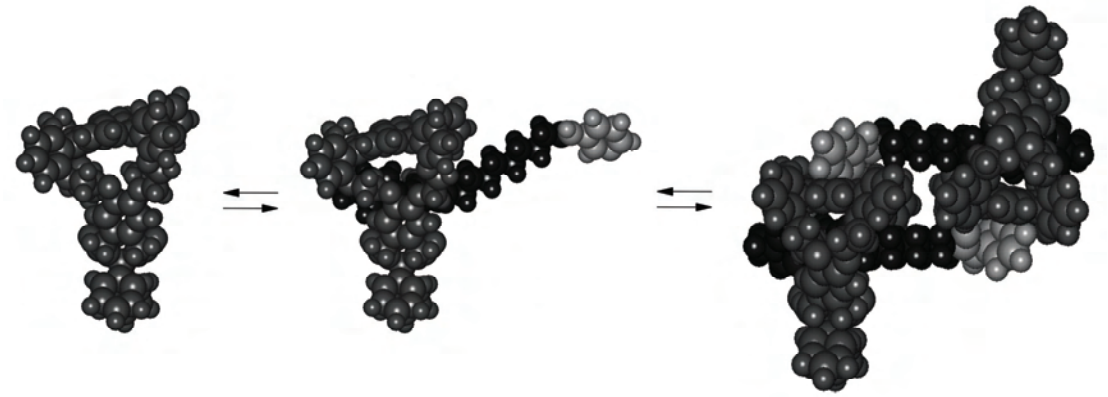

c)

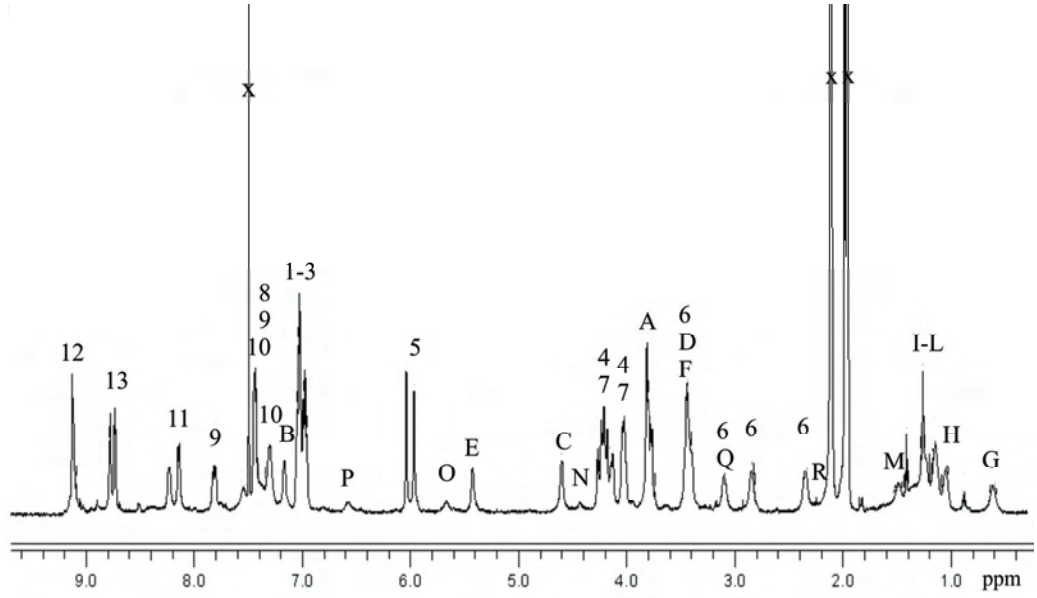

Figure 8. *a) Titration curve obtained for the binding of **VPy** in **ZnMC** measured by UV-Vis spectroscopy in $CHCl_3/CH_3CN$ 1:1 (v/v). b) Computer modelled structure of the 2:2 assembly of **ZnMC** and **VPy**. c) ^1H NMR spectrum (400.15 MHz, $CDCl_3/CD_3CN$ = 1/1 (v/v), 298K, [**ZnMC**] = 1.06 x 10^{-3} M) of a 1:1 mixture of **ZnMC** and **VPy** mixture.*

From the assembly studies above, it can be concluded that the formation of discrete assemblies is favoured over supramolecular oligomers or polymers, probably because the spacers of all the bifunctional guest have the same length. Entropy works against this discrete assembly process; the bringing together of more than a handful of molecules, however, is apparently even more unfavourable. Furthermore, the last step in the formation of the complexes of **ZnMC** with either **VPy** or with **PyPy** and **VV** consists of a cyclisation (whether it is the binding of a viologen moiety inside the host cavity or the axial ligation of a pyridine moiety to the zinc ion), increasing the stability of these complexes, as described by the effective molarity factor mentioned in Chapter 1. To investigate whether a *mismatch* with regard to the alkyl spacers between a **VV** guest and **PyPy** guest in combination with **ZnMC** would disfavour the self-assembly of the components into a discrete complex and favour the formation of polymeric structures (Figure 9b), a fourth bifunctional guest was synthesised, containing two viologen moieties, separated by an alkyl spacer of 16 CH_2-units (**V-C_{16}-V**; Figure 9a). The addition of half an equivalent of **V-C_{16}-V** and half an equivalent of **PyPy** to a solution of **ZnMC** in $CDCl_3/CD_3CN$ 1:1 (v/v) ([**ZnMC**] = 2 x 10^{-3} M) resulted in the formation of a discrete self-assembled 1:1:1 complex. This was concluded from the observation that only the signals arising from one viologen moiety of **V-C_{16}-V** and one pyridine moiety of **PyPy** showed an upfield shift in the ^{1}H NMR upon addition of the host. The formation of supramolecular polymers as depicted in Figure 9b is even in this case entropically not favourable when compared to the formation of the observed discrete host-guest complexes.

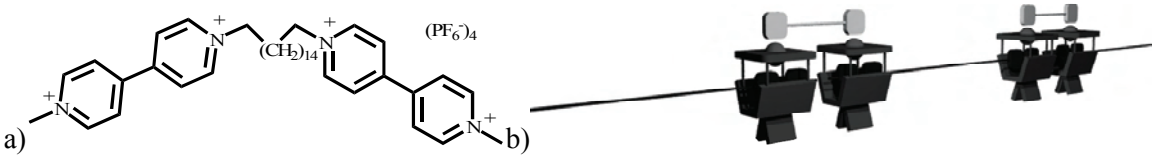

Figure 9. *a) **V-C_{16}V**. b) Host-guest polymer based on **ZnMC**, **PyPy** and **V-C16-V**.*

4.4 Self-assembled complexes containing ZnDC

In order to avoid the formation of discrete, low molecular weight self-assembled allosteric complexes as observed in the case of **ZnMC**, it was decided to switch to a double cavity host. It has been previously shown that the double-cavity porphyrin molecule **DC** exhibits negative homotropic allosteric binding behaviour upon the binding of two viologen guests (Figure 10a and b).[8a] Positive heterotropic binding behaviour was also exhibited upon complexation of **V** and **py** to the zinc porphyrin analogue of this host, **ZnDC** (Chapter 2).

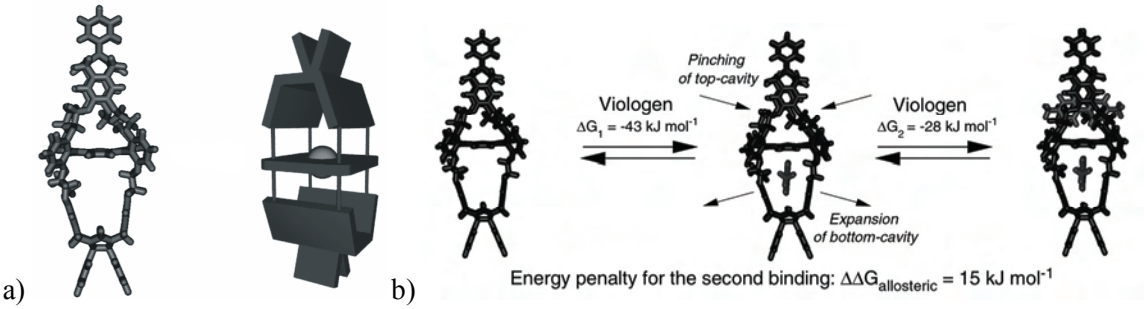

Figure 10. *a)* ***ZnDC*** *and its schematic representation. b) Negative homotropic allosteric binding behaviour of* ***DC****.*

Since the two cavities of **ZnDC** are oriented orthogonal to each other, the combination of **VPy** with **ZnDC** or **VV** and **PyPy** with **ZnDC** should in principle not result in the formation of discrete low-order assemblies, as was found for the complexes with **ZnMC**.

The binding affinities of the three different bifunctional guests for ZnDC were measured, again assuming independent (non-cooperative) binding between the two binding moieties of the bifunctional guests (Table 3). The titration curve obtained from UV-vis titration studies for the binding of **PyPy** in **ZnDC** revealed a binding constant higher than that observed for **ZnDC** and pyridine (K_a= 2.2 x 10^4 M^{-1}). This increase is probably again due to the combination of hydrogen bonding between the amide group of the guest and the carbonyl moiety of the host molecule, with the affinity of cavity porphyrins for alkyl spacers.[8]

Table 3. *Association constants* K_a[a] *and binding free energies* ΔG *for the complexation of* ***ZnDC*** *with different guests.*

Guest	K_a (M^{-1})	ΔG (kJ mol^{-1})
PyPy	4 x 10^5	-32
VV	1 x 10^8	-46
VV[b]	7 x 10^9	-56
VPy	1 x 10^6 ; 1 x 10^8	-34 ; -46

[a] *Determined by UV-vis and fluorescence spectroscopy (excitation wavelength = 426 nm; emission wavelength(max) = 605 nm). Association constants obtained from fluorescence data have been compared with the reported* K_a*-values determined from UV-vis data. They were found to be similar and are therefore not mentioned.* $CHCl_3/CH_3CN$ *= 1:1 (v/v), 298 K,* [***ZnDC***] = 2.3 x 10^{-6} *M.* [b] *Association constant in the presence of 1 equivalent* ***PyPy****.*

The bifunctional guest **VV** also had a much greater apparent affinity for the host (association constant of 1 x 10^8 M^{-1}). The observed K_a is significantly higher than for **ZnMC** (K_a= 4.6 x 10^6), assuming only a [3]pseudo-rotaxane binding motif. It is expected that **ZnDC** displays similar negative allosteric binding behaviour upon the binding of two

viologen moieties as its free-base analogue **DC**. Despite this assumption, which probably is not completely correct, an excellent fit was obtained (Figure 11b).

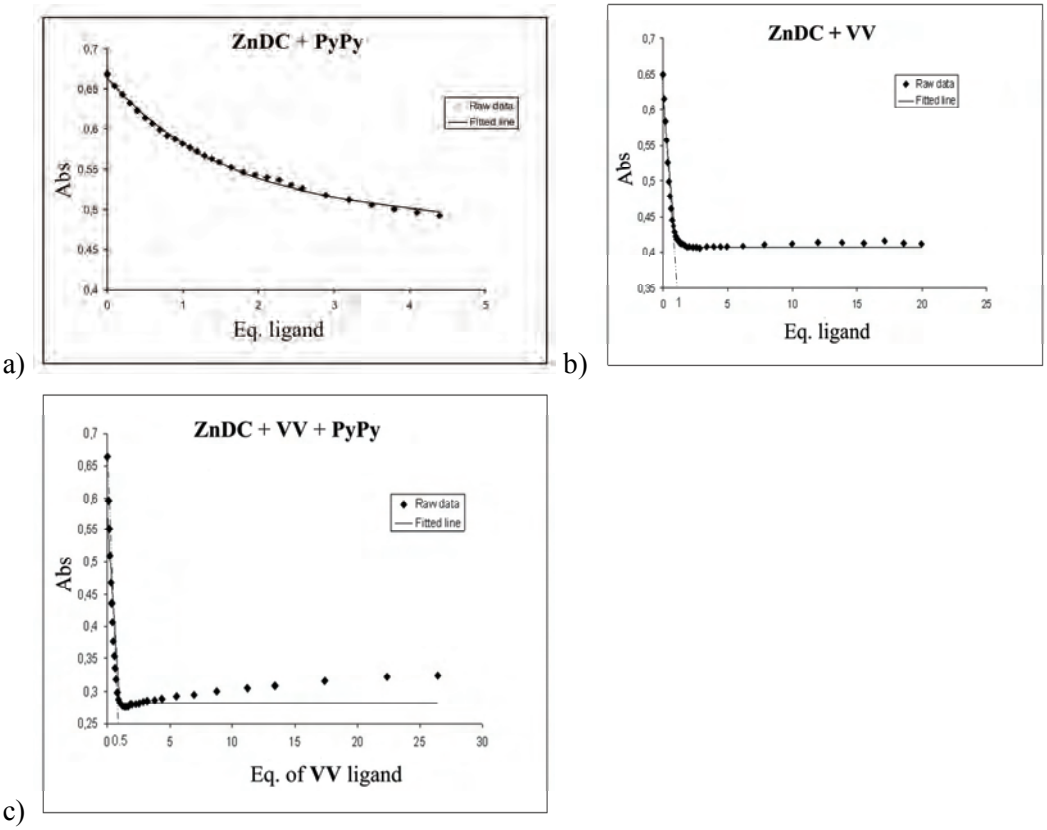

Figure 11. *a) Titration curve obtained for the binding of **PyPy** in **ZnDC** obtained by UV-vis spectroscopy in $CHCl_3/CH_3CN$ 1:1 (v/v). b and c) Titration curves obtained for the binding of **VV** in **ZnDC** obtained by UV-vis spectroscopy in $CHCl_3/CH_3CN$ 1:1 (v/v); b) in the absence of **PyPy**, and c) in the presence of 1 equivalent of **PyPy**.*

The binding titration with **VV** was repeated in the presence of 1 equivalent of **PyPy**, to study the allosteric properties of the complex. A 70-fold increase in binding constant of **VV** was observed, confirming a strong allosteric behaviour (Figure 11c). In the presence of 1 equivalent of **PyPy** only half an equivalent of **VV** was required to completely quench the fluorescence emission of the host zinc porphyrin. In the absence of **PyPy** a whole equivalent was required. A deviation between the calculated model and the observed change in absorption was observed in the latter stage of the titration. It was assumed that a 2:1 complex between **VV** and two **ZnDC** hosts exists, in which both hosts have a **PyPy** guest in one of their cavities. The mismatch between the calculated binding mode and the one that is observed, indicates that several different self-assembled structures are also being formed at higher concentrations. The formation of non-discrete self-assembled oligomers, together with the formation of [4]pseudo-rotaxanes, are the most obvious

possibilities. Further studies are in progress to see if these binding modes can be observed.

Assuming a simple 2:1 model binding geometry it was impossible to fit the binding curve of the titration of **VPy** with **ZnDC**. Similar to what was observed in the binding of the **VV** guest in the presence of 1 equivalent of **PyPy,** already the addition of half an equivalent of **Vpy** was sufficient to achieve full binding and complete fluorescence quenching. By assuming that only the viologen moiety would be engaged in binding, no adequate fit could be obtained. When it was assumed that both ends of the guest could bind, an excellent fit between the observed and calculated binding curves could be obtained, assuming two association constants $K_a(1)= 1 \times 10^6\ M^{-1}$ and $K_a(2)= 1 \times 10^8\ M^{-1}$ (Figure 12a). These values are assumed to be the K_a-values for the pyridine and the viologen moiety, respectively, since they correspond reasonably well to the K_a-values found for the two other bifunctional guests. The above assumption would indicate that for this guest the pyridine moiety does not act as an allosteric effector, since the association constants correspond to the binding of **VV** and **PyPy** separately to **ZnMC** in simple 1:2 complexes. A possible reason for this observation is that there are other factors that influence the allosteric binding, for example geometric or steric ones.
To obtain more information about the geometry of the formed complexes, ^{1}H NMR experiments were carried out on a 1:1 mixture of **ZnDC** and **VPy** in $CDCl_3/CD_3CN$ 1:1 (v/v). In contrast to the good fit in the UV-vis titration, a broad NMR spectrum was obtained in which no peaks could be assigned and no conclusions could be drawn about the structure of the complexes present in solution. When the host and guest were dissolved in a the less polar solvent mixture $CDCl_3/CD_3CN$ 19:1 (v/v), the peaks in the ^{1}H NMR sharpened up a little, but only the separate regions of the **ZnDC** could be assigned, e.g. between 8.5 and 9 ppm the signals for the β-pyrrolic protons and between 2 and 5 ppm the signals for the crown-ether moiety of the host (Figure 12b). The broadness and numerous peaks found between 5.7 and 6.4 ppm (which is the region in which normally the signal for the protons of the aromatic side-walls of **ZnDC** can be found) indicate that there are numerous different and exchanging complexes in solution. ESI-MS spectroscopic studies of this solution revealed an isotope pattern of the peak corresponding to a mass of $[\mathbf{ZnDC}:\mathbf{VPy}\text{-}PF_6]_n^{n+}$, suggesting at least four molecules of each component were present in the complex. In MALDI-TOF MS studies of the complexes in this 1:1 mixture, no finite species could be observed, due to decomplexation upon laser excitation.

a)

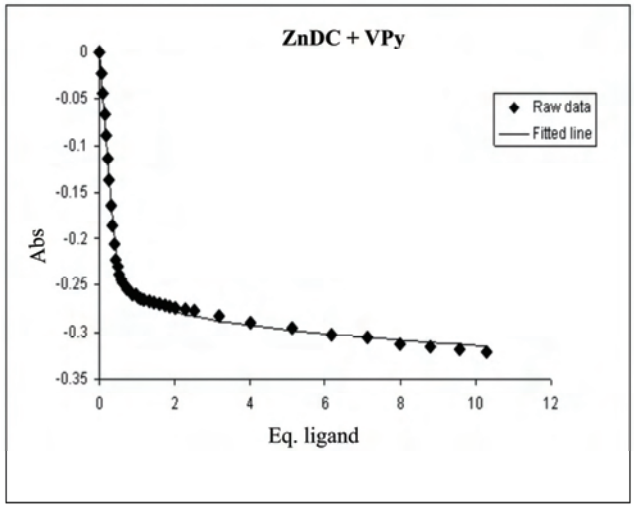

b)

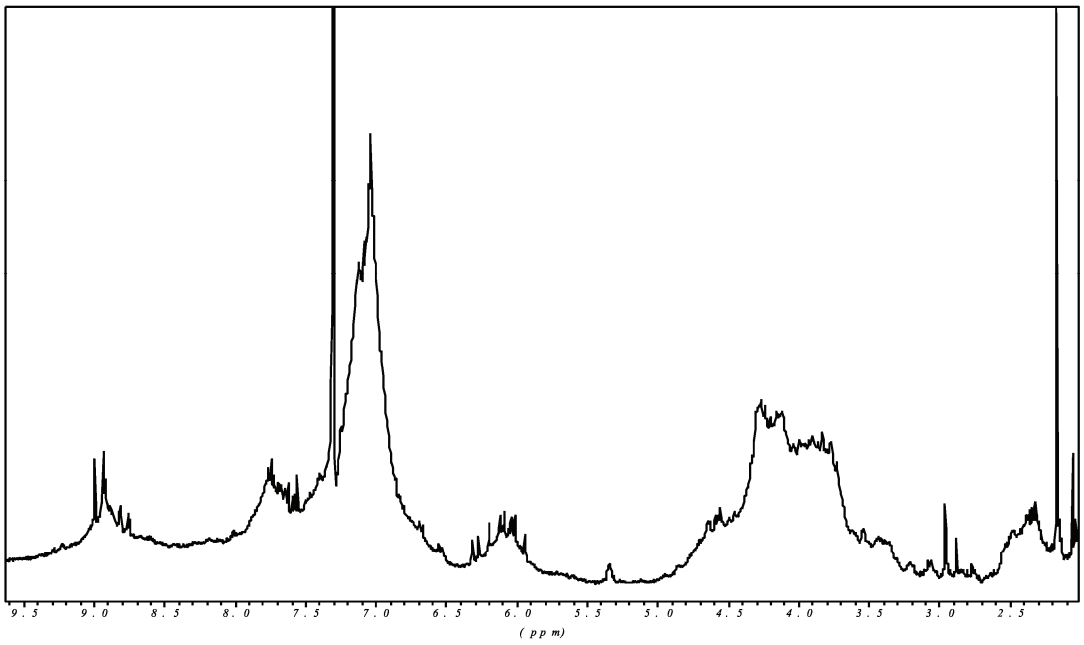

Figure 12. *a) Titration curve obtained for the binding of* ***VPy*** *in* ***ZnDC*** *obtained by UV-vis spectroscopy in $CHCl_3/CH_3CN$ 1:1 (v/v). b) ^1H NMR spectrum (400.15 MHz, $CDCl_3/CD_3CN$ = 19:1 (v/v), 298K, [**ZnDC**] = 1.10 x 10^{-3} M) of a 1:1 mixture of* ***ZnDC*** *and* ***VPy*** *.*

As an alternative investigative tool to study the complexes, a diffusion-ordered NMR (DOSY NMR) spectrum of the 1:1 mixture of **ZnDC** and **VPy** was recorded in $CDCl_3/CD_3CN$ 1:1 (v/v; [**ZnDC**] = 10^{-3} M).[11] The DOSY NMR spectrum showed only one complex with a well-defined diffusion coefficient, not multiple complexes. Using the Einstein-Stokes equation it was possible to estimate an approximate radius of this complex of 193 Å (see Experimental section). Although the concentration is not a factor in the Einstein-Stokes equation, at different concentrations, different diffusion rate values were obtained for single reference compounds. This is, however, not surprising for

supramolecular complexes. It must also be noted that the pseudo-rotaxanes are far from spherical. Due to both these factors, the obtained radius for the self-assembled complexes is not an accurate value. This observation, however, does point towards the formation of a defined complex that contains multiple host and guest molecules. Apart from supramolecular polymer structures, also "allosteric squares" can be formed, in which four host and four guest molecules form a thermodynamic structure (Figure 13, right). The possibility to assemble into different diastereoisomers can be readily envisaged, which might explain the broad and complex ^{1}H NMR spectrum. From the UV-vis studies, the DOSY NMR and the ESI-MS, it is proposed that a square 4:4 complex is formed.

Figure 13. *Schematic representation of possible self-assembled allosteric complexes in which* ***ZnDC*** *and* ***VPy*** *are incorporated in a 1:1 component.*

Additional techniques usually used for the analysis of supramolecular assemblies, e.g. viscometry and vapour pressure osmometry, are not applicable for these systems, since they require amounts of the components that are not available, in view of the low yield in the synthesis of **ZnDC**.

4.5 Conclusions

An array of bifunctional guests has been synthesised containing either two viologens or two pyridine moieties, or one viologen and one pyridine moiety. In combination with **ZnMC** these guests were shown to form discrete self-assembled complexes in solution, which according to UV-vis and fluorescence titrations displayed allosteric interactions. In order to increase the size and complexity of the assemblies, the bifunctional guests were combined with the double-cavity host **ZnDC**. The binding behaviour of this host towards the bifunctional guests proved to be complex and suggests formation of allosterically driven tetrameric assemblies. The combination of allosterism and self-assembly as demonstrated elegantly by Nature, opens genuine possibilities for the construction of hierarchical architectures. The present studies are just a first step in this direction.

4.6 Experimental

Acetonitrile-d_3 was distilled over CaH_2 and chloroform-*d* was distilled over $CaCl_2$ prior to use. **ZnMC** was synthesised according to literature procedures.[10] **ZnDC** was synthesised as described in Chapter 2. NMR spectra were obtained on Varian Unity Inova 400 and Bruker DRX 500 instruments at 298 K. All NMR studies of host-guest complexes were performed in freshly prepared $CDCl_3/CD_3CN$ 1:1 (v/v) mixtures at 1 x 10^{-3} M concentrations. All the ratios that are mentioned with regard to mixtures of hosts and guests are molar ratios. UV-vis spectra were measured on a Varian Cary 50 UV-vis spectrophotometer and MALDI-TOF MS spectra were recorded on a Bruker Biflex III spectrometer. Fluorescence titrations were performed on a Perkin Elmer Luminescence Ls50B spectrometer. UV-vis and fluorescence titration experiments and the calculation of binding constants were carried out following the standard methods reported earlier by our group.[8a,c]

Diffusion rate values were obtained using data analysis in Mestre-C 4.7.0.0 on the DOSY NMR data. The diffusion rate that was used for the calculation of the radius was an average of the diffusion rates obtained for at least six different peaks in the DOSY NMR spectrum to minimise errors. The radius was calculated from the diffusion rate, with the assumption that the viscosity of a 1:1 (v/v) mixture of $CDCl_3$ and CD_3CN is the average (0.4435×10^{-3} kg m^{-1} s^{-1}) of the viscosity values of the two individual solvents, using the rearranged Einstein-Stokes equation: $r = kT/6\pi D\eta$, in which:

r = radius (m)
k = Boltzmann's constant (JK^{-1})
T = temperature (K)
D = diffusion rate (m^2 s^{-1})
η = viscosity of the medium (kg m^{-1} s^{-1})

Synthesis of PyPy.

To 3.3 ml of triethylamine (24 mmol) and 1.6 g of 3-aminopyridine (17 mmol) in 40 mL of CH_2Cl_2 was added drop-wise at 0˚C a solution of 2.1 g of suberoyl chloride (9.8 mmol) in 3 mL of CH_2Cl_2. This mixture was stirred at 0˚C for 1 h and subsequently at room temperature for 2 h. The mixture was poured into water and a white solid was isolated *via* filtration, which was dissolved in little DMSO and this solution was again poured into water. After filtration, the resulting solid was recrystallised from boiling MeOH and by diffusion of Et_2O into a saturated MeOH solution of the compound. Yield: 73% of a white solid.

^{1}H-NMR (300 MHz, $CD_3CN/CDCl_3$ 1:1 (v/v), for proton numbering see Figure 3): δ = 8.64 (s, H_A, 2H), 8.26 (d, 2H, ^3J= 3.9 Hz, H_B), 8.19 (s, 2H, H_E), 8.08 (d, 2H, ^3J= 8.3 Hz,

H_D), 7.22 (dd, 2H, ^3J= 8.3 Hz, ^3J= 3.9 Hz, H_C), 2.37 (t, 4H, ^3J= 7.2 Hz, H_F), 1.73 (m, 4H, H_G), 1.43 (m, 4H, H_H); $^{13}C\{^1H\}$NMR (50 MHz, CD_3OD): δ = 174.59, 144.60, 141.32, 137.1, 128.47, 124.88, 37.27, 29.55, 26.08; EI-MS m/z 326 (M^+); UV-vis (MeOH) λ/nm (log(ε/$M^{-1}cm^{-1}$): 240 (4.3), 278 (3.8).

Synthesis of VV.

A mixture of 1.0 g of 1,10-dibromodecane (3.3 mmol) and 7.4 g of 4,4'-dipyridyl (47 mmol) in 50 mL of CH_3CN was refluxed overnight under nitrogen. After cooling, the resulting precipitate was filtered off and washed with Et_2O and CH_3CN. The residue was dissolved in water and after addition of a saturated aqueous NH_4PF_6 solution a precipitate was formed, which was filtered off, washed with water and dried *in vacuo*. A solution of 0.99 g of the resulting white solid and 0.33 mL pf iodomethane (5.3 mmol) in 35 mL of CH_3CN was refluxed under nitrogen for 64 h. The precipitate was filtered off and dissolved in water, and this solution was added slowly to a saturated aqueous solution of NH_4PF_6 resulting in the formation of a precipitate. The suspension was heated until the entire solid redissolved again. Upon cooling, a white solid formed, which was filtered off, washed with water and recrystallised by the diffusion of Et_2O into a saturated CH_3CN solution of the compound. Yield: 28% as a white solid.

Dp = 250 °C; ^{1}H NMR (400.15 MHz, CD_3CN, for proton numbering see Figure 3): δ = 8.85 (m, 8H, H_{B+E}), 8.37 (m, 8H, H_{C+D}), 4.60 (t, 4H, ^3J= 7.6 Hz, H_F), 4.40 (s, 6H, H_A), 2.00 (m, 4H, H_G), 1.37 (m, 12H, H_{H-J}); $^{13}C\{^1H\}$NMR (50 MHz, CD_3CN): δ = 150.83, 150.61, 147.45, 146.48, 139.98, 63.07, 49.56, 31.96, 29.93, 29.58, 26.56; MALDI-TOF m/z 628 $(M - 3\ PF_6)^+$; UV-vis (CH_3CN) λ/nm (log(ε/$M^{-1}cm^{-1}$): 265 (4.6).

Synthesis of 1-methyl-4-(4'-pyridyl)-pyridinium hexafluoro-phosphate.

A solution of 1.2 g of 4,4'-dipyridyl (7.7 mmol) and 0.57 mL of methyl iodide (9 mmol) in 5 mL of CH_2Cl_2 was refluxed overnight under nitrogen. The resulting precipitate was filtered off, redissolved in MeOH, precipitated by the addition of Et_2O, filtered off and washed with EtOH. To an aqueous solution of the resulting solid, a saturated aqueous NH_4PF_6 solution was added, which resulted in the formation of a precipitate that was filtered off. Yield: 74% of a white solid. Physical properties were in agreement with those previously reported.[12]

Synthesis of 9-bromo-(N-3-pyridyl)nonamide (4).

To a solution of 3.5 g of chromium oxide (35 mmol) in 5 mL of water at 0˚C was added drop-wise 3 mL of concentrated sulphuric acid and 10 ml of water. This solution was slowly added at -5˚C to a solution of 5.4 g of 9-bromononanol (24.2 mmol) in 250 mL of acetone. After stirring at room temperature for 2 h a green precipitate had formed, which was filtered off and discarded. The filtrate was evaporated and a solution of the resulting

solid in Et_2O was washed three times with water. The organic layer was dried with $MgSO_4$, filtered and evaporated, resulting in a product that was purified by column chromatography (silica; hexane/ethylacetate 20:1 (v/v)), yielding a white solid. A mixture of 0.41 g of this solid (1.7 mmol) and 2 mL of thionyl chloride was stirred overnight, after which excess liquid was evaporated until an oil remained that was dissolved in 5 mL of diethylether. This solution was added drop-wise to an ice-cold solution of 0.16 g 3-aminopyridine (1.7 mmol) in 15 mL of Et_2O. After warming to room temperature, the mixture was stirred overnight under nitrogen. The resulting suspension was filtered and the residue dissolved in water, after which $NaHCO_3$ was added until a pH of 8 was reached. The product was extracted with Et_2O, the organic layer washed with a saturated aqueous $NaHCO_3$ solution, dried with $MgSO_4$, filtered and evaporated. Yield: 53% of a white solid.
^{1}H NMR (300 MHz, $CDCl_3$): δ = 8.51 (d, 1H, ^3J= 2.1 Hz, NC*H*CN), 8.31 (d, 1H, ^3J= 4.2 Hz, NC*H*CC), 8.16 (d, 1H, ^3J= 8.1 Hz) , NCCC*H*, 7.35 (s, 1H, N*H*), 7.24 (m, 1H, NCC*H*C), 3.39 (t, 2H, ^3J= 6.9 Hz) , BrCH_2, 2.39 (t, 2H, ^3J= 7.5 Hz, C(O)CH_2), 1.86 (m, 2H, BrCCH_2), 1.82 (m, 2H, C(O)CCH_2), 1.35 (m, 8H, CH_2-rest).

Synthesis of VPy.
A solution of 0.1 g of 9-bromo-(N-3-pyridyl) nonamide (0.32 mmol) and 0.5 g of 1-methyl-4-(4'-pyridyl)-pyridinium hexafluorophosphate (1.58 mmol) in 500 mL of CH_3CN was stirred for 2 weeks. The precipitate was filtered off and washed three times with CH_3CN, dissolved in water, and this solution was added drop-wise to a saturated aqueous NH_4PF_6 solution. The resulting precipitate was isolated *via* centrifugation and recrystallised by diffusion of $CHCl_3$ into a saturated CH_3CN solution of the compound. Yield: 4% of a white solid.
^{1}H NMR (400.15 MHz, CD_3CN, for proton numbering see Figure 3): δ = 8.85 (m, 4H, H_{B+E}), 8.70 (s, 1H, H_R), 8.35 (m, 5H, H_{C+D+N}), 8.24 (d, 1H, ^3J= 6.6 Hz, H_Q), 8.00 (d, 1H, ^3J= 11 Hz, H_O), 7.30 (dd, 1H, ^3J= 6.6 Hz, ^3J= 11Hz, H_P) 4.60 (t, 2H, ^3J= 10 Hz, H_F), 4.39 (s, 3H, H_A) 2.34 (t, 2H, ^3J= 9.6 Hz, H_M), 2.02 (m, 2H, H_G), 1.65 (m, 2H, H_L), 1.40 (m, 8H, H_{H-K}); MALDI-TOF m/z 550 $(M - PF_6)^+$.

Synthesis of *N*1-(3-pyridyl)butanamide.
A solution of 0.45 g of butyryl chloride (4.22 mmol) in 2 mL of CH_2Cl_2 was added drop-wise to an ice-cold solution of 0.40 g of 3-aminopyridine (4.25 mmol) in 10 mL of CH_2Cl_2 and 0.82 ml of triethylamine (6 mmol). This solution was stirred for 1 h at 0ºC and at room temperature for 2 hrs, after which it was washed with water. The product that was obtained after evaporation of the organic layer, and was purified by column chromatography (silica; 6% MeOH in $CHCl_3$) to yield an off-white oil. Yield: 68%.

^{1}H NMR (400.15 MHz, $CDCl_3$): δ = 8.56 (d, 1H, ^4J= 2.4 Hz, *H2*), 8.33 (d, 1H, ^3J= 3.9 Hz, *H6*), 8.21 (d, 1H, ^3J= 8.32 Hz, *H3*), 7.86 (br s, 1H, N*H*), 7.28 (t, 1H, ^3J= 4.64 Hz, *H3*), 2.38 (t, 2H, ^3J= 7.08 Hz, C(O)CH_2), 1.77 (se, 2H, ^3J= 7.60 Hz, C(O)CCH_2), 1.01 (t, 3H, ^3J= 7.36 Hz, CH_3).

Synthesis of V-C_{16}-V.

To a suspension of 1.0 g of 1,16-dihydroxyhexadecane (3.8 mmol) in 20 mL of Et_2O was added drop-wise 0.24 mL of PBr_3 (2.5 mmol), after which the suspension was refluxed for 5 h, during which the solid dissolved. After cooling, the solution was poured into 50 mL of water and this suspension was extracted three times with CH_2Cl_2. The combined organic layers were dried with Na_2SO_4, filtered and the solvent was evaporated. The resulting solid was recrystallised from boiling EtOH to yield 1,16-dibromohexadecane. A mixture of 0.556 g of 1,16-dibromohexadecane (1.44 mmol) and 2.25 g of 4,4'-dipyridyl (14.4 mmol) in 25 mL of DMF was stirred at 90°C for 3 days under nitrogen. After cooling, the resulting precipitate was filtered off and washed with Et_2O and CH_3CN. The filtrate was evaporated and the residue was dissolved in DMSO. After the addition of a saturated aqueous NH_4PF_6 solution a precipitate was formed, which was filtered off, washed with water and dried *in vacuo*. A solution of 65 mg of the resulting white solid and 1 mL of iodomethane (16 mmol) was refluxed in 15 mL of CH_3CN for 14 h under nitrogen. The precipitate was filtered off and added to a saturated aqueous NH_4PF_6 solution. This mixture was heated to 100°C three times after which the precipitate that formed upon cooling was white. This solid was filtered off, washed with water and Et_2O and dried *in vacuo*. Yield: 30% as a white solid.

^{1}H NMR (400.15 MHz, $CDCl_3$/CD_3CN 1:1 (v/v), proton numbering see Figure 3 for the **VV** analogue): δ = 8.86 (m, 8H, H_{B+E}), 8.38 (m, 8H, H_{C+D}), 4.59 (t, 4H, ^3J= 7.6 Hz, H_F), 4.41 (s, 6H, H_A), 2.10 (m, 4H, H_G), 1.35 (m, 24H, CH_2-rest).

References

1. a) *Supramolecular Polymers*, 2nd ed.; Ciferri, A., Ed.; CRC Press: Taylor and Francis: Boca Raton, FL, 2005.
   b) C. Fouquey, J.-M. Lehn, A.M. Levelut, *Adv. Mater.* **1990**, *2*, 254-257.
2. G.B.W.L. Ligthart, H. Ohkawa, R.P. Sijbesma, E.W.Meijer, *J. Am. Chem. Soc.,* 2005, **127**, 810-811.
3. a) A. Gesquiere, S. De Feyter, F.C. De Schryver, F. Schoonbeek, J. Van Esch, R.M. Kellogg, B.L. Feringa, *Nano Lett.,* 2001, ***1***, 201-206.
   b) F. Lortie, S. Boileau, L. Bouteiller, C. Chassenieux, F. Lauprêtre, *Macromolecules*, 2005, **38**, 5283-5287.
   c) S. Sivakova, D.A. Bohnsack, M.E. Mackay, P. Suwanmala, S.J. Rowan, *J. Am. Chem. Soc.,* 2005, **127**, 18202-18211.

d) E. Kolomiets, E. Buhler, S.J. Candau, J.-M. Lehn, *Macromolecules,* 2006, **39**, 1173-1181.

4. a) L. Brunsveld, B.J.B. Folmer, E.W. Meijer, R.P. Sijbesma, *Chem. Rev.,* 2001, **101**, 4071-4097.
   b) M. Sayar, S.I. Stupp, *Phys. Rev. E: Stat., Nonlin., and Soft Matter Phys.,* 2005, **72**, 011803/1.
   c) N.C. Gianneschi, M.S. Masar III, C.A. Mirkin, *Acc. Chem. Res.*, 2005, **38**, 825-837.
   d) D. Knapton, P.K. Iyer, S.J. Rowan, C. Weder, *Macromolecules*, 2006, **39**, 4069-4075.
   e) L. Zhao, W.-Y. Wong, T.C.W. Mak, *Chem. Eur. J.,* 2006, **12**, 4865-4872.
   f) J.M.J. Paulusse, J.P.J. Huijbers, R.P. Sijbesma, *Chem. Eur. J.,* 2006, **12**, 4928-4934.
   g) V.H.G. Tellini, A. Jover, J.C. García, L. Galantini, F. Meijide, J.V. Tato, *J. Am. Chem. Soc.,* 2006, **128**, 5728-5734.
5. a) M. Takeuchi, M. Ikeda, A. Sugasaki, S. Shinkai, *Acc. Chem. Res.,* 2001, **34**, 865-873.
   b) L. Kovbasyuk, R. Kramer, *Chem. Rev.,* 2004, **104**, 3161-3188.
   c) J.D. Badjíc, A. Nelson, S.J. Cantrill, W.B. Turnbull, J.F. Stoddart, *Acc. Chem. Res.,* 2005, **38**, 723-732.
6. *An example of a cooperative supramolecular polymer:* H. Kautz, D.J.M. van Beek, R.P. Sijbesma, E.W. Meijer, *Macromolecules*, 2006, **39**, 4265-4267.
7. J. Monod, J. Wyman, J.P. Changeux, *J. Mol. Biol.,* 1965, **12**, 88-118.
8. a) P. Thordarson, E.J.A. Bijsterveld, J.A.A.W. Elemans, P. Kasák, R.J.M. Nolte, A.E. Rowan, *J. Am. Chem. Soc.,* 2003, **125**, 1186-1187.
   b) P. Thordarson, E.J.A. Bijsterveld, A.E. Rowan, R.J.M. Nolte, *Nature,* 2003, **424**, 915-918.
   c) P. Thordarson, R.G.E. Coumans, J.A.A.W. Elemans, P.J. Thomassen, J. Visser, A.E. Rowan, R.J.M. Nolte, *Angew. Chem. Int. Ed.,* 2004, **43**, 4755-4759.
   d) J.A.A.W. Elemans, E.J.A. Bijsterveld, A.E. Rowan, R.J.M. Nolte, *Eur. J. Org. Chem.*, 2007, 751-757.
9. K. Tranchepain, F. Le Berre, A. Dureault, Y. Le Merrer, J.C. Depezay, *Tetrahedron*, 1989, **45**, 2057-2065.
10. J.A.A.W. Elemans, M.B. Claase, P.P.M. Aarts, A.E. Rowan, A.P.H.J. Schenning, R.J.M. Nolte, *J. Org. Chem.*, 1999, **64**, 7009-7016.
11. *Reviews on DOSY NMR:*
    a) D. Wu, A. Chen, C.S. Johnson Jr., *Bull. Magn. Res.*, 1995, **17**, 21-26.
    b) G.A. Morris, H. Barjat, *Anal. Spectrosc. Libr.*, 1997, **8**, 211-226.
    c) C.S. Johnson Jr. *Prog. Nucl. Magn. Reson. Spectrosc.*, 1999, **34**, 203-256.
    d) M.J. Shapiro, J.S. Gounarides, *Prog. Nucl. Magn. Reson. Spectrosc.*, 1999, **35**, 153-200.
    e) G.A. Morris, *Encycl. Nucl. Magn. Reson.*, 2002, **9**, 35-44.
    f) R. Huo, R.Wehrens, J. van Duynhoven, L.M.C. Buydens, *Anal. Chim. Acta*, 2003, **490**, 231-251.
    g) J.C. Cobas, P. Groves, M. Martin-Pastor, A. de Capua, *Curr. Anal. Chem.*, 2005, **1**, 289-305.
    Examples of DOSY NMR on supramolecular complexes:
    g) R.S.K. Kishore, T. Paululat, M. Schmittel, *Chem. Eur. J.*, 2006, **12**, 8136-8149.
    h) L. Allouche, A. Marquis, J.-M. Lehn, *Chem. Eur. J.*, 2006, **12**, 7520-7525.

i) C.-C. You, C. Hippius, M. Gruene, F. Wuerthner, *Chem. Eur. J.*, 2006, **12**, 7510-7519.
j) H. Jiang, W. Lin, *J. Am. Chem. Soc.*, 2006, **128**, 11286-11297.
Example of DOSY NMR in a mixed solvent system:
k) G. Pages, C. Delaurent, S. Caldarelli, *Anal. Chem.*, 2006, **78**, 561-566.
12. Park, Y. S.; Lee, E. J.; Chun, Y. S.; Yoon, Y. D.; Yoon, K. B. *J. Am. Chem. Soc*, 2002, **124**, 7123-7135.

Chapter 5. Self-assembly studies of allosteric photosynthetic antenna model systems

5.1 Introduction

One of the most fundamental steps in the process of photosynthesis is the photo-induced charge separation, which takes place in the photosynthetic reaction centre.[1] At this centre a photon of solar energy is delivered from the antenna and converted into chemical energy.[2] The study of synthetic chromophoric arrays capable of electron and energy transfer has therefore been of great biological relevance and consequently a large number of covalently linked porphyrin-containing donor-acceptor systems have been synthesised and their photodynamic properties have been studied in great detail.[3,4] Zinc and copper porphyrins are typical examples of electron donors, whereas gold porphyrins are commonly used as electron acceptors.[5-7] More commonly quinones, viologens and fullerenes have been used as electron acceptors in the electron transfer cascade reactions following the photo-excitation of the donor.[8-10]

In Nature, however, the chromophores are all *non-covalently* attached to a protein scaffold, which positions them at the correct spatial separation and orientation which allows for the fast, unidirectional and efficient electron transfer (**ET**). This supramolecular assembly of donor and acceptor, as simple biomimetic photosynthetic reaction centres, has also been extensively mimicked.[11]

In contrast to the above, the use of cooperative and allosteric interactions for the self-assembly of photo-active complexes has so far been largely unexplored. It has been shown, however, that the exploitation of cooperative coordination interactions between chromophores has considerable advantages over using hydrogen-bonding or standard non-cooperative coordination chemistry.[12]

A special case of cooperativity, in which a binding event in a multivalent host at one site causes a discrete, reversible alteration in the structure of the host at a remote binding site, is called allosterism.[13] Allosteric interactions can be both positive and negative, and can act between a host and identical guests (homotropic), or between a host and different guests (heterotropic).

Recently our group has developed several porphyrin-based host-guest systems that display unique allosteric effects.[14] One of these systems was based on a mono-cavity-appended zinc porphyrin host **ZnMC** that has a strong affinity for both viologen guests (**V**) and axial ligands and exhibits a positive heterotropic binding behaviour (see Chapter 1).[14b, 15]

It was demonstrated that these allosteric interactions can be employed in the self-assembly of host-guest systems to increase the percentage ratio of the host-guest complex

in solution relative to their separate, uncomplexed components, a form of allosteric magnification.

In the above mentioned systems the fluorescence of zinc porphyrins upon photo-excitation can be readily quenched *via* electron transfer to nearby viologens (4,4'-bipyridines). These energy acceptors can be either covalently bound or complexed *via* supramolecular interactions and have been often used as a useful tool for the determination of the association constants for viologen guests inside the cavity of **ZnMC**.[15-17] The aforementioned gold porphyrins are known to possess an energy level even lower than that of viologens. In principle if a central gold porphyrin were to be decorated with one or more covalently attached viologen electron-acceptor moieties, which also have an affinity for the cavity of **ZnMC,** a unique electron transfer complex could be assembled. In such a system, a photo-excited electron could be transferred upon excitation from the zinc porphyrin *via* the viologen to the gold porphyrin to form a (usually short-lived) charge-separated state. In addition such a supramolecular complex of this nature could be manipulatable and fine-tuned by the employment of allosteric interactions.

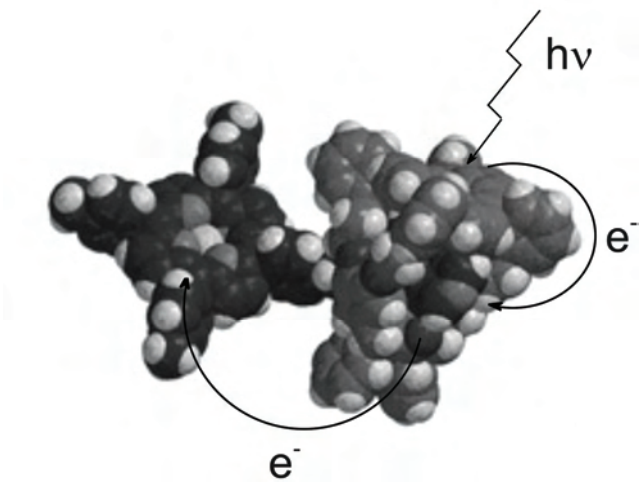

Figure 1. *Schematic representation of possible* ***ET*** *processes in [2]-pseudo-rotaxane containing* ***ZnMC*** *and a gold porphyrin functionalised with a viologen-like moiety.*

Towards the goal of developing a supramolecular complex that exhibits both electron transfer upon photo-excitation as well as allosteric binding behaviour, two new model antenna systems have been constructed using allosteric interactions to tune the assembly. The molecular components used in this study are **ZnMC**, the axial ligand 4-*tert*-butylpyridine (**tbpy**), non-methylated-4,4'-bipyridine appended Au-porphyrin (**AuP-bipy)**, and its analogue with *four* non-methylated-4,4'-bipyridines covalently attached to the Au-porphyrin (**AuP-(bipy)$_4$**; Figure 2a). Self-assembly of these components in solution results in equilibrium mixtures containing the pseudo-rotaxane complexes (**AuP-bipy**)-**ZnMC** and (**AuP-(bipy)$_4$**)-(**ZnMC**)$_4$, respectively (Figure 2b). Following from the

known allosteric binding properties of **ZnMC**, this chapter describes the studies into whether the addition of the ligand **tbpy**, which axially binds to the porphyrin zinc ion, effects these equilibriums, driving them through to completion of the formation of the complexes, resulting in the pseudo-rotaxanes (**AuP-bipy**)-**ZnMC**-**tbpy** and (**AuP-(bipy)$_4$**)-(**ZnMC**)$_4$-(**tbpy**)$_4$, respectively.

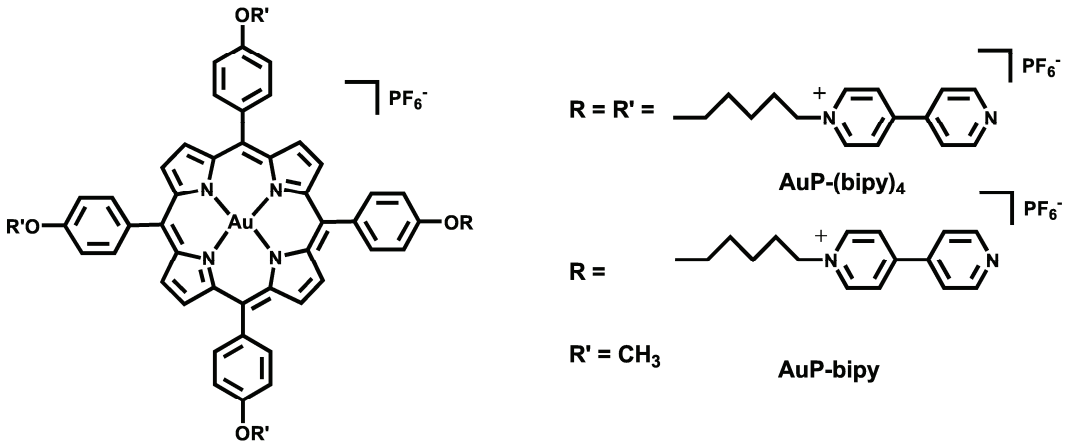

a)

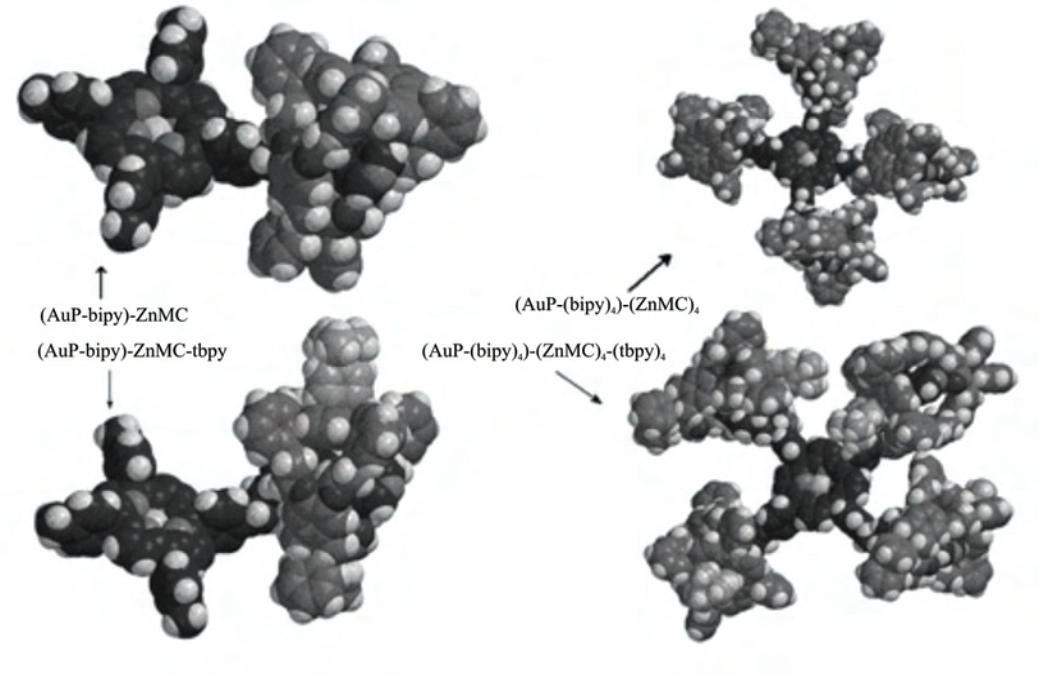

b)

Figure 2. *a) Gold porphyrin building blocks used in the construction of rotaxane antenna systems. b) Molecular modelled (PM3) optimised structures of (**AuP-bipy**)-**ZnMC**, (**AuP-bipy**)-(**ZnMC**)-**tbpy** and the (MMFF) optimised structures of the (**AuP-(bipy)$_4$**)-(**ZnMC**)$_4$ and (**AuP-(bipy)$_4$**)-(**ZnMC**)$_4$-(**tbpy**)$_4$ pseudo-rotaxane complexes.*

5.2 Model studies using mono-substituted bipyridines

In earlier work it has been demonstrated that **ZnMC** binds viologen derivatives very strongly inside its cavity ($K_{ass}>10^5$ M^{-1}) and that the bulky ligand **tbpy** can coordinate simultaneously to the porphyrin zinc ion at the outside of the cavity.[16]
To establish whether mono-substituted bipyridines would also display strong binding inside the cavity of **ZnMC,** three different model compounds of this class were synthesised, **M-bipy, P-bipy** and **T-bipy** (Scheme 1). Mono-substituted bipyridine moieties were used in these studies in contrast to viologens, because previous research had suggested that the association constants of these last moieties were lower than of their mono-substituted analogues for binding to **ZnMC**. This turned out not to be true, during the investigations performed for this chapter.

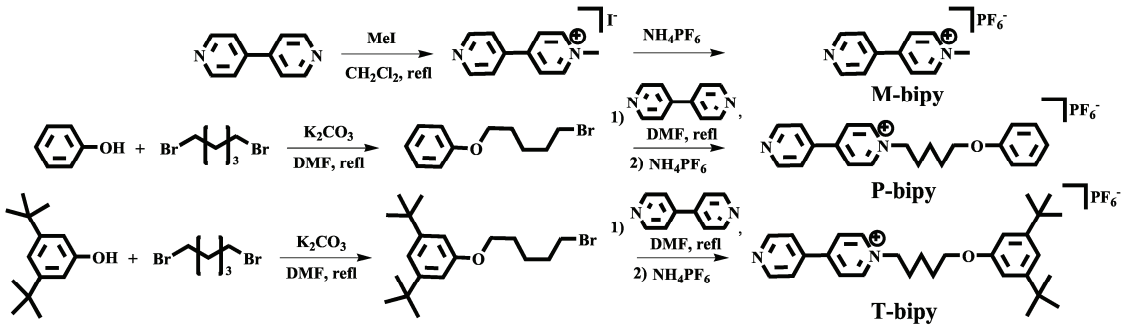

Scheme 1. *Synthesis of mono-substituted bipyridines.*

5.2.1 Synthesis

M-bipy was synthesised by refluxing 4,4'-bipyridine with one equivalent of methyl iodide in dichloromethane for 14 hours, followed by an exchange of the iodide anion for a hexafluorophosphate anion through the addition of an aqueous ammonium hexafluorophosphate solution to an aqueous solution of the iodide salt, resulting in the precipitation of the desired compound (Scheme 1).
The reaction of phenol with one equivalent of 1,5-dibromopentane in DMF yielded 1-[(5-bromopentyl)oxy]benzene, which was subsequently reacted with an excess of 4,4'-bipyridine in DMF to yield the bromide salt of **P-bipy**. The same procedure as for **M-bipy** was employed to yield the desired hexafluorophosphate salt. **T-bipy** was synthesised analogous to **P-bipy**, but with 3,5-di(*tert*-butyl)phenol instead of phenol.

5.2.2 Binding studies

^{1}H-NMR measurements revealed that the mono-functionalised **M-bipy** complexes inside the cavity of **ZnMC** at a concentration of 10^{-3} M in $CDCl_3/CD_3CN$ 1:1 (v/v). This binding is reflected in both the crown-ether proton signals and the proton signals of the aromatic side-walls of **ZnMC** being severely broadened and shifted upfield by -0.3 ppm (Table 1, for the proton numbering see Figure 4). The broadening is attributed to the non-symmetry of the host-guest complex and a rapid exchange between the free species and the complex in solution. This complexation-decomplexation process is too rapid on the NMR timescale (400MHz) and hence a broad average signal is observed. The proton signals of **M-bipy** were not observed, due to coalescence of the signals of the bound and unbound species at the measured temperature.

A fluorescence titration study, in which **M-bipy** was titrated with **ZnMC,** revealed a 6% quenching of the fluorescence of the zinc porphyrin at 605 nm (excitation 426 nm) after the addition of 1 equivalent and of 97% after the addition of 100 equivalents of this guest (Figure 3, Table 2). Upon addition of the guest the Soret band of **ZnMC** was observed to shift to higher wavenumbers. From UV-vis titrations, a binding constant of $K_a = 7.5 \times 10^4$ M^{-1} was calculated. At a ratio of **ZnMC**/**M-bipy** = 1:1, this value indicates an occupation of the host cavity of only 7% at a concentration of 10^{-6} M and of 95% at a ratio host:guest ratio of 1:100, which corresponds well with the observed fluorescence quenching of 6% and 97% at the same ratios. The observed fluorescence behaviour confirms the conclusion by Milgrom *et al.* that mono-substituted bipyridines, just like viologens, are effective quenchers of Zn porphyrin fluorescence as a result of fast **ET** from the porphyrin to the mono-alkylated bipyridinium unit, which was tentatively attributed by them to a weak ligation of the latter to the zinc ion.[17]

As a control experiment the binding of **M-bipy** to a simple Zn tetrakis-meso-*p*-toluyl-porphyrin (**ZnTTP**) showed no axial ligation at a concentration of 10^{-3} M in $CDCl_3/CD_3CN$ 1:1 (v/v), according to ^{1}H-NMR. It can therefore be concluded that binding of this guest occurs on the inside of the cavity of **ZnMC**. A fluorescence titration in which **M-bipy** was added to **ZnTTP** gave only a maximum of 13% quenching of fluorescence after the addition of 500 eq of **M-bipy** (Table 2). This quenching may be attributed to several factors; a) a solvent effect, which is the result of an increase in ionic strength of the solution, and b) a binding mode of **M-bipy** parallel to the porphyrin plane due to weak π-π interactions which allows for quenching, or c) a very weak binding of the pyridine moiety of the guest to **ZnMC**, which is too small to be seen by NMR.

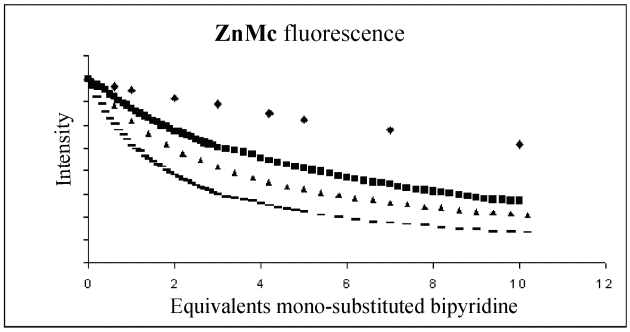

Figure 3. *Fluorescence quenching of **ZnMC** by **M-bipy**, **P-bipy** and **T-bipy** in the presence of 500 eq of **tbpy**. ♦ **ZnMC** + **M-bipy**; ■ **ZnMC** + **P-bipy**; ─ **ZnMC/tbpy** + **P-bipy**; ▲**ZnMC** + **T-bipy**. $CHCl_3/CH_3CN$ = 1:1 (v/v). T = 298 K. Excitation wavelength = 426 nm. Emission wavelength = 605 nm. [**ZnMC**] = 10^{-6} M.*

To investigate what effect an alkyl chain spacer between the porphyrin and the viologen in the guest has on the host-guest binding properties and the photophysical properties of the system, model studies were carried out with compound **P-bipy**. ^{1}H-NMR measurements of the complexes at a concentration of 10^{-3} M in $CDCl_3/CD_3CN$ 1:1 (v/v) again showed that the guest was bound inside the cavity of the **ZnMC** host. In contrast to the studies with **M-bipy**, sharp signals were observed for the bipyridine protons, which were shifted strongly upfield (Table 1). Apparently, the presence of the alkyl chain spacer allows for a better binding and a stronger complex to be formed, slowing down the exchange process between bound and unbound species. From the observed chemical shifts it can be concluded that the **P-bipy** guest is bound in a non-symmetrical geometry in the **ZnMC** host. The porphyrin is shifted towards the alkyl chain (the induced chemical shift of the signals of the α-protons is larger than that of the signals of the α'-protons; Figure 4), which is in agreement with the previously reported affinity of porphyrin clips for viologens with alkyl chains.[16b]

From UV-vis titrations a binding constant K_a= 2.2 x 10^5 M^{-1} was determined. The observed slower complexation-decomplexation process can be attributed to this increase in binding constant when compared to **M-bipy**. The addition of 10 eq of **P-bipy** to **ZnMC** resulted in the quenching of the fluorescence emission of 66%, which corresponds perfectly with the calculated 67% occupation of the host at the used concentration of 10^{-6} M (Table 2).

When the UV-vis titration of **ZnMC** with **P-bipy** was carried out in the presence of 500 eq of **tbpy**, the K_a-value increased to 6.8 x 10^5 M^{-1} as a result of allosteric effects.[14b] In this case, the quenching of the fluorescence of **ZnMC** after addition of 10 eq **P-bipy** rose to 84%, as a result of "allosteric quenching magnification" (AQM) which corresponds well with the calculated 86% abundance of the host-guest complex at this concentration.

In a reverse approach, the addition of 500 eq of **tbpy** to a 1:1 mixture of **ZnMC** and **P-bipy** in $CHCl_3/CH_3CN$ 1:1 (v/v), resulted in an AQM of the initial fluorescence by 46%. By using the respective binding constants and a simple host-guest equilibrium, an increase in population of the host-guest complex from 16% to 32% can be calculated. The addition of 500 eq **tbpy** to a solution of exclusively **ZnMC** resulted in a fluorescence quenching of only 10% (this being the result of solvent effects).

Table 1. *Induced chemical shifts[a] ($\Delta\delta$, ppm) of proton signals in the ^{1}H-NMR upon binding of mono-substituted bipyridine guests in the cavity of **ZnMC**.*

	α	β	α'	β'	γ	1a	2a	2b	3a	3b
Ref.[b]	8.83	8.27	8.74	7.71	4.56	6.20	3.52	3.23	4.17	4.07
M-bipy	-	-	-	-	-	-0.3[c]	-0.3[c]	-0.3[c]	-0.3[c]	-0.3[c]
P-bipy	-5.07	-3.95	-2.97	-3.83	-1.43	-0.17	-0.14	-0.10	0.14	0.01
T-bipy	-5.14	-4.00	-2.98	-3.84	-1.44	-0.16	-0.12[d]	-0.42[d]	0.15[d]	-0.23[d]
							-0.39[e]	-0.85[e]	-0.02[e]	-0.23[e]
AuP-bipy	-5.37	-4.14	-2.97	-3.76	-1.42	-0.06	-0.06[d]	-0.36[d]	0.23[d]	-0.30[d]
							-0.32[e]	-[f]	-0.03[e]	-0.30[e]
AuP-bipy$_4$	-	-	-2.94	-	-1.41	0.03	0.01	-0.08	0.24	0.09

*[a] $CDCl_3/CD_3CN$ = 1:1 (v/v). [**ZnMC**] = [guest] = 10^{-3} M. T = 298 K. A shift with a negative value represents an upfield shift and vice versa. For proton numbering see Figure 4. [b] Proton signals of **ZnMC** or the respective guests in the uncomplexed form. [c] Broad signals. [d] Proton signals from the side of **ZnMC** where the unfunctionalised pyridine ring of the guest is situated. [e] Proton signals from the side of **ZnMC** where the R-group is situated. [f] The signal can not be distinguished from the H_2O signal.*

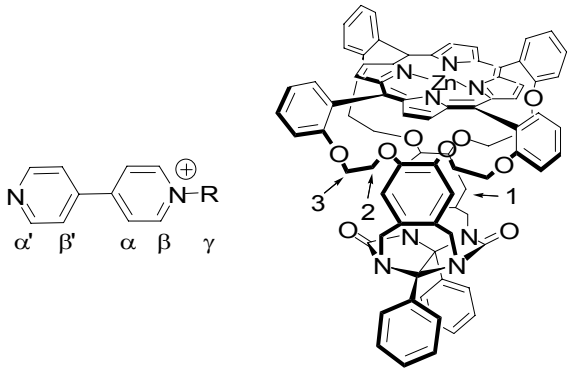

Figure 4. *Proton numbering of **ZnMC** and mono-substituted bipyridine molecules.*

As a third reference compound, **T-bipy** was also investigated. This guest is terminated with a 3,5-di-*tert*-butyl-benzene stopper group which is so bulky that **ZnMC** can only bind to the bipyridine unit from one side (Scheme 1). ^{1}H-NMR experiments of the complex at a concentration of 10^{-3} M in $CDCl_3/CD_3CN$ 1:1 (v/v) showed a similar

binding geometry as to that found for the complex of **ZnMc** with **P-bipy** (Table 1). As seen above, the bipyridine unit is complexed non-symmetrically in the cavity. In addition, the crown ether signals of **ZnMC** also show asymmetric splitting into two sets of signals, indicating a 'front'- and a 'back'-side, where the front side is defined as the side of the **ZnMC** host where the alkyl chain protrudes from the cavity. The signals of the β-pyrrolic protons situated above the cavity side-walls are also split into two singlets, again highlighting the loss of symmetry in the host upon binding of an unsymmetric guest. The sharpness of the signals also indicates that the complex is even more defined than the complex for **ZnMC** with **P-bipy**.

UV-vis titrations in which **T-bipy** was added to **ZnMC** showed an increase in binding constant compared to **P-bipy** (Table 2). This increase in complexation strength is reflected in an increased observed fluorescence quenching of the zinc porphyrin by this guest than the quenching by **P-bipy** under the same conditions (from 66% to 74%).

Table 2. *Quenching (Q_F) of Zn porphyrin (P) fluorescence[a] and calculated association constants K_a (M^{-1}) and free energies ΔG (kJ mol^{-1}) with various ligands L in the absence and presence of substrates R.*

P	L	R	Q_F (1 eq)	Q_F (10 eq)	Total Q_F	K_{ass}[b]	ΔG	Q_F[c]
ZnMC	**M-bipy**		6%	35%	97% (100 eq)	7.5×10^4	-28	
ZnMC	**P-bipy**		19%	66%		2.2×10^5	-30	
ZnMC	**P-bipy**	**tbpy**	36%	84%		6.8×10^5	-33	1.9
ZnMC	**T-bipy**		22%	74%		3.6×10^5	-32	
ZnMC	**tbpy**				10% (500 eq)	4×10^2	-15	
ZnMC	**tbpy**	**P-bipy**			46%[d] (500 eq)	1.9×10^3	-19	
ZnTTP	**M-bipy**			3%	13% (500 eq)	7.6×10^3	-22	
ZnMC	**AuP-bipy**		17%	75%		3×10^5	-31	
ZnMC	**AuP-bipy**	**tbpy**	34%	90%		8×10^5	-34	2.0
ZnMC	**tbpy**	**AuP-bipy**			14%[d] (500 eq)			
ZnMC	**AuP-(bipy)$_4$**		20%[e]	88%[e]		7×10^5	-33	
ZnMC	**AuP-(bipy)$_4$**	**tbpy**	18%[e]	83%[e]		4×10^5	-32	0.9
ZnMC	**tbpy**	**AuP-(bipy)$_4$**			10%[d]			

[a] *Excitation wavelength = 426 nm. Emission wavelength = 560 nm. T = 298 K. $CHCl_3/CH_3CN$ = 1/1 (v/v). [**ZnMC**] = [**ZnTTP**] = 10^{-6} M.* [b] *Association constants obtained from fluorescence data have been compared with the reported K_{ass}-values determined from UV-vis data. They were found to be similar and are therefore not mentioned. In their calculation it was assumed that the quantum yield of the host and of the host-guest complexes are the same.* [c] *Allosteric Quenching Magnification Factor: (observed percentage zinc porphyrin quenching by 1 eq of guest in the absence of **tbpy**)/(observed percentage zinc porphyrin quenching by 1 eq of guest in the presence of 500 eq **tbpy**).* [d] *Observed percentage of the quenching of zinc porphyrin fluorescence relative to the fluorescence in the absence of **tbpy**.* [e] *Equivalents of mono-substituted bipyridine guest (corresponds to 4 x [**AuP-(bipy)$_4$**]).*

5.3 Gold porphyrin antenna systems

A wide variety of both free base and zinc porphyrin-viologen arrays have been studied in the literature.[9] In those studies it was found that linked viologens are efficient quenchers of both the excited singlet and triplet states of the central porphyrin. In general a through-solvent **ET** process from the central porphyrin to the viologen was cautiously suggested.[9c,d] It was of interest to see if such a process would also occur in our host-guest systems.

5.3.1 Synthesis

The insertion of gold into the central porphyrin shifts the absorption of this porphyrin away from that of a zinc porphyrin, allowing the selective excitation of the latter without exciting the former.[7] The use of gold porphyrins as electron acceptors for electron-donating photo-excited zinc porphyrins has been well-described in literature, however, the precise process of electron transfer still remains unclear.[18]
To construct the gold porphyrin rotaxane mimics, the free-base porphyrin-bipyridine arrays were first synthesised according to the procedure described in literature.[9a,b] Gold was then inserted into these compounds by refluxing them in the presence of $KAuCl_4$ and NaOAc in acetic acid to give quantitatively **AuP-bipy** and **AuP-(bipy)$_4$** .[19]

5.3.2 Binding studies

The UV-vis absorption spectrum of a 1:1 mixture of **ZnMC** and **AuP-bipy** in $CHCl_3/CH_3CN$ = 1:1 (v/v) at a concentration of 10^{-6} M is almost a superposition of the UV-vis spectra of the respective pure compounds (Figure 5). The Soret band of **ZnMC** is, however, observed to be red-shifted by 3 nm, because even at this low concentration a percentage of the bipyridine units of **AuP-bipy** is complexed inside the host. The absence of large shifts or appearance of new peaks suggests that there is no significant ground-state electronic interaction between the two components.
The ^{1}H-NMR spectrum of a 1:1 mixture of **AuP-bipy** and **ZnMC** in $CDCl_3/CD_3CN$ 1:1 (v/v) is similar to that observed for the complex between **ZnMC** and **T-bipy**, implying a similar binding mode. Large upfield shifts were observed for the bipyridine proton signals and a splitting of the signals belonging to the β-pyrrolic protons above the cavity side-walls and of the crown ether proton signals into a set for the 'front' side and one for the 'back' side of **ZnMC** were observed (Figure 6).

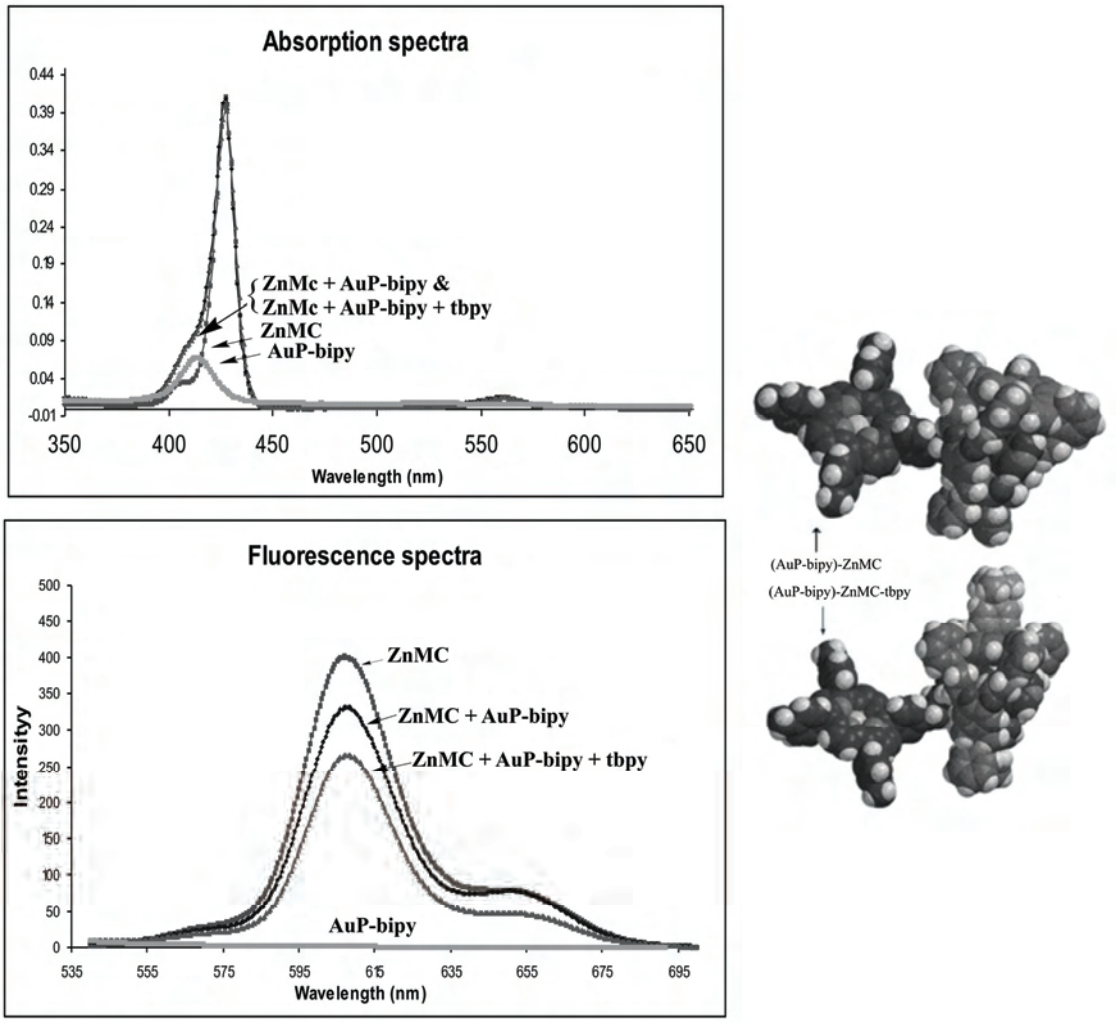

Figure 5. *UV-vis absorption and fluorescence emission spectra of* ***ZnMC*** *and* ***AuP-bipy*** *and of a 1:1 mixture of these components in the absence and in the presence of 500 eq of* ***tbpy****. $CHCl_3/CH_3CN$ = 1/1 (v/v). T = 298 K.* ***[ZnMC] = [AuP-bipy]*** *= 10^{-6} M. Excitation (****ZnMC****) 426 nm; excitation (****AuP-bipy****) 411 nm.* ***ZnMC*** *(UV-vis): λ = 426, 545 nm; (fluor) λ = 605 nm.* ***AuP-bipy*** *(UV-vis): λ = 411, 521 nm; no fluorescence emission detected.*

The addition of **AuP-bipy** to a solution of **ZnMC** in $CHCl_3/CH_3CN$ = 1:1 (v/v) resulted in quenching of the zinc porphyrin fluorescence at 605 nm upon excitation at 426 nm. The amount of quenching increases from 17% at a 1:1 host-guest ratio to 75% at a ratio of 1:10 (Figure 7, Table 2). The same titrations when carried out in the presence of 500 eq of **tbpy**, resulted in 34% (which indicates a AQM factor of 2) and 90% quenching, respectively, at these ratios (Figure 8, Table 2).

UV-vis titration experiments confirmed that this increase in quenching was the consequence of only a slight increase in binding constant from $K_a = 3 \times 10^5\ M^{-1}$ to $K_a = 8 \times 10^5\ M^{-1}$ in the presence of the axial ligand **tbpy**. In energy terms this corresponds to a

$\Delta\Delta G$ of only -3 kJmol^{-1}, which, although small, does demonstrate the first example of an allosteric effect being employed in the self-assembly of synthetic photo-active systems.

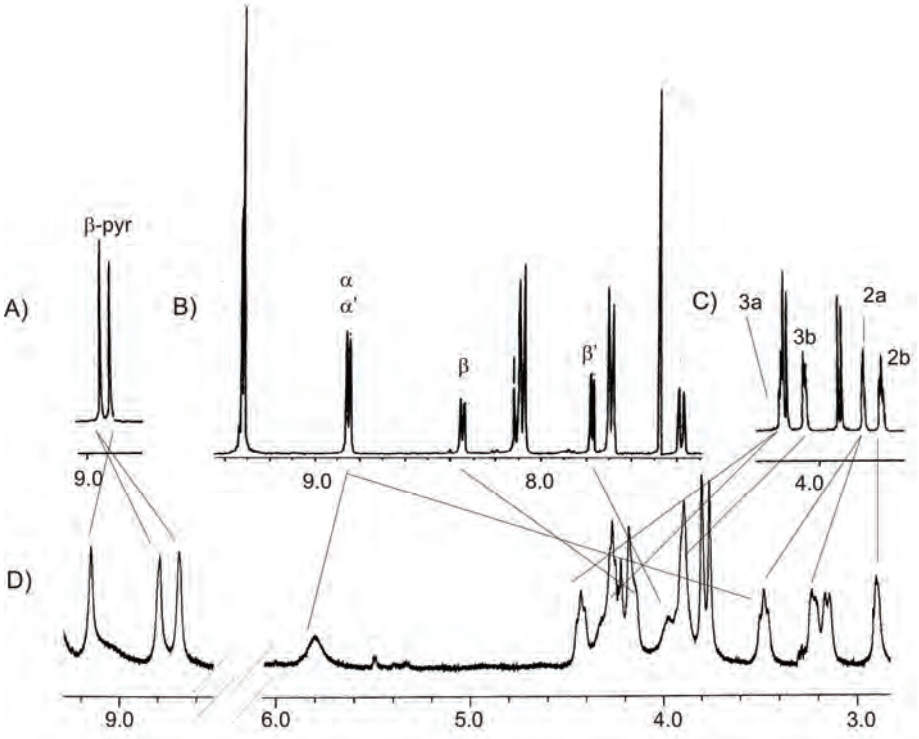

Figure 6. *^{1}H-NMR spectra (400.15 MHz, $CDCl_3/CD_3CN$ = 1:1 (v/v), 298 K). A) β-pyrrolic region of **ZnMC**. B) Aromatic region of **AuP-bipy**. C) Crown ether region of **ZnMC**. D) Partial spectrum of the 1:1 complex between (**AuP-bipy**) and **ZnMC**.*

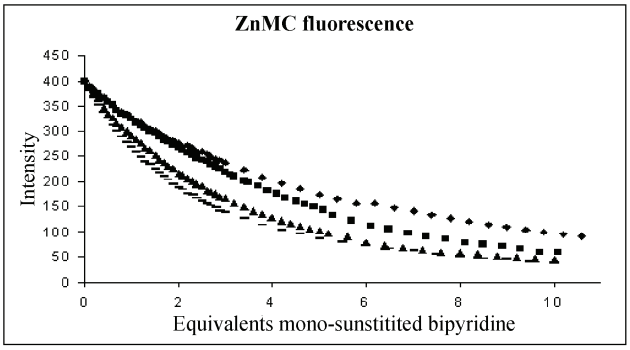

Figure 7. *Fluorescence quenching of **ZnMC** by **AuP-bipy** and **AuP-(bipy)$_4$** in the absence and in the presence of 500 eq of **tbpy**. ♦ **ZnMC** + **AuP-bipy**; ▬ **ZnMC/tbpy** + **AuP-bipy**; ▲ **ZnMC** + **AuP-(bipy)$_4$**; ■ **ZnMC/tbpy** + **AuP-(bipy)$_4$**. $CHCl_3/CH_3CN$ = 1:1 (v/v). T = 298 K. Excitation = 426 nm. Emission = 605 nm. [**ZnMC**] = 10^{-6} M.*

The reverse titration approach in which **tbpy** was added to a 1:1 mixture of **ZnMC** and **AuP-bipy** in $CHCl_3/CH_3CN$ = 1:1 (v/v) resulted in an increase in quenching of 14% (Figure 8).

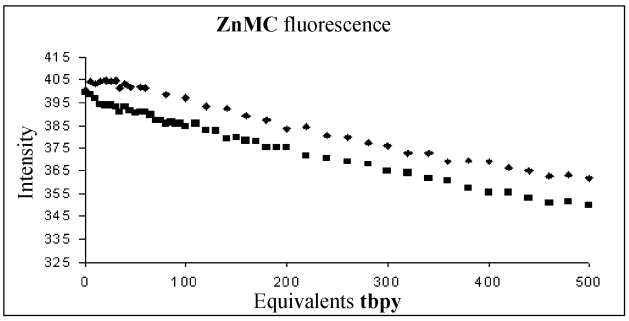

Figure 8. *Fluorescence quenching of **ZnMC** by **AuP-bipy** and **AuP-(bipy)$_4$** during the addition of 500 eq **tbpy**. ■ **ZnMC/AuP-bipy** + **tbpy**; ♦ **ZnMC/AuP-(bipy)$_4$** + **tbpy**. $CHCl_3/CH_3CN$ = 1:1 (v/v). T = 298 K. Excitation = 426 nm. Emission = 605 nm. [**ZnMC**] = [**AuP-bipy**] =10^{-6} M. [**AuP-(bipy)$_4$**] = 2.5 x 10^{-5} M.*

In order to investigate the fluorescence quenching behaviour of the tetrafunctional **AuP-(bipy)$_4$** guest, it was first tested whether or not four zinc porphyrin hosts could be complexed to a single guest. A ^{1}H-NMR spectrum of a mixture of **ZnMC** and **AuP-(bipy)$_4$** in the ratio 4:1 at a concentration of [**ZnMC**] = 10^{-3} M in $CDCl_3/CD_3CN$ 1:1 (v/v) did not show the presence of uncomplexed bipyridine units, indicating that the the 4:1 host-guest complex is the predominant species in solution. The crown ether proton signals of **ZnMC** were significantly broadened, which made the proton signals of the bipyridine moieties of the complex hardly visible. From the peaks that could be identified, a similar binding geometry as for the complexes of **ZnMC** with **P-bipy** was deduced (Table 1).

The quenching behaviour induced by the **AuP-(bipy)$_4$** guest was subsequently studied. The addition of 0.25 eq of **AuP-(bipy)$_4$** to **ZnMC** resulted in a quenching of the fluorescence of the latter porphyrin of 20%, a similar value as measured for the complex of **ZnMC** with **AuP-bipy** at a host-guest ratio of 1:1 (Figure 7, Table 2). The quenching of **ZnMC** fluorescence after the addition of 2.5 eq of **AuP-(bipy)$_4$** increased to 88%, which is a little higher than observed for the quenching of the **ZnMC-AuP-bipy** complex. The binding constant obtained from UV-vis titrations, between **ZnMC** and **AuP-(bipy)$_4$**, was K_a= 7 x 10^5 M^{-1} (for **ZnMC** and **AuP-bipy**: K_a= 3 x 10^5 M^{-1}).

Repetition of this titration in the presence of 500 eq of **tbpy** in $CHCl_3/CH_3CN$ 1:1 (v/v) surprisingly did not result in a further increase in fluorescence quenching. At a host-guest ratio of 1:1 (**AuP-(bipy)$_4$**:**ZnMC**= 1:4), a fluorescence quenching of 18% was observed and after the addition of 2.5 eq of **AuP-(bipy)$_4$** the total quenching of **ZnMC** fluorescence was 83%. This is in both cases a little lower than observed for the titration experiment in the absence of **tbpy**, demonstrating a small negative cooperative effect and an AQM factor of 0.9 (Figure 6, Table 2). The binding constant that was calculated from these titration experiments is also slightly lower than that for the **AuP-bipy**/**ZnMC**/**tbpy**-

system, namely $K_a = 4 \times 10^5\ M^{-1}$. The reverse approach of adding **tbpy** to a 1:4 mixture of **ZnMC** and **AuP-(bipy)$_4$** resulted in only 10% extra quenching (Figure 9), which is equal to the quenching observed for the addition of **tbpy** to **ZnMC** in the absence of any guest molecules (Table 2).
We ascribe this observed inability of **tbpy** to enhance binding and increase fluorescence quenching to steric hindrance and crowding around the central porphyrin, which increases in the order ((**AuP-bipy**)-**ZnMC**)<((**AuP-bipy**)-**ZnMC**-**tbpy**)<((**AuP-(bipy)$_4$**)-(**ZnMC**)$_4$)<((**AuP-(bipy)$_4$**)-(**ZnMC**)$_4$-(**tbpy**)$_4$) (Figure 2b). As a consequence of this crowding the effective binding actually decreases upon the addition of **tbpy**.

5.4 Photophysical studies on ZnMC complexes

In literature, the electron transfer from zinc porphyrins to either viologens or gold porphyrins has been well described.[7,9,17,18] Comparing both electron acceptor molecules, it is clear that gold porphyrins have a smaller negative reduction potential than viologens, which makes these molecules more favourable for electron acceptance. Electron transfer (**ET**) in our systems, however, has to occur 'through space', which is a process that is exponentially dependant on the distance between the electron donor and acceptor. From a simple modelling of the (**AuP-bipy**)-**ZnMC** complex, the distance between the porphyrin zinc ion and the positively charged nitrogen and between the porphyrin zinc ion and the porphyrin gold ion can be estimated to be 5 Å and 20 Å, respectively. In view of these distances, a direct **ET** from the zinc porphyrin to the gold porphyrin will be negligible compared to an **ET** to the mono-substituted bipyridine. A successive charge shift, however, from the latter moiety to the gold porphyrin should be possible and is probable. The positively charged nitrogen atom and the central porphyrin gold ion are only 18 Å apart, and the studies on zinc tetraviologen complexes have already shown that **ET** across this distance is very feasible.[17] The occurrence of two subsequent **ET** steps would make our systems unique allosterically sensitive photosynthetic antenna model systems.

The initial studies to investigate the processes occurring after photo-excitation of the zinc porphyrin, emission spectra of the [2]-pseudo-rotaxane (**AuP-bipy**)-**ZnMC** recorded at 77 K revealed no phosphorescence from the gold porphyrin after excitation of the zinc porphyrin. Energy transfer to the gold porphyrin can therefore be ruled out and electron transfer seems to be the dominant process, which compares well with literature examples of systems with analogous chromophores.[7]
The photophysical processes occurring in the **ZnMC** – mono-substituted bipyridine complexes were further investigated using time correlated single-photon fluorescence counting in collaboration with the University of Leuven, Belgium.

Since chloroform is not a photostable solvent, it was decided to switch to the commonly used solvent benzonitrile. The association constants between the mono-substituted bipyridine guests and **ZnMC** in this solvent were determined by UV-vis and fluorescence spectroscopy (Table 3), and found to be comparable to the values obtained in $CHCl_3/CH_3CN$ 1:1 (v/v).

Table 3. *Association constants[a] K_a (M^{-1}) and free energies ΔG (kJ mol^{-1}) between mono-functionalised bipyridine guests and **ZnMC**.*

	$CHCl_3/CH_3CN$ 1:1 (v/v)	Benzonitrile	THF
M-bipy	7.5×10^4 ; -28	5.5×10^5 ; -33	
P-bipy	2.2×10^5 ; -30	8.2×10^4 ; -28	7.0×10^5 ; -33
AuP-bipy	3×10^5 ; -31	1.8×10^5 ; -30	3×10^4 ; -26
AuP-(bipy)$_4$	7×10^5 ; -33	3.3×10^5 ; -31	

*[a] Excitation wavelength = 426 nm. Emission wavelength = 560 nm. T = 298 K. [**ZnMC**] = 10^{-6} M. Association constants obtained from fluorescence data have been compared with the reported K_{ass}-values determined from UV-vis data. They were found to be similar and are therefore not mentioned. In their calculation it was assumed that the quantum yield of the host and of the host-guest complexes are the same.*

Except for **M-bipy**, the association constants dropped by only a factor of 2-3 compared to the values measured in $CHCl_3/CH_3CN$ 1:1 (v/v). Molecular modelling suggests that benzonitrile can occupy the cavity of **ZnMC**, however only with severe steric strain in the conformation where the nitrile group points towards the zinc ion. The crown-ether moiety of **ZnMC**, however, has an affinity for electron poor aromatic molecules, e.g. 1,3-dinitrobenzene, benzonitrile and viologens.[14,20] The weaker host-guest binding in this solvent is the result of competition for binding to **ZnMC** between benzonitrile and mono-substituted bipyridine guests resulting in lower association constants. (The higher association constant for **M-bipy** is as yet unexplained.)

Although the association constants in benzonitrile were found to be lower than in $CHCl_3/CH_3CN$ 1:1 (v/v), they were sufficiently high to readily give complexes between **ZnMC** and the bipyridine guests and therefore attempts were made to investigate the photophysical processes occurring upon the photo-excitation of **ZnMC** in our systems.
Since in the host-guest complexes the fluorescence of the zinc(II) porphyrin is severely quenched, a single-photon fluorescence experiment needs to be carried out for at least three hours in order to yield enough photons for a reliable measurement. This means that the solutions under investigation are irradiated by a laser for the same period of time and therefore the photostability of the host molecule and host-guest complexes in solution was first tested. Solutions of **ZnMC** and the 1:1 complex of **ZnMC** and **AuP-bipy** at 10^{-5} M concentration in benzonitrile were stable for at least 2 days while standing in

daylight, and upon irradiation of the Soret or Q-bands by a laser for up to 4 hours, as was concluded from the absence of changes in the UV-vis spectra of these solutions.

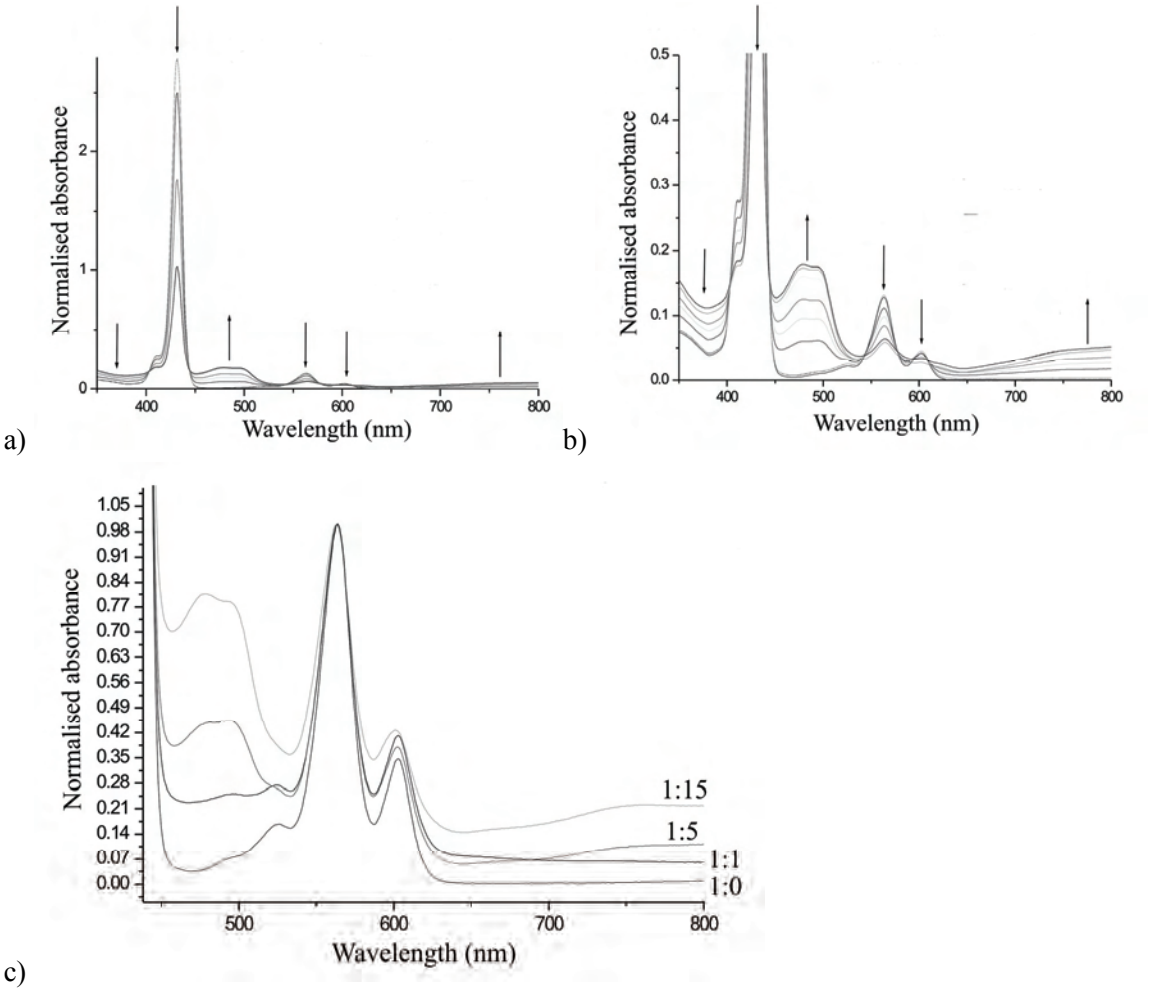

Figure 9. *a) Changes in UV-vis spectra recorded over a period of 7 h of the complex between* ***ZnMC*** *and* ***P-bipy*** *in benzonitrile ([**ZnMC**]= 1.1 x 10^5 M). b) Zoom-in of a). c) UV-vis spectra recorded after 3 hours of irradiation of solutions containing the complex between* ***ZnMC*** *and* ***P-bipy*** *at different host:guest ratios in benzonitrile ([**ZnMC**] = 1.1 x 10^{-5} M).*

Interestingly, when the Soret band of **ZnMC** (10^{-5} M) in the complex with **P-bipy** was irradiated by the laser, both the Soret and the Q-bands in the UV-vis spectrum gradually decreased in intensity until almost total disappearance, accompanied by the emergence of a new band at 475 nm, with the presence of two isosbestic points at 445 nm and 540 nm (Figure 9a and b). These spectral changes continued to occur when the solution was placed in the dark, however, they were accelerated in daylight or upon a continuous irradiation by the laser. The spectral changes were more pronounced in solutions containing increasing amounts of the guest molecule (Figure 9c), while irradiation in the presence of 500 eq of the axial ligand **tbpy** did not cause any changes in the UV-vis

spectra. At ten times lower concentration, a 1:5 mixture of **ZnMC** and **P-bipy** in benzonitrile showed similar changes in the UV-vis spectra upon standing in daylight. These changes, however, were in contrast to the situation observed for the 10^{-5} M solutions of **ZnMC** and **P-bipy,** since in this case the original UV-vis spectrum could be observed again once the solution was kept in the dark for 14 hours.
A possible origin of the band at 475 nm is the formation of a charge-transfer complex between the guest and the host. This possibility is in line with the fact that the intensity of the band increases at higher concentrations of the guest. The question remains as to why the presence of **tbpy** would prevent the formation of this complex, and why its formation would be light-dependent.

To examine whether the photolability of **ZnMC**:**P-bipy** complexes only occurred in benzonitrile, the photostability was tested by UV-vis spectroscopy in $CHCl_3/CH_3CN$ 1:1 (v/v). In this solvent mixture, the 1:1 complex between **ZnMC** and **P-bipy** ([**ZnMC**] = 10^{-6} M) showed an asymptotic decrease in intensity of the Soret and Q-bands upon storing the sample in daylight, while in the dark only marginal changes were observed (Figure 10a). No new bands emerged during these experiments.
A $CHCl_3/CH_3CN$ 1:1 (v/v) solution containing the 1:1 complex between **ZnMC** and **P-bipy** at a concentration of 10^{-5} M showed different behaviour in its UV-vis spectra upon storing the sample in daylight. Also in this sample no new bands appeared, and the intensities of the Soret- and Q-bands decreased asymptotically. The absorption increased again upon storing the sample in the dark, although not to their full original intensities (Figure 10b). The commonly observed photodegradation of porphyrin molecules upon prolonged irradiation would not give such an asymptotic decrease in the intensities and can therefore not explain the observed photolabile behaviour.[21] Viologens are known to be photostabile and are employed as photostabilisers in liquid crystal displays.[22] Their mono-reduced radical species, however, are known to irreversibly react with oxygen.[23] Assuming that the same behaviour applies to mono-substituted bipyrines, this could provide a clue towards the observed photolability of the complexes. A reaction with oxygen of the reduced guest, which is only expected to form upon photo-excitation, could alter the UV-vis absorption properties of the complex. This reaction would, however, have to be reversible in order to explain the observations as reported in Figure 10b.

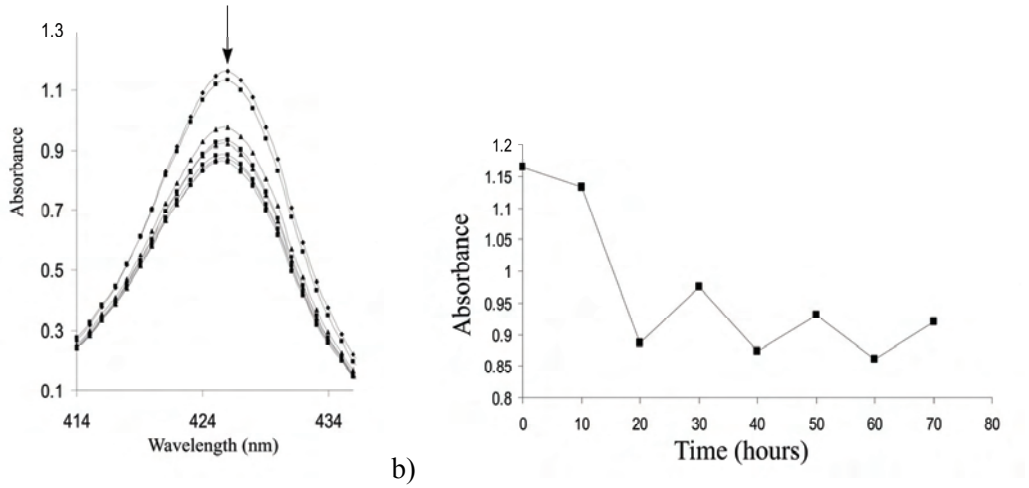

a) b)

Figure 10. *a) Zoom-in of the Soret-band region in the UV-vis spectra of a solution containing the 1:1 complex between* ***ZnMC*** *and* ***P-bipy*** *in $CHCl_3/CH_3CN$ 1:1 (v/v) ([**ZnMC**] = 10^{-6} M) upon storing the sample alternating 10 h in the dark and 10 h in daylight. b) Changes in absorbance of the Soret-band of a solution containing the 1:1 complex between* ***ZnMC*** *and* ***P-bipy*** *in $CHCl_3/CH_3CN$ 1:1 (v/v) ([**ZnMC**] = 10^{-5} M) upon storing the sample alternating 10 h in the dark and 10 h in daylight.*

Since solutions of complexes between **ZnMC** and **P-bipy** in benzonitrile appeared to be photosensitive, it was decided to switch to another commonly used solvent for photo-physical studies, namely THF. A disadvantage of using THF as a solvent is that it can also bind to metal ions. The binding of THF to **ZnMC** and thereby the possibility that this solvent would be in strong competition for binding with the mono-substituted bipyridine guests, was initially investigated. ^{1}H NMR experiments suggested that THF could occupy the cavity of **ZnMC** in a $CDCl_3$ solution, since upon the addition of excess THF the crown ether signals shifted slightly upfield by 0.2 ppm and the porphyrin signals became very broad (Figure 11). No signals for THF bound inside the cavity were observed indicating fast exchange between bound and unbound guest.

The association constant for the binding of THF to the zinc ion of **ZnMC** is expected to be lower than the association constants of acetonitrile and benzonitrile, since the soft metal zinc(II) has a higher affinity for nitrogen donor than for oxygen donor ligands. For this reason, it is expected that THF competes less for binding of mono-substituted bipyridine guests than acetonitrile. In Table 3 the association constants between **ZnMC** and some of these guests in THF are summarised. The K_a-value between **ZnMC** and **P-bipy** in THF is slightly higher than the values determined in benzonitrile and $CHCl_3/CH_3CN$ 1:1 (v/v), in accordance with the hypothesis of less competitive binding by the solvent. The K_a-value of **AuP-bipy**, however, is a factor 10 lower than the values in the other solvent systems. So far the reason for this difference is unknown.

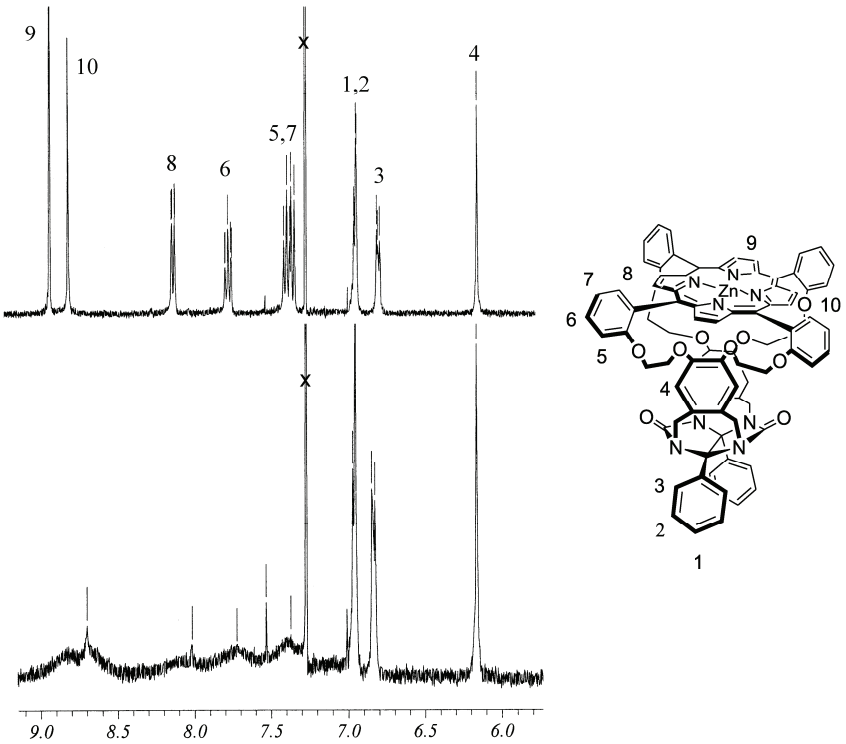

Figure 11. *Downfield region of ^1H NMR spectra of* ***ZnMC*** *in $CDCl_3$ in the absence (top spectrum) and presence (bottom spectrum) of an excess of THF, together with the relevant proton numbering.*

The addition of **tbpy** to a solution of **ZnMC** in THF did not result in changes in the UV-vis spectrum, indicating that no axial binding of the nitrogen donor ligand occurred. This was confirmed by a ^{1}H NMR experiment in which in a mixture of **tbpy** and **ZnMC** in THF-d_8 revealed no complexation induced shifts for **tbpy**. In spite of the fact that THF has a lower association constant than **tbpy**, it is present in much higher concentrations, preventing the **tbpy** from binding.

Solutions of **ZnMC,** the 1:1 complex of **ZnMC** and **P-bipy** and the 1:1 complex of **ZnMC** and **AuP-bipy** in THF at a concentration range of 10^{-6} M to 10^{-4} M were found to be photostable for at least 2 days upon storing the sample in daylight, and upon irradiation of the Soret or Q-bands by a laser for up to 24 hours. This conclusion was the drawn from the absence of changes in the UV-vis and fluorescence spectra of these solutions. Although the solvent THF does not allow for the allosteric manipulation of the pseudo-rotaxane systems by the addition of the axial ligand **tbpy**, the photostability of the complexes does allow for investigation of the photophysical processes occurring upon photo-excitation of the zinc porphyrin and therefore further investigations were carried out in this solvent.

Time resolved fluorescence measurements in THF upon irradiation into a Q-band of **ZnMC** at 552 nm ([**ZnMC**] = 10^{-5} M) showed that whereas the fluorescence decay kinetics of **ZnMC** can be fitted to a single exponential, the fluorescence decays for the 1:1 complexes between **ZnMC** and both guests are multi-exponential (Figure 12). In the case of **ZnMC**, the single exponential decay of τ_1= ~2.4 ns is representative of the S_1 singlet excited-state lifetime.[4g,22] In the case of the host-guest complex, in addition to a ~2.4 ns decay component, which is attributed to uncomplexed host **ZnMC**, decay components of ~40 ps and ~350 ps were found. The time resolved emission spectra did not exhibit spectral shifts in time, which suggests that the populations in the S_1 state are converted into a non-radiative state by means of a photoreaction occurring with ~40 and ~350 ps time constants.

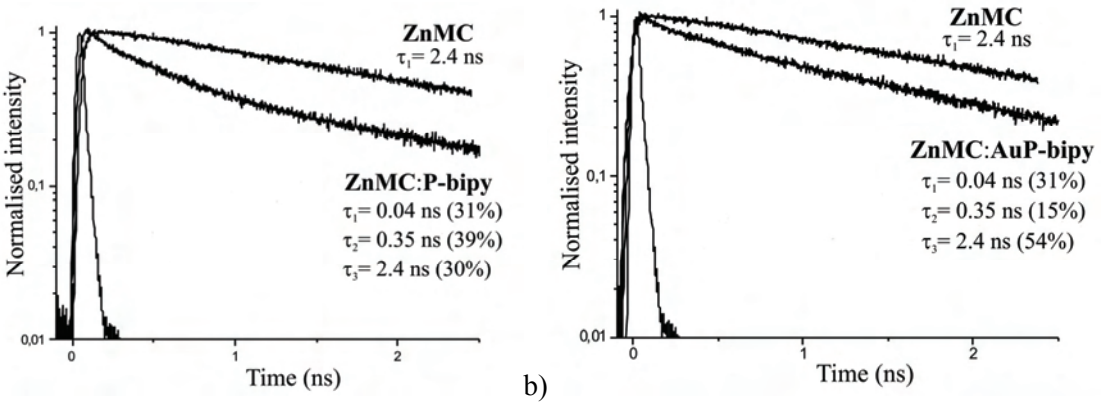

Figure 12. *Fluorescence transients of **ZnMC** and the 1:1 complex between **ZnMC** and **P-bipy** (a) and the 1:1 complex between **ZnMC** and **AuP-bipy** (b) in THF. $\lambda_{excitation}$ = 552 nm; $\lambda_{detection}$ = 660nm; [**ZnMC**] = [**P-bipy**] = [**AuP-bipy**] = 10^{-5} M.*

These time components can be associated with an excited state **ET** process occurring from the zinc porphyrin host to the mono-substituted bipyridine moiety of the guest.[24] It is suggested that the double exponential decay of the fluorescent reactant state originates from structural inhomogeneities in the host-guest binding mode, which in turn originate from the rather loose complexation of the bipyridine moiety inside the cavity, as is evidenced by the equivalency of the protons on the 'top'- and 'bottom' side of the bipyridine group. In the ^{1}H NMR spectra these protons are averaged into a single signal. The fluorescence kinetics are thus considered as multi-exponential, where the double exponential decay is merely indicative of a spread of excited-state lifetimes. This conclusion can be drawn since no indication for the binding of more than one guest molecule to the host has been found in ^{1}H NMR and UV-vis measurements in studies with different host:guest ratios and concentrations. The higher ratio of the 2.4ns decay component for the solution containing **AuP-bipy** compared to the solution containing **P-bipy** is in line with the higher association constant of the complex of **ZnMC** with the latter guest relative to the former one (Figure 12).

Based on the ratios between the fluorescence transients arising from the free host and the **ZnMC**:**P-bipy** complex, the association constants of **P-bipy** and **AuP-bipy** with **ZnMC** can be determined. Averaging the time dependant fluorescence measurements performed at different host:guest ratios allows one to obatin an indication of the K_a-values, by applying the following mathematical equations:

$$\mathbf{ZnMC} + \mathrm{L} \underset{\leftarrow}{\overset{\rightarrow}{}} \mathbf{ZnMC}\text{-L}$$

Parameters:
a: total concentration **ZnMC**
b: total concentration mono-substituted bipyridine guest,
x: concentration 1:1 complex between **ZnMC** and the mono-substituted bipyridine guest

The fluorescence that can be measured at each point in time can be defined as:

$$I(t) = \alpha_1 \exp(-t/t_1) + \beta_2 \exp(-t/t_2)$$

I(t) = fluorescence intensity at time *t,* α_1 = contributing factor for fluorescence from uncomplexed **ZnMC**, *T* = time (ns), t_1 = single exponential decay constant of uncomplexed **ZnMC** (2.4 ns), β_2 = contributing factor for fluorescence from 1:1 complex between **ZnMC** and mono-substituted bipyridine guest, t_2 = exponential decay of 1:1 complex between **ZnMC** and mono-substituted bipyridine guest.

If it is assumed that the electronic properties do not change upon complexation, then:

$$x = \frac{\beta_2}{\alpha_1 + \beta_2} \mathrm{a}$$, and:

$$K_a = \frac{\frac{\beta_2}{\alpha_1 + \beta_2} a}{\left(a - \frac{\beta_2}{\alpha_1 + \beta_2} a\right)\left(b - \frac{\beta_2}{\alpha_1 + \beta_2} a\right)}$$, which rearranges to:

$$K_a = \frac{\beta_2}{\alpha_1\left(b - \frac{\beta_2}{\alpha_1 + \beta_2} a\right)}$$

The average association constants based on time resolved fluorescence measurements at various concentrations of host and guest for **P-bipy** was calculated to be $K_a = 7.7 \times 10^4$ M^{-1} and $K_a = 1.93 \times 10^4$ M^{-1} for **AuP-bipy** of which the second value corresponds quite well with the value obtained via UV-vis titrations for **AuP-bipy** being $K_a = 3 \times 10^4$ M^{-1}.

At present, femtosecond transient absorption experiments are being initiated at the University of Leuven to investigate the excited-state kinetics and to characterize the non-emissive states involved in the electron transfer reaction. Concomitantly with the decay of the fluorescent S_1 state, the **ZnMC** porphyrin radical cation is being formed. (The transient absorption spectrum of this species has been well documented.[4g,24,25]) If the lifetime of the radical-cation state is sufficiently long lived, it can be probed by means of pump-probe spectroscopy. Indirect evidence for such a radical cation can also be found by probing the ground-state hole repopulation dynamics, since the ground state populations are being formed by means of charge recombination.[24] The observation of a gold(II) porphyrin species in the transient absorption spectrum of the complex between **ZnMC** and **AuP-bipy** upon photo-excitation, would confirm the occurrence of **ET** to the gold(III)porphyrin moiety.[7,18,26]

5.5 Conclusions

In this chapter we have described studies in which allosteric interactions are employed to enhance electron transfer in a reaction-centre mimic. This is the first example of such studies in the literature. Binding of an axial ligand (**tbpy**) to an electron-donating zinc porphyrin host (**ZnMC**), was shown to increase the complexation strength of this host to a series of electron-accepting mono-substituted bipyridine guests, resulting in a more pronounced electron transfer process upon excitation of the zinc porphyrin. The allosteric increase in the binding strength is accompanied by a more efficient quenching of the zinc porphyrin fluorescence by the guest. This effect can be quite dramatic, since upon the addition of an excess of **tbpy** to 1:1 solutions of **ZnMC** and either **P-bipy** or **AuP-bipy,** the only slight increase in the binding efficiency ($\Delta\Delta$G-value = 3 kJ) is accompanied by a doubling of the fluorescence quenching. After electron transfer from the host to the bipyridine guest, a charge-shift to an appended gold porphyrin was tentatively suggested. During the investigations of the details of the electron transfer processes it was found that benzonitrile solutions of the 1:1 complex between **ZnMC** and **P-bipy** are not photophysically stable when they are stored in daylight or when they are irradiated by a laser. One or more unknown processes, reversible or irreversible depending on the concentration of the solution, are occurring under these circumstances. In contrast, THF solutions of the same complex were stable upon irradiation or when stored in daylight. Unfortunately this solvent blocks the outside face of **ZnMC** by competitive binding to the porphyrin zinc ion, preventing the binding of the axial ligand **tbpy**. Photophysical studies revealed that that solutions containing the 1:1 complex between **ZnMC** and **P-bipy**, as well as solutions containing **ZnMC** and **AuP-bipy**, show a multi-exponential decay in the time resolved fluorescence kinetics measurements. The decay profiles

consist of one component which is attributed to uncomplexed **ZnMC** and two other components that are ascribed to the 1:1 complex.

5.6 Experimental

UV-vis spectra were recorded on a Varian Cary 50 UV-vis spectrophotometer. Fluorescence titrations were performed on a Perkin Elmer Luminescence Ls50B spectrometer. ^{1}H-NMR spectra were obtained on a Varian Unity Inova 400. The time correlated single-photon fluorescence counting measurements were performed employing the pump-probe experimental set-up described elsewhere.[27] In brief, the output pulses of a regenerative amplifier system (Spitfire, Spectra Physics) (970 uJ/pulse at 1khZ repetition rate) were split by a beam splitter, the main part was used to pump an optical parametric amplifier (OPA 800-II Spectra Physics) and only a small fraction was used to generate a white light continuum. The output pulses of the OPA (500 μW) were used and attenuated to photoexcite the sample at 552 nm at the absorption maximum of the donor **ZnMC** molecule. Average pump power was about 150-250 μW. Laser fluorescence was kept at a level where signal linearity was ensured. The other part of the RGA output was focused into a sapphire plate to generate a white light continuum that served as probe pulses for the photoexcited sample. The probe beam, after passing through the photoexcited volume, was then spectrally dispersed onto a CCD camera by means of a spectrograph (SP300i, Acton research). The detection range was between 350 and 750 nm. The instrumental response time was ~300 fs FWHM. The actual transient signals were obtained via a sequence of measurements in which pump and/or probe beams were selectively blocked. The solution was contained in a quartz cuvette with an optical pathlength of 1 mm and deoxygenated by four consecutive freeze-pump-thaw cycles.
$CHCl_3$ was distilled over $CaCl_2$ and CH_3CN was distilled over CaH_2 before use. **ZnMC** and **M-bipy** were synthesised according to literature procedures.[15a,28]
UV-vis and fluorescence titration experiments and the calculation of binding constants were carried out following the standard methods reported earlier by our group.[14b]

Synthesis of (5-(4,4'-bipyridinium)pentoxy)benzene hexafluorophosphate (P-bipy).
To dibromopentane (14.5 ml, 106 mmol) and K_2CO_3 (3 g) in DMF (70 ml) was added phenol (1 g, 10.6 mmol), after which the mixture was refluxed under a N_2 atmosphere for 3 hrs. After cooling and filtration all liquids were distilled off under reduced pressure. The remaining solid was dissolved in diethyl ether (20 ml) and this solution was added drop-wise to methanol (200 ml). The resulting precipitate was filtered off, washed with methanol and purified by column chromatography (silica; *n*-hexane/CH_2Cl_2 = 7:3 (v/v)) and the product was dried *in vacuo*. A portion of the resulting white solid (2.32 g, 9.55 mmol) was dissolved in DMF (50 ml) and 4,4'-bipyridine was added (5.9 g, 38.2 mmol).

This mixture was stirred under a N_2 atmosphere at 90˚C for 72 hrs. After concentration of the solution under reduced pressure, it was added to a saturated NH_4PF_6 (aq) solution (200 ml). The precipitate was filtered off, washed with water and purified by column chromatography (silica; CH_2Cl_2/MeOH/$MeNO_2$ = 6/1/1) and the product was dried *in vacuo*. Yield: 70% of a white solid.
^{1}H-NMR ($CDCl_3$/CD_3CN = 1:1 (v/v), 300.13 MHz, 25ºC): δ = 8.79 (d, 2H, Py*H*-2,6, ^3J= 6.3 Hz), 8.73 (d, 2H, Py*H*-2',6', ^3J= 6.9 Hz), 8.26 (d, 2H, Py*H*-3,5, ^3J= 5.1 Hz), 7.71 (d, 2H, Py*H*-3',5', ^3J= 6.3 Hz), 7.24 (t, 2H, Ar*H*-3,5, ^3J= 6.6 Hz), 6.86 (m, 3H, Ar*H*-2,4,6), 4.56 (t, 2H, N-CH_2, ^3J= 7.6 Hz), 3.97 (t, 2H, O-CH_2, ^3J= 7.9 Hz), 2.07 (m, 2H, N-C-CH_2), 1.85 (m, 2H, O-C-CH_2), 1.57 (m, 2H, C-CH_2-C). FAB-MS: m/z = 319 [**P-bipy** – PF_6]$^+$.

Synthesis of 3,5-di-*tert*-butyl-1-(5-(4,4'-bipyridinium)pentoxy)benzene hexafluorophosphate (T-bipy).
This compound was synthesised following a route analogous to **P-bipy,** however 3,5-di-*tert*-buylphenol (2.2 g, 10.6 mmol) was used instead of phenol. Yield: 76% of a white solid.
^{1}H-NMR ($CDCl_3$/CD_3CN = 1:1 (v/v), 300.13 MHz, 25ºC): δ = 8.85 (d, 2H, Py*H*-2,6, ^3J= 6.3 Hz), 8.73 (d, 2H, Py*H*-2',6', ^3J= 6.9 Hz), 8.26 (d, 2H, Py*H*-3,5, ^3J= 5.1 Hz), 7.71 (d, 2H, Py*H*-3',5', ^3J= 6.3 Hz), 6.99 (s, 1H, Ar*H*-4), 6.69 (s, 2H, Ar*H*-2,6), 4.58 (t, 2H, N-CH_2, ^3J= 7.6 Hz), 3.98 (t, 2H, O-CH_2, ^3J= 7.9 Hz), 2.10 (m, 2H, N-C-CH_2), 1.85 (m, 2H, O-C-CH_2), 1.60 (m, 2H, C-CH_2-C), 1.26 (s, 18H, CH_3). FAB-MS: m/z = 431 [**T-bipy** – $2PF_6$]$^+$.

Synthesis of 5-(4-(5-(4,4'-bipyridinium)-1-pentoxy)phenyl)-10,15,20-tri(4-toluyl) gold(III) porphyrin dihexafluorophosphate (AuP-bipy).
The free base compound was synthesised according to a literature procedure.[9a,b] This compound (100 mg, 96 μmol) was dissolved in acetic acid (60 ml) and $KAuCl_4$ (363 mg, 0.96 mmol) and NaOAc (31 mg, 378 μmol) were added. The mixture was purged with N_2 for 30 min and then refluxed under a N_2 atmosphere and under exclusion of light for 7 days. After cooling, the solvent was evaporated and the remaining solid was dissolved in CH_2Cl_2 (40 ml). This solution was washed with an aqueous 10% Na_2CO_3 solution. After evaporation of the organic layer, the residue was dissolved in DMF (5 ml) and this solution was added drop-wise, with vigorous stirring, to a saturated aqueous NH_4PF_6 solution. The precipitate was filtered off, washed with water and methanol and dried *in vacuo*. Purification by column chromatography (silica, CH_2Cl_2/CH_3OH/CH_3NO_2 = 6:1:1 (v/v/v)) yielded the desired product in 25% yield as an orange solid.

^{1}H-NMR (CD_2Cl_2, 400.15 MHz, 25ºC): δ = 9.34 (bs, 8H, β-pyrrole*H*), 8.97 (d, 2H, Py*H*-2,6, ^3J= 6.5 Hz), 8.92 (d, 2H, Py*H*-2',6', ^3J= 6.9 Hz), 8.40 (d, 2H, Py*H*-3,5, ^3J= 6.7 Hz), 8.10 (d, 2H, Ar*H*-2,6 *meta to O(CH$_2$)$_5$-bipy* , ^3J= 7.7 Hz), 8.08 (d, 6H, Ar*H*-2,6, ^3J= 7.5 Hz), 7.92 (d, 2H, Py*H*-3',5', ^3J= 5.8 Hz), 7.68 (d, 6H, Ar*H*-3,5, ^3J= 8.2 Hz), 7.37 (d, 2H, Ar*H*-3,5 *ortho to O(CH$_2$)$_5$-bipy* , ^3J= 8.7 Hz), 4.75 (t, 8H, N-CH_2, ^3J= 7.4 Hz), 4.40 (t, 8H, O-CH_2, ^3J= 6.9 Hz), 2.73 (s, 9H, CH_3), 2.38 (m, 2H, N-C-CH_2), 2.20 (m, 2H, O-C-CH_2), 1.95 (m, 2H, C-CH_2-C). UV-vis (CH_2Cl_2): 415, 525. MALDI-TOF: m/z = 1238 [**AuP-bipy** – PF_6]$^+$.

Synthesis of 5,10,15,20-tetrakis(4-(5-(4,4'-bipyridinium)-1-pentoxy)phenyl) gold(III) porphyrin penta(hexafluorophosphate) (AuP-(bipy)$_4$).

The free base analogue was synthesised according to a literature procedure.[12a,b] Gold was inserted in an analogous fashion as to described for the synthesis of **AuP-bipy**, also starting with 100 mg (63 μmol) of free base compound. After evaporation of the acetic acid, the mixture was dissolved in DMF (5 ml) and this solution was added drop-wise to a saturated aqueous NH_4PH_6 solution. The precipitate was washed with water and methanol. It was then dissolved in CH_3CN (5 ml), after which any insoluble material was filtered off. The filtrate was evaporated and the product was dried *in vacuo*. Yield: 30% of an orange solid.

^{1}H-NMR (CD_3CN, 400.15 MHz, 25ºC): δ = 9.30 (s, 8H, β-pyrrole*H*), 8.84 (d, 8H, Py*H*-2,6, ^3J= 6.4 Hz), 8.80 (bs, 8H, Py*H*-2',6'), 8.36 (d, 8H, Py*H*-3,5, ^3J= 6.8 Hz), 8.13 (m, 8H, Ar*H*-2,6), 7.79 (d, 8H, Py*H*-3',5', ^3J= 4.6 Hz), 7.41 (d, 8H, Ar*H*-3,5, ^3J= 8.6 Hz), 4.67 (t, 8H, N-CH_2, ^3J= 7.6 Hz), 4.31 (t, 8H, O-CH_2, ^3J= 6.1 Hz), 2.20 (m, 8H, N-C-CH_2), 2.04 (m, 8H, O-C-CH_2), 1.70 (m, 8H, C-CH_2-C). UV-vis (CH_3CN): 419, 523. MALDI-TOF: m/z = 2354 [**AuP-(bipy)$_4$** – PF_6]$^+$.

References

1. J. Deisenhofer, J.R. Norris, in *The Photosynthetic Reaction Center*, Academic Press, San Diego, California, 1993.
2. J.D. Rawn, *Biochemistry*, Neil Patterson Publishers, Burlington, North Carolina, 1989.
3. a) G. McLendon, R. Hake, *Chem. Rev.*, 1992, **92**, 481-490.
   b) M.R. Wasielewski, *Chem. Rev.*, 1992, **92**, 435-461.
   c) D. Gust, A.T. Moore, A.L. Moore, *Acc. Chem. Res.*, 1993, **26**, 198-205.
   d) H. Hurreck, M. Huber, *Angew. Chem. Int. Ed. Eng.*, 1995, **34**, 849-866.
   e) A. Harriman, J.-P. Sauvage, *Chem. Soc. Rev.*, 1996, **25**, 41-48.
4. a) K.D. Jordan, M.N. Paddon-Row, *Chem. Rev.*, 1992, **92**, 395-410.
   b) M.-J. Blanco, M. Consuelo Jiménez, J.-C. Chambron, V. Heitz, M. Linke, J.-P. Sauvage, *Chem. Soc. Rev.*, 1999, **28**, 293-305.
   c) F. Diederich, M. Gómez-López, *Chem. Soc. Rev.*, 1999, **28**, 263-277.

d) F.D. Lewis, R.L. Letsinger, M.R. Wasielewski, *Acc. Chem. Res.*, 2001, **34**, 159-170.
e) L. Flamigni, F. Barigelletti, N. Armaroli, J.-P. Collin, I.M. Dixon, J.-P. Sauvage, J.A.G. Williams, *Coord. Chem. Rev.*, 1999, **190-192**, 671-682.
f) S. Fukuzumi, K. Ohkubo, H. Imahori, J. Shao, Z. Ou, G. Zheng, Y. Chen, R.K. Pandey, M. Fujistuka, O. Ito, K.M. Kadish, *J. Am. Chem. Soc.*, 2001, **123**, 10676-10683.
g) I.-W. Hwang, M. Park, T.K. Ahn, Z.S. Yoon, D.M. Ko, D. Kim, F. Ito, Y. Ishibashi, S.R. Khan, Y. Nagasawa, H. Miyasaka, C. Ikeda, R. Takahashi, K. Ogawa, A. Satake, Y. Kobuke, *Chem. Eur. J.*, 2005, **11**, 3753-3761.

5. a) Y. Sakata, H. Tsue, M.P. O'Neil, G.P. Wiederrecht, M.R. Wasielewski, *J. Am. Chem. Soc.*, 1994, **116**, 6904-6909.
   b) R. Sadamoto, N. Tomioka, T. Aida, *J. Am. Chem. Soc.*, 1996, **118**, 3978-3979.
   c) L. Flamigni, I.M. Dixon, J.-P. Collin, J.-P. Sauvage, *Chem. Commun.*, 2000, 2479-2480.
   d) K. Pettersson, K. Kilså, J. Mårtensson, B. Albinsson, *J. Am. Chem. Soc.*, 2004, **126**, 6710-6719.
6. a) M. Inamo, H. Kumagai, U. Harada, S. Itoh, S. Iwatsuki, K. Ishihara, H.D. Takagi, *Dalton Trans.*, 2004, 1703-1707.
   b) M. Inamo, K. Aoki, N. Ono, H.D. Takagi, *Inorg. Chem. Commun.*, 2005, **8**, 979-982.
7. a) S. Prathapan, T.E. Johnson, J.S. Lindsey, *J. Am. Chem. Soc.*, 1993, **115**, 7519-7520.
   b) J. Seth, V. Palaniappan, T.E. Johnson, S. Prathapan, J.S. Lindsey, D.F. Bocian, *J. Am. Chem. Soc.*, 1994, **116**, 10578-10592.
   c) J.-S. Hsiao, B.P. Krueger, R.W. Wagner, T.E. Johnson, J.K. Delaney, D.C. Mauzerall, G.R. Fleming, J.S. Lindsey, D.F. Bocian, R.J. Donohoe, *J. Am. Chem. Soc.*, 1996, **118**, 11181-11193.
8. a) J.S. Van den Brink, P. Gast, A.J. Hoff, *J. Chem. Phys.*, 1996, **104**, 1805-1812.
   b) E.G. Alexov, M.R. Gunner, *Biochem.*, 1999, **38**, 8235-8270.
   c) E. Turcsanyi, I. Vass, *Photochem. Photobiol.*, 2000, **72**, 513-520. d) I. Vass, *Photosynth. Res.*, 2003, **76**, 303-318.
9. a) L.R. Milgrom, *J. Chem. Soc. Perkin Trans. I*, 1983, 2535-2539.
   b) A. Harriman, G. Porter, A. Wilowska, *J. Chem. Soc. Faraday Trans. 2*, 1984, **80**, 191-204.
   c) A. Harriman, *Inorg. Chim. Act.*, 1984, **88**, 213-216.
   d) J.D. Batteas, A. Harriman, Y. Kanda, N. Mataga, A.K. Nowak, *J. Am. Chem. Soc.*, 1990, **112**, 126-133.
   e) S. Noda, H. Hosono, I. Okura, Y. Yamamoto, Y. Inoue, *J. Chem. Soc. Faraday Trans.*, 1990, **86**, 811-814.
   f) J. Hirota, I. Okura, *J. Phys. Chem.*, 1993, **97,** 6867-6870.
   g) H. Hosono, M. Kaneko, *J. Chem. Soc. Faraday Trans.*, 1997, **93**, 1313-1319.
10. a) A. De la Escosura, V.M. Martinez-Diaz, D.M. Guldi, T. Torres, *J. Am. Chem. Soc.*, 2006, **128**, 4112-4118.
    b) S.A Vail, D.I. Schuster, D.M. Guldi, M. Isosomppi, N. Tkachenko, H. Lemmetyinen, A. Palkar, L. Echegoyen, X. Chen, J.Z.H. Zhang, *J. Phys. Chem. B*, 2006, **110**, 14155-14166.
    c) B. Wang, Y. Zhou, X. Ding, K. Wang, X. Wang, J. Yang, J.G. Hou, *J. Chem. Phys. B*, 2006, **110**, 245050-24512.

d) F. D'Souza, R. Chitta, S. Gadde, L.M. Rogers, P.A. Karr, M.E. Zandler, A.S.D. Sandanayaka, Y. Araki, O. Ito, *Chem. Eur. J.*, 2007, **13**, 916-922.

11. a) D.M. Guldi, H. Imahori, *J. Porphyrins Phtalocyanines*, 2004, **8**, 976-983, and references therein.
    b) M.-S. Choi, T. Yamazaki, I. Yamazaki, T. Aida, *Angew. Chem. Int. Ed.*, 2004, **43**, 150-158, and references therein.
12. C.A. Hunter, R.K. Hyde, *Angew. Chem. Int. Ed. Eng.*, 1996, **35**, 1936-1939.
13. J. Monod, J. Wymann, J.P. Changeux, *J. Mol. Biol.*, 1965, **12**, 88-118.
14. a) P. Thordarson, E.J.A. Bijsterveld, J.A.A.W. Elemans, P. Kasák, R.J.M. Nolte, A.E. Rowan, *J. Am. Chem. Soc.*, 2003, **125**, 1186-1187.
    b) P. Thordarson, R.G.E. Coumans, J.A.A.W. Elemans, P.J. Thomassen, J. Visser, A.E. Rowan, R.J.M. Nolte, *Angew. Chem. Int. Ed.*, 2004, **43**, 4755-4759.
15. a) A.E. Rowan, P.P.M. Aarts, K.W.M. Koutstaal, *Chem. Commun.*, 1998, 611-612.
    b) J.A.A.W. Elemans, M.B. Claase, P.P.M. Aarts, A.E. Rowan, A.P.H.J. Schenning, R.J.M. Nolte, *J. Org. Chem.*, 1999, **64**, 7009-7016.
16. a) J.A.A.W. Elemans, E.J.A. Bijsterveld, A.E. Rowan, R.J.M. Nolte, *Chem. Commun.*, 2000, 2443-2444.
    b) P.Thordarson, E.J.A. Bijsterveld, A.E. Rowan, R.J.M. Nolte, *Nature*, 2003, **424**, 915-918.
17. G. Blondeel, D. De Keukeleire, A. Harriman, L.R. Milgrom, *Chem. Phys. Lett.*, 1985, **118**, 77-82.
18. a) A.M. Brun, A. Harriman, V. Heitz, J.-P. Sauvage, *J. Am. Chem. Soc.*, 1991, **113**, 8657-8663.
    b) M. Linke, J.-C. Chambron, V. Heitz, J.-P. Sauvage, S. Encinas, F. Barigelletti, L. Flamigni, *J. Am. Chem. Soc.*, 2000, **122**, 11834-11844.
    c) K. Kilså, J. Kajanus, A.N. Macpherson, J. Mårtensson, B. Albinsson, *J. Am. Chem. Soc.*, 2001, **123**, 3069-3080.
    d) S. Fukuzumi, K. Ohkubo, W. E, Z. Ou, J. Shao, K.M. Kadish, J.A. Hutchison, K.P. Ghiggino, P.J. Sintic, M.J. Crossley, *J. Am. Chem. Soc.*, 2003, **125**, 14984-14985.
19. A.M. Brun, S.J. Atherton, A. Harriman, V. Heitz, J.-P. Sauvage, *J. Am. Chem. Soc.*, 1992, **114**, 4632-4639.
20. a) R.P. Sijbesma, R.J.M. Nolte, *J. Am. Chem. Soc.*, 1991, **113**, 6695-6696.
    b) R.P. Sijbesma, R.J.M. Nolte, *J. Phys. Org. Chem.*, 1992, **5**, 649-655.
21. a) A. Granzhan, A. Penzkofer, G. Hauska, *J. Photochem. Photobiol.*, 2004, **165**, 75-89.
    b) J.M. Lupton, *Appl. Phys. Lett.*, 2002, **81**, 2478-2480; J. Moan, P. Juzenas, S. Bagdonas, *Recent Res. Develop. Photochem. Photobiol.*, 2000, **4**, 121-132.
22. a) C. Yuang, G. He, R. Wang, Y, Li, *Thin Solid Films*, 2000, **363**, 218-220.
    b) E. Dayalan, S. Qutubuddin, *Langmuir*, 1990, **6**, 715-721.
23. a) A. Martre, H. Laguitton-Pasquier, A. Deronzier, A. Harriman, *J. Phys. Chem. B*, 2003, **107**, 2648-2692.
    b) T. Itoh, A. Ishii, Y. Kodera, A. Matsushima, M. hiroto, H. Nishimura, T. Tsuzuki, T. Kamachi, I. Okura, Y. Inada, *Bioconjugate Chem.*, 1998, **9**, 409-412.

24. S. Prathapan, S.I. Yang, J. Seth, M.A. Miller, D.F. Bocian, D. Holten, J.S. Lindsey, *J. Chem. Phys. B*, 2001, **105**, 8237-8248.
25. a) T. Hayashi, T. Takimura, H. Ogoshi, *J. Am. Chem. Soc.*, 1995, **117**, 11606-11606. b) H. Imahori, K. Tamaki, H. Yasuyuki, T. Hasobe, O. Ito, A. Shimomura, S. Kundu, T. Okada, Y. Sakata, S. Fukuzumi, *J. Phys. Chem. A*, 2002, **106**, 2803-2814.
c) Y. Shibano, M. Sasaki, T. Mikio, A. Hayato, I. Yasuyuki, T. Osamu, K. Tamao, *J. Organomet. Chem.*, 2007, **692**, 356-367.
d) S. Fukuzumi, Y. Kashiwagi, *J. Porphyrins Phthalocyanines*, 2007, **11**, 368-374.
26. K.M. Kadish, W. E, Z. Ou, J. Shao, P.J. Sintic, K. Ohbuko, S. Fukuzumi, M.J. Crossley, *Chem. Commun.*, 2002, 356-357.
27. M. Maus, E. Rousseau, M. Cotlet, G. Schweitzer, J. Hofkens, M. Van der Auweraer, F.C. De Schryver, *Rev. Sci. Instrum.*, 2001, **72**, 36-40.
28. Y.S. Park, E.J. Lee, Y.S. Chun, Y.D. Yoon, K.B. Yoon, *J. Am. Chem. Soc.*, 2002, **24**, 7123-7135.

Chapter 6. Allosterically driven assembly as a tool to construct complex supramolecular architectures

6.1 Introduction

One of Nature's ways to influence the function and composition of self-assembled structures is the use of cooperative effects. A very elegant and powerful subtype of cooperativity, allosterism, occurs when the activity at a substrate-binding site is modulated by the complexation of an effector molecule at a second site, sometimes nanometres away from the substrate-binding site. The area of artificial allosteric interactions is of great general interest, not only because of its crucial role in Nature, but also because it may be of help in the construction of functional and finite artificial nanoscale objects.[1]

Anderson and Taylor have shown that the bifunctional base diazabicyclo[2.2.2]octane (**dabco**) binds to zinc(II) porphyrins with negative cooperativity, with an interaction cooperativity parameter ($\alpha = 4K_{2ass}/K_{1ass}$) that varies between 0.01 and 0.2, depending on the solvent.[2,3] When **ZnMC** was titrated with **dabco**, a similar negative cooperativity was observed (Figure 1).[4b] The cooperativity parameter was estimated to be approximately 0.05, with the association constant $K_{1ass} = 5 \times 10^4\ M^{-1}$. Only binding of **dabco** to the "outside" of **ZnMC** was observed, as has been seen for the ligand **tbpy**. It was concluded that due to the bulkiness of the ligand, it can not be easily accommodated within the cavity of **ZnMC**. Upon the addition of viologen (**V**), K_{1ass} was found to increase by one order of magnitude ($K_a = 4 \times 10^5\ M^{-1}$; Figure 1). The differences in binding affinity of **dabco** for **ZnMC** in the presence and absence of **V** were most clearly observed in the ^{1}H NMR spectra of the complexes. The porphyrin resonances of **ZnMC** bound and unbound to **dabco** are in fast exchange on the NMR timescale in the absence of **V**, but in slow exchange upon the addition of **V**. The latter observation allowed for the direct measurement of the ratio between the ternary **V**:**ZnMC**:**dabco** complex ($\delta_{\mathbf{dabco}} = 0.87$ and -2.88 ppm) and the pentameric **V**:**ZnMC**:**dabco**:**ZnMC**:**V** complex ($\delta_{\mathbf{dabco}} = -4.74$ ppm) and thus the K_{1ass}/K_{2ass} ratios could be directly measured.[5] A cooperativity interaction parameter $\alpha = 0.07$, which is similar to the value found in the absence of **V,** was calculated. The allosteric magnification observed in this case was observed to have a pronounced effect on the distribution of species present in the solution. Calculations using the measured association constants at concentrations of [**ZnMC**] = 1 mM and [**dabco**] = 0.5 mM predicted that the sandwich species **ZnMC**:**dabco**:**ZnMC** accounts for only 22% the total amount of **ZnMC** present in solution. Upon the addition of **V** (and based on the assumption that **ZnMC**, **V**:**ZnMC**:**dabco** and **V**:**ZnMC**:**dabco**:**ZnMC**:**V** are the only species in the mixture), 57% of **ZnMC** was calculated to participate in the

sandwich complex, which illustrates how the binding of **V** promotes the assembly of **ZnMC** around the **dabco** ligand in an allosteric fashion. The equilibrium, however, was not exclusively driven through to the pentameric complex owing to the negative cooperativity of the **dabco** ligand. This chapter describes efforts to form a pentameric [5]pseudo-rotaxane complex by using a modified porphyrin clip. The dimerisation of this [5]pseudo-rotaxane to form a well-defined 14-component complex by allosteric self-assembly, was also studied.

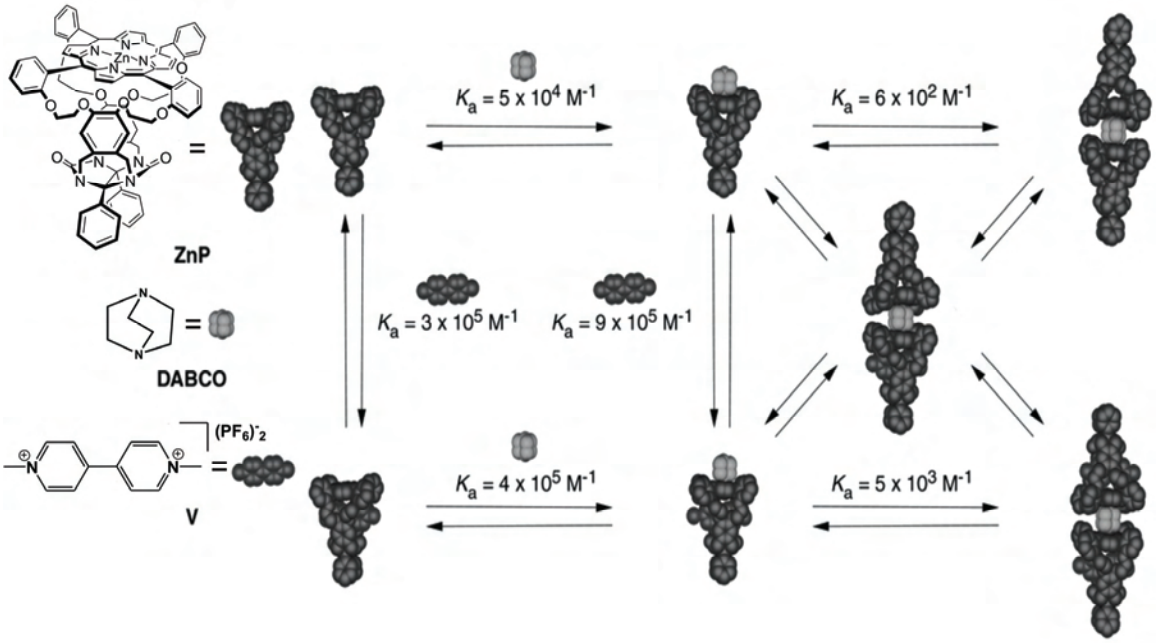

Figure 1. *Allosteric dimerisation of* ***ZnMC*** *by the addition of* ***dabco*** *in the presence and absence of* ***dabco*** *(**V** = PF_6 salt of 4,4'-dimethyl-viologen).*

6.2 'Simple' dimerisation of ZnOHP

It was reasoned that the negative cooperativity of the bridging **dabco** ligand could be overcome by the introduction of functional groups on top of the zinc porphyrin host which could interact with the other zinc porphyrin host in the sandwich complex in a positive cooperative mode. A cavity-appended zinc(II) porphyrin was therefore synthesised with 4 hydroxy functions positioned on the meso phenyl rings which might serve as additional interactive elements (**ZnOHP**, Figure 2a). Molecular modelling studies indicated that the OH functions of **ZnOHP** would be 3 Å apart when two molecules of this compound are self-assembled by a **dabco** ligand. These OH functions can form hydrogen bonds upon dimerisation, in principle overcoming the negative cooperativity of **dabco**. NMR, UV-vis and fluorescence spectroscopy studies of a 1:1 mixture of **ZnOHP** and **dabco** ($CHCl_3/CH_3CN$ 1:1 (v/v)) revealed an association constant of $K_a = 1.5 \times 10^5\ M^{-1}$, but no indication for the formation of sandwich complexes

was observed. In the presence of **V**, however, upon the addition of **dabco** the pentameric sandwich complex **V**:**ZnOHP**:**dabco**:**ZnOHP**:**V** (Figure 2b) became visible and the association constants between the ligand and the two hosts were measured to be K_{1ass}= 2 x 10^6 M^{-1} and K_{2ass}= 9 x 10^6 M^{-1}, respectively. These association constants give an α-value of 17, which points to an exceptionally positive cooperative assembly process. A consequence of the cooperative process is that at concentrations of [**ZnOHP**]= 1 mM and [**dabco**]= 0.5 mM, a remarkable 98.5% of **ZnOHP** is involved in the pentameric sandwich complex (Figure 2b). This compares to the unfunctionalised host which at the same concentrations is only 57% bound in the pentameric complex. The above indicates that the addition of an extra factor, namely the OH-groups in **ZnOHP**, combined with the allosteric magnification that **V** exerts on the binding of **dabco**, results in the assembly of a single, well-defined species from a complex equilibrium mixture.

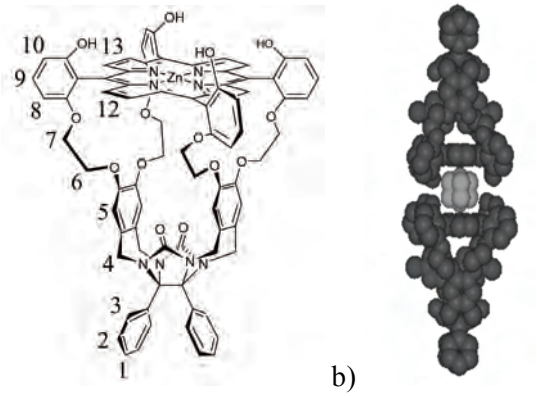

Figure 2. *a) Structure of porphyrin host* ***ZnOHP*** *with proton numbering. b) Structure of the allosteric sandwich complex* ***ZnOHP****:V:****dabco****:V:****ZnOHP****.*

6.3 Self-assembly of a 14-component complex

As a continuation of this research it was attempted to create larger and more complex architectures based on this allosteric self-assembly process. Research was directed towards the dimerisation of [5]pseudo-rotaxanes composed of four **ZnOHP** hosts complexed to a central free base porphyrin with four pendant viologens connected *via* pentylene (**FbP-(C_5-V)$_4$**) or propylene spacers (**FbP-(C_3-V)$_4$**. Dimerisation of these [5]rotaxanes will be induced by the addition of **dabco**, with the aim to form a finite 14-component complex by allosteric self-assembly (Figure 3).

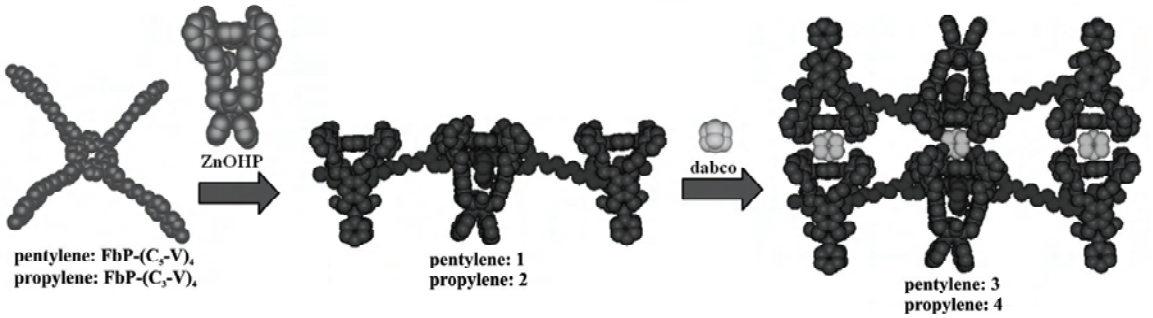

Figure 3. *Schematic representation of the allosteric self-assembly of a 14-component complex induced by the addition of* ***dabco*** *to two [5]pseudo-rotaxanes consisting of four* ***ZnOHP*** *hosts and one central tetra-viologen porphyrin (****FbP-(C$_n$-V)$_4$*** *(Figure 2 and 5a)).*

Before attempting the dimerisation of the [5]pseudo-rotaxanes, a simple free base porphyrin with one covalently attached viologen moiety (**FbP-(C$_5$-V)**) reference guest was complexed with the **ZnOHP** host (Figure 3 and 4a). According to ^{1}H-NMR, the addition of one equivalent of **ZnOHP** to this compound in a $CDCl_3/CD_3CN$ 1:1 (v/v) solution at a concentration of 10^{-3} M, resulted in the quantitative formation of a [2]pseudo-rotaxane. In this complex the viologen proton signals were shifted significantly upfield with respect to the free species, which is indicative of complexation of the guest inside the cavity of **ZnOHP**. In addition, the aromatic side-wall proton signals of the host at 6.0 ppm were split into two signals, indicative of a non-symmetric complexation geometry, and NOE contacts were observed between the C and E protons of the guest with the 6 protons of the host in a 2D-NOESY-NMR spectrum. The subsequent addition of one equivalent of **dabco** to the solution gave rise to the appearance of a signal corresponding to the doubly complexed ligand at -4.8 ppm (3 in Figure 4d), and two signals corresponding to the single complexed ligand at 0.87 and -2.75 ppm, respectively (1 and 2 in Figure 4d), showing that not a single species is formed. The fact that no other significant changes in the chemical shifts were observed in the ^{1}H-NMR spectrum and no new NOE contacts could be observed compared to the situation before the addition of **dabco**, suggest that the dimerised [2]pseudo-rotaxane sandwich adopts a conformation in which on average the two free base porphyrin ligands are not in close proximity to each other, as shown (Figure 4b).

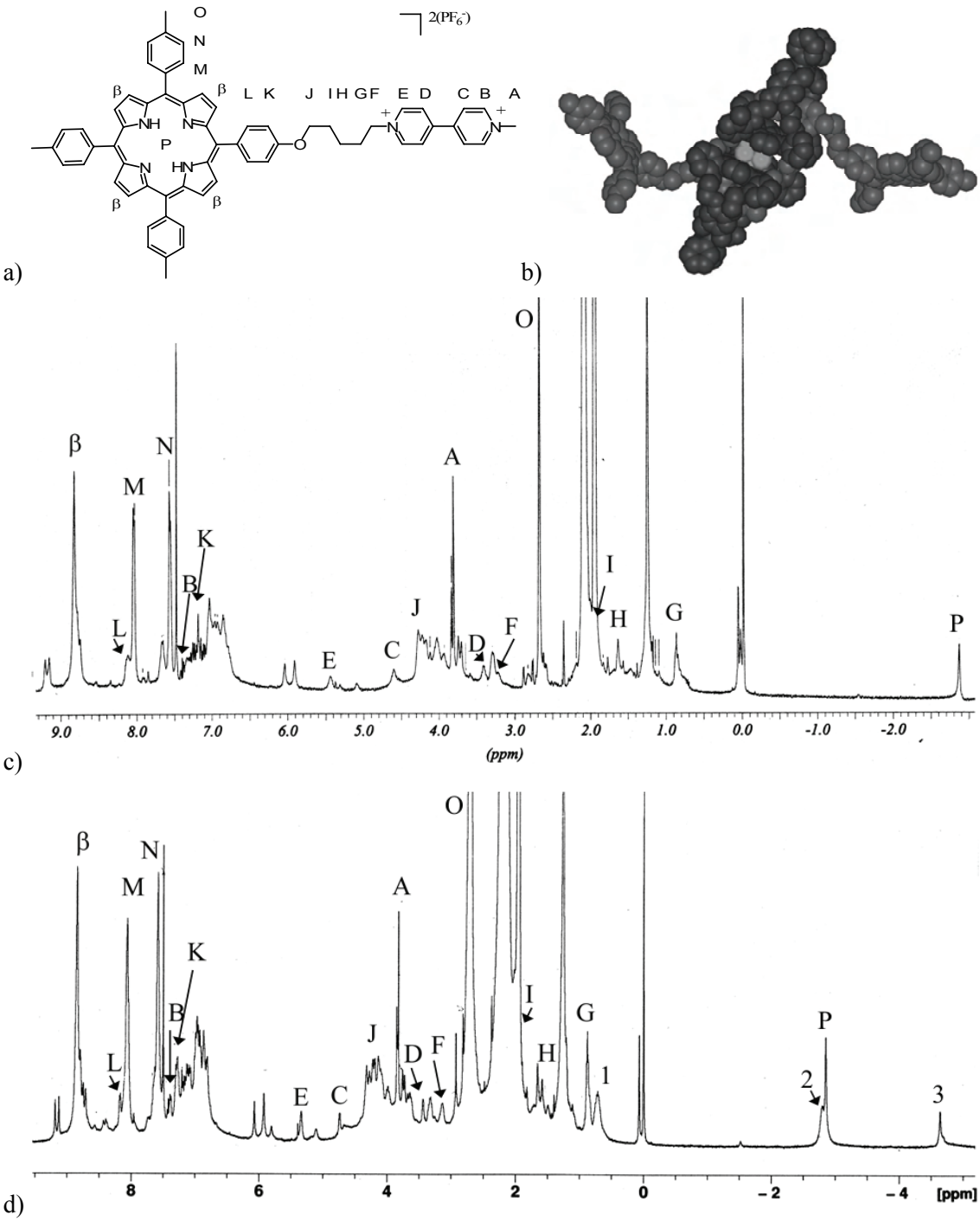

Figure 4. *a) Structure and proton assignment of* ***FbP-(C5-V)****. b) MMFF optimised structure of the complex* ***(FbP-(C5-V))2-(ZnOHP)2-dabco****. c)* ^{1}*H-NMR spectrum of* ***(FbP-(C5-V))-ZnOHP*** *(400.15 MHz, $CDCl_3/CD_3CN$ = 1:1 (v/v)). d)* ^{1}*H-NMR spectrum of* ***(FbP-(C5-V))-ZnOHP*** *in the presence of one equivalent of* ***dabco*** *(500.13 MHz, $CDCl_3/CD_3CN$ = 1:1 (v/v)).*

Upon the step-wise addition of 4 equivalents of **ZnOHP** to **FbP-(C_5-V)$_4$** ($CDCl_3/CD_3CN$ 1:1 (v/v); [**FbP-(C_5-V)$_4$**] = 10^{-3} M) an upfield shift in the ^{1}H-NMR spectrum for the

proton signals of the viologen moiety and the side-wall of the host were observed, indicating the formation of [5]pseudo-rotaxane **1** (Figure 3). Concomitantly, a small 0.1 ppm downfield shift and a splitting of the pyrrole N*H* protons of **FbP-(C_5-V)$_4$** into three distinct new peaks was observed (Figure 5b). Molecular modelling calculations on the 4:1 complex showed that the pentylene spacers of the central porphyrin guest are long and flexible enough to allow conformations in which one or more of the **ZnOHP** hosts are situated above and/or below the porphyrin plane of **FbP-(C_5-V)$_4$** (Figure 5c). When such conformations exchange slowly on the NMR timescale, a shift and a splitting of the pyrrole N*H* protons would be expected.

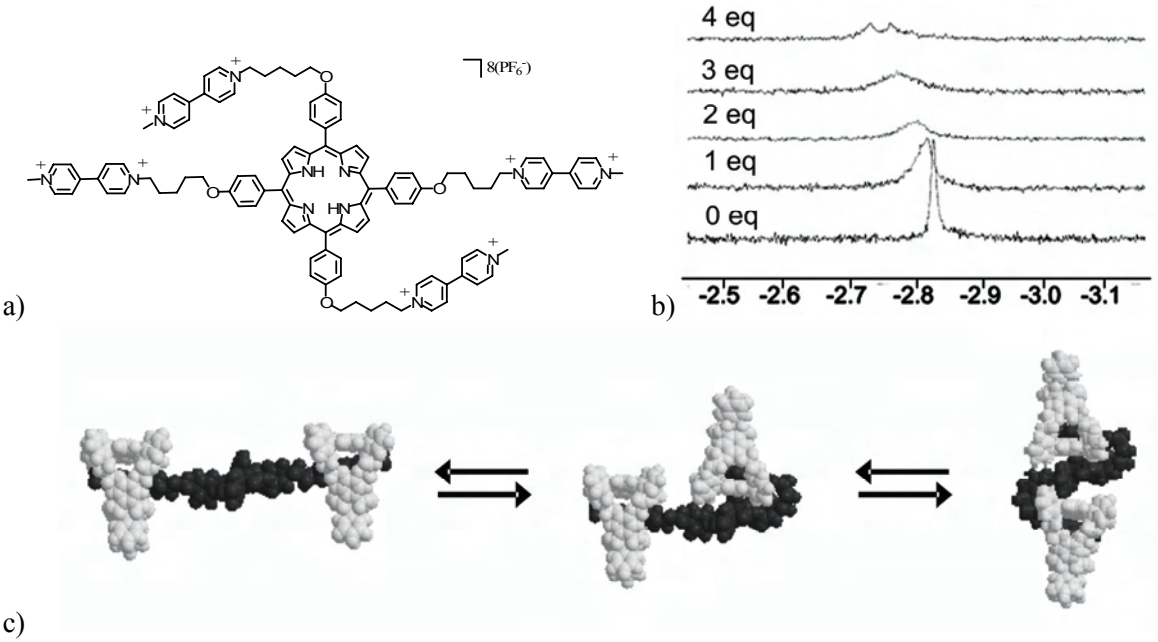

Figure 5. *a) Structure of **FbP-(C_5-V)$_4$**. b) Upfield region of the ^{1}H-NMR spectra during the addition of 4 equivalents of **ZnOHP** to **FbP-(C_5-V)$_4$** (400.15 MHz, $CDCl_3/CD_3CN$ = 1:1 (v/v)). c) Molecular models showing the possible folding of bound **ZnOHP** above and/or below the porphyrin plane of **FbP-(C_5-V)$_4$**. (For clarity, two pendant viologens with complexed host molecules are omitted.)*

The subsequent addition of **dabco** to the presumed [5]pseudo-rotaxane complex **1** gave rise to the emergence of two separate double-coordinated **dabco** signals at -4.73 and -4.76 ppm in the ^{1}H-NMR spectrum. This doubling is characteristic of the formation of a dimer. After the addition of more than 2 equivalents of **dabco** with respect to **FbP-(C_5-V)$_4$**, signals at 0.9 and -2.8 ppm corresponding to mono-coordinated **dabco** started to appear, indicative of the formation of complex **9** (Figure 6e). During the titration, the signal of the pyrrole N*H* protons of **FbP-(C_5-V)$_4$** at -2.75 ppm experienced a small downfield shift. During the early part of the titration, several N*H* proton resonances were observed, while after the addition of 2 equivalents of **dabco** only two singlets remained at

-2.4 and -2.6 ppm. These signals were reduced to one signal at -2.6 ppm after the addition of 10 equivalents of the ligand relative to the porphyrin guest (Figure 6a).

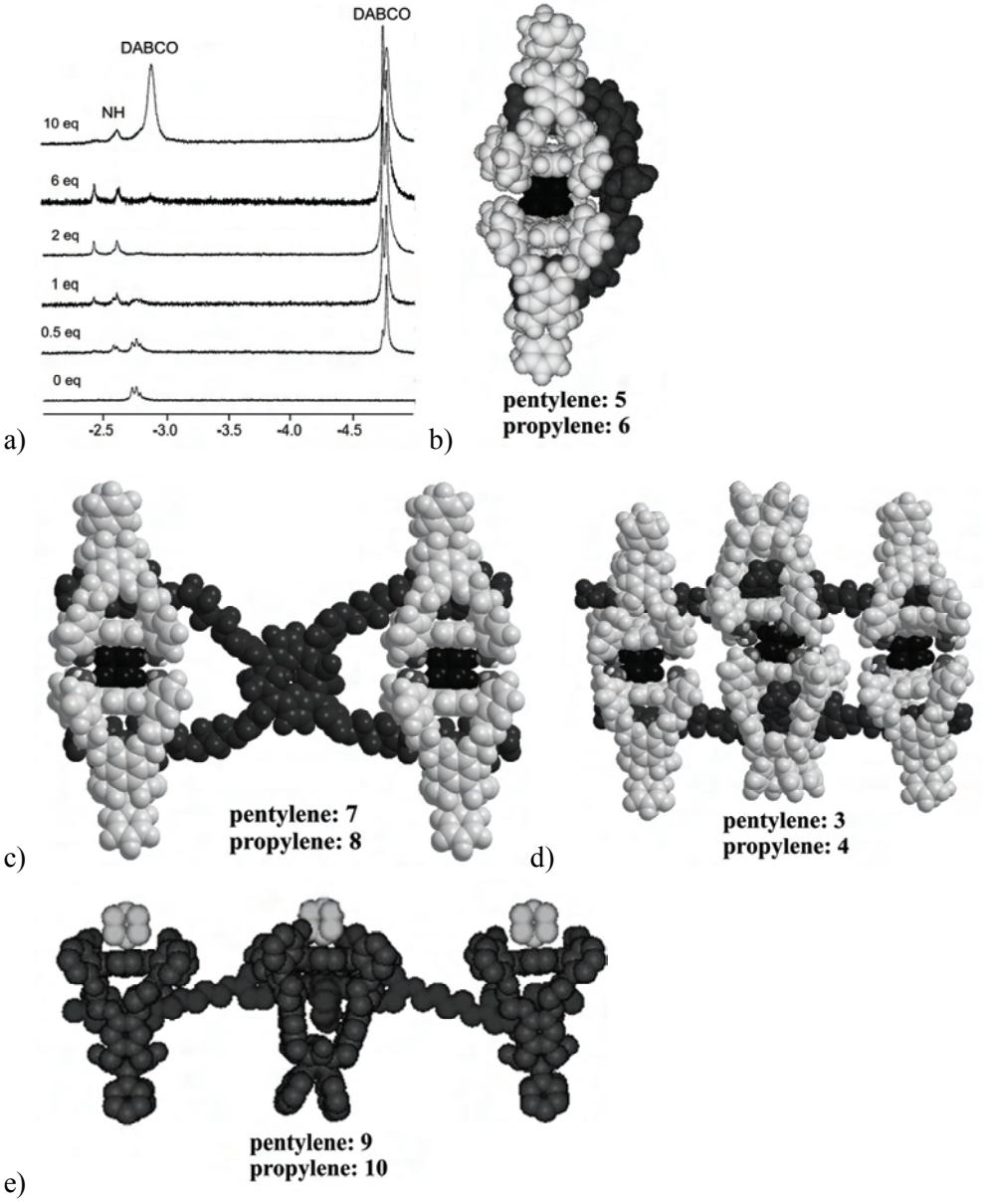

Figure 6. *a) Upfield region of the ^{1}H-NMR spectra during the addition of 10 equivalents of* ***dabco*** *to a 4:1 mixture of* ***ZnOHP*** *and* ***FbP-(C_5-V)$_4$*** *(400.15 MHz, $CDCl_3/CD_3CN$ = 1:1 (v/v)). b) Molecular model of the complex in which* ***dabco*** *is intramolecularly sandwiched between two porphyrin hosts on opposite viologen moieties. (For clarity, two pendant viologens with complexed host molecules are omitted.) c) Molecular model of the complex in which* ***dabco*** *is intramolecularly sandwiched between two porphyrin hosts on neighbouring viologen moieties. d) Molecular model of the complex in which* ***dabco*** *is intermolecularly sandwiched between two porphyrin hosts. e) Molecular model of the pentameric complex* ***FbP-(C_n-V)$_4$:(ZnOHP)$_4$*** *with four* ***dabco*** *molecules singly coordinated.*

A possible explanation for this complex NMR behaviour was sought with the help of modelling calculations. Molecular models indicated that the pentylene spacers of the guest molecule are flexible enough to allow the **ZnOHP** hosts within the same [5]pseudo-rotaxane to dimerise with each other upon the addition of **dabco**. This dimerisation can be between two hosts complexed on neighbouring viologen moieties (**7**; Figure 6c) or between two **ZnOHP** hosts complexed on opposite viologen moieties (**5;** Figure 6b). Together with the 14-component self-assembled complex **3**, which consists of two [5]pseudo-rotaxanes dimerised by four **dabco** molecules, and complexes in which one or more **dabco** ligands are mono-coordinated to **ZnOHP**, several different complexes can be envisaged to be formed and to be in fast exchange during the stepwise addition of the ligand.

In order to inhibit self-dimerisation within one [5]pseudo-rotaxane, the spacers between the central porphyrin and the viologen moieties were shortened from pentylene to propylene (**FbP-(C_3-V)$_4$**; Figure 7a). Molecular modelling calculations suggested that these spacers would be too short to easily allow intramolecular dimerisation of two neighbouring **ZnOHP** hosts through the coordination of **dabco**, as in complex **8** (Figure 6b).
In contrast to the observation in the titration using **FbP-(C_5-V)$_4$**, the stepwise addition of 4 equivalents of **ZnOHP** to a solution of **FbP-(C_3-V)$_4$** in $CDCl_3$/CD_3CN 1:1 (v/v) ([**FpP-(C3-V)$_4$**] = 10^{-3} M) did not result in a splitting of the pyrrole N*H* protons of the guest in the ^{1}H-NMR spectra. The signal shifted downfield by 0.15 ppm and experienced significant broadening (Figure 7b). All other signals of the complex appeared approximately at the same position as in the analogous complex based on **FbP-(C_5-V)$_4$**, indicating the formation of the [5]pseudo-rotaxane **2** (Figure 3, 4c and d). All this indicated that the propylene spacers inhibit the conformations with one or more **ZnOHP** hosts above and/or below the porphyrin plane of **FbP-(C_3-V)$_4$**.
The subsequent stepwise addition of 4 equivalents of **dabco** to **2** resulted in similar changes in the signals of the pyrrole N*H* protons of **FbP-(C_3-V)$_4$** as were observed when **FbP-(C_5-V)$_4$** was used as the central guest. Again two other peaks appeared at -2.4 and -2.6 ppm, shifted downfield with respect to the original peak at -2.7 ppm. After the addition of 2 equivalents of **dabco**, the integral of the signal at -2.4 ppm reached a maximum, constituting 70% of the overall integral of the N*H* signals, and decreased in size upon the addition of more equivalents of the ligand. After the addition of 1.5 eq of **dabco**, the original N*H* signal at -2.7 ppm had disappeared. In addition, similar to the case in which **FbP-(C_5-V)$_4$** was used, two separate signals appeared between -4.5 and -5 ppm, corresponding to **dabco** bound in a sandwich geometry. After the addition of more than 2 equivalents of **dabco**, signals for the monodentate complexed ligand appeared at 0.87 and -2.75 ppm. The observation of distinct double-complexed **dabco** signals show

that different double-complexed **dabco** conformations exist. Molecular modelling studies indicated that the formation of **6** is possible, which suggests that the solution contains complexes **4**, **6**, **10** and perhaps oligomeric architectures, in fast exchange.

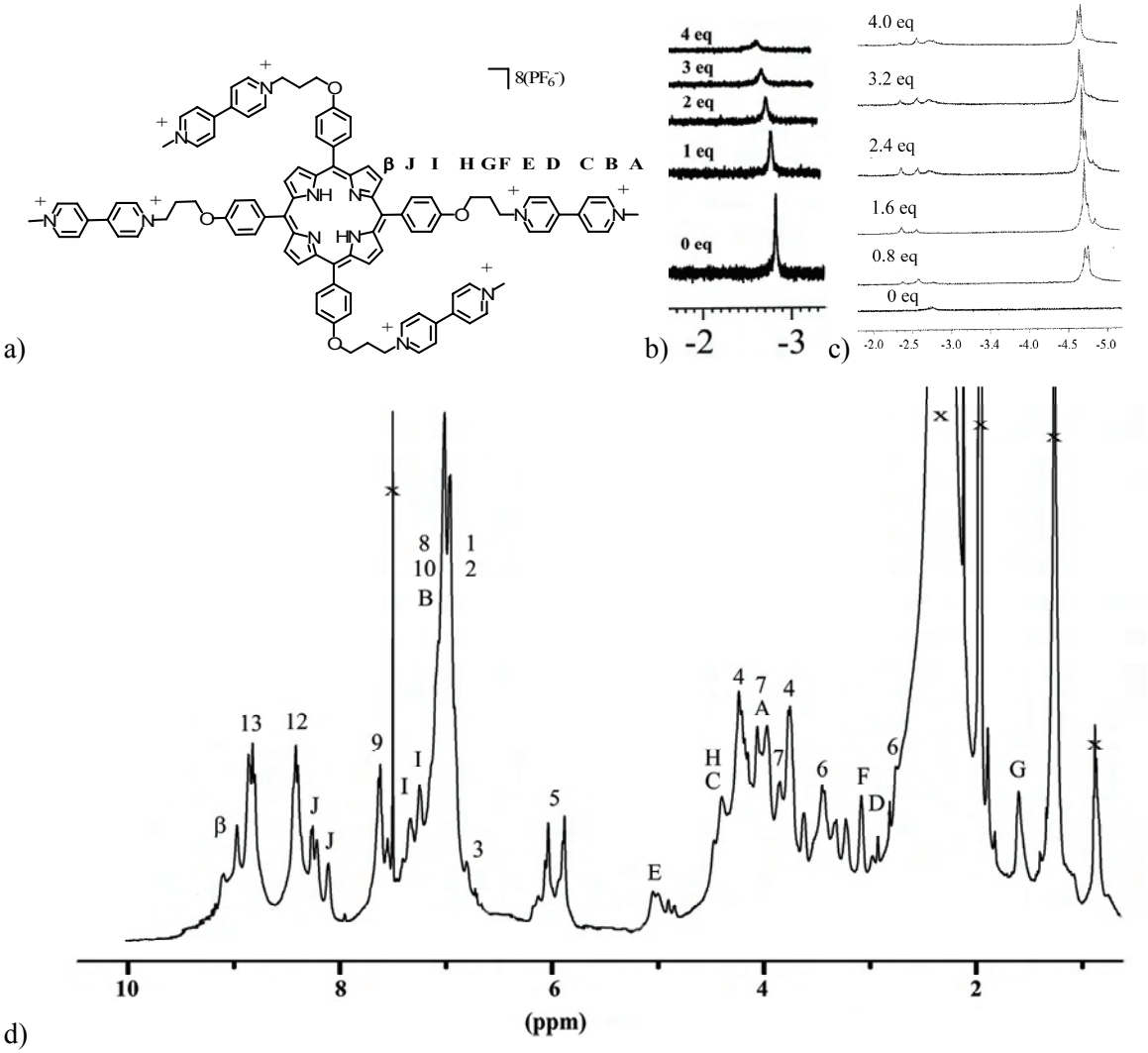

Figure 7. *a) Structure of* ***FbP-(C₃-V)₄*** *with proton assignment. b) Upfield region of the* ^{1}*H-NMR spectra during the addition of 4 equivalents of* ***ZnOHP*** *to* ***FbP-(C₃-V)₄*** *(500.13 MHz, $CDCl_3/CD_3CN$ = 1:1 (v/v)). c) Upfield region of the* ^{1}*H-NMR spectra during the addition of 4 equivalents of* ***dabco*** *to a 4:1 mixture of* ***ZnOHP*** *and* ***FbP-(C₃-V)₄*** *(500.13 MHz, $CDCl_3/CD_3CN$ = 1:1 (v/v)). d) Downfield region of the* ^{1}*H-NMR spectrum of the 4:1* ***ZnOHP*****:*****FbP-(C₃-V)₄*** *mixture with assignment of the signals belonging to* ***FbP-(C₃-V)₄*** *and* ***ZnOHP*** *(500.13 MHz, $CDCl_3/CD_3CN$ = 1:1 (v/v)).*

The overall ^{1}H-NMR spectrum of a 4:1 mixture of **ZnOHP** and **FbP-(C_3-V)$_4$** in $CDCl_3/CD_3CN$ 1:1 (v/v) was relatively sharp, allowing the assignment of many of the peaks in the region downfield from 0 ppm with the help of COSY and NOESY 2D NMR techniques (Figure 7d). Upon the addition of **dabco**, this region showed almost no

changes in the proton signals, except for the appearance of some relatively small, broad peaks between 9.0 and 9.5 ppm, making it of little use in distinguishing between the different possible self-assembled complexes. A tentative explanation for the peaks between 9.0 and 9.5 ppm might be that they belong to the β-pyrrolic protons of **ZnOHP** that point towards the porphyrin moiety in **FbP-(C_3-V)$_4$**, such as in complex **6** (Figure 6b), however, no NOE contacts were found for these peaks and therefore the formation of such a complex can not be proven.

Mass spectroscopy, unfortunately, proved to be of little use for the analysis of the complexes, since even using the mildest techniques, such as MALDI-TOF and ESI, the complexes appeared to fall apart into their separate components. As an alternative investigative tool diffusion-ordered NMR (DOSY NMR) spectra of the separate components and their mixtures were recorded in $CDCl_3/CD_3CN$ 1:1 (v/v; [**FbP-(C_3-V)$_4$**] = 10^{-3} M).[6] Using the Einstein-Stokes equation it was possible to estimate the approximate radii of the different compounds and complexes (see Experimental section).

From a DOSY NMR spectrum of a $1x10^{-3}$ M solution of **ZnOHP** in $CDCl_3/CD_3CN$ 1:1 (v/v), a radius of 8.6 Å was calculated for the host molecule. This value was compared with a PM3 model of the molecule, from which a radius of 8-9 Å could be estimated using a spherical approximation of this molecule (Figure 8a).

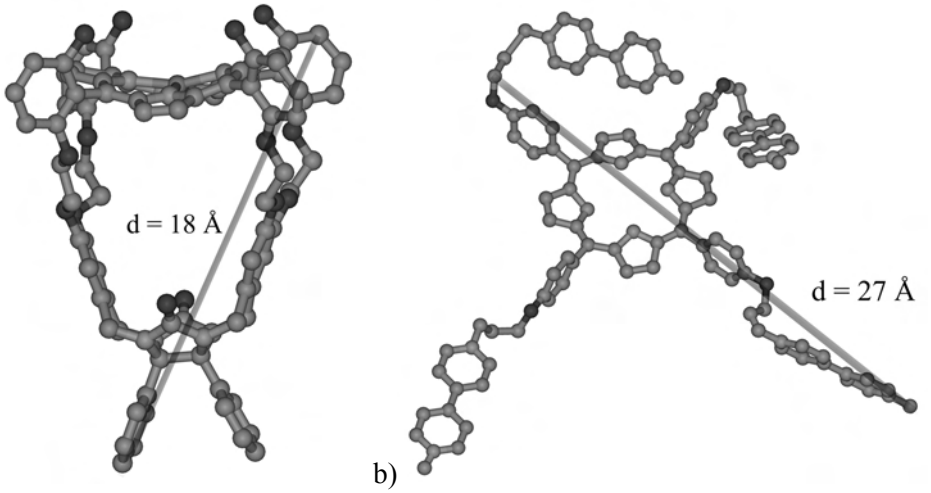

a) b)

Figure 8. *PM3 optimised structures with relevant distances of a)* ***ZnOHP*** *and b)* ***FbP-(C_3-V)$_4$,*** *which correlate well with the diameter calculated from DOSY NMR.*

From a DOSY NMR spectrum of a $1x10^{-3}$ M solution of **FbP-(C_3-V)$_4$** in $CDCl_3/CD_3CN$ 1:1 (v/v), a radius of 11.7 Å was obtained for the molecule, which compares well with a spherical approximation of this molecule calculated at the PM3 level which assumes that the viologen side chains are not fully stretched (Figure 8b).

Upon mixing the two compounds in $CDCl_3/CD_3CN$ 1:1 (v/v), using a concentration of 10^{-3} M for the central porphyrin, the DOSY NMR spectra showed the presence of only

one species with a well-defined diffusion rate, both in the absence and presence of **dabco**. The calculated radii that were obtained by DOSY NMR did not fit well with calculated models for **2** and **4**. A radius of 21 Å can be estimated for **2** (Figure 3), however, a radius of only 3.8 Å was obtained from the DOSY NMR spectrum of a 4:1 solution of **ZnOHP** and **FbP-(C_3-V)$_4$**. Upon the addition of one equivalent of **dabco** relative to **ZnOHP**, a radius of 19.3 Å for the resulting complex was obtained, whereas a radius of 23 Å is estimated from the PM3 model of **4** (Figure 3). The increase by a factor of 5 upon the addition of **dabco** for the average radius seems to indicate the formation of a large self-assembled system, and compares well with the estimated radii of complexes **6** and **8** (19 and 21 Å, respectively). Although the concentration is not a factor in the Einstein-Stokes equation, at different concentrations, different diffusion rate values were obtained for single compounds. It must also be noticed that the pseudo-rotaxanes are far from spherical. Due to both these factors, the obtained radii for the self-assembled complexes can only be tentatively obtained from DOSY NMR spectra.

6.4 Discussion

The combination of data obtained from the different NMR techniques and molecular modelling studies, unfortunately was not conclusive enough to allow a precise geometry of the self-assembled 4:2:1 (and/or 8:4:2) **ZnOHP**:**dabco**:**FbP-(C_n-V)$_4$** complexes to be obtained. From an energetic point of view, the enthalpy of the self-assembly of these complexes is expected to be relatively equal, because all the interactions between the components are equal, displaying similar allosteric increases in association constants. Entropically, however, the complexation of **dabco** within one [5]pseudo-rotaxane would be more favourable than between two of these complexes. In both cases the alkyl spacers of the guest have to give up their conformational flexibility, by bending or stretching, respectively, however in the formation of the 14-component systems **3** and **4**, more molecules have to self-assemble compared to the formation of complexes **5-8**, which in general is entropically even less favourable. The latter effect is valid especially in the case of the guest **FbP-(C_5-V)$_4$** in which intramolecular complexation of **dabco** is not hindered. The formation of 14-component complex **3** is therefore only tentatively proposed. In the case of guest **FbP-(C_3-V)$_4$**, in which the formation of complex **8** is hindered according to modelling calculations, the formation of the 14-component complex **4** may indeed occur. The formation of a large complex is supported by DOSY NMR data, however the estimated radius, however inaccurate, corresponds better with the formation of complex **6**. This also agrees with the tentative assignment of the peaks between 9 and 9.5 ppm in the ^{1}H NMR spectrum of this 4:2:1 mixture.
Overall it seems that during the stepwise addition of the ditopic ligand **dabco** to the complexes **1** and **2** (with the porphyrin N*H* signal in ^{1}H NMR at -2.7 ppm) both are

converted into at least two different complexes (with N*H* signals at -2.4 and -2.6 ppm). The addition of more than two equivalents of the ligand resulted in the formation of the complexes **9** and **10** (with the N*H* signal at -2.6 ppm) in which **dabco** is only single-coordinated.

6.5 Conclusions

Allosterically controlled assembly, although not easy as demonstrated herein, opens up numerous possibilities for directing complex equilibrium mixtures to a desired product that mimics the hierarchical self-assembly processes found in Nature.

The sandwich-like complexation of the ditopic ligand **dabco** by two hydroxy-functionalised cavity-appended zinc(II) porphyrins (**ZnOHP**) was proven to be only possible in the presence of viologen guests, resulting in an allosteric complex with an α-value of 17, which is an exceptionally positive cooperative assembly process.

NMR studies have shown that upon the addition of 4 equivalents of **ZnOHP** to the tetra-viologen-appended free base porphyrin **FbP-(C_5-V)$_4$** a [5]pseudo-rotaxane complex **1** is formed. The flexibility of the pentylene spacers in complex **1** allowed two of the hosts to fold above and below the plane of the central porphyrin, which prevented the formation of larger complex self-assembled architectures upon the addition of **dabco**. To avoid these interactions within one [5]pseudo-rotaxane, a tetra-viologen-appended free base porphyrin **FbP-(C_3-V)$_4$** with shorter spacers was studied. ^{1}H NMR spectra showed for this guest that in the [5]pseudo-rotaxane **2** this folding did not occur. The subsequent addition of half an equivalent of **dabco** to **2** resulted in the formation of a minimum of at least two distinct complexes, as was concluded from the ^{1}H NMR signals for the pyrrole N*H* protons of the central guest. One of these complexes is tentatively ascribed to the 7-component complex **6**, consisting of two **dabco** molecules, four host molecules and one tetra-viologen porphyrin (the existence of complex **8** is unlikely based on the conclusions of molecular modelling studies; in complex **8** two adjacent **ZnOHP** hosts are dimerised by **dabco**, while in complex **6** two opposite **ZnOHP** hosts sandwich the ditopic ligand.) Upon the addition of half an equivalent of **dabco** the desired self-assembled complex **4**, a 14-component system with a molecular weight of 15,272 Da (excluding the 16 PF_6^- counter-ions) could also be formed. The formation of a single, large self-assembled complex is supported by a significant decrease in the average diffusion coefficient of the complex upon the addition of **dabco**, however, entropically the formation of either complex **6** or **8** seems more favourable than the formation of complex **4**. Further experiments are needed to conclusively prove what species is formed.

6.6 Experimental

Acetonitrile-d_3 was distilled over CaH_2 and chloroform-d was distilled over $CaCl_2$ prior to use. The mono-substituted bipyridinium analogues of **FbP-(C_5-V)$_4$**, **FbP-(C_3-V)$_4$** and **FbP-(C_5-V)** were synthesised according to the procedure described in Chapter 4. **ZnOHP** was synthesised according to literature procedures.[7] All other solvents and chemicals were commercial materials and used without purification.
NMR spectra were obtained on Varian Unity Inova 400 and Bruker DRX 500 instruments at 298 K. All NMR studies of host-guest complexes were performed in freshly prepared $CDCl_3$/CD_3CN 1:1 (v/v) mixtures at a 1 x 10^{-3} M for the central porphyrin guest. All the ratios that are mentioned with regard to host:guest mixtures are molar ratios.
Diffusion rate values were obtained using data analysis in Mestre-C 4.7.0.0 on the DOSY NMR data. The diffusion rates for the single molecules and complexes that were used for the calculation of their radii were an average of the diffusion rates obtained for at least six different peaks in the DOSY NMR spectrum to minimise errors. The radii were calculated from the diffusion rates, with the assumption that the viscosity of a 1:1 (v/v) mixture of $CDCl_3$ and CD_3CN is the average (0.4435×10^{-3} kg m^{-1} s^{-1}) of the viscosity values of the two individual solvents, using the rearranged Einstein-Stokes equation: $r = kT/6\pi D\eta$, in which:

r = radius (m)
k = Boltzmann's constant (JK^{-1})
T = temperature (K)
D = diffusion rate (m^2 s^{-1})
η = viscosity of the medium (kg m^{-1} s^{-1})

Synthesis of FbP-(C_5-V), FbP-(C_5-V)$_4$ and FbP-(C_3-V)$_4$.
The bipyridinium molecules were functionalised with a methyl group by stirring them in DMF at a concentration of 0.01 M with a 1000-fold excess of MeI under N_2 for 24 hrs. The solution was quenched in water, extracted with $CHCl_3$, and the organic layer was evaporated. The remaining solid was dissolved in CH_3CN, after which a saturated aqueous $NaHCO_3$ solution was added until the solution turned from green to purple. The solution was extracted with $CHCl_3$ and the organic layer evaporated. The remaining solid was dissolved in CH_3CN and this solution was added to a saturated aqueous KPF_6 solution. The resulting precipitate was filtered off and dissolved in CH_3CN. This solution was added to diethyl ether and the resulting precipitate was isolated *via* centrifugation and drying *in vacuo*. Yield: 94% (**FbP-(C_5-V)**, 93% (**FbP-(C_5-V)$_4$**), 95% (**FbP-(C_3-V)$_4$**.
^{1}H NMR **FbP-(C_3-V)** (CD_3CN, 298K, 400.13 MHz): δ = 9.13 (d, 2H, Py*H*-2,6 ^3J= 4.6 Hz), 8.88 (s, 8H, β-pyrrole*H*), 8.84 (d, 2H, Py*H*-2',6', ^3J= 5.2 Hz), 8.50 (d, 2H, Py*H*-3,5,

^3J= 4.4 Hz), 8.44 (d, 2H, Py*H*-3',5', ^3J= 4.4 Hz), 8.14 (d, 8H, Ar*H*-2,6, ^3J= 7.4 Hz), 7.29 (d, 8H, Ar*H*-3,5, ^3J= 7.7 Hz), 4.97 (t, 2H, N-CH_2, ^3J= 7.6 Hz), 4.47 (s, 3H, N-CH_3), 4.40 (t, 2H, O-CH_2, ^3J= 7.1 Hz), 2.73 (bs, 11H, CH_3, C-CH_2-C), -2.84 (s, 2H, N*H*). MALDI-TOF: 886 [**FbP-(C_5-V)** - 2 PF_6]$^+$.

^{1}H NMR **FbP-(C_5-V)$_4$** ($CDCl_3$/CD_3CN 1:1 (v/v), 298K, 400.13 MHz): δ = 8.98 (d, 8H, Py*H*-2,6 ^3J= 4.7 Hz), 8.87 (s, 8H, β-pyrrole*H*), 8.84 (d, 8H, Py*H*-2',6', ^3J= 5.1 Hz), 8.46 (d, 8H, Py*H*-3,5, ^3J= 4.4 Hz), 8.40 (d, 8H, Py*H*-3',5', ^3J= 4.4 Hz), 8.09 (d, 8H, Ar*H*-2,6, ^3J= 7.3 Hz), 7.29 (d, 8H, Ar*H*-3,5, ^3J= 7.9 Hz), 4.73 (t, 8H, N-CH_2, ^3J= 7.7 Hz), 4.40 (s, 12H, N-CH_3), 4.28 (t, 8H, O-CH_2, ^3J= 6.8 Hz), 2.24 (m, 8H, N-C-CH_2-C), 2.10 (m, 8H, O-C-CH_2-C), 1.75 (m, 8H, C-C-CH_2-C-C), -2.85 (s, 2H, N*H*). MALDI-TOF: 1640 [**FbP-(C_5-V)$_4$** - 8 PF_6]$^+$.

^{1}H NMR **FbP-(C_3-V)$_4$** (CD_3CN, 298K, 400.13 MHz): δ = 9.12 (d, 8H, Py*H*-2,6 ^3J= 4.6 Hz), 8.89 (s, 8H, β-pyrrole*H*), 8.85 (d, 8H, Py*H*-2',6', ^3J= 5.1 Hz), 8.51 (d, 8H, Py*H*-3,5, ^3J= 4.4 Hz), 8.44 (d, 8H, Py*H*-3',5', ^3J= 4.4 Hz), 8.12 (d, 8H, Ar*H*-2,6, ^3J= 7.3 Hz), 7.28 (d, 8H, Ar*H*-3,5, ^3J= 7.8 Hz), 4.96 (t, 8H, N-CH_2, ^3J= 7.5 Hz), 4.46 (s, 12H, N-CH_3), 4.39 (t, 8H, O-CH_2, ^3J= 7.0 Hz), 2.72 (m, 8H, C-CH_2-C), -2.85 (s, 2H, N*H*). MALDI-TOF: 1528 [**FbP-(C_3-V)$_4$** - 8 PF_6]$^+$.

References

1. a) J. Rebek Jr., *Acc. Chem. Res.,* 1984, **17**, 258-264.
   b) I. Tabushi, *Pure Appl. Chem.,* 1988, **60**, 581-586.
   c) R.P. Sijbesma, R.J.M. Nolte, *J. Am. Chem. Soc.,* 1991, **113**, 6695-6696.
   d) S. Shinkai, M. Ikeda, A. Sugasaki, M. Takeuchi, *Acc. Chem. Res.,* 2001, **34**, 494-503.
   e) M. Takeuchi, M. Ikeda, A. Sugasaki, S. Shinkai, *Acc. Chem. Res.,* 2001, **34**, 865-873.
   f) L. Kovbasyuk, R. Krämer, *Chem. Rev*., 2004, **104**, 3161-3188.
   g) H. Sato, K. Tashiro, H. Shinmori, A. Osuka, Y. Murata, K. Komatsu, T. Aida, *J. Am. Chem. Soc.,* 2005, **127**, 13086-13087.
   h) J.D. Badjić, A. Nelson, S.J. Cantrill, W.B. Turnbill, J.F. Stoddart, *Acc. Chem. Res.,* 2005, **38**, 723-732.
   i) R. Wakabayashi, Y. Kubo, O. Hirata, M. Takeuchi, S. Shinkai, *Chem. Commun.,* 2005, 5742-5744.
   j) N.C. Gianneschi, M.S. Masar III, C.A. Mirkin, *Acc. Chem. Res.,* 2005, **38**, 825-837.
   k) S. Le Gac, J. Marrot, O. Reinaud, I. Jabin, *Angew. Chem. Int. Ed.,* 2006, **45**, 3123-3126.
   l) B. Botta, F. Caporuscio, D. Subissati, A. Tafi, M. Botta, A. Filippi, M. Speranza, *Angew. Chem. Int. Ed.,* 2006, **45**, 2717-2720.
2. P.N. Taylor, H.L. Anderson, *J. Am. Chem. Soc.*, 1999, **121**, 11538-11545.
3. a) K.A. Connors, *Binding Constants*, Wiley, New York, 1987.
   b) K.A. Connors, A. Paulson, D. Toledo-Velasquez, *J. Org. Chem*., 1988, **53**, 2023-2026.

4. a) P. Thordarson, E.J.A. Bijsterveld, A.E. Rowan, R.J.M. Nolte, *Nature,* 2003, **424**, 915-918.
b) P. Thordarson, R.G.E. Coumans, J.A.A.W. Elemans, P.J. Thomassen, J. Visser, A.E. Rowan, R.J.M. Nolte, *Angew. Chem. Int. Ed.,* 2004, **43**, 4755-4759;
c) P.J. Thomassen, J. Foekama, R. Jordana i Lluch, P. Thordarson, J.A.A.W. Elemans, R.J.M. Nolte, A.E. Rowan, *New J. Chem.*, 2006, **30**, 148-155.
5. H.L. Anderson, C.A. Hunter, M.N. Meah, J.K.M. Sanders, *J. Am. Chem. Soc.,* 1990, **112**, 5780-5789.
6. *Reviews on DOSY NMR:*
a) D. Wu, A. Chen, C.S. Johnson Jr., *Bull. Magn. Res.*, 1995, **17**, 21-26.
b) G.A. Morris, H. Barjat, *Anal. Spectrosc. Libr.*, 1997, **8**, 211-226.
c) C.S. Johnson Jr. *Prog. Nucl. Magn. Reson. Spectrosc.*, 1999, **34**, 203-256.
d) M.J. Shapiro, J.S. Gounarides, *Prog. Nucl. Magn. Reson. Spectrosc.*, 1999, **35**, 153-200.
e) G.A. Morris, *Encycl. Nucl. Magn. Reson.*, 2002, **9**, 35-44.
f) R. Huo, R.Wehrens, J. van Duynhoven, L.M.C. Buydens, *Anal. Chim. Acta*, 2003, **490**, 231-251.
g) J.C. Cobas, P. Groves, M. Martin-Pastor, A. de Capua, *Curr. Anal. Chem.*, 2005, **1**, 289-305.
Examples of DOSY NMR on supramolecular complexes:
g) R.S.K. Kishore, T. Paululat, M. Schmittel, *Chem. Eur. J.*, 2006, **12**, 8136-8149.
h) L. Allouche, A. Marquis, J.-M. Lehn, *Chem. Eur. J.*, 2006, **12**, 7520-7525.
i) C.-C. You, C. Hippius, M. Gruene, F. Wuerthner, *Chem. Eur. J.*, 2006, **12**, 7510-7519.
j) H. Jiang, W. Lin, *J. Am. Chem. Soc.*, 2006, **128**, 11286-11297.
Example of DOSY NMR in a mixed solvent system:
k) G. Pages, C. Delaurent, S. Caldarelli, *Anal. Chem.*, 2006, **78**, 561-566.
7. P. Thordarson, E.J.A. Bijsterveld, J.A.A.W. Elemans, P. Kasák, R.J.M. Nolte, A.E. Rowan, *J. Am. Chem. Soc.,* 2003, **125**, 1186-1187.

Chapter 7. Synthesis of a "double-decker" porphyrin clip

7.1 Introduction

In chapter 6 two tetra-hydroxy zinc porphyrin clips (**ZnOHP**) were shown to dimerise by means of allosteric supramolecular interactions (Figure 1a).[1] The double-decker porphyrin clip molecule that would arise from a covalent coupling of two of these hydroxy-functionalised porphyrin clips (Figure 1b), would also be of interest in particular as a novel catalyst. Such a molecule could bind two viologen guests with equally high binding constants allowing for the formation of supramolecular host-guest assemblies, although no allosteric behaviour would be expected for this molecule. The coordination of **dabco** in between the two zinc porphyrin moieties might facilitate a communicative interaction between the two cavities, resulting in allosteric binding behaviour. In addition, a double-decker porphyrin clip with two different metal centres should be capable of performing two different catalytic reactions simultaneously or in tandem with information transferred from one cavity to the other, making it an interesting molecule for cascade catalysis.

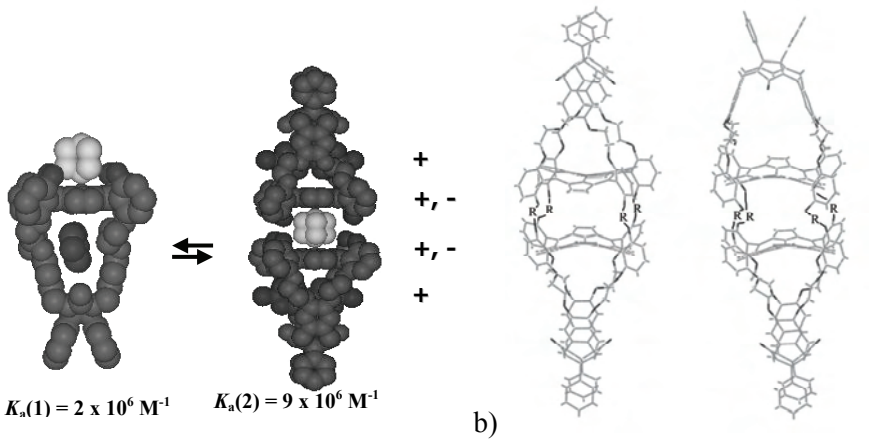

Figure 1. *a) Dimerisation of the tetra-hydroxy functionalised zinc porphyrin clip by* ***dabco*** *in the presence of a dimethyl viologen guest. The association constants for the binding of the dimethyl viologen guest are reported below the complexes. The + and – signs indicate positive and negative cooperativity. b) Double-decker porphyrin clip isomers formed by covalently linking two tetra-hydroxy porphyrin clips. The R-symbols indicate linker groups.*

7.2 Synthesis

Several attempts were undertaken to synthesise a double-decker porphyrin clip. Inspired by standard alcohol-coupling chemistry, the first attempt involved the introduction of carbonate linkers between the two clips (Figure 2, Approach a). To this end, 2.5 equivalents of triphosgene ($(CCl_3O)_2CO$) and an excess of triethylamine were added to a

dichloromethane solution of the free base tetra-hydroxy porphyrin clip (**OHP**) and this mixture was stirred for two hours. No reaction was however observed to occur, based upon analysis of the reaction products by both ^{1}H NMR and MALDI-TOF MS.

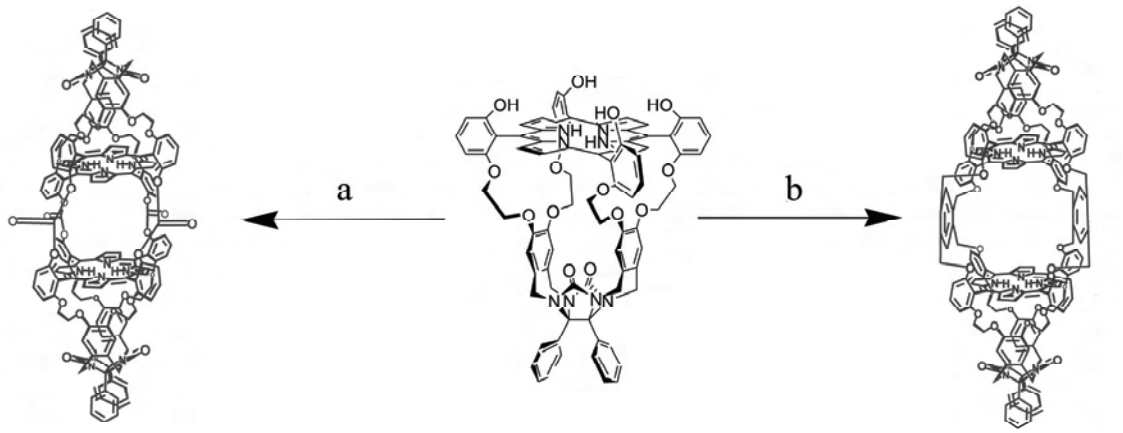

1 **OHP** **2**

Figure 2. *Attempted syntheses of free-base double-decker porphyrin clip. Only one of the possible double-decker porphyrin clip isomers is depicted. Approach a: Triphosgene, Et_3N, CH_2Cl_2, RT, 2 hrs. Approach b: 1,2,4,5-tetrakis(bromomethyl)benzene, K_2CO_3, DMF, RT, 3 days.*

The second attempt was based on the use of a durene linker (Figure 2, Approach b). In order to first test the feasibility of this approach, an acetonitrile solution of tetrakis-meso-*o*-hydroxyphenyl porphyrin was refluxed for four hours with one equivalent of tetrakisbromodurene using potassium carbonate as a base (Figure 3). According to a sample taken from the reaction mixture that was analysed by MALDI-TOF MS the bis-durene linked bisporphyrin molecule had formed. When **OHP** was subjected to the same procedure, even after three days the reaction had not proceeded to completion. The main products were a dimer with one durene linker and four unreacted hydroxy groups and dimers with two durene linkers and a varying number of unreacted hydroxy groups.

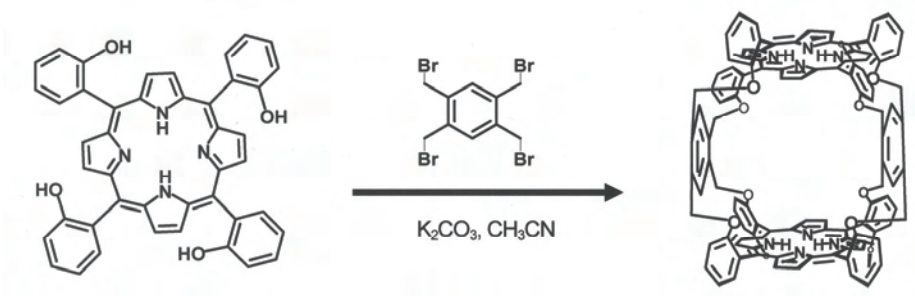

Figure 3. *Dimerisation of two tetra-hydroxy porphyrins into a bis-durene linked bisporphyrin.*

Cram *et al*. have reported several procedures to alkylate cavitand molecules via their hydroxy groups.[2] For instance, 1,2-dichloroquinoxaline was used to increase the volume of a hydroxy-functionalised cavity (Figure 4a),[3] and two hydroxy-functionalised cavitands were dimerised by a reaction with chlorobromomethane to give a carceplex (Figure 4b).[4]

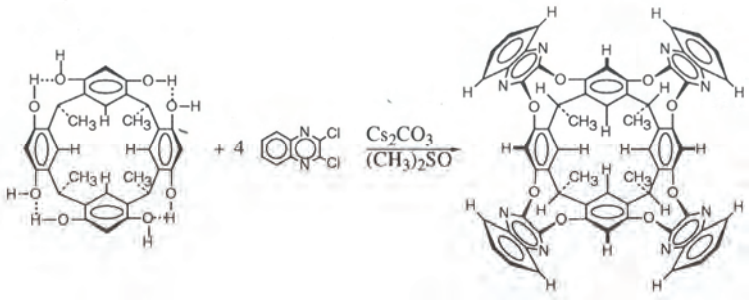

a)

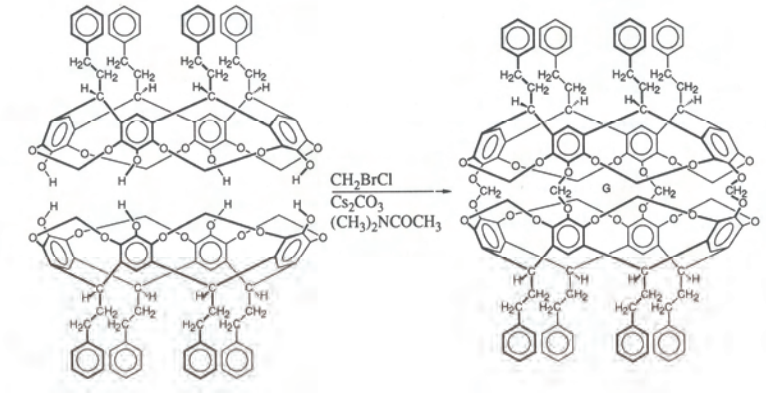

b)

Figure 4. *a) Reaction of an octahydroxy-functionalised cavitand with 1,2-dichloroquinoxaline. b) Dimerisation of two cavitands with chlorobromomethane to give a carceplex with a solvent molecule incarcerated.*

Since the hydroxy groups in the cavitand in Figure 4a were pre-organised, a similar approach was considered for the coupling of the porphyrin clips. Instead of **OHP**, **ZnOHP** was used in the presence of a small excess of dimethyl viologen (**V**) and half an equivalent of **dabco** in a $CHCl_3/CH_3CN$ 1:1 (v/v) solution, in order to preorganise two clips in a supramolecular dimer. A coupling reaction was then carried out with 1,2-dichloroquinoxaline using cesium carbonate as a base.[3] According to MALDI-TOF MS analysis of samples taken from the reaction mixture covalent dimerisation had occurred. Even after three weeks of reaction, however, and upon the addition of extra amounts of base and 1,2-dichloroquinoxaline, the main product was the dimer with three quinoxaline bridges with two unreacted hydroxy groups opposite each other. Dimers with two quinoxaline bridges and four unreacted hydroxy groups were also detected, as well as a species that could be identified as containing two quinoxaline bridges, one quinoxaline-

mono-chloride moiety with an opposite unreacted hydroxy groups and two unreacted hydroxy groups opposite each other.

Since it was apparent that the complete closing of the macrocycle has a significant energy barrier, a new attempt was performed, but this time in DMF in order to be able to carry out the reaction at a higher temperature. Since DMF is a much stronger acceptor of hydrogen bonds than acetonitrile, the formation of supramolecular dimers of **ZnOHP** through intermolecular hydrogen bonds is not expected in this solvent. Therefore in this attempt no **dabco** or **V** were added to the reaction mixture. Reaction with 1,2-dichloroquinoxaline in the presence of excess cesium carbonate at 120ºC again only gave covalently linked dimers with a maximum of three bridging quinoxaline groups.

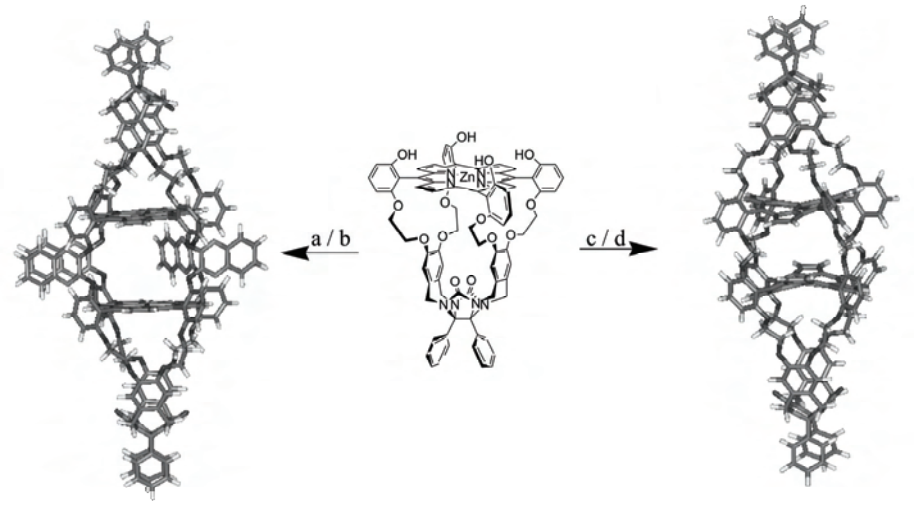

3 **ZnOHP** **4**

Figure 5. *Attempted syntheses of zinc double-decker porphyrin clips. Only one of the possible isomers is depicted. a) 1,2-Dichloroquinoxaline, dimethyl viologen,* ***dabco****, Cs_2CO_3, $CHCl_3/CH_3CN$ 1:1 (v/v), reflux, 3 weeks. b) 1,2-Dichloroquinoxaline, Cs_2CO_3, DMF, 120ºC, 3 weeks. c) CH_2BrCl, dimethylviologen,* ***dabco****, Cs_2CO_3, $CHCl_3/CH_3CN$ 2:1 (v/v), reflux, 12 days. d) CH_2BrCl, Cs_2CO_3, DMF, 105ºC, 4 weeks.*

Since the 1,2-dichloroquinoxaline approach was found not to work, the use of chlorobromomethane was tried. In a first attempt, **ZnOHP** was reacted with an excess of chlorobromomethane in the presence of cesium carbonate and a small excess of viologen and half an equivalent of **dabco** in $CHCl_3/CH_3CN$ 2:1 (v/v). Upon refluxing this mixture for 12 days, some of the desired covalently linked dimer was formed, according to MALDI-TOF MS. Isolation of this trace amount of dimer, however, was unsuccessful. When **ZnOHP** was reacted in DMF with chlorobromomethane in the presence of cesium carbonate at 105ºC for four weeks, MALDI-TOF MS analysis again revealed the formation of the covalent dimer. Isolation of the "double-decker" porphyrin clip (**ZnDDC**) by preparative TLC yielded the desired product, however in impure form (~80% pure) with a very low yield (<2%). The product could be analysed by ^{1}H NMR,

COSY and NOESY techniques, which confirmed that the desired dimer had indeed been obtained.

The ^{1}H NMR spectra of **ZnDC**, **ZnOHP** and **ZnDDC** were found to be very similar. Strikingly, the signals for the β-pyrrole protons of **ZnDDC** had been shifted upfield by -0.3 ppm, when compared to the other two hosts. In contrast, the signal for *H10* experienced a downfield shift of 0.4 ppm. Both shifts could be caused by the presence of another porphyrin moiety in close proximity. The signal for the aromatic side-wall protons was shifted upfield by -0.2 ppm, which indicates a slight widening of the cavity of **ZnDDC** when compared to the other two hosts. The ^{1}H NMR spectrum of **ZnDDC** showed no signal for phenolic protons, which indicated complete coupling of two **ZnOHP** molecules by four methylene linkers, for which the signal could be found at 2 ppm. From these data it could not be determined which of the two possible isomers had been formed or if it was a mixture of the two isomers.

Table 1. *Induced chemical shifts[a] (ppm) of proton signals in the ^{1}H-NMR for three different zinc porphyrin clip molecules.*

Proton signal (ppm)	**ZnDC**[b]	**ZnOHP**[c]	**ZnDDC**[d]
1	6.97-6.91	7.08-6.93	6.96-6.82
2	6.97-6.91	7.08-6.93	6.96-6.82
3	6.83-6.78	6.79	6.74
4a	4.24	4.17	4.10
4b	3.74	3.66	3.62
5	6.18	6.28	6.02
6a	3.43-3.28	3.40-3.31	3.41-3.22
6b	3.25-3.10	3.24-3.13	3.13-2.94
7a	4.25-4.20	4.12-4.03	4.08-3.93
7b	4.00-3.80	4.01-3.93	3.91-3.78
8	7.07	7.08-6.93	7.05
9	7.69	7.54	7.70
10		7.08-6.93	7.39
β-pyrrole	8.75	8.69	8.39
β-pyrrole		8.53	8.31
O-CH_2-O			2.08-1.92

*[a] 298 K, $CDCl_3$. [b] 500.14 MHz, for proton numbering see chapter 2, Figure 3c. [c] 400.15 MHz, for proton numbering see chapter 6, Figure 2a. [d] 400.15 MHz, proton numbering analogous to **ZnDC** and **ZnOHP**.*

A UV-vis spectrum of the product in $CHCl_3$/CH_3CN 1:1 (v/v) showed a slightly blue-shifted Soret-band at 424 nm (the Soret-band of the tetra-hydroxy porphyrin clip is at 426 nm), which is expected for porphyrins that are stacked face-to-face on top of each other.[5]

Since no pure sample of **ZnDDC** has been obtained and time was limited, no binding studies were performed and no attempts have been undertaken to exchange the zinc ions for different, catalytically active, metal ions. This remains the next step in the development of an allosteric catalyst.

7.3 Conclusions

The synthesis of double-cavity, double porphyrin 'double-decker' molecules appeared to be possible, however not trivial. Several synthetic routes were explored, of which so far only the coupling of two tetrahydroxy-functionalised porphyrin clips using bromochloromethane gave the most promising result. A small amount of an as yet not completely pure "double decker" compound was obtained, which could be identified with the help of NMR and mass spectroscopy. Future studies to optimise the synthesis of this "double decker" molecule are necessary in order to obtain a catalyst in which cross-communication could occur; a genuine polymerase mimic.

7.4 Experimental

^{1}H-NMR spectra were recorded on a Varian Unity Inova 400 instrument at 298 K. MALDI-TOF MS spectra were recorded on a Bruker Biflex III spectrometer.
All solvents were distilled under nitrogen prior to use. Acetonitrile was distilled from CaH_2, chloroform from $CaCl_2$ and dichloromethane from CaH_2. DMF was predried over BaO for one week and then distilled under reduced pressure, and the first and last 25% of the distillate was discarded. All other solvents and chemicals were commercial materials and used without purification. **OHP** and **ZnOHP** were synthesised according to literature procedures,[6] as was tetrakis-meso-*o*-hydroxyphenyl porphyrin.[7]

Synthesis of carbonate-linked double-decker porphyrin clip 1.
In 2 mL of CH_2Cl_2 was dissolved 4.8 mg (3.41 μmol) of **OHP**, 53 μL (0.38 mmol) of triethylamine and 2.5 mg (6.53 μmol) of triphosgene and this mixture was stirred under N_2 for 2 hours. The mixture was washed with water and the organic layer was dried with Na_2SO_4, the drying agent was filtered off and the solvent was evaporated to dryness. Both MALDI-TOF MS and ^{1}H NMR spectroscopy showed the presence of only starting material.

Synthesis of bis-durene-linked bis-porphyrin.
A mixture of 14.4 mg (21.2 μmol) tetrakis-meso-*o*-hydroxyphenyl porphyrin, 10.6 mg (23.6 μmol) of 1,2,4,5-tetrakis(bromomethyl)benzene and 26 mg (0.19 mmol) of K_2CO_3 in 50 mL acetonitrile was refluxed for 4 hrs. Any solids were filtered off, washed with

water and the organic layer was dried with Na_2SO_4 and evaporated to dryness. MALDI-TOF MS showed the peak corresponding to the dimer. MALDI-TOF: 1610 $[dimer + H]^+$.

Synthesis of durene-linked double-decker porphyrin clip 2.

A mixture of 7 mg (4.97 μmol) of **OHP**, 2.5 mg (5.6 μmol) of 1,2,4,5-tetrakis(bromomethyl)benzene and 10 mg (72.4 μmol) of K_2CO_3 in 5 mL DMF was stirred under N_2 at RT for 3 days. The solvent was removed *in vacuo* and the remaining solid was extracted with water and $CHCl_3$. The organic layer was dried with Na_2SO_4, the drying agent was filtered off and evaporated to dryness. MALDI-TOF MS and ^1H NMR showed mainly dimers in which not all hydroxy groups had reacted.

Synthesis of quinoxaline-linked double-decker porphyrin clip 3.

Method **a**

ZnOHP (5.0 mg, 3.5 μmol) 1.7 mg (3.6 μmol) of dimethyl viologen hexafluorophosphate , 9.3 mg (28 μmol) of cesium carbonate and 1.4 mg (7.0 μmol) of 1,2-dichloroquinoxaline were added to 200 μL of a solution of **dabco** (8.8 μM) in $CHCl_3/CH_3CN$ 1:1 (v/v), after which the mixture was sonicated. The resulting green solution was heated refluxed for 5 days under N_2. MALDI-TOF MS of a sample taken from the reaction mixture showed that only dimeric products were formed with less than four quinoxaline linkers.

Method **b**

ZnOHP (10.5 mg, 7.14 μmol), 18.7 mg (57.4 μmol) of cesium carbonate and 3.0 mg (15.1 μmol) of 1,2-dichloroquinoxaline were added to 7 mL of DMF. This solution was heated to 120 ºC and stirred for 3 weeks under N_2. MALDI-TOF MS of a sample taken from the reaction mixture revealed that only dimeric products had been formed with less than four quinoxaline linkers.

Synthesis of methyl-linked double-decker porphyrin clip 4.

Method **c**

A mixture of 5.0 mg (3.5 μmol) of **ZnOHP**, 1.7 mg (3.6 μmol) of dimethyl viologen hexafluorophosphate and 9.3 mg (28 μmol) of cesium carbonate was added to 200 μL of a solution of **dabco** (8.8 μM) in $CHCl_3/CH_3CN$ 2:1 (v/v), after which the mixture was sonicated. The resulting green solution was heated to 60 ºC and 1.5 μL (22 μmol) of bromochloromethane in 30 μL $CHCl_3/CH_3CN$ 2:1 (v/v) was added, after which the solution was heated to reflux. Over the course of 5 days 50 μL of (0.8 μmol) bromochloromethane was added stepwise. After 5 days MALDI-TOF showed that a trace amount of **4** had been formed. The product could not be isolated.

Method **d**

To a mixture of 20.0 mg (13.6 μmol) of **ZnOHP** and 44 mg (135 μmol) of cesium carbonate in 8 mL of DMF was added 100 μL (1.5 mmol) of bromochloromethane. The mixture was heated to 105 ºC and stirred for 4 weeks under N_2. After cooling, the mixture any solids were filtered off and the solvent was removed *in vacuo*. The remaining solid was subjected to preparative TLC (toluene / ethyl acetate / methanol 5:3:1 (v/v/v)) and the second band was collected to yield 0.5 mg of impure double-decker porphyrin clip (~80% pure).

^{1}H-NMR ($CDCl_3$, 400.15 MHz): δ = 8.39 (bs, 8H, β-pyrrole*H*), 8.31 (bs, 8H, β-pyrrole*H*), 7.70 (t, 8H, ^3J= 8.6 Hz, *H9*), 7.39 (d, 8H, ^3J= 8.8 Hz, *H10*), 7.05 (d, 8H, ^3J= 8.3 Hz, *H8*), 6.96-6.82 (m, 12H, *H1,2*), 6.74 (d, 8H, ^3J= 3.7 Hz, *H3*), 6.02 (s, 8H, *H5*), 4.10 (d, 8H, ^2J= 14.9 Hz, *H4*), 4.08-3.93 (m, 8H, *H7*), 3.91-3.78 (m, 8H, *H7*), 3.62 (d, 8H, ^2J= 15.4 Hz, *H4*), 3.41-3.22 (m, 8H, *H6*), 3.13-2.94 (m, 8H, *H6*), 2.08-1.92 (m, 8H, O-CH_2-O) ppm; MALDI-TOF: 2991 [**4** + H]$^+$. The proton numbering is analogous to that for **ZnOHP** (chapter 6, Figure 2a).

References

1. P. Thordarson, R.G.E. Coumans, J.A.A.W. Elemans, P.J. Thomassen, J. Visser, A.E. Rowan, R.J.M. Nolte, *Angew. Chem. Int. Ed.*, 2004, **43**, 4755-4759.
2. D.J. Cram, J.M. Cram, in *Container Molecules and Their Guests*, The Royal Society of Chemistry, U.K., **1994**.
3. J.R. Moran, J.L. Ericson, E. Dalcanale, J.A. Bryant, C.B. Knobler, D.J. Cram, *J. Am. Chem. Soc.*, **1991**, *113*, 5707-5714.
4. J.C. Sherman, C.B. Knobler, D.J. Cram, *J. Am. Chem. Soc.*, **1991**, *113*, 2194-2204.
5. M. Kasha, H.R. Rawls, M.A. El-Bayoumi, *Pure Appl. Chem.*, 1965, **11**, 371-392.
6. P. Thordarson, E.J.A. Bijsterveld, J.A.A.W. Elemans, P. Kasák, R.J.M. Nolte, A.E. Rowan, *J. Am. Chem. Soc.,* 2003, **125**, 1186-1187.
7. a) A.E. Rowan, P.P.M. Aarts, K.W.M. Koutstaal, *Chem. Commun.*, 1998, 611-612.
   b) J.A.A.W. Elemans, M.B. Claase, P.P.M. Aarts, A.E. Rowan, A.P.H.J. Schenning, R.J.M. Nolte, *J. Org. Chem.*, 1999, **64**, 7009-7016.

Summary

Cooperative interactions play a ubiquitous role in Nature, where they are employed to influence the composition and function of hierarchical self-assembled systems. A special case of cooperativity, in which a binding event in a multivalent host at one binding site causes a discrete, reversible alteration in its structure at a remote binding site, is called allosterism. This thesis describes the studies in which a number of different cavity-appended porphyrins, namely **MC**, **OHP**, **DC,** and derivatives of these compounds (Figure 1), are used as hosts for a variety of different guests in order to form, with the assistance of cooperative interactions, multi-component supramolecular architectures.

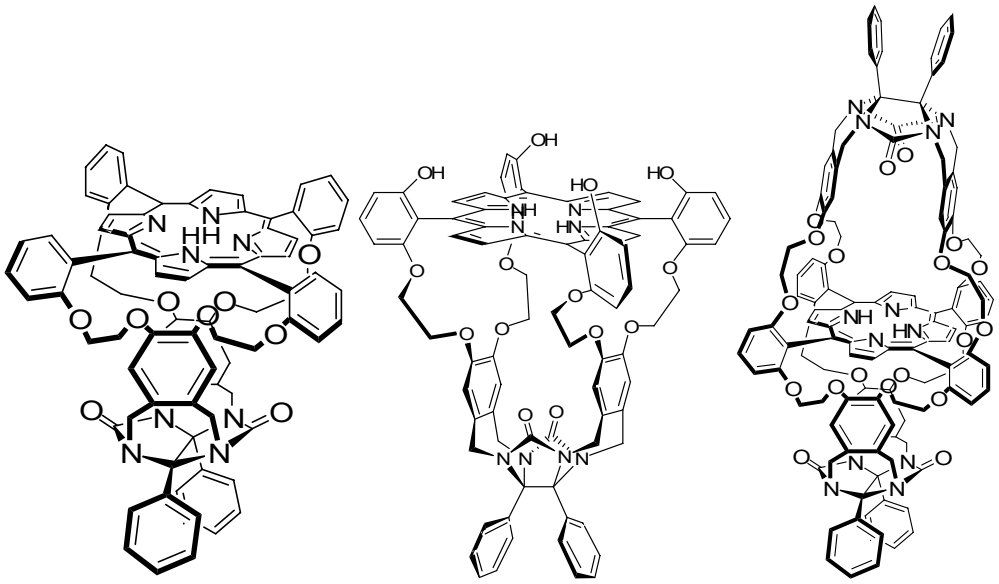

MC **OHP** **DC**

Figure 1. *Three different cavity-appended porphyrin hosts that have been employed to create multi-component self-assembled architectures with the help of cooperative interactions.*

Chapter 1 gives a literature overview on the recent developments in the field of cooperative assembly of porphyrins. This chapter also introduces the mono-cavity appended porphyrin molecule **MC** and its zinc analogue, **ZnMC**. The positive allosteric binding behaviour of the latter compound is reported, namely the coordination of 4-*tert*-butyl-pyridine (**tbpy**) to the zinc ion at the "outside" of the host which increases the association constant of 4,4'-bipyridinium (**V**) guests inside the cavity of **ZnMC**, and *vice versa*. The highly negative allosteric binding of two **V** guests in the cavities of the double-cavity porphyrin **DC** is also reported here.

In Chapter 2, efforts to improve the yield of the synthesis of **DC** are described, as well as the isolation and characterisation of two of its isomers, in which the porphyrin bridges the clip moieties in a "sideways" geometry. The concomitant binding of one

molecule of pyridine (**py**) and one molecule of **V** inside the cavities of **ZnDC**, the zinc analogue of **DC**, was shown to display positive allosteric binding behaviour.

The remarkable stability of **MnMC**, the manganese derivative of **MC,** in the presence of **tbpy** in the epoxidation of simple alkenes has been reported before. In Chapter 3, the synthesis and the investigations of the catalytic properties of **MnDC**, the manganese derivative of **DC**, are described. It was found that the epoxidation rates of the catalyst **MnDC** in the presence of 1 equivalent of **py** were considerably lower than those of **MnMC** for the same substrates and the same reaction conditions. This difference was attributed to the unfavourable binding of the substrate into a cavity of **DC** that is pinched because of the binding of **py** into the opposite cavity. Epoxidation rates in the absence and in the presence of an excess of **py** were found to be even lower. The catalyst remained stable for at least two weeks, without any signs of decomposition.

In Chapter 4 the synthesis of three different bifunctional guests, containing pyridine and/or viologen moieties, are reported. These guest molecules were incorporated *via* allosteric interactions into discrete self-assembled complexes when they were combined with **ZnMC**. They were also combined with **ZnDC** in order to increase the complexity and size of the assemblies. The binding behaviour of the latter host toward these guests proved to be complex and suggested the formation of tetrameric assemblies.

The synthesis and binding behaviour of three 'simple' mono-N-substituted bipyridine guests towards **ZnMC** are described in Chapter 5. The addition of **tbpy** to solutions containing these guests and **ZnMC** resulted in an increase of the quenching of the fluorescence of the zinc porphyrin, as a result of an allosterically induced increase in the number of **ZnMC** molecules that contain a guest molecule. In such a complex, electron transfer from the porphyrin to the bipyridine guest occurs upon photo-excitation. The same positive cooperative behaviour upon the addition of **tbpy** was observed for a mixture of **ZnMC** and a gold porphyrin that was functionalised with a mono-N-substituted bipyridine moiety, whereas negative cooperative behaviour was observed when a gold porphyrin with four appended mono-N-substituted bipyridine moieties was employed as the guest. This latter effect was ascribed to steric crowding around the central gold porphyrin. The fluorescence decay kinetics of uncomplexed **ZnMC** was found to be mono-exponential, whereas this kinetics was multi-exponential for the investigated host-guest complexes.

The negative cooperativity that is normally observed upon the dimerisation of two zinc porphyrins by the addition of diazabicyclo[2.2.2]octane (**dabco**) also occurred in the case of **ZnMC**, as is described in Chapter 6. The dimerisation of the tetra-hydroxy derivative of this host, **ZnOHP,** by the addition of **dabco** was shown to be accompanied by positive cooperative behaviour in the presence of 1 equivalent of **V**, resulting in the formation of discrete self-assembled complexes. The binding processes that take place upon the addition of **dabco** to a solution of a complex consisting of four **ZnOHP** hosts

and one guest consisting of a central free-base porphyrin appended with four viologen moieties were also investigated, the target being the formation of a discrete 14-component complex formed by allosteric self-assembly. It was found that dimerisation of the **ZnOHP** hosts by bidentate **dabco** coordination within one porphyrin-host complex was more favourable than dimerisation between two porphyrin-host complexes, although the former effect could be hindered by decreasing the length of the alkyl spacers between the free-base porphyrin and the viologen moieties of the guest.

In Chapter 7, several attempted routes to synthesize a double-porphyrin, double-cavity "double-decker" molecule are reported. The covalent dimerisation of two **ZnOHP** molecules using bromochloromethane resulted in the formation of a small amount of a so far not completely pure sample of a "double decker" compound.

Samenvatting

Coöperatieve interacties zijn alom vertegenwoordigd in de natuur, waar ze worden gebruikt om de vorming en functie van complexe, geaggregreerde systemen te beïnvloeden. Een speciaal geval van coöperativiteit is allosterie, waarbij het binden van een gast-molecuul A aan een gastheer-molecuul met meerdere bindingsplaatsen B een morfologische, reversibele verandering teweeg brengt in één van de andere bindingsplaatsen van B, waardoor het binden van een ander gast-molecuul C aan de veranderende bindingsplaats gehinderd danwel vergemakkelijkt wordt.
In dit proefschrift worden studies beschreven waarin een aantal gastheer-moleculen (**MC**, **OHP** en **DC** en afgeleiden daarvan) zijn gebruikt om in combinatie met verschillende gast-moleculen en door middel van coöperative interacties te komen tot de vorming van supramoleculaire constructies, die uit meerdere componenten bestaan (Figuur 1).

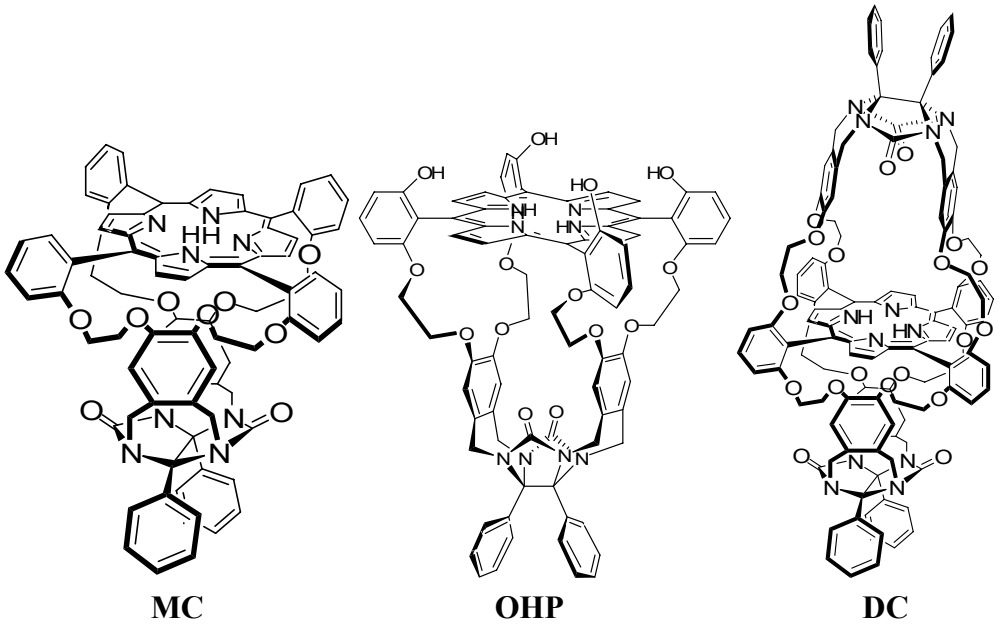

Figuur 1. *Drie verschillende porfyrine gastheer-moleculen met één of meerdere afgeschermde holtes, welke zijn gebruikt om cooperatieve, geaggregeerde systemen bestaande uit meerdere componenten te creëren.*

Hoofdstuk 1 is een literatuuroverzicht van de recente ontwikkelingen op het gebied van het coöperatief aggregeren van porfyrines. Hier wordt ook het molecuul **MC** geïntroduceerd, dat bestaat uit een porfyrine waaraan een afgeschermde holte is bevestigd. Van de zink-analoog van **MC** wordt het positieve allostere bindingsgedrag beschreven; de coordinatie van 4-*tert*-butyl-pyridine (**tbpy**) aan het zinkion aan de "buitenkant" van het gastheer-molecuul vergemakkelijkt de binding van een 4,4'-bipyridinium gast-molecuul (**V**) in de holte van ditzelfde molecuul, en vice versa. Ook

het negatieve allostere bindingsgedrag van **DC** in combinatie met twee **V** gasten is hier vermeld.

In Hoofdstuk 2 zijn de pogingen beschreven om de opbrengst van de synthese van **DC** te verhogen, samen met de isolatie en karakterisatie van twee isomeren van deze verbinding waarin het porfyrine molecuul zijdelings over de holtes gespannen is in plaats van er bovenop. Verder is gebleken dat het gelijktijdig binden van een molecuul pyridine (**py**) en een molecuul **V**, elk in één van de holtes van **ZnDC**, de zink-analoog van **DC**, een duidelijk positief allosteer bindingsgedrag oplevert.

Het was al bekend dat **MnMC**, de mangaan-analoog van **MC**, opmerkelijk stabiel is wanneer dit molecuul wordt gebruikt als katalysator voor de epoxidatie van eenvoudige olefines in het bijzijn van **tbpy** als axiaal ligand. In Hoofdstuk 3 is de synthese en de katalytische eigenschappen van **MnDC**, de mangaan-analoog van **DC**, beschreven. Voor dezelfde substraten en onder dezelfde omstandigheden bleken de epoxidatiesnelheden van **MnDC** aanmerkelijk lager te zijn dan die van **MnMC**, in het bijzijn van 1 equivalent van het axiaal ligand **py**. Dit wordt waarschijnlijk veroorzaakt door het samentrekken van de lege holte die gelegen is tegenover de holte waarin **py** gebonden is, en als gevolg daarvan wordt minder gemakkelijk een substraat toegelaten in de lege holte. De epoxidatiesnelheid, zowel in afwezigheid van **py** als in aanwezigheid van een overmaat **py**, werd nog lager dan in de situatie waarin maar 1 equivalent aanwezig is. Opmerkelijk was dat **MnDC** minstens twee weken stabiel was en daarna nog geen tekenen van degradatie vertoonde.

In Hoofdstuk 4 is de synthese van drie verschillende bifunctionele gast-moleculen beschreven die elk een pyridine- en/of een viologeen-gedeelte bevatten. In combinatie met **ZnMC** werden deze gasten door middel van allostere interacties ingebouwd in goed gedefinieerde en discrete zelf-geassembleerde complexen. Om de complexiteit en grootte van deze structuren te vergroten, werden dezelfde gasten gecombineerd met **ZnDC**. Het bindingsgedrag van dit laatste gastheer-molecuul met de gasten bleek zeer complex te zijn. Voorlopige experimenten wezen op de vorming van allostere tetramere structuren.

De synthese en het bindingsgedrag met **ZnMC** van drie eenvoudige mono-N-gesubstitueerde bipyridine moleculen is beschreven in Hoofdstuk 5. Het toevoegen van **tbpy** aan oplossingen die zowel **ZnMC** en deze gasten bevatten, resulteerde in een afname van de fluorescentie van de porfyrines, vanwege een verhoging van het aantal gastheer-moleculen dat betrokken is bij de vorming van een gastheer-gastcomplex. Wanneer het porfyrinegedeelte wordt aangeslagen met licht vindt in zo'n complex overdracht plaats van een electron van het porfyrine naar de mono-gesubstitueerde gast. Een vergelijkbaar positief coöperatieve gedrag werd waargenomen wanneer **tbpy** werd toegevoegd aan een oplossing van **ZnMC** en een goudporfyrine dat gefunctionaliseerd was met een mono-N-gesubstitueerde bipyridinegroep, terwijl negatief coöperatief gedrag duidelijk zichtbaar was wanneer een analoog experiment werd uitgevoerd met **ZnMC** en

een goud porfyrine met vier mono-N-gesubstitueerde bipyridinegroepen. Als reden voor de negatieve cooperativiteit werd sterische hindering voorgesteld. De fluorescentieafnamekinetiek van niet-gecomplexeerde **ZnMC** was mono-exponentieel, terwijl de **ZnMC**-complexen met mono-N-gesubstitueerde bipyridine gasten een multi-exponentieel verval te zien gaven.

De negatieve coöperativiteit die normaal gesproken optreedt wanneer twee zinkporfyrines dimeriseren als gevolg van de toevoeging van diazabicyclo[2.2.2]octaan (**dabco**), werd ook waargenomen in het geval van **ZnMC**. Deze experimenten zijn beschreven in Hoofdstuk 6. Wanneer echter **dabco** werd toegevoegd aan een oplossing van het tetrahydroxyderivaat van dit gastheer-molecuul, **ZnOHP** en 1 equivalent **V**, verliep de dimerisatie met positief coöperatief bindingsgedrag, hetgeen resulteerde in de vorming van een discreet en goed gedefinieerd zelf-geassembleerd complex. Tevens zijn in dit hoofdstuk studies beschreven naar bindingsprocessen die optraden wanneer **dabco** werd toegevoegd aan een complex bestaande uit vier **ZnOHP** gastheer-moleculen en één gast-porfyrine met daaraan bevestigd vier viologeengroepen. Het doel van dit experiment was het verkrijgen van een discreet zelf-geassembleerd complex dat bestaat uit 14 componenten. Dimerisatie van **ZnOHP** gastheermoleculen binnen één porfyrine-gastheercomplex bleek echter gunstiger te zijn dan dimerisatie tussen twee porfyrine-gastheercomplexen, waarbij de eerstgenoemde dimerisatie deels verhinderd kon worden door de alkylverbindingen tussen de porfyrine en de viologeen-gedeelten te verkorten.

In Hoofdstuk 7 zijn verschillende routes beschreven om een "dubbeldekker"-verfbinding met twee holtes en twee porfyrines te synthetiseren. De covalente dimerisatie van twee **ZnOHP**-moleculen met behulp van broomchloormethaan heeft tot een kleine hoeveelheid van een tot nog toe onzuiver monster van een dergelijke "dubbeldekker"-verbinding geleid.

Dankwoord

Hè hè, het zit er bijna op. Op dit moment kan dit boekje bijna naar de drukker en ik kan niet wachten om het uit te gaan delen, zodat ik iedereen meteen naar het dankwoord kan zien bladeren om alleen dat gedeelte te lezen. En dat is helemaal niet erg, heb ik zelf ook met genoeg proefschriften gedaan.
In de afgelopen jaren heb ik heel wat geleerd, zoals chemisch als op persoonlijk vlak. Een promotietraject gaat vrijwel altijd gepaard met toppen en dalen, en het mijne was niet anders. Gelukkig heb ik de voorbije jaren altijd mensen om me heen gehad op wie ik terug kon vallen, doordat je eens even lekker tegen ze kon vloeken en gillen, doordat ze je een schouderklopje gaven en je naar huis stuurden om daar even lekker te gaan balen, doordat ze altijd een glimlach op je gezicht tevoorschijn wisten te toveren, en doordat je altijd met ze een pilsje kon gaan pakken en gewoon gezellig kon gaan zitten keuvelen zonder aan het werk te hoeven denken.

Eerst wil ik prof. Alan Rowan bedanken voor het mij aanbieden van een promotieplek ondanks een rampzalige sollicitatiepresentatie. Door je enthousiasme en creativiteit had ik nooit een gebrek aan ideeën over hoe door te gaan als er eens een onderwerp was afgerond en hoewel het soms lang kan duren, als je eenmaal iets hebt gecorrigeerd dan is het ook goed.
Natuurlijk net zo belangrijk was prof. Roeland Nolte. Ook jij had genoeg vertrouwen in me om me in jouw groep te laten promoveren en met een paar vriendelijke, geïnteresseerde vragen kon je altijd meteen inschatten hoe het met iemand stond en iemand weer enthousiast maken wanneer dit nodig was. Dank je!
De allerbelangrijkste persoon tijdens mijn promotie was toch wel mijn dagelijks begeleider dr. Hans Elemans. Met je grote kennis had je antwoord op alle vragen, je had altijd een luisterend oor en opbeurende glimlach klaar, en al met al was het gewoon heel prettig om met je te werken. Daarvoor hartelijk dank en nogmaals gefeliciteerd met je VIDI beurs.
De manuscripcommissie wil ik bedankt voor hun tijd, moeite en nuttige suggesties. Dr. Paul Toele en prof. M. van der Auweraer hartelijk dank voor al het werk in Leuven.
Uiteraard ook erg bedankt aan alle mensen die onmisbaar zijn bij het draaiende houden van een succesvolle chemie-afdeling: Paula, Désirée, Jacky, Peter vD, Peter vG, Helene, Paul S, Ad en Jan.

Zoals al eerder vermeld zijn collega's (in een ruime zin van het woord) onmisbaar tijdens je promotie. En er zijn er een hele hoop geweest! Ik zal er vast een aantal vergeten en daarvoor mijn welgemeende excuses. Palli (you were an excellent mentor to share an office and lab with in dear old UL and you taught me a lot. Thanks also for the association constant calculations and all your support down under), Paul vG (ook zo lekker cynisch; bedankt voor mijn ergste kater ooit!), Mark (heerlijk om bij te hebben tijdens oefenen voor 4 daagse), Nuria (great to see how you blossomed in the end), Marga (klikte meteen, veel succes in Berlijn!), Pili (great neighbour!), Marta (zo vriendelijk), Erik (gezellige vent!), Marco (Italians shouldn't be so tall!), Paul K (bridgen is leuk! Succes met de kleine), Arend (klein maar fijn), Michiel (harig maar fijn), Richard (onbehouwen maar fijn), Edward (bedankt voor alle hulp zelfs nadat je al weg was), Ton

(bedankt voor de hulp met de kaft!), Johan H (kon van jou om de 1 of andere reden altijd heel veel hebben; komt helemaal goed bij Mallinckrodt), Ruud (wat een geweldige vader en doorzetter), Joost C (geweldig fitness- en kletsmaatje), Matthijs (als we uurloon hadden gekregen voor de uren die wij gekletst hebben, waren we nu schatrijk), Irene (kan altijd alles bij je kwijt en ik kan altijd helemaal mezelf zijn bij je, geweldig!), Femke, Pieter, Jurry, Aurélie, Kelly, Jeroen, Alexander, Friso, Victor, Heather, Cyril, Linda, Nikos, Raquel, Dennis vdM, Maria en Andrés.
Een heel speciaal bedankje aan de studenten die hebben bijgedragen aan de inhoud van dit boekje: Johan V (doe iets aan die ene wenkbrauwhaar!), Alistair (eigenwijs, maar altijd enthousiast), Nico (superchemicus; succes met je eigen promotie!) and last but not least to Ribera a big Thank You (it's an honour you want to come all the way from Catalonia for my defence ceremony).
En natuurlijk ook buiten de Nolte-groep waren er mensen die ik graag wil bedanken: Joost O (go Boekel!), Joris (altijd behulpzaam!), Rosalie (met doorntjes, maar toch zeker met een heel mooie bloem!), Henri (typisch vriendelijke Tukker), Suzanne (staat in het woordenboek onder 'sarcasme'), Bram (lekker over motoren kletsen), Dennis H (als je wat zei was het altijd leuk), Onno (zet hem op!), Stan (wat een kok), Jasper (Duitsers kunnen wel aardig zijn), Sander (sexy kalend) en Sjef (onderhevig aan metamorfoses, maar altijd een goede vriend). Natuurlijk zijn ook de partners van bovengenoemde (en onderstaande) personen ingesloten in de dankbetuiging, maar ik wil toch graag een paar namen noemen: PP (ik bewonder je enorm), Francis (succes met de kleine), Manon (komt helemaal goed), Ilona (de enige vrouw die me om zou kunnen turnen) en Annemiek (hoe langer ik je ken, hoe meer ik je waardeer en ik ken je al lang!).
Ook buiten de universiteit mocht ik me nog rijk rekenen met goede vrienden: Karin (ik bewonder je durf om te stoppen), Linda (nog nooit boos gezien), Guido (waarom toch?) en Lizette (altijd fijn om weer bij te kletsen).

Of course I need to send a very big "Cheers" to the people who have made my time in Oz so fantastic. First the people from Sydney University: Max (thanks for hiring me), Dianne (country girls are so refreshing!), Maxine (keep on riding bikes!), Ben (wee), Adam (also wee), Grace (it's all in the name), Peter (stereotypical Ozzie: very good!), Christine (someone's gotta do it), Felicia (good luck with the twins!), James (thanks for the skydive!), Allan (snorkeling is supergood!), Jarod (not a word!), Sabrina (if I was straight…), Josh (Americans are so easy to get along with), Paul (great to reminisce about Europe), Leon (heerlijk om samen Oz en Holland te vergelijken), Simon (f-ing A!), Aleisha (one of the prettiest brides ever) and last but not least Iain (never met anyone I've agreed with more on issues and people; sweet as a nut!). And outside of university: Andrew (I want your abs!), Brendan (Beyond is so much fun!), Chris (one of my first mates), Colin and Tony (thanks for a great Pool Party and Fair Day), Colin (wish we had met earlier), David (one of my first buddies), David M (had a great last weekend), Davo (have fun with the bike), Grant and Kelley (definitely A+!), Harry (thanks for the pillion rides), Jason (thanks for getting me involved in the MG parade), Lawrence (the best neighbor in a parade anyone could wish for), Mark (thanks for the pillion rides and so much more), Melody and Scott (great landlords), Michael T (great guy to share a house with), Michael (you're too kind), Nathan (what can I say? One day…), Rob (thanks for the couch and all the help), Sarge (always a good friend), Srdjean (great smile), Thomas

(sorry for not caring about your Aston Martin), Timo (also a great housemate), and last but not least Chris T (thanks for being a great friend; you could always make me smile). I wish you all nothing but the best and I hope to see you all again in the future.

Na terugkeer uit Australië kon ik gelukkig tijdelijk aan de slag bij Encapson en daarvoor wil ik Dennis en Lee van harte bedanken. Heb het erg naar mijn zin gehad en ik hoop dat het bedrijf een glorieuze toekomst tegemoet gaat. Verder was het meestal fijn met Dennis zijn ballen te spelen en ik kon altijd heerlijk kletsen (en militairtjes kijken) met Marieke.

Verder wil ik nog Bill Gates en al die andere lieve, lieve mensen bedanken die zich tot taak hebben gesteld het leven van de mens onmogelijk te maken zonder op zijn minst ekele uren per dag gebruik te maken van een computer. Zonder al die lieve, lieve mensen zou ik niet tot uitspraken zijn gekomen als “Ik beitel mijn proefschrift wel uit in steen! Dat is sneller!” of “Deze laptop gaat zo vliegles krijgen!”, en zouden mijn hart en bloedvaten een stuk saaier leven leiden. Waarbij ik even wil opmerken dat een goede vloek zeker wèl oplucht en iedereen die het daar niet mee eens is, kan een Dell door zijn strot gedouwd krijgen.

Tot slot kom je dan nog bij de mensen onder het kopje familie. Ik prijs me ontzettend gelukkig met een schoonfamilie als de mijne en ik wil graag Maria, Cees, Marike, Cees, Carmen, Axel, Irene, Saar en Jet erg bedanken voor de fijne tijden die we ondertussen al gedeeld hebben. Veronique, je bent een fantastische zus en je bent altijd een geweldig vertrouwenspersoon geweest. Ik hoop dat Jeroen je erg gelukkig gaat maken (en heb daar alle vertrouwen in, ik mag hem graag) en ook dat je carrière een wending gaat nemen in een richting die je graag wilt. Pap en mam: jullie hebben me door dik en dun, met raad en daad gesteund, ondanks dat ik wel eens verrassende en misschien onverstandige beslissingen nam. Het is altijd fijn om weer in Rosmalen te zijn en ik houd ontzettend veel van jullie. Pap, op het moment heb je het erg moeilijk en dat vind ik heel rot om te zien, maar ik weet zeker dat het helemaal goed met je komt. Je bent er altijd voor mij geweest en ik hoop nu dat ik er voor jou kan zijn. Ik had me geen betere vader kunnen wensen. Heel veel sterkte en beterschap gewenst. En dan natuurlijk mama: we hoeven nooit veel tegen elkaar te zeggen, want we kennen onszelf en daardoor elkaar blindelings. En dat is een band welke ik nooit met iemand anders zal delen.

En toen was er Jaap. Hoewel mijn afwezigheid gedurende ruim 13 maanden veel veranderd heeft, is de plek in mijn hart die jij inneemt nog net zo groot. Ondanks dat we elkaar ontzettend kunnen irriteren en opjutten, is mijn tijd met jou ontzettend fijn geweest en ik kon altijd bij je terecht voor wat voor zaken dan ook. Ik ben geen gemakkelijk persoon, maar jij heb mij met al mijn fouten en eigenaardigheden altijd geaccepteerd en dat vergt een groot hart, waarvoor ik je niet genoeg kan danken. Ik hoop je nog lang in mijn leven te mogen houden en ik houd heel veel van je.

En nu: hora est! Tijd voor bier….

Paul

Appendix

In this enclosure some of the Figures in Chapters 1 through 7 are printed in color, where the author has felt that the grayscale Figures might have been indistinct.

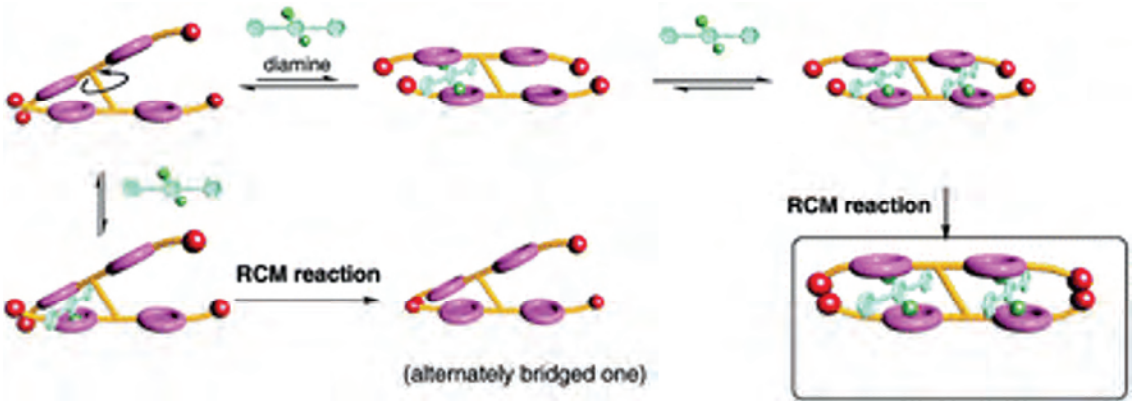

Chapter 1, Figure 3c

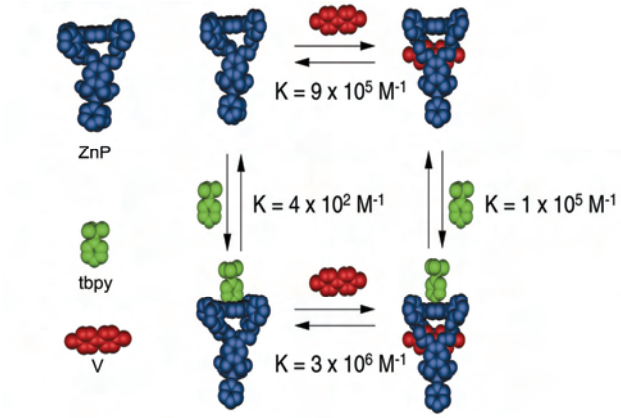

Chapter 1, Figure 13b; Chapter 2, Figure 1b; Chapter 4, Figure 1b

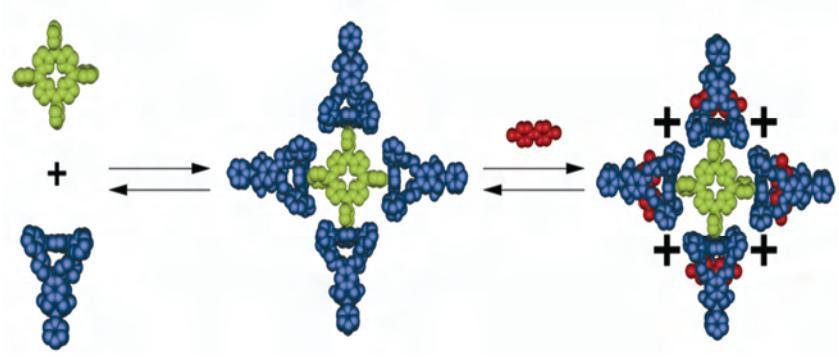

Chapter 1, Figure 13c

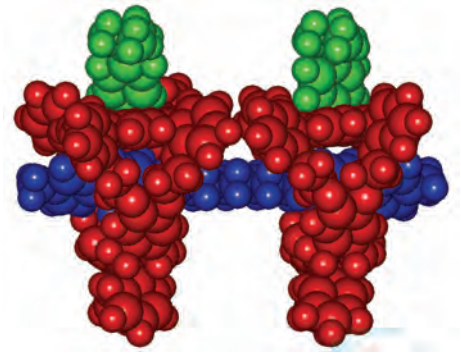

Chapter 4, Figure 5a

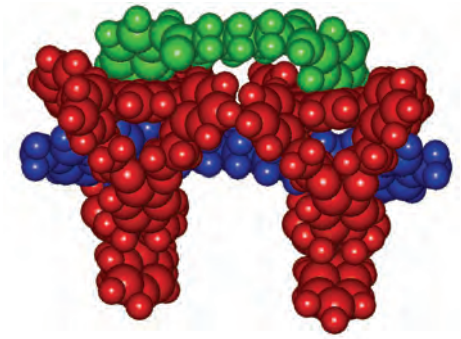

Chapter 4, Figure 7a

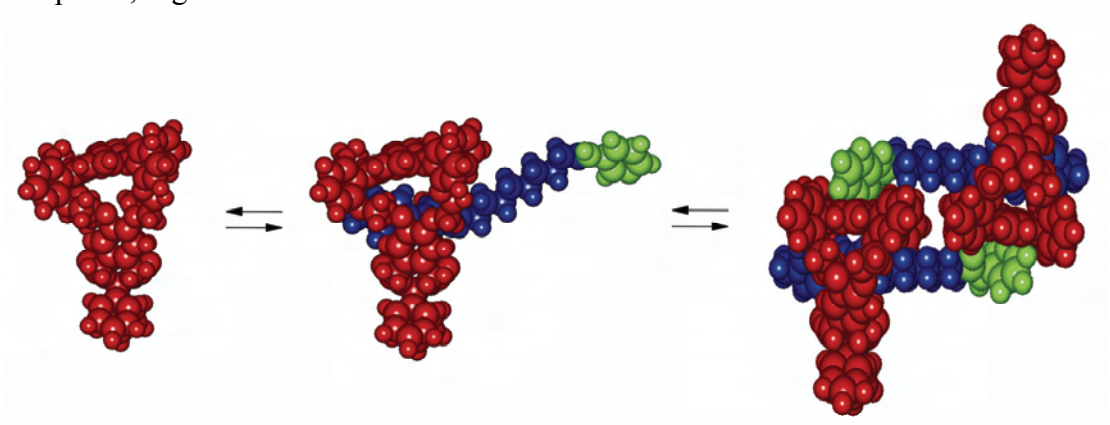

Chapter 4, Figure 8b

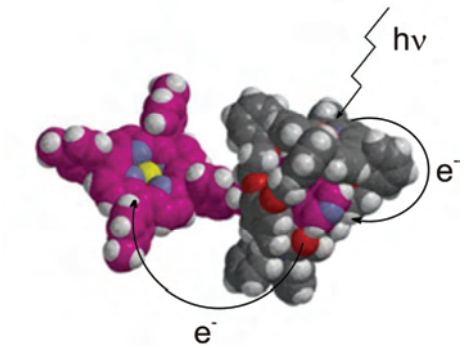

Chapter 5, Figure 1

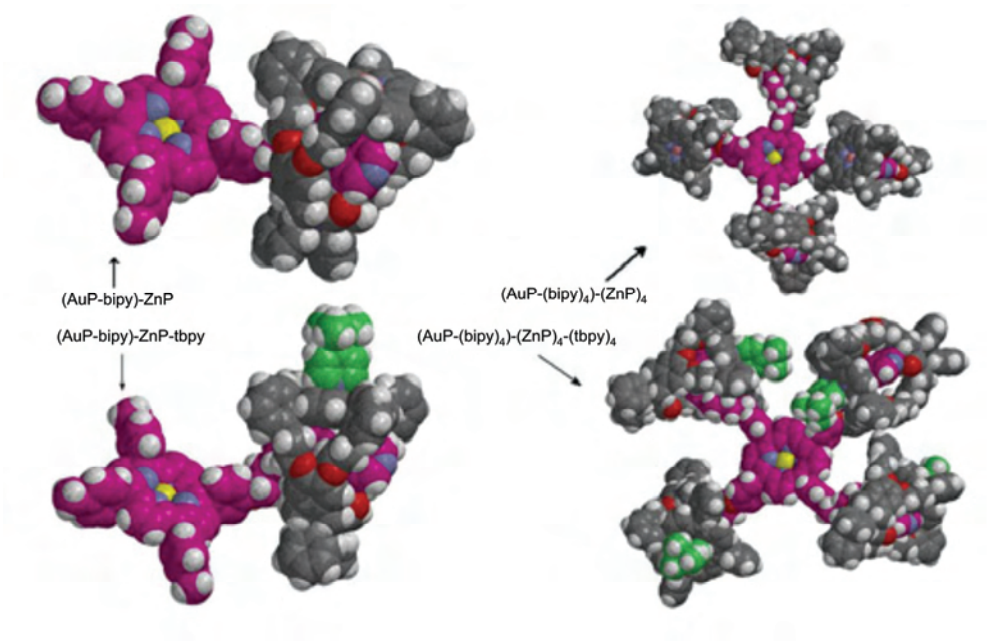

Chapter 5, Figure 2b

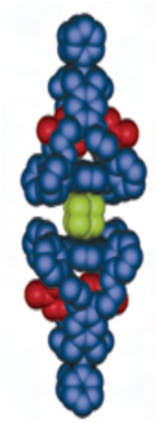

Chapter 6, Figure 2b

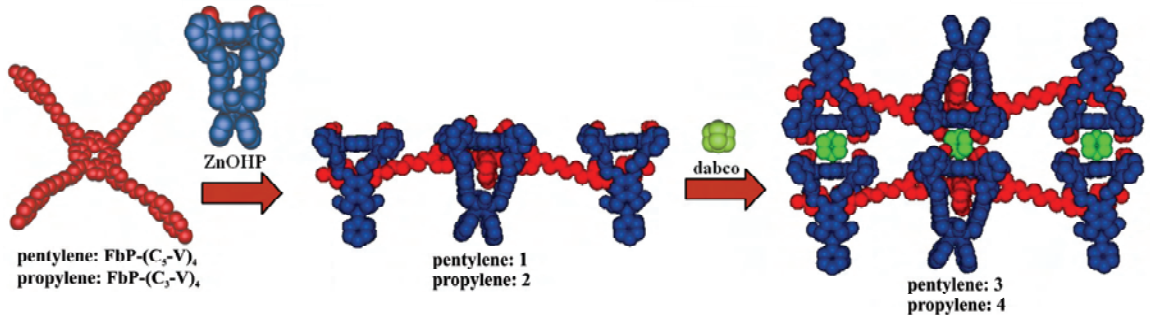

Chapter 6, Figure 3

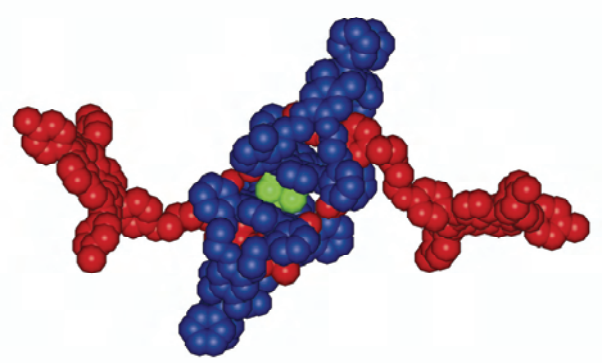

Chapter 6, Figure 4b

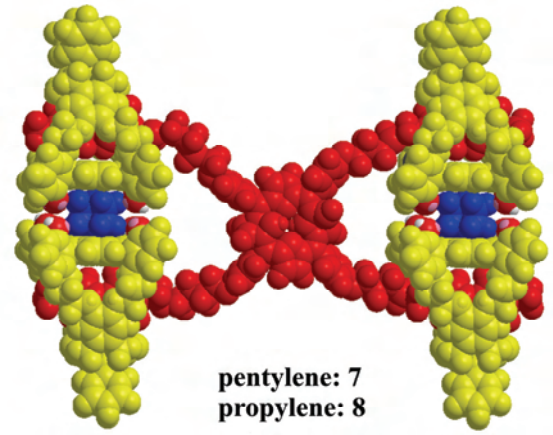

Chapter 6, Figure 6c

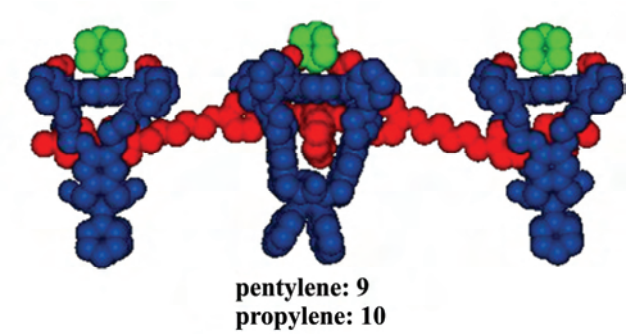

Chapter 6, Figure 6e

Curriculum Vitae

Paul Thomassen was born on September 14th 1979 in ‘s-Hertogenbosch. After attending R.K.B.S. ‘t Ven primary school in Rosmalen, he entered Gymnasium Bernrode in Heeswijk in 1991. He started his chemistry study at the Radboud University in Nijmegen in 1997 and received his M.Sc. degree there in 2002. His major was in Inorganic Chemistry, under the supervision of Prof. dr. A.W. Gal and Dr. B. de Bruin, studying hydrogen bonding nitrogen donor ligands for platinum(II) olefin complexes. His minor was a collaboration between the “Performance Materials Competence Centre” at DSM, Geleen (under Dr. A. Heise), the “Biocatalysis and Bioprocessing of Macromolecules” research group at the Brooklyn Polytechnic University, New York (under Prof. dr. R.A. Gross and Dr. B. Kalra), the “Macro-Organic Chemistry” research group at the Eindhoven University of Technology (under Dr. A.R.A. Palmans) and the “Bio-Organic Chemistry” group at the Radboud University Nijmegen (under Prof. dr. J.C.M. van Hest). Research was performed at the first three locations of this collaboration and was focussed on the synthesis of block-copolymers employing the combination of enzymatic ROMP and living free radical polymerisation techniques.

In October 2002 he started his PhD project as a junior researcher under guidance of Dr. J.A.A.W. Elemans. The project was a collaboration between the “Physical-Organic and Supramolecular Chemistry” group of Prof. dr. R.J.M. Nolte and the “Molecular Materials” research group of Prof. dr. A.E. Rowan. Cooperative systems employing cavity-appended porphyrin host molecules were investigated. The results thereof are presented in this thesis.

From February 2007 Paul was employed as a Post-Doctoral Fellow at the University of Sydney in the “Synthesis of Functional Organic Molecules” research group of Prof. dr. M.J.C. Crossley. Porphyrinic systems were investigated that could be switched between a “0” and a “1” state and could therefore be employed as miniature computer chips.

In April 2008 he was employed as a Research Scientist at Encapson BV in Nijmegen, investigating the self-assembly of polymers into capsules. Since August 2008 he has been employed as Application Engineer Solar at Mallinckrodt Baker.